



HAL
open science

Rational development of kinase inhibitors dedicated to treatment of neoplastic diseases and diabetic complications

Matus Hlavac

► **To cite this version:**

Matus Hlavac. Rational development of kinase inhibitors dedicated to treatment of neoplastic diseases and diabetic complications. Medicinal Chemistry. Université de Strasbourg; Univerzita Komenského (Bratislava), 2020. English. NNT : 2020STRAF063 . tel-03641751

HAL Id: tel-03641751

<https://theses.hal.science/tel-03641751v1>

Submitted on 14 Apr 2022

HAL is a multi-disciplinary open access archive for the deposit and dissemination of scientific research documents, whether they are published or not. The documents may come from teaching and research institutions in France or abroad, or from public or private research centers.

L'archive ouverte pluridisciplinaire **HAL**, est destinée au dépôt et à la diffusion de documents scientifiques de niveau recherche, publiés ou non, émanant des établissements d'enseignement et de recherche français ou étrangers, des laboratoires publics ou privés.

École Doctorale des Sciences Chimiques
UMR CNRS 7042, LIMA

THÈSE

Présentée par:

Matúš HLAVÁČ

soutenue le: 14 Décembre, 2020

Pour obtenir le grade de: **Docteur de l'université de Strasbourg**

Discipline: **Chimie organique et médicinale**

**Développement rationnel d'inhibiteurs de kinases
dédiés au traitement de maladies néoplasiques et
des complications diabétiques**

THÈSE dirigée par: **Dr. Gilles HANQUET**, Université de Strasbourg, ECPM, UMR
CNRS 7509, Strasbourg, France

Co-directeur: **assoc. Prof. Andrej Boháč**, Univerzita Komenského v Bratislave
Faculté des Sciences Naturelles, Bratislava, Slovaquie

RAPPORTEURS: **Prof. Philippe BELMONT**, Université Paris Descartes, Faculté des
Sciences Pharmaceutiques et Biologiques, UMR 8638 CNRS
Prof. Viktor MILATA, Slovak Technical University in Bratislava,
Faculty of Chemical and Food Technology, Bratislava, Slovaquie

AUTRES MEMBRES: **Prof. Fernanda BORGES**, Université de Porto, Departamento de
Química e Bioquímica, Faculty of Sciences, Porto, Portugal
Prof. Danijel KIKELJ, Univerza v Ljubljani, Faculté de Pharmacie,
Ljubljana, Slovénie
assoc. Prof. Daniele PASSARELLA, Università degli studi di Milano,
Dipartimento di Chimica, Milano, Italie
Dr. Pavol Koiš, MultiplexDX, Bratislava, Slovaquie

Acknowledgement

Firstly, I would like to express my sincere gratitude to my both tutors Dr. Gilles Hanquet and assoc. prof. RNDr. Andrej Boháč, PhD. for their valuable advice, guidance, professional help and continuous support of my PhD study and related research.

Besides of my tutors, I would like to thank my fellow labmates and advisors at both universities for their stimulating discussions and useful advice, and for all the fun we have had in the last years.

I also thank Biomagi, Ltd. for the proposed structures of VEGFR2 TK and ALR2 inhibitors. My sincere thanks goes to French Institute in Bratislava for an opportunity to complete my PhD study at Université de Strasbourg in frame of “Cotutelle“ program and to the organizations Collège Doctoral Européen and Campus France for their support and valuable help during my stay in Strasbourg.

Last but not the least, I would like to thank my family and girlfriend for their patient and for supporting me during last three years.

Summary

SUMMARY

Résumé en français	21
1. Introduction	27
2. Les récepteurs de la tyrosine kinase VEGFR2	33
2.1. VEGFR2 tyrosine kinase.....	34
2.2. Inhibiteurs du VEGF	36
2.3. Résultats et discussions	37
3. L'aldose réductase (ALR2) dans le diabète sucré	45
3.1. La voie des polyols.....	46
3.2. Diabète sucré (DM) et complications du diabète	47
3.3. Propriétés et fonction d'ALR2.....	48
3.4. Un site actif d'ALR2.....	48
3.5. Aldéhyde réductase	49
3.6. Inhibiteurs d'ALR2.....	49
3.6.1. Dérivés d'acide carboxylique	49
3.6.2. Spirohydantoïne et dérivés du spirosuccinimide.....	51
3.7. Résultats et discussions	52
4. Conclusion générale	57
Manuscript en Anglais	59
Resume of the thesis	59
5. Introduction	65
6. Vascular endothelial growth factor receptor (VEGFR)	71
6.1. VEGFR2 tyrosin kinase	72
6.2. Inhibitors of VEGF.....	74
6.3. Inhibitors of VEGFR2 TK.....	74
6.4. Biological assay activity (VEGFR2 TK)	76
7. Synthesis of aminooxazole VEGFR2 TK inhibitors	79
7.1. Synthesis of <i>N</i> ,5-diaryloxazole-2-amines	79
7.2. Synthesis of <i>N</i> ,4-diaryloxazole-2-amines	83
8. Palladium-catalyzed cross-coupling reactions	89
8.1. Suzuki-Miyaura (SM) cross-coupling reaction	89
8.1.1. Types of boronic derivatives	91
8.1.2. Ligands in SM-cross coupling reactions	92
8.2. Stille cross-coupling reaction	95

SUMMARY

8.2.1. Additives in Stille coupling reactions.....	96
9. Development of novel <i>N</i>,4-diaryloxazol-2-amine VEGFR2 TK inhibitors NBM(1-7)	101
9.1. Synthesis of <i>N</i> ,5-diaryloxazole-2-amine intermediate (28) and VEGFR2 TK inhibitor (BM7).....	103
9.2. Synthesis of <i>N</i> ,4-diaryloxazole-2-amine precursor (10).....	105
9.3. Determination of biological activity and evaluation of the project	110
9.4. Experimental part.....	112
9.4.1. Synthesis of isothiocyanate (5) and urea (6).....	112
8.4.2. Synthesis of <i>N</i> ,4-diaryloxazole-2-amine general intermediate (10)	119
9.4.2. Synthesis of tributylstannylimidazole (15) and pyrrol pinacol boronic ester (19) coupling partners	124
9.4.3. Synthesis of <i>N</i> ,4-diaryloxazole-2-amine VEGFR2 TK inhibitors NBM(1-7).....	131
9.4.4. Synthesis of 5-[3-(1 <i>H</i> -imidazol-5-yl)phenyl]- <i>N</i> -[5-(ethylsulfonyl)-2-methoxyphenyl]oxazol-2-amine (BM7)	146
10. Development of three-point interacting SBCP VEGFR2 TK inhibitors BM(8-16)	153
10.1. Synthesis of the general intermediate <i>N</i> ,5-diaryloxazol-2-amine (36).....	157
10.2. Synthesis of pyrazole inhibitors BM(11-13)	163
10.3. Synthesis of imidazole inhibitors BM(14-16)	163
10.4. Synthesis of <i>N</i> ,4-diaryloxazole-2-amine precursor (69).....	164
10.5. Evaluation of biological activity.....	168
10.6. Experimental part.....	169
10.6.1. Synthesis of a general intermediate <i>N</i> ,5-diaryloxazol-2-amine (36).....	169
10.6.2. Synthesis of <i>N</i> ,5-diaryloxazol-2-amine VEGFR2 TK inhibitors BM(8-16)	178
10.6.3. Synthesis of <i>N</i> ,4-diaryloxazole-2-amine precursor (69)	193
11. Aldose reductase (ALR2) in diabetes mellitus.....	201
11.1. The polyol pathway	202
11.2. Diabetes mellitus (DM) and diabetic complications	203
11.3. Properties and function of ALR2.....	204
11.4. An active site of ALR2	205
11.5. Aldehyde reductase.....	205
11.6. Inhibitors of ALR2	206
11.6.1. Carboxylic acid derivatives	206

SUMMARY

11.6.2. Spirohydantoin and spirosuccinimide derivatives	208
11.6.3. Discovery of the indole-1-acetic acid ALR2 inhibitor (CMTI).....	209
11.7. Biological assay activity (ALR2).....	211
12. Synthesis of ALR2 inhibitors possessing triazinoindole scaffold	215
12.1. Preparation of a 1,2,4-triazine-3-(2 <i>H</i>)-thione catalysed by base	215
12.2. Preparation of the 1,2,4-triazine-3-(2 <i>H</i>)thione catalysed by HOAc or NaOAc / HOAc	217
12.3. Formation of the 1,2,4-triazin-3(2 <i>H</i>)-one	218
13. Project 3 - Isosteric sulphur/oxygen replacement in the ALR2 inhibitor centirestat (CMTI).....	223
13.1. Synthesis of centirestat (CMTI).....	224
13.2. Synthesis of an oxo CMTI isostere (OTI) and its dicarboxylic derivative (OTI-1) 224	
13.3. Synthesis of other OTI derivatives OTI-(2-5).....	225
13.4. Evaluation of OTIs ALR2 inhibition and selectivity	227
13.5. Experimental part	230
13.5.1. Synthesis of triazinoindol ALR2 inhibitor centirestat (CMTI)	230
13.5.2. Synthesis of an oxo CMTI isostere (OTI) and its dicarboxylic derivative (OTI- 1) 236	
13.5.3. Synthesis of OTI derivatives OTI-(2-5).....	248
14. Project 4 - Synthesis and SAR study of novel OTI derivatives OTI-(6-9)	263
14.1. Synthesis of OTI-6	264
14.2. Synthesis of OTI-(7-9)	265
14.3. Evaluation of OTI-(6-9) ALR2 inhibitory activity	265
14.4. Experimental part	268
14.4.1. Synthesis of benzyl derivative (OTI-6)	268
14.4.2. Synthesis of benzyl analogues OTI-(7-9)	277
15. Conclusion	287
16. Future perspective	291
17. Characterization of the prepared compounds	297
Scientific contribution	303

Abbreviations

Abbreviations

Abs	Absolut, dry, not containing water
ALL	Acute lymphotic leukemia
ALR1	Aldehyde reductase
ALR2	Aldose reductase
AN	Acetonitrile
Ar	Argon atmosphere
ARIs	Aldose reductase inhibitors
ATP	Adenosine triphosphate
Brine	Saturated aq solution of NaCl
cHex	cyclohexane
CML	Chronic myelogenous leukemia
DCM	Dichloromethane
DM	Diabetes Mellitus
DMA	<i>N,N</i> -Dimethylacetamide
DMF	<i>N,N</i> -Dimethylformamide
DMSO	Dimethylsulfoxide
DPPH	A free radical of 2,2-diphenyl-1-(2,4,6-trinitrophenyl)hydrazyl
EA	Ethyl acetate
ED ₅₀ (e.g., mg / kg, mmol / kg or mg / L, mmol / L when a tissue is perfused)	A half maximal effective dose – the dose of a drug that produces a specific <i>in vivo</i> response in 50 % of a tested population compare to a blank assay
EGFR	Epidermal growth factor receptor
ESI	Electrospray ionization
FDA (US FDA)	The US Food and drug administration agency
FLC	Flash liquid chromatography
GIST	Gastrointestinal stromal tumor

Abbreviations

GSH	Glutathione (reduced state)
GSSG	Glutathione disulphide (oxidized state)
Hex	Hexol (a mixture of hexanes)
HexLi	Hexyllithium
HRMS	High resolution mass spectrometry
HV	High vacuum (< 0.1 Torr)
IC ₅₀	A half maximal inhibitory concentration – the concentration of an antagonist required for 50 % inhibition of particular biological target compared to a blank assay
IR	Infrared spectroscopy
K _i (M)	An equilibrium dissociation constant for ligand receptor interactions determined in inhibition studies
MIDA	<i>N</i> -methyliminodiacetic acid
MW	Microwave irradiation
NADH	Nicotinamide adenine dinucleotide (reduced form)
NADPH	Nicotinamide adenine dinucleotide phosphate (reduced form)
NIDDM	Non-insulin-dependent diabetes mellitus
NMR	Nuclear Magnetic Resonance
PDB	<i>(The Protein Data Bank)</i> the crystallographic database of the 3D structural data of biomolecules and / or their complexes
PPTS	Pyridinium <i>p</i> -toulenesulfonate
rt	room temperature
RVE	Rotavap, Rotatory vacuum evaporator
SAR	Structure activity relationship – the relationship between the structure of a molecule and its biological activity
SBCP	The Salt Bridge Containing Pocket

Abbreviations

SF	Selectivity factor (IC_{50} (ALR1) / IC_{50} (ALR2))
SM	Suzuki-Miyaura
TFA	Trifluoroacetic acid, CF_3CO_2H
THF	Tetrahydrofuran
TK	Tyrosine kinase
TKI	Tyrosine kinase inhibitor
TLC	Thin layer chromatography
TMEDA	Tetramethylethylenediamine
VEGF	Vascular endothelial growth factor
VEGFR2 TK (KDR)	Vascular endothelial growth factor receptor 2 (Kinase Inserted Domain Receptor)

General considerations for the experimental sections

Commercially available compounds were purchased from Sigma-Aldrich, Alfa Aesar, Fluorochem, TCI Europe or Acros Organics vendors. Solvents were purchased from Sigma-Aldrich or Mikrochem in an analytical grade, technical grade or reagent grade quality. Anhydrous solvents were used; Acetonitrile (AN), dichloromethane (DCM), 1,4-dioxane, ethyl acetate (EA) and triethylamine (Et₃N) were dried and distilled from CaH₂ under Ar. Tetrahydrofuran (THF) was distilled over sodium / benzophenone, dimethylformamide (DMF) over P₂O₅. Methanol (MeOH) was dried and stored over molecular sieves. A reaction progress was monitored by Thin Layer Chromatography (TLC) analysis (Merck Millipore Silica gel 60 F254). UV lamp (254 nm), iodine vapors and KMnO₄ solution were used for visualization of TLC spots. Crude mixtures were purified by trituration, crystallization, distillation or Flash Liquid Chromatography (FLC) on the silica gel 60 (230-400 mesh, 0.040-0.063 mm) purchased from Merck.

Prepared compounds were characterized by their M.p., NMR (textual assignment and NMR diagram), IR and MS spectrometry, elemental and X-Ray analysis. NMR diagrams represent clear information about assigned ¹H and ¹³C-NMR data of a particular chemical structure. ¹H-NMR diagrams allow fast check of both chemical shifts and pairs of coupling constants. Numbers used on the diagrams mean chemical shift in δ ppm and numbers in parenthesis represent corresponding coupling constants in Hz. The other reason why NMR diagrams were used is to read and compare the NMR data more conveniently.

Nuclear Magnetic Resonance (NMR) spectra were measured on Varian Gemini 300, Varian Gemini 600 or Bruker AC 400 machines with the peak of TMS as a reference. In the NMR diagrams and assignments, coupling constants (*J*) are expressed in Hertz (Hz), multiplicity is described with s (as singlet) br s (as broad singlet), d (as doublet), dd (as doublet of doublets), ddd (as doublet of doublets of doublets), t as (triplet) and q (as quadruplet).

Melting points were measured on Büchi Melting Point M-565 instrument. Infrared (IR) spectra were obtained neat using Agilent Technologies Cary 630 104 FTIR with diamond probe and MTS detector. Microwave experiments were carried out in an *Initiator*TM from Biotage (400 W) or Anton Paar – monowave 300 (850 W). Liquid Chromatography-Mass Spectrometry (LC-MS) analysis was performed on an Agilent Technologies 1200 Series instrument equipped with Mass spectrometer Agilent Technologies 6100 Quadrupole using electrospray ionization (ESI). Elemental and X-Ray analysis were obtained from the science analytical service at University of Strasbourg or at Comenius University in Bratislava.

General considerations for the experimental sections

Résumé en français

Matúš Hlaváč: Développement rationnel d'inhibiteurs de kinases dédiés au traitement de maladies néoplasiques et des complications diabétiques

Université de Strasbourg, Ecole européenne de Chimie, Polymères et Matériaux (ECPM), UMR CNRS 7042 LIMA, Strasbourg, France. Univerzita Komenského v Bratislave, Faculté des Sciences Naturelles, Bratislava, Slovaquie

Les récepteurs de la tyrosine kinase VEGFR2 sont des protéines transmembranaires cruciales pour la régénération tissulaire, la régulation des cycles cellulaires importants et la fonction des cellules endothéliales vasculaires. D'autre part, une activité accrue de VEGFR2 TK provoque une division incontrôlée des cellules cancéreuses et la formation de tumeurs. En conséquence, le développement de petites molécules inhibitrices de la VEGFR2 TK est devenu un moyen prometteur et efficace pour le traitement du cancer. D'un autre côté, une maladie tout aussi grave est le diabète, caractérisée par une hyperglycémie due à l'absence de sécrétion d'insuline ou de son inactivité, ou encore la conjonction des deux. Dans ce cadre, l'aldose réductase (ALR2), qui joue un rôle important dans la survenue de diverses complications, est devenue une cible thérapeutique importante dans le traitement des maladies liées au diabète. Dans la première partie de cette thèse, nous décrivons le développement de 14 inhibiteurs potentiels de l'aminooxazole VEGFR2 TK. Nous avons réussi à synthétiser de nouveaux inhibiteurs aminooxazoles *N*,4-disubstitués **NBM(1-7)**, qui sont des paires régioisomères des inhibiteurs *N*,5-disubstitués **BM(1-7)** que nous avons précédemment développés. Ensuite, nous avons proposé les dérivés **BM(8-6)** potentiellement plus efficaces et six d'entre eux ont été préparés. L'évaluation de l'activité biologique de ces inhibiteurs est en cours. La deuxième partie de la thèse est consacrée au développement d'inhibiteurs d'ALR2. Sur la base de la structure du composé principal **CMTI** précédemment développé, nous avons préparé un composé oxotriazinoindole **OTI** et trois de ses analogues **OTI-(1-3)** plus actifs et sélectifs. Une étude du site actif d'ALR2 nous a conduit à découvrir une poche inoccupée et mené au développement de nouveaux dérivés *N*-benzyliques **OTI-(6-9)** ainsi que plusieurs autres dérivés.

Mots clés: inhibiteurs de tyrosine kinase, aldose réductase, VEGFR2 TK, ALR2, aminooxazoles, oxotriazinoindoles

Introduction

1. Introduction

Le cancer est sans aucun doute l'une des maladies les plus graves et potentiellement plus mortelles au monde. Le développement d'un cancer est un processus en plusieurs étapes impliquant une initiation et un état de progression. Lors de l'initiation de la tumeur, une seule cellule est mutée par des modifications de l'ADN entraînant ensuite une prolifération anormale. Cette prolifération donne lieu à un grand nombre de cellules filles contenant la mutation créée par l'initiateur. La progression tumorale se poursuit alors que des mutations supplémentaires se produisent dans les cellules de la population tumorale, suivies d'une sélection pour des cellules à croissance plus rapide. Cette sélection contribue au développement de la tumeur, de sorte que la tumeur devient à croissance plus rapide et maligne.

L'angiogenèse est un processus complexe contrôlé par des facteurs de croissance produits dans le corps. Au cours de l'angiogenèse, de nouveaux vaisseaux sanguins sont formés à partir de vaisseaux préexistants et ce processus est physiologiquement crucial pendant le développement embryonnaire et la guérison des plaies. D'autre part, l'angiogenèse est également impliquée dans la croissance des tumeurs. La compréhension des processus de signalisation cellulaire au cours des dernières décennies a conduit à l'identification du VEGFR2 TK comme cible intéressante pour une thérapie anticancéreuse. Il a été démontré que de petites molécules inhibitrices de VEGFR2 TK suppriment la croissance du cancer et les métastases, conduisant à un traitement efficace du cancer, principalement en combinaison avec d'autres agents.

Le Diabète sucré (DM) est également une maladie bien connue induite par un groupe de troubles métaboliques caractérisés par un taux anormalement élevé de sucre dans le sang. Les personnes atteintes de diabète sucré (DM) ont soit un manque de sécrétion d'insuline (DM type I), soit l'insuline ne peut pas être utilisée correctement (DM type II), ce qui conduit à diverses pathologies. Il peut endommager les minuscules vaisseaux des reins, du foie, des yeux ou du système nerveux entraînant une cataracte diabétique, une rétinopathie, une neuropathie ou encore une néphropathie. Toutes ces complications pathologiques diabétiques sont associées à une voie polyol, qui dans un premier temps convertit le glucose en sorbitol par une enzyme, l'aldose réductase. Outre une concentration élevée de sorbitol, il en résulte une accumulation excessive d'espèces intracellulaires réactives de l'oxygène (ROS) dans divers tissus. Des études récentes ont montré que les inhibiteurs de l'ALR2 pouvaient prévenir ou retarder l'apparition des complications diabétiques chroniques, par conséquent, l'inhibition de l'activité de l'ALR2 a ouvert une voie prometteuse pour le traitement des complications liées au diabète.

Introduction

La première partie de la thèse est consacrée au développement d'aminooxazoles inhibiteurs de VEGFR2 TK prédits *in silico*. La deuxième partie de la thèse est axée sur le développement d'oxotriazinoindoles comme nouveaux inhibiteurs d'ALR2, y compris la conception, la synthèse, l'activité biologique et l'évaluation des résultats obtenus. Ces études et les résultats obtenus peuvent servir d'outil précieux pour une meilleure compréhension de la conception des médicaments.

Dans le cadre du premier projet, nous visons à synthétiser une série d'inhibiteurs prédits de VEGFR2 TK comportant le noyau *N*,4-diaryloxazole-2-amine **NBM(1-5,7)** représentant un ensemble de régioisomères comportant le noyau *N*,5-diaryloxazole-2-amine **BM(1-6)** préparés antérieurement à ce travail. Etant donné qu'un oxygène est un isostère d'un azote dans un cycle oxazole et *vice versa*, des interactions de liaison similaires des inhibiteurs avec Cys917 à partir du site de liaison ATP sont attendues pour les deux régioisomères. Un composé manquant pour cette étude **BM7** a également été synthétisé. Enfin nous avons également déterminé les activités biologiques des nouveaux composés préparés afin d'évaluer notre hypothèse de bioisostérie régioisomérique (*RegBio*). (Figure 1)

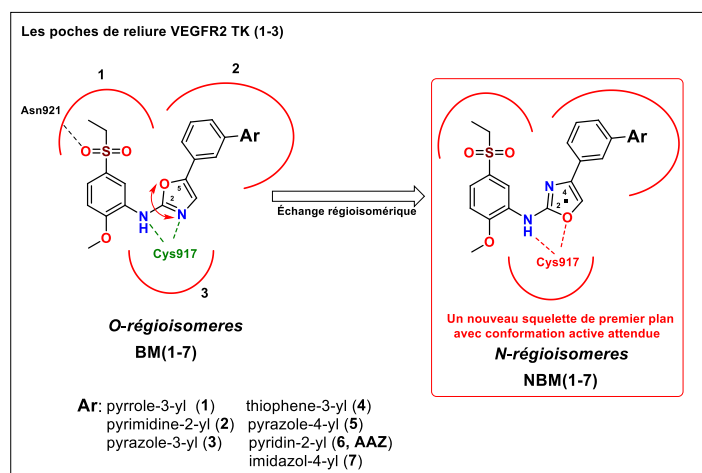


Figure 1 Bioisostérie régioisomérique (*RegBio*) - série des aminooxazoles *N*,5-disubstitués **BM(1-7)** les plus actifs et leurs paires régioisomères **NBM(1-7)** possédant un noyau aminooxazole *N*,4-disubstitué.

Dans le cadre du deuxième projet, nous nous sommes concentrés sur le développement et la synthèse de la deuxième classe d'inhibiteurs de VEGFR2 TK **BM(8-16)**, contenant des hétérocycles pyrrole, pyrazole et imidazole en position *mé*ta et un groupement *para*-cyano, -amide et -acide carboxylique sur le cycle phényle terminal. Ils devraient posséder des

Introduction

interactions en trois points avec une poche de SBCP récemment découverte et améliorer les affinités de liaison récepteur-ligand. (Figure 2)

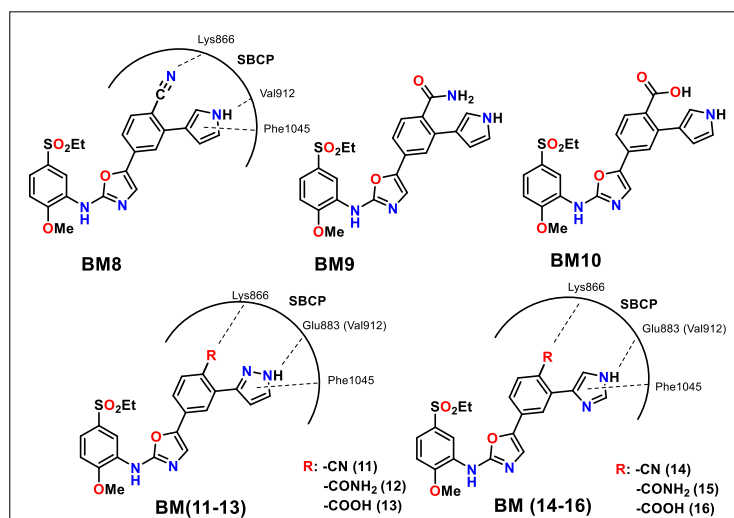


Figure 2. Structures des inhibiteurs de 2^{ème} génération **BM(8-16)** avec une interaction en trois points proposée avec le SBCP.

Dans le troisième projet, nous avons cherché à développer une méthodologie synthétique pour l'inhibiteur de l'aldose réductase (ALR2) **CTMI** récemment découvert et hautement actif. Nous nous sommes ensuite concentrés sur le développement de l'analogue isostérique soufre / oxygène **CMTI OTI** et de ses dérivés **OTI-(1-5)** possédant un squelette oxotriazinoindole. Finalement, les activités et les sélectivités de tous les composés préparés ont été déterminées. (Figure 3)

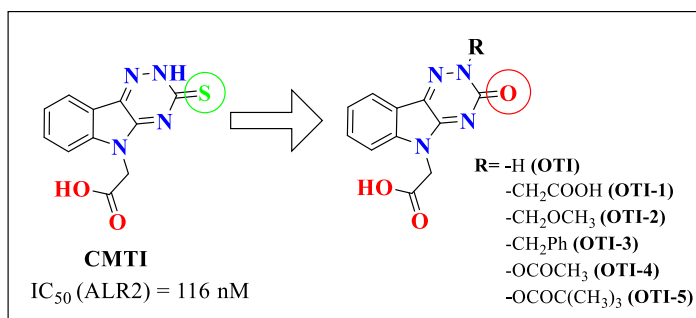


Figure 3. Remplacement bioisostérique du soufre par de l'oxygène dans le **CMTI** et la structure de l'**OTI** et analogues proposés **OTI-(1-5)**.

Introduction

Dans le dernier projet, nous nous sommes concentrés sur la synthèse et l'étude SAR de **OTI-3** (**6-9**) en tant que nouveaux analogues *N*-benzyliques de **OTI-3** afin d'améliorer l'activité inhibitrice d'ALR2 en exploitant davantage la poche interactive avec le benzyle. (Figure 4)

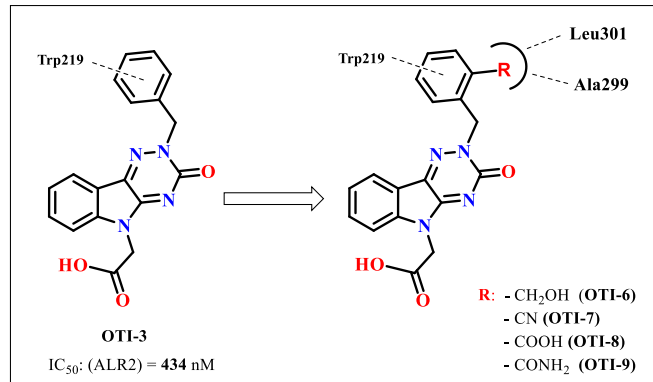


Figure 4. Les structures des dérivés de *N*-benzyl(oxotriazinoindole) proposés **OTI- (6-9)**.

Chapitre 1. Les récepteurs de la tyrosine kinase VEGFR2

2. Les récepteurs de la tyrosine kinase VEGFR2

Les facteurs de croissance endothéliaux vasculaires (VEGF) sont des protéines de signalisation très importantes qui stimulent la formation de nouveaux vaisseaux sanguins. Cette sous-famille de facteurs de croissance est produite par les cellules et elle est aussi impliquée dans la vasculogénèse (production de nouvelles cellules endothéliales) et l'angiogénèse (production de nouveaux vaisseaux à partir de vaisseaux préexistants). La fonction normale des VEGF est de créer de nouveaux vaisseaux sanguins après une blessure et pendant le développement embryonnaire. D'autre part, les VEGF sont surexprimés dans de nombreuses cellules tumorales, ce qui entraîne une angiogénèse tumorale, une prolifération cellulaire et des métastases. Chacun des ligands du VEGF se lie d'une manière spécifique à trois récepteurs VEGF de la tyrosine kinase (VEGFR TK). Les tyrosines kinases sont des enzymes qui phosphorylent spécifiquement les résidus d'acides aminés tyrosine de cibles peptidiques par des molécules ATP à haute énergie. Il existe trois importantes catégories de VEGFR, numérotés 1, 2 et 3. VEGFR1 (Flt-1) est exprimé sur les cellules souches hématopoïétiques, les monocytes et les macrophages, le VEGFR2 (Flk-1, KDR) régule principalement la fonction des cellules endothéliales vasculaires et favorise leur prolifération, migration, perméabilité et leur survie. Par conséquent, VEGFR2 est crucial pour le développement d'une tumeur. Enfin, VEGFR3 (Flt-4) régule les fonctions des cellules endothéliales lymphatiques. (Figure 5)

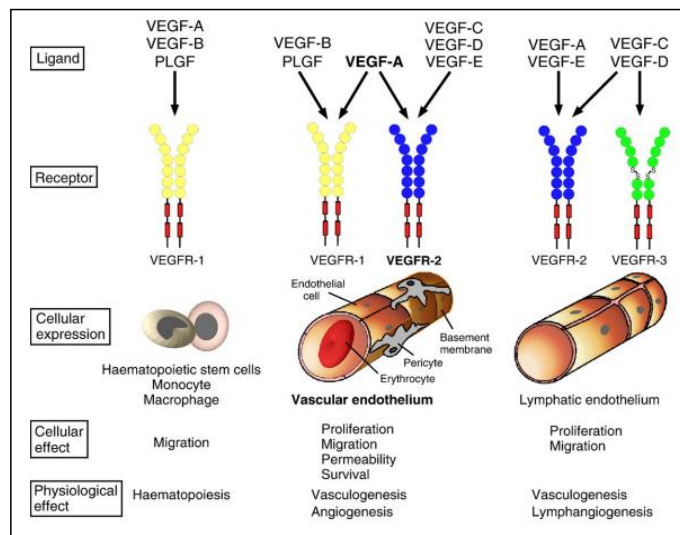


Figure 5. Illustration schématique de chaque récepteur de facteur de croissance endothélial vasculaire (VEGFR) avec leurs facteurs de croissance (VEGF (A-E), PLGF) et leurs effets cellulaires et physiologiques.

2.1. VEGFR2 tyrosine kinase

VEGFR2 TK (kinase insert domain receptor (KDR) ou foetal liver kinase (Flk-1)) est un récepteur transmembranaire de la tyrosine kinase composé d'une région extracellulaire (composée de sept domaines de type immunoglobuline (Ig)), d'un court domaine transmembranaire et d'une région intracellulaire (contenant le domaine tyrosine kinase). (Figure 6)

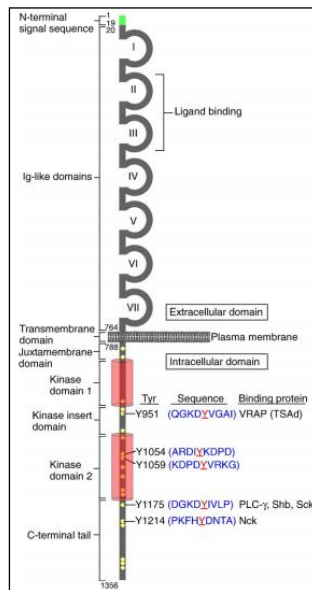


Figure 6. La structure de la tyrosine kinase VEGFR2 humaine.

Le VEGFR2 TK est activé lorsqu'un ligand (VEGF) se lie au domaine extracellulaire d'un récepteur, ce qui conduit à sa dimérisation avec son voisin et à la stabilisation de ce complexe. Après cela, plusieurs résidus tyrosine intracellulaires de chaque monomère de récepteur sont transphosphorylés par son récepteur partenaire. La phosphorylation et l'activation de ces deux protéines réceptrices conduisent à une activation et à l'initiation de diverses réponses et voies cellulaires. (Figure 7)

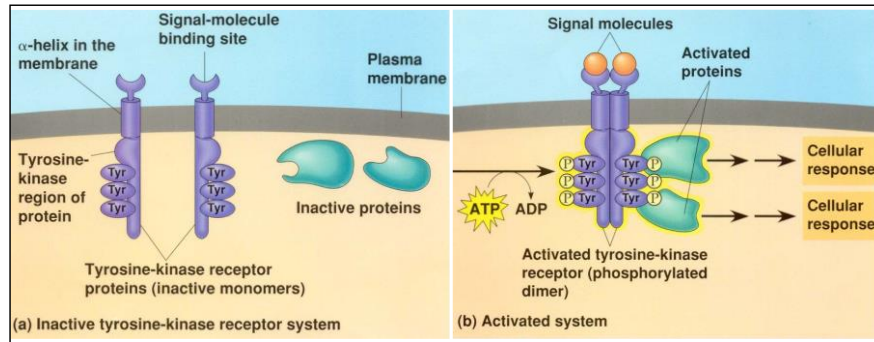


Figure 7. a) Etat inactif du récepteur tyrosine kinase b) Un récepteur tyrosine kinase homodimère activé.

L'expression de VEGFR2 dans les cellules cancéreuses est régulée à la hausse pendant la croissance tumorale par des stimuli environnementaux tels que l'hypoxie ou certaines mutations génétiques. L'état d'hypoxie favorise la sécrétion de VEGF-A, qui se lie au VEGFR2 TK exprimé sur les cellules endothéliales vasculaires (Figure 8). L'expression du VEGF-A est un marqueur pronostique chez les patients atteints de diverses tumeurs malignes. Par conséquent, l'inhibition de l'angiogenèse avec des médicaments anti-angiogéniques efficaces peut entraîner la suppression de la croissance tumorale. Ces agents sont divisés en plusieurs classes selon leur mécanisme d'action. (Figure 8)

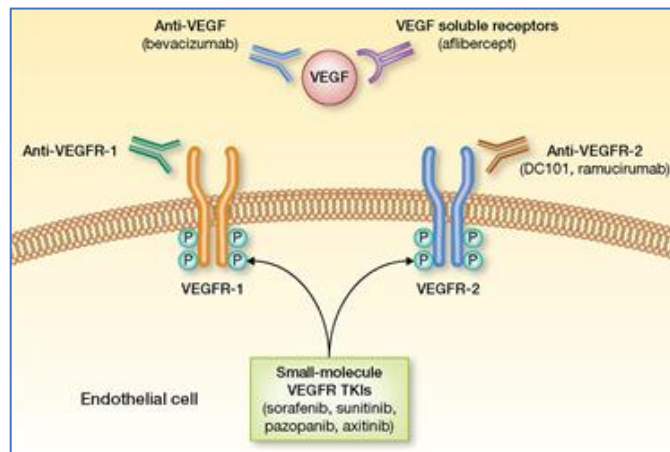


Figure 8. Inhibition de VEGFR2 TK par diverses voies.

2.2. Inhibiteurs du VEGF

Le **bevacizumab** (nom commercial : Avastin®) est devenu le premier inhibiteur de l'angiogenèse en tant qu'anticorps monoclonal recombinant humanisé en se liant au VEGF-A. Le bevacizumab a été approuvé pour la première fois par la FDA USA en 2004 pour un traitement du cancer colorectal et plus tard pour d'autres types graves de cancers tels que les tumeurs du poumon, du sein ou encore du cerveau. Les principaux effets indésirables du bevacizumab sont l'hypertension, les saignements de nez, les maux de tête et les éruptions cutanées. L'**aflibercept** (noms commerciaux : Eylea® et Zaltrap®) est un médicament principalement utilisé pour traiter le cancer colorectal métastatique et la dégénérescence maculaire humide (un trouble oculaire chronique). C'est une protéine recombinante qui agit comme un récepteur leurre avec une forte affinité caractéristique envers le VEGF et le facteur de croissance placentaire (PIGF). En 2014, l'Aflibercept était indiqué pour le traitement des patients atteints de maladies visuelles et en 2019 il a été approuvé par la FDA pour le traitement de la rétinopathie diabétique. Le **ramucirumab** (nom commercial : Cyramza®) est un anticorps monoclonal humain, qui se lie au domaine extracellulaire du VEGFR2 et bloque la liaison des facteurs de croissance naturels (VEGF-A, VEGF-C et VEGF-D). Il a été approuvé par la FDA pour le traitement du cancer gastrique avancé, du carcinome pulmonaire non à petites cellules (CPNPC), du cancer colorectal et récemment pour le carcinome hépatocellulaire (CHC). L'**imatinib** (nom commercial Gleevec®) est un inhibiteur compétitif des TK utilisé pour le traitement de la leucémie lymphoblastique aiguë (FDA en 2013), du cancer gastro-intestinal rare (FDA en 2012) et des tumeurs stromales gastro-intestinales (GIST) (FDA en 2002). L'imatinib occupe un site actif TK des protéines fusionnées bcr et abl (appelé bcr-abl), conduisant au verrouillage du site de liaison à l'ATP et donc à l'inhibition de l'activité enzymatique de la bcr-abl kinase. (Figure 9) Le **sunitinib** (commercialisé sous le nom de Sutent® par Pfizer) est un inhibiteur de la tyrosine kinase (RTK) à récepteurs multiples qui a été approuvé par la FDA en 2006 pour le traitement du carcinome rénal (RCC) et de la tumeur stromale gastro-intestinale (GIST). Il inhibe également les récepteurs des facteurs de croissance dérivés des plaquettes (PDGF-R), les CLK et les récepteurs VEGFR qui jouent à la fois un rôle d'angiogenèse tumorale et de prolifération cellulaire. Ainsi, le sunitinib a été le premier médicament anticancéreux approuvé simultanément pour deux indications différentes. Les principaux effets indésirables sont le syndrome main-pied (rougeur et douleur aux mains et/ou aux pieds) ainsi que la stomatite (inflammation de la bouche et des lèvres). Le **sorafenib** (commercialisé sous le nom de Nexavar® par Bayer) est un inhibiteur de plusieurs tyrosines

kinases telles que le PDGFR, le VEGFR et les kinases de la famille Raf (C-Raf, B-Raf). En 2005, il a été approuvé par la FDA USA pour le traitement du cancer des reins (carcinome rénal avancé) en 2007 pour les carcinomes hépatocellulaires (CHC) et en 2013 pour le traitement du carcinome thyroïdien. Un inhibiteur très efficace et sélectif du VEGFR2 TK commercialisé sous le nom d'**apatinib** a été approuvé en 2014 pour les patients atteints d'un carcinome gastrique de stade avancé en Chine. Il existe aussi d'autres inhibiteurs actifs du VEGFR2 TK tel que le **lenvatinib**, le **vandetanib** et le **cediranib**. (Figure 9)

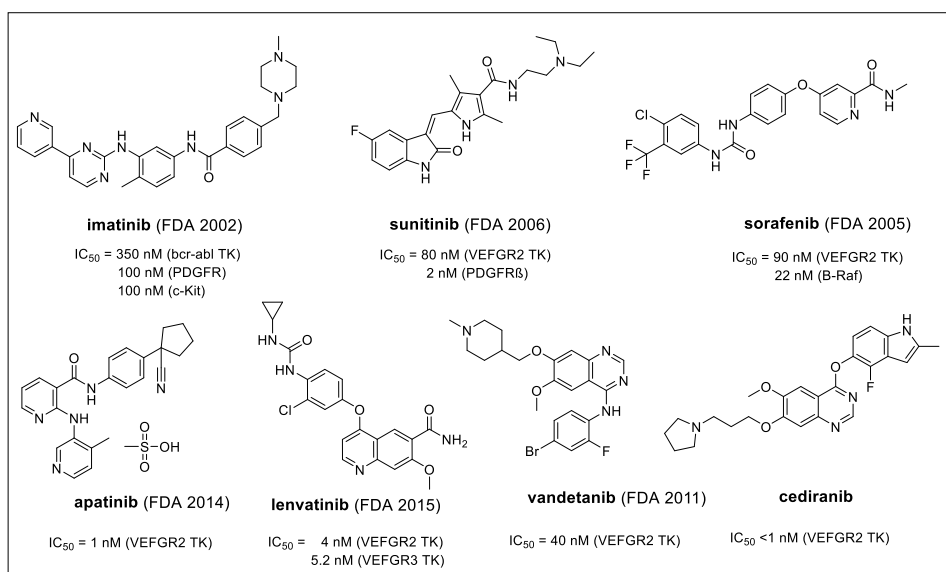


Figure 9. Structures et activités des inhibiteurs de tyrosine kinases VEGFR2.

2.3. Résultats et discussions

En 2005, GlaxoSmithKline a développé l'inhibiteur de VEGFR2 TK **AAZ** comportant une *N*,5-diaryloxazole-2-amine et présentant une forte activité inhibitrice ($IC_{50} = 22$ nM) et de bonnes propriétés pharmacocinétiques. Après docking, nous avons proposé et développé des dérivés plus actifs **BM(1-5,7)** contenant le noyau aminooxazole, et divers substituants hétérocycliques sur le phényle en position *mé*ta en place du groupe pyrid-2-yle présent dans **AAZ**. (Figure 10)

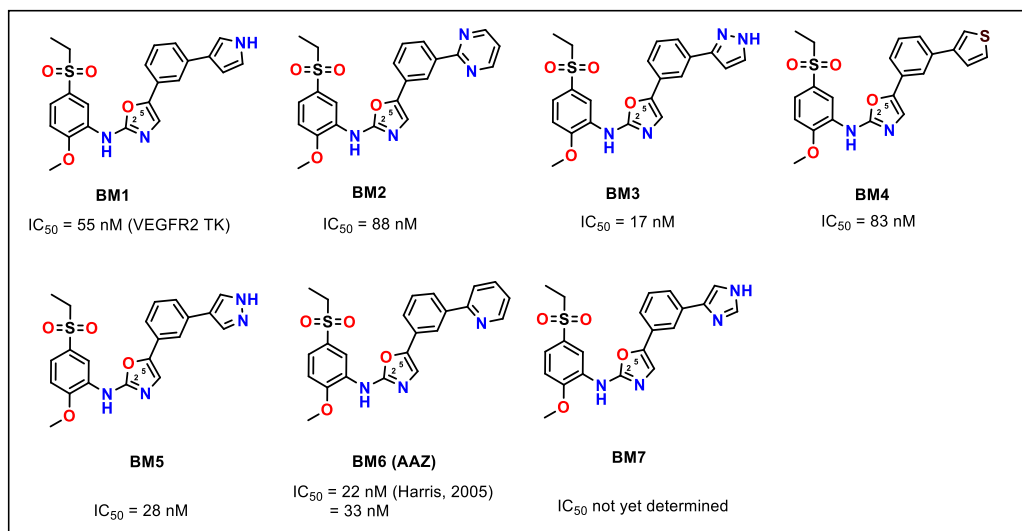


Figure 10. Structures des inhibiteurs les plus actifs de VEGFR2 TK **BM(1-7)** s'appuyant sur le motif oxazole-2-amine *N,5*-disubstituée.

Tous les inhibiteurs **BM(1-7)** représentent une classe d'oxazole-2-amines *N,5*-disubstituées que nous appelons *O*-régioisomères. Dans ce projet, nous avons développé une série d'analogues *N*-régioisomères (*N,4*-oxazole-2-amines **NBM(1-7)**) dans lesquels le substituant est placé en α de l'atome d'azote. (Figure 11) Un oxygène dans le cycle 1,3-oxazolique est un isostère d'un azote oxazolique. Par conséquent, des interactions de liaison similaires dans le site de liaison à l'ATP sont attendues pour les deux régioisomères avec la Cys917.

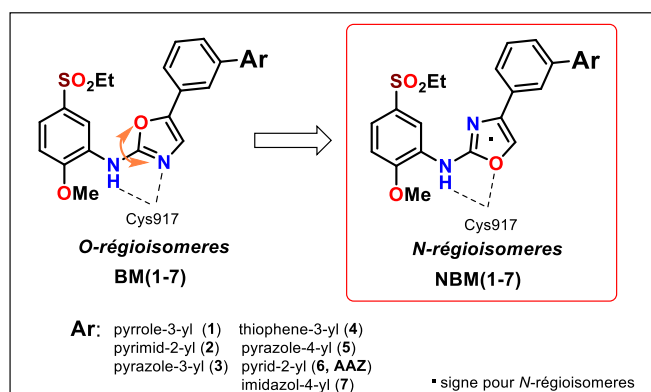


Figure 11. Une structure générale d'oxazole-2-amines *N,4*-disubstituées **NBM(1-7)** proposée basée sur des oxazole-2-amines *N,5*-disubstituées **BM(1-7)** possédant divers substituants hétérocycliques (Ar) dans une position *mé*ta.

La mise au point de cette stratégie nous permettrait de préparer de nouveaux inhibiteurs non encore brevetés.

Notre synthèse débute avec l'acétophénone **7**, qui subit une α -oxydation avec $\text{PhI}(\text{OAc})_2$ et une hydrolyse pour donner **8** avec un rendement de 69 %. La réaction de l'hydroxycétone **8** avec de l'anhydride triflique en présence de 2,6-lutidine fournit le triflate **9**. En raison de la stabilité généralement faible des triflates, le composé **9** a été utilisé dans l'étape suivante sans autre purification. De plus, le triflate **9**, instable, et présentant une faible vitesse de réaction vis-à-vis de l'urée **8**, a dû être ajouté par portions au mélange réactionnel à 45 °C toutes les 12 h en 2 jours. Le précurseur **10** de *N*,4-diaryloxazole-2-amine résultant a été obtenu avec un rendement de 67 %. (Schéma 1)

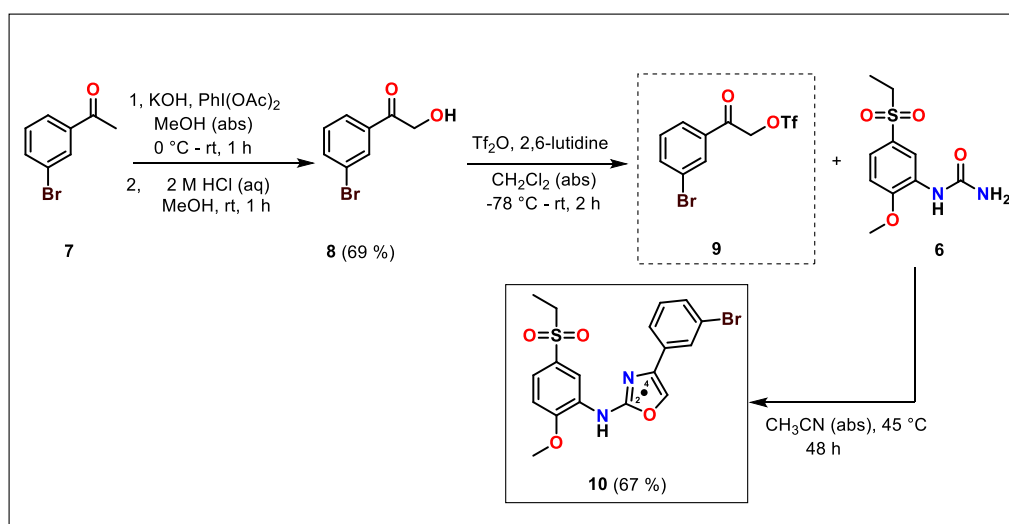


Schéma 1. Synthèse du précurseur *N*,4-diaryloxazole-2-amine **10** à l'aide du triflate **9** et d'arylurée **6**.

La préparation des composés **NMB(1-7)** a été réalisée avec succès grâce à des réactions de couplage catalysées au palladium (réactions de couplage des Suzuki et de Stille). (Schéma 2)

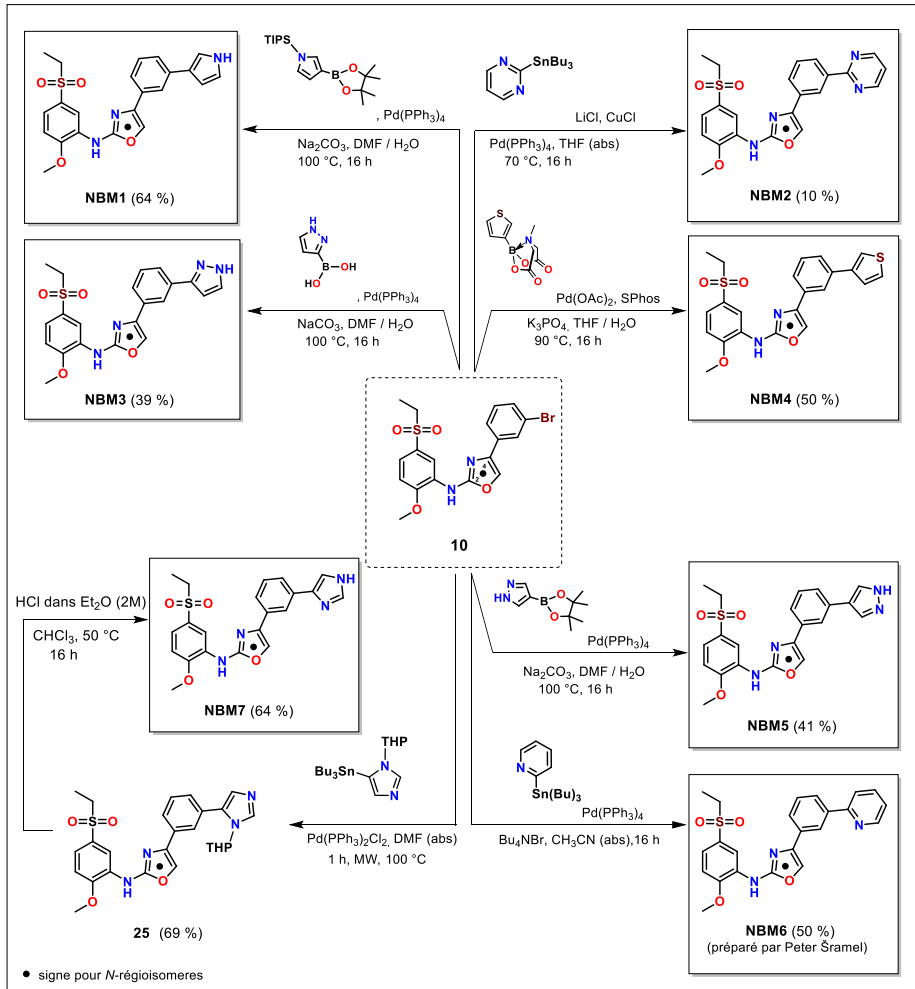


Schéma 2. Étape finale (réaction de couplage) de préparation des inhibiteurs NBM(1-7).

Comparés aux *O*-régioisomères **BM(1-7)**, dont les IC₅₀ sur VEGFR2 TK sont nanomolaires, les *N*-régioisomères **NBM(1-7)** présentent pour leur part une activité micromolaire, validant ainsi notre hypothèse. (Figure 12)

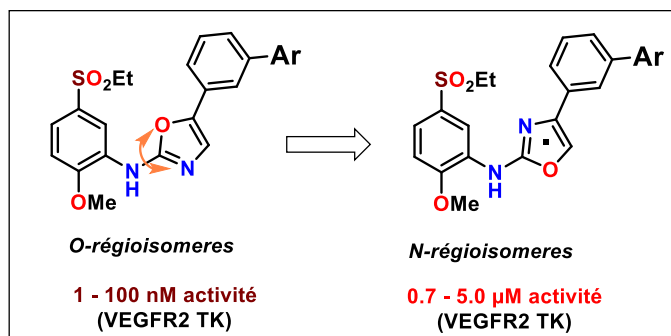


Figure 12. Comparaison de l'inhibition VEGFR2 TK des régioisomères *O* et *N*.

Récemment, nous avons mis en évidence à partir d'une structure cristallographique par diffraction des rayons X (PDB: 1Y6A) une poche interactive inutilisée, appelée Salt Bridge Containing Pocket (SBCP), composée de Lys866-Glu883-Phe1045. Elle se trouve au-dessus du phényle terminal des inhibiteurs précédemment développés **BM(1-7)** et **NBM(1-7)**. Ainsi, nous avons développé et synthétisé des inhibiteurs d'aminooxazole disubstitués **BM8** et **BM(11-15)** visant à avoir des interactions supplémentaires au sein du SBCP pour conduire à une amélioration de leur activité inhibitrice. Leurs valeurs IC_{50} sont en cours d'évaluation. (Figure 13)

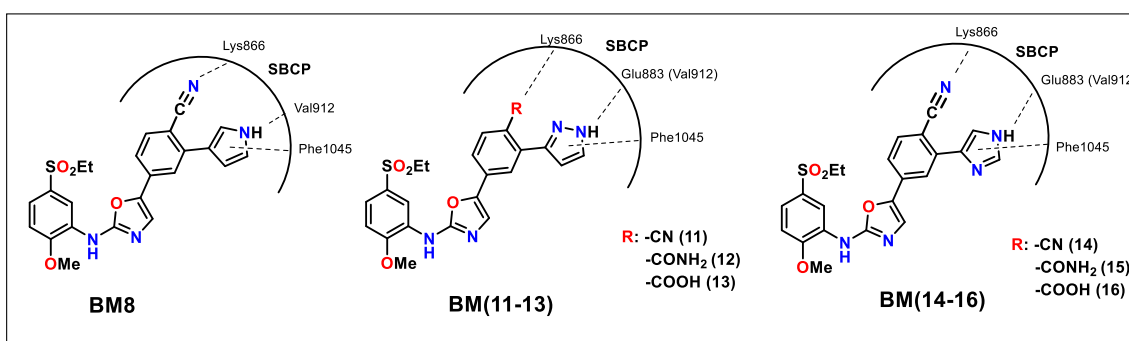


Figure 13. Structures des inhibiteurs de 2^e génération conçus **BM8** et **BM(11-15)** possédant la capacité d'effectuer des interactions en trois points avec le SBCP.

Chapitre 2. L'aldose réductase (ALR2) dans le diabète sucré

3. L'aldose réductase (ALR2) dans le diabète sucré

La deuxième partie de cette thèse est consacrée à une autre maladie grave et bien connue du diabète sucré (DM). Le facteur le plus important impliqué dans le DM et ses maladies connexes est la glycémie. Le glucose est un sucre hexose, qui circule dans le sang humain et qui représente une source d'énergie importante pour les cellules, il est aussi également stocké sous forme de polymère appelé glycogène dans le foie. Dans les conditions aérobies normales (conditions non diabétiques), le *D*-glucose est phosphorylé par l'hexokinase et est ensuite métabolisé en plusieurs étapes métaboliques en dioxyde de carbone et en eau. Cette cascade produit de l'énergie principalement sous forme de molécules riches en énergie comme le NADH et l'ATP (adénosine triphosphate).

La glycolyse est une voie métabolique qui convertit le glucose en pyruvate et l'énergie libre est libérée sous forme d'ATP et de NADH. Les molécules de pyruvate produites sont ensuite transportées dans la matrice mitochondriale, où elles sont oxydées par la Coenzyme A (CoA) pour former du CO₂, de l'acétyl-CoA et du NADH. Les molécules d'acétyl-CoA résultantes entrent dans le cycle de l'acide citrique (ou cycle de Krebs) et par la série de réactions sont oxydées en CO₂ et produisent de l'ATP riche en énergie. Le cycle réduit également le NAD⁺ en NADH, qui est utilisé dans la voie de phosphorylation oxydative (transport d'électrons) pour générer de l'ATP riche en énergie. Le rendement théorique d'ATP par oxydation d'une molécule du *D*-glucose en glycolyse en passant par le cycle de Krebs et la phosphorylation oxydative est de 36 molécules d'ATP. (Schéma 3)

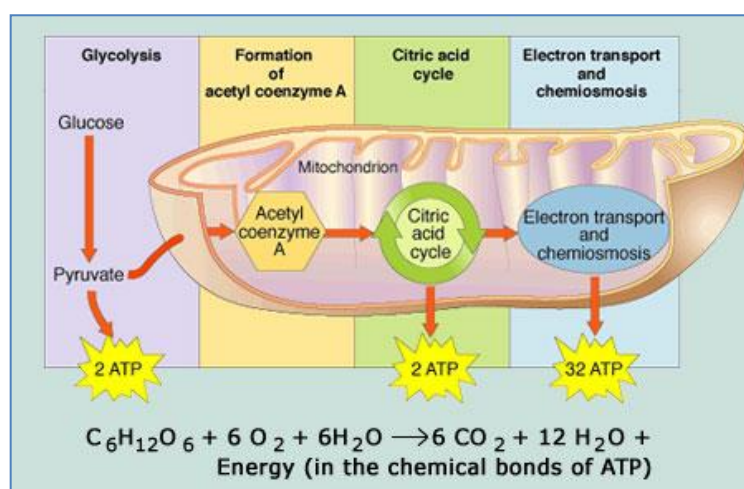


Schéma 3. Un aperçu du métabolisme du D-glucose.

Cependant, si de grandes quantités de glucose sont présentes dans des conditions d'hyperglycémie, l'hexokinase est saturée et environ 33% du glucose global est métabolisé par une voie polyol. Alors que la plupart des cellules nécessitent l'action de l'insuline pour que le glucose pénètre dans la cellule, les cellules de la rétine, des reins et des tissus nerveux sont indépendantes de l'insuline, de sorte que le glucose se déplace à travers la membrane cellulaire, quelle que soit l'action de l'insuline. Les cellules utiliseront le glucose comme énergie comme d'habitude, et l'excès de glucose entrera dans la **voie des polyols**.

3.1. La voie des polyols

La voie des polyols est un processus en deux étapes qui convertit le glucose en fructose. Il utilise une aldose réductase (ALR2) et une sorbitol déshydrogénase comme catalyseurs. (Figure 14) La voie polyol réduit le *D*-glucose et oxyde le NADPH en NADP⁺. Par la suite, la sorbitol déshydrogénase oxyde le sorbitol en fructose, qui produit du NADH à partir de NAD⁺. Le NADPH favorise la production de glutathion *via* la voie des polyols et conduit à une carence en NADPH provoquant un stress oxydatif et une hémolyse. Le NADPH est important pour empêcher l'accumulation d'espèces réactives de l'oxygène (ROS) et l'endommagement des cellules. En outre, le fructose produit provoque la glycation des protéines et des graisses et améliore la formation de produits finaux de glycation avancée (AGE), dont la production provoque un stress oxydatif ainsi qu'une inflammation. De plus, le sorbitol est un composé hautement polaire et pénètre à peine à travers les membranes cellulaires. Son accumulation provoque un gonflement des cellules conduisant à des déséquilibres osmotiques et entraîne diverses complications diabétiques telles que la cataracte, la rétinopathie, la neuropathie et la néphropathie.

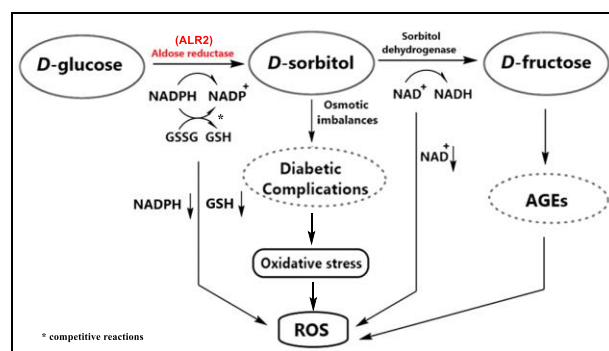


Figure 14. Une illustration de la voie des polyols et de son implication dans les complications diabétiques.

3.2. Diabète sucré (DM) et complications du diabète

Le diabète sucré de type I est un trouble métabolique du pancréas, un organe qui produit l'hormone insuline. Cette dernière est une hormone peptidique, qui joue un rôle clé dans la régulation de diverses bio-macromolécules, en particulier la régulation de la glycémie. Normalement, lorsque le taux de glucose est élevé, les cellules bêta du pancréas sécrètent l'insuline et la libèrent dans la circulation sanguine. Ensuite, le glucose est absorbé dans la cellule grâce à un transporteur de glucose activé par un complexe d'insuline avec son récepteur et le glucose peut être converti directement en énergie ou en stockage d'énergie : soit du glycogène via la glycogénèse, soit des graisses *via* la lipogénèse. (Figure 15)

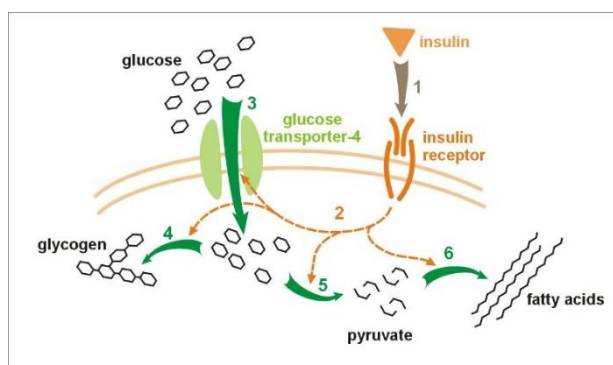


Figure 15. Transport du glucose à travers la membrane cellulaire, médié par l'insuline.

Les personnes atteintes de diabète sucré (DM) ont soit un manque de sécrétion d'insuline (DM type I), soit l'insuline ne peut pas être utilisée correctement (DM type II), ce qui entraîne un taux élevé de sucre dans le sang qui conduit à diverses pathologies telles que la cataracte diabétique, la neuropathie et la néphropathie. Il peut aussi endommager les minuscules vaisseaux des reins, du foie, des yeux ou du système nerveux. Toutes ces complications pathologiques diabétiques sont associées à une voie polyol qui, dans un premier temps, transforme le glucose en sorbitol par une enzyme, l'aldose réductase. Par conséquent, l'inhibition de l'activité d'ALR2, qui peut empêcher l'accumulation anormale de sorbitol et supprimer indirectement le stress oxydatif de la cellule, est devenue un moyen prometteur pour éviter ou ralentir les complications diabétiques tardives.

3.3. Propriétés et fonction d'ALR2

L'aldose réductase (ALR2) est l'une des premières enzymes d'une voie polyol et appartient à la superfamille des enzymes aldo-céto réductases. Elle catalyse la réduction dépendante du NADPH d'une grande variété de composés carbonylés, par ex. le glucose. L'enzyme est un domaine polypeptidique unique composé de 315 résidus d'acides aminés repliés en un motif structurel en tonneau β / α contenant huit brins β parallèles. Le site actif est situé dans une grande cavité à l'extrémité C-terminale du tonneau β et le cofacteur NADPH est situé au sommet du tonneau β / α avec l'anneau nicotinamide se détachant au centre du canon.

3.4. Un site actif d'ALR2

D'après l'analyse des structures cristallines d'ALR2, une structure de son site actif a été proposée. La première poche de liaison du site actif d'ALR2 est constituée d'une poche de liaison anionique rigide, composée de chaînes latérales d'acides aminés Trp20, Trp111, Tyr48, His110 et d'un groupe amide de NADP⁺. La seconde, est une poche de spécificité et est constituée de Leu 300, Cys298, Cys303, Trp111 et Phe122. Cette poche est caractéristique par son degré élevé de flexibilité et les résidus d'acides aminés tapissant cette poche ne sont pas présents dans d'autres aldo-céto réductases telles que l'aldéhyde réductase, par ex. ALR1. La troisième est une poche hydrophobe formée de résidus Phe122, Trp219, Trp20 et Trp111. (Figure 16)

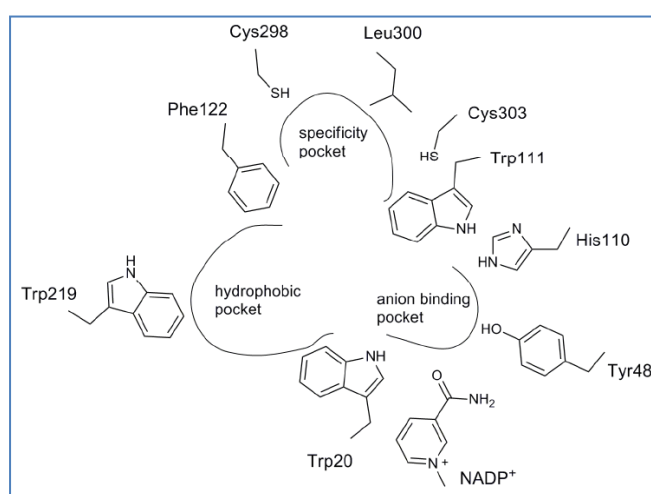


Figure 16. La structure du site actif de l'enzyme ALR2.

3.5. Aldéhyde réductase

L'aldéhyde réductase (ALR1) est une autre oxydoréductase étroitement liée à l'aldose réductase (ALR2). Les deux enzymes partagent 65% de l'homologie structurale et ces similitudes jouent un rôle important dans la non-sélectivité des inhibiteurs. La co-inhibition des oxydoréductases apparentées peut créer des effets secondaires indésirables. Le rôle principal de l'ALR1 est la détoxification, car elle métabolise spécifiquement les aldéhydes toxiques tels que la 3-désoxyglucosone (3DG) ou l'hydroxynonéal (HNE), qui peuvent résulter du stress oxydatif dans le cadre d'une hyperglycémie. De plus, il est également responsable de la synthèse de l'acide ascorbique chez les animaux par réduction du *D*-glucuronate en *D*-gulonate. Par conséquent, ALR1 est un "antitarget" comparé à la cible antidiabétique importante ALR2.

3.6. Inhibiteurs d'ALR2

Au cours des 40 dernières années, de nombreux inhibiteurs d'ALR2 ont été développés, mais seulement un candidat (epalrestat) a été approuvé comme médicament au Japon, en Chine et en Inde. La plupart des autres inhibiteurs mis au point n'ont pas été approuvés pour les essais cliniques, principalement à cause de leurs faibles efficacités *in vivo*, leurs inconvénients pharmacocinétiques et leurs effets secondaires liés à l'inhibition non sélective de l'aldéhyde réductase (ALR1).

3.6.1. Dérivés d'acide carboxylique

Les acides carboxyliques représentent la classe la plus importante et la plus grande des ARI, car le groupe carboxylate de l'inhibiteur occupe une poche de liaison anionique du site actif d'ALR2. Par contre, de faibles valeurs de pK_a entravent la perméabilité de la membrane dans des conditions de pH physiologiques et conduisent à un mauvais profil pharmacocinétique de ces ARI. À l'instar de ces inhibiteurs, l'epalrestat, un inhibiteur non compétitif et réversible de l'ALR2 (contenant un anneau de rhodanine) utilisé pour le traitement de la neuropathie diabétique, a été développé en 1983 et approuvé au Japon, en Chine et en Inde pour l'amélioration des symptômes de neuropathie subjective et des modifications anormales du rythme cardiaque associées à une neuropathie diabétique périphérique. (Figure 17)

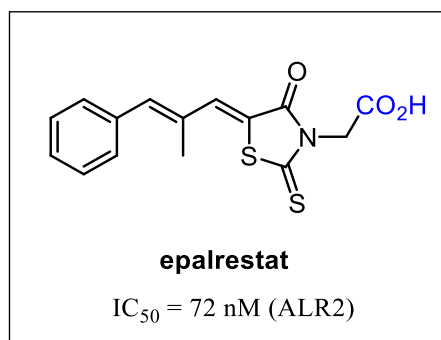


Figure 17. Structure et activité de l'epalrestat.

Le deuxième inhibiteur très important de l'ALR2 est le tolrestat, un médicament candidat pour le traitement des complications diabétiques, qui a été approuvé sur plusieurs marchés, mais retiré en 1997 en raison de sa toxicité hépatique en 3^{ème} phase d'un essai clinique et n'a finalement jamais reçu l'approbation de la FDA. (Figure 18) Le zenarestat a été pressenti comme candidat pour le traitement de la cataracte, de la rétinopathie diabétique et de la neuropathie. Le zenarestat et le zopolrestat ont été soumis à des essais cliniques. Dans la 2^{ème} phase de l'étude clinique, ils ont montré un effet bénéfique sur la vitesse de conduction nerveuse, mais la 3^{ème} phase des essais a montré que le zenarestat était associé à une toxicité rénale chez un petit nombre de patients. Un inhibiteur structurellement similaire nommé ponalrestat a également échoué dans les essais cliniques en raison du manque d'efficacité. (Figure 18)

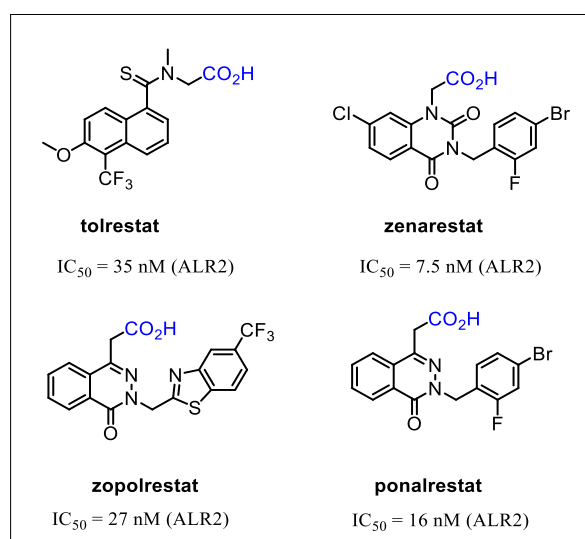


Figure 18. Structures des ARI les plus développées possédant une fonctionnalité carboxylique.

3.6.2. Spirohydantoïne et dérivés du spirosuccinimide

La deuxième classe importante d'inhibiteurs d'ALR2 comprend les dérivés de la spirohydantoïne, où le groupe hydantoïne occupe la poche de liaison anionique de la même manière que le groupe anionique des dérivés carboxyliques. Le sorbinil, un puissant inhibiteur de l'ALR2 avec une sous-structure chromane, s'est avéré un excellent inhibiteur de l'ALR2 pour les tests *in vivo* et *in vitro*. Malheureusement, les essais cliniques ont montré que le sorbinil augmente le risque de développer une hypersensibilité telle que des éruptions cutanées, de la fièvre et des myalgies (douleurs musculaires). Ces effets indésirables peuvent être attribués à la faible sélectivité du sorbinil envers l'aldéhyde réductase (ALR1). Sur la base de la structure du sorbinil, plusieurs analogues de la spirohydantoïne ont été développés. L'addition d'un groupe carbamoyle ou méthyle au niveau du squelette du sorbinil a donné le fidarestat et le M79175, respectivement. Le remplacement de l'anneau chromane par l'isoquinoline-1,3 (2*H*, 4*H*)-dione et l'introduction de l'anneau spirosuccinimide conduisent à la synthèse du minalrestat. Un autre inhibiteur similaire nommé ranirestat, a été développé pour le traitement de la neuropathie diabétique et est maintenant en phase 3 des essais cliniques au Japon. L'imirestat, contenant un anneau fluorène planaire, a également atteint la phase 3 mais a été retiré par la suite en raison de sa toxicité. (Figure 19)

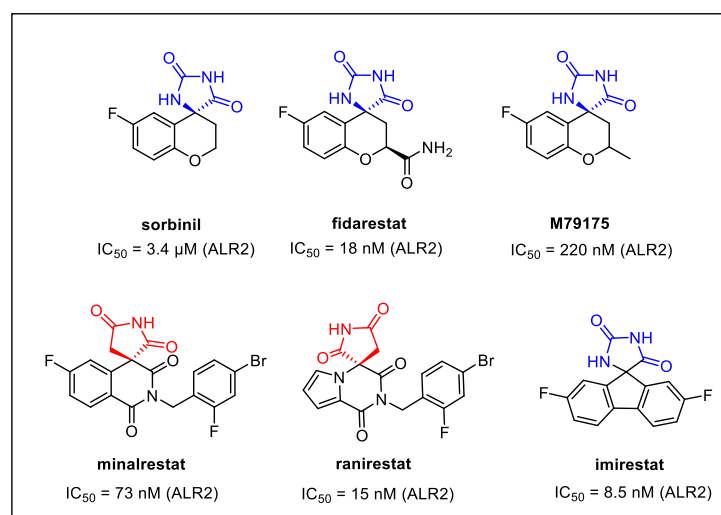


Figure 19. Structures et activités des plus importants inhibiteurs de la spirohydantoïne ALR2.

En conclusion, ces acides carboxyliques ainsi que les dérivés de spirohydantoïne n'ont pas été approuvés par la FDA en tant qu'inhibiteurs d'ALR2. Par conséquent, dans la recherche récente d'inhibiteurs ARI efficaces, il est nécessaire de trouver de nouveaux squelettes actifs.

3.7. Résultats et discussions

Le point de départ du deuxième projet est l'acide 2-(3-thioxo-2H-[1,2,4]triazino[5,6-b]indol-5(3H)-yl) acétique (**CMTI** ou Cemtirestat) qui a été identifié comme un puissant inhibiteur de l'ALR2 possédant une bonne sélectivité ALR2 / ALR1 et des propriétés thérapeutiques. Sur la base de calculs *in silico*, nous avons proposé et synthétisé plusieurs analogues potentiels du **CMTI**. Parmi eux, le composé **OTI** ($IC_{50} = 42$ nM) a montré une activité inhibitrice presque 3 fois plus élevée dans un essai enzymatique ALR2 *in vitro* et une sélectivité 8 fois plus élevée par rapport à ALR1 ($IC_{50} > 100$ μ M) que **CMTI** ($IC_{50} = 116$ nM ALR2 et 35,10 μ M ALR1). Sur la base de ces résultats, nous pouvons conclure que le remplacement isostérique du soufre par de l'oxygène joue un rôle important à la fois pour l'inhibition de l'ALR2 et sa sélectivité.

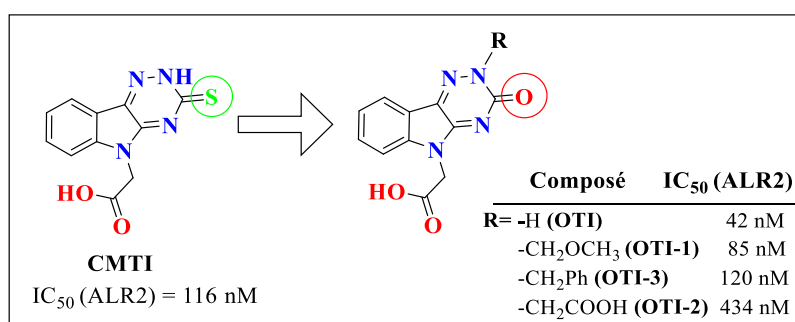


Figure 20. Les structures du **CMTI**, ses dérivés analogues de l'oxygène **OTI** et **OTI-(1-3)** avec des activités IC_{50} .

L'inhibiteur de **CMTI** a été préparé en 3 étapes à partir d'isatine disponible dans le commerce. (Schéma 4) Son oxo-analogue **OTI** a été préparé à partir de **CMTI** avec du $KMnO_4$ en solution aqueuse de NaOH. (Schéma 4)

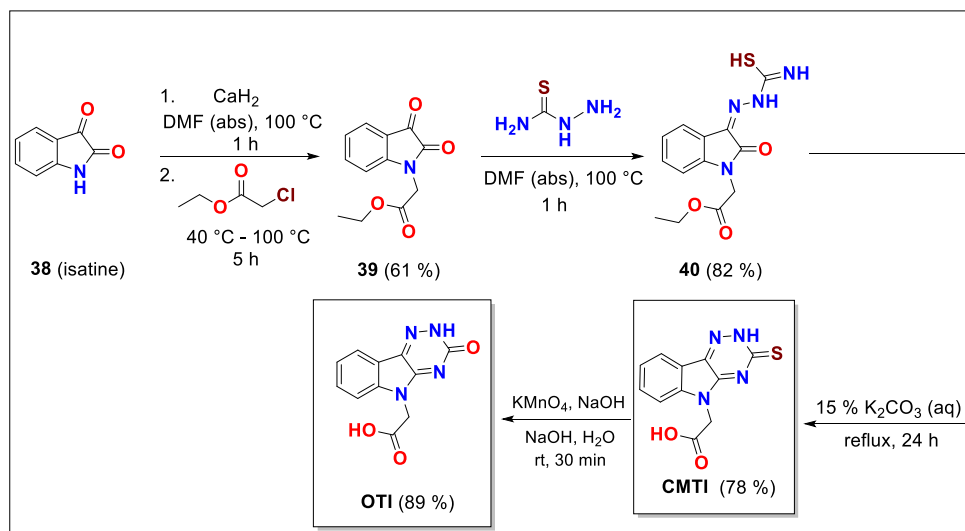


Schéma 4. Synthèse du CMTI et de son oxo-analogue OTI.

Nous avons ensuite étudié une poche interactive dans le site actif d'ALR2. Après docking, nous avons proposé et synthétisé de nouveaux dérivés benzylques de l'inhibiteur OTI-3. (Figure 21) Les évaluations biologiques ont montré une activité inhibitrice plus élevée pour tous les inhibiteurs substitués OTI-(6-9) par rapport à l'analogue OTI-3 non substitué qui possède une IC_{50} inférieure. (Figure 21)

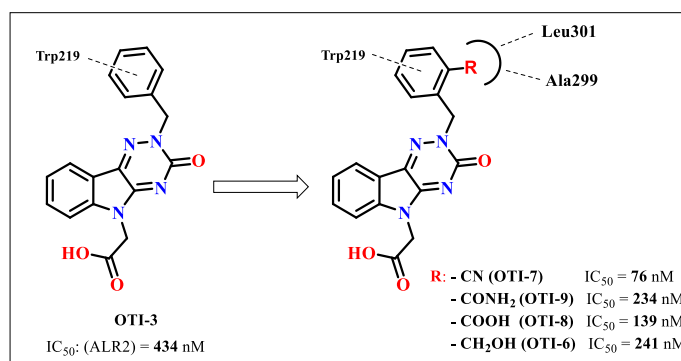


Figure 21. Proposition de nouveaux N-benzyl(oxotriazinoindole) inhibiteurs de l'aldose réductase (ALR2).

Conclusion générale

4. Conclusion générale

La thèse a été divisée en deux parties : 1) Développement d'inhibiteurs de VEGFR2 et 2) Développement d'inhibiteurs d'ALR2. Nous avons mis au point avec succès une nouvelle synthèse des régioisomères *N*,4-oxazole-2-amines **NBM(1-7)** de **AAZ** et évalué leur activité inhibitrice. Comparés à leurs analogues *O*-régioisomères (*N*,5-oxazole-2-amines **BM(1-7)**), ils présentent une activité inhibitrice plus faible (IC_{50} micromolaire). La découverte d'une poche **SBCP**, située dans le site actif de VEGFR2 nous a permis de développer de nouveaux inhibiteurs de structure aminooxazole disubstitué **BM8** et **BM(11-15)**. Leur activité inhibitrice n'a pas encore été déterminée. Dans la deuxième partie de la thèse, nous avons développé plusieurs inhibiteurs d'ALR2. Parmi eux, le dérivé **OTI** présente une excellente activité inhibitrice et une excellente sélectivité. Là aussi, la découverte d'une poche interactive dans le site actif d'ALR2 a été l'occasion de développer de nouveaux inhibiteurs **OTI** substitués **OTI-(6-9)**. Les résultats montrent sans ambiguïté la présence d'une interaction supplémentaire dans la poche du récepteur. Les inhibiteurs ALR2 substitués **OTI-(6-9)** ont montré une activité inhibitrice plus élevée que l'inhibiteur non substitué de référence **OTI-3**.

Manuscript en Anglais

Resume of the thesis

Matúš Hlaváč: Rational development of kinase inhibitors dedicated to treatment of neoplastic diseases and diabetic complications

Université de Strasbourg, Ecole européenne de Chimie, Polymères et Matériaux (ECPM), UMR CNRS 7042 LIMA, Strasbourg, France. Comenius University in Bratislava, Faculty of Natural Sciences, Bratislava, Slovakia.

VEGFR2 tyrosine kinase receptors are transmembrane proteins that are crucial for tissue regeneration, regulation of important cell cycles and vascular endothelial cell function. On the other hand, enhanced activity of VEGFR2 TK causes uncontrolled division of cancer cells and formation of tumor. Accordingly, a development of small molecule VEGFR2 TK inhibitors has become a promising and effective way for cancer treatment. Another equally serious disease is diabetes mellitus, characterized by absence of insulin or its resistance. Aldose reductase (ALR2) plays an important role in a formation of various heart and diabetic complications and has become an important therapeutic target in treatment of illnesses related to diabetes mellitus.

Within the first part of this dissertation thesis we described a development of 14 predicted aminooxazole VEGFR2 TK inhibitors. We successfully synthesized novel *N*,4-disubstituted aminooxazole inhibitors **NBM(1-7)**, which are regioisomeric pairs to the previously developed *N*,5-disubstituted inhibitors **BM(1-7)**. Afterwards, we proposed more effective derivatives **BM(8-16)** and six from them prepared. Evaluation of their activity is currently in progress. Second part of the thesis was dedicated to the development of ALR2 inhibitors. Based on the structure of the previously developed lead compound **CMTI** we developed more active and selective oxotriazinoindole inhibitor **OTI** and its 3 analogues **OTI(1-3)**. Subsequent investigation of an active site of ALR2 led to detection of an unoccupied pocket and novel *N*-benzyl derivatives **OTI(6-9)** were developed and other several derivatives proposed.

Key words: tyrosine kinase inhibitors, aldose reductase, VEGFR2 TK, ALR2, aminooxazoles, oxotriazinoindoles

Introduction

5. Introduction

Cancer is undoubtedly one of the most serious and potentially life-threatening illnesses in the World.¹ The development of a cancer is a multistep process involving an initiative and a progressive state. In the tumor initiation, a one single cell is mutated by changes in DNA, which results to abnormal proliferation. This proliferation giving rise to large number of daughter cells containing the mutation created by the initiator.² Tumor progression continues as additional mutations occur within cells of tumor population followed by selection for more rapidly growing cells. This selection continues to tumor development, so tumor become more rapid-growing and malignant.³

Angiogenesis is a complex process controlled by growth factors produced in the body. During the angiogenesis new blood vessels are formed from pre-existing ones and it's physiologically crucial during an embryonic development and healing of wounds.⁴ On the other hand, angiogenesis is also involved in growth of tumors. The understanding of cell signaling processes in the last decades led to the identification of VEGFR2 TK as an interesting target for an anticancer therapy. It has been demonstrated that small-molecule VEGFR2 TK inhibitors suppress cancer growth and metastasis leading to an effective cancer treatment mainly in combination with other agents.

Diabetes mellitus (DM) is also a well-know disease characterised by abnormal high level of blood sugar. People with diabetes mellitus (DM) have either a lack of secretion of insulin (DM type I) or insulin can't be used properly (DM type II), which lead to variety of pathology conditions. It can damage the tiny vessels in kidneys, hearth, eyes or nervous system leading to diabetic cataract, retinopathy, neuropathy and nephropathy.⁵ All these diabetic pathological complications are associated with a **polyol pathway**, which in the first step converts glucose to sorbitol by an enzyme **aldose reductase**. Beside of high concentration of sorbitol it results to an excessive accumulation of intracellular reactive oxygen species (ROS) in various tissues. Recent studies have shown that ALR2 inhibitors could prevent or delay the onset chronic diabetic complications, therefore inhibition of ALR2 activity has opened a promising way for a treatment of complications connected with DM.

¹ <http://www.who.int> (accessed April 14th, 2020)

² Yamagiwa, K.; Ichikawa, K. *CA Cancer J. Clin.* **1977**, *27*, 174 - 181.

³ Cooper, G.M. *The Cell: A Molecular Approach* (2nd ed.), Sinauer Associates, Boston University, 2000, ISBN 0-87893-106-6.

⁴ Birbrair, A.; Zhang, T.; Wang, Z.; Messi, M.L.; Olson, J.D.; Mintz, A.; Delbono, O. *Am. J. Physiol. - Cell Ph.*, **2014**, *307*, 25 - 38.

⁵ www.webmd.com (accessed April 8th, 2020)

The first part of the dissertation thesis is devoted to the development of *in silico* predicted aminooxazole VEGFR2 TK inhibitors. The second part of the thesis is focused on the development of novel oxotriazinoindole ALR2 inhibitors including design, synthesis, biological assay and evaluation of obtained results. These studies and achieved results may provide a great insight into a medicinal chemistry and could serve as a valuable tool for better understanding of drug design.

Within the first project we aimed to synthesize a series of predicted *N*,4-diaryloxazole-2-amine VEGFR2 TK inhibitors **NBM(1-5,7)** as a set of regioisomers to the previously prepared, highly active *N*,5-diaryloxazole-2-amine analogues **BM(1-6)**. Since an oxygen is an isostere to a nitrogen in an oxazole ring and vice versa, similar binding interactions with Cys917 from ATP-binding site is expected for both regioisomers. A missing compound for this study **BM7** was synthesized as well. After successful preparation we also determined biological activities for novel compounds in order to evaluate our hypothesis of Regioisomeric Bioisostery (*RegBio*). (Figure 22)

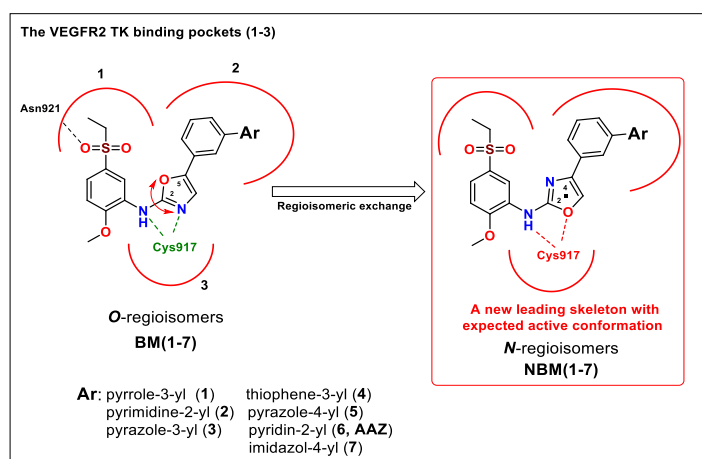


Figure 22. Regioisomeric bioisostery (*RegBio*) - series of the most active *N*,5-disubstituted aminooxazoles **BM(1-7)** and their regioisomeric pairs **NBM(1-7)** possessing *N*,4-disubstituted aminooxazole core.

Within the second project we were focus on a development of the second class of VEGFR2 TK inhibitors **BM(8-16)**, containing pyrrole, pyrazole and imidazole heterocycles in *meta* position and *para* cyano, amide and carboxylic acid functioning group on a terminal phenyl ring. They should possess three-point interactions with a recently discovered SBCP pocket and improve ligand binding affinities. (Figure 23)

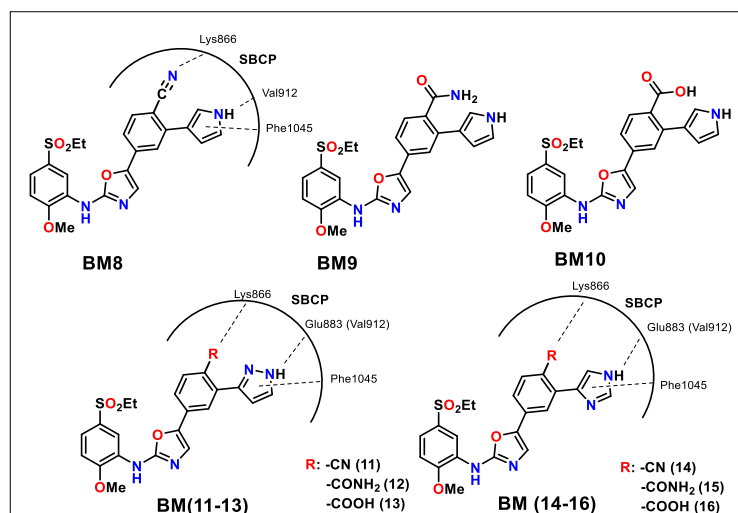


Figure 23. Structures of the 2nd generation inhibitors **BM(8-16)** with proposed three-point interaction with the SBCP.

In the third project we aimed to develop a synthetic methodology for recently discovered and highly active aldose reductase (ALR2) inhibitor **CMTI**. After that, we were focus on a development of **CMTI** sulfur/oxygen isosteric analogue **OTI** and its derivatives **OTI-(1-5)** possessing oxotriazinoindole scaffold. At the end activities and selectivities of all prepared compounds were determined. (Figure 24)

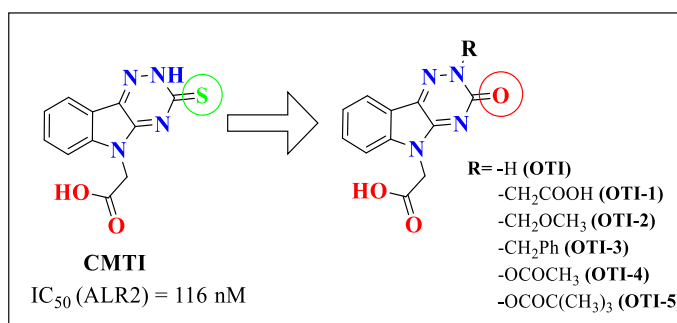


Figure 24. Bioisosteric replacement of sulphur with oxygen in **CMTI** and the structure of **OTI** and its proposed derivatives **OTI-(1-5)**.

Within the last project we were focus on a synthesis and a SAR study of novel *N*-benzyl **OTI-3** analogues **OTI-(6-9)** in order to improve ALR2 inhibitory activity by further exploitation of a benzyl interactive pocket.

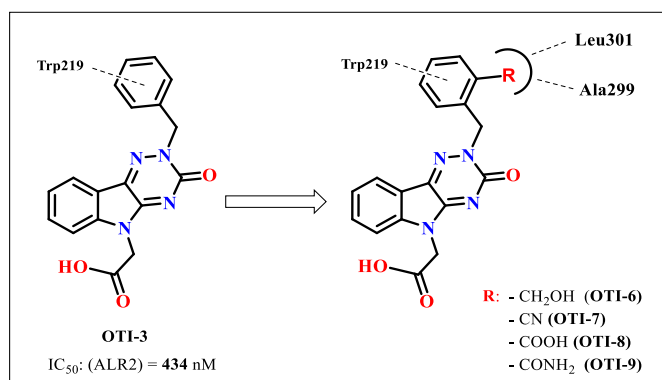


Figure 25. The structures of proposed *N*-benzyl(oxotriazinoindole) derivatives **OTI-(6-9)**.

Chapter 3. Vascular endothelial growth factor receptor (VEGFR)

6. Vascular endothelial growth factor receptor (VEGFR)

Very important signal proteins that stimulate the formation of new blood vessels are **vascular endothelial growth factors (VEGFs)**. This sub-family of growth factors are produced by cells and are involved in vasculogenesis (*de novo* production of endothelial cells) and angiogenesis (production of new vessels from pre-existing ones).⁶ The normal function of VEGFs is to create new blood vessels after injury and during an embryonic development. On the other hand, VEGFs are overexpressed in many tumor cells leading to tumor angiogenesis, proliferation and metastasis. Each from VEGF ligands binds in a specific manner to three **VEGF receptors of tyrosin kinase (VEGFR TKs)**.⁷ Tyrosin kinases are enzymes that specifically phosphorylate tyrosine amino acid residues of peptide targets by high-energy containing molecules ATP.

There are three main subtypes of VEGFR TKs, numbered 1, 2 and 3. VEGFR1 (Flt-1) is expressed on haematopoietic stem cells, monocytes and macrophages, VEGFR2 (Flk-1, KDR) mainly regulates vascular endothelial cell function and promotes their proliferation, migration, permeability and survival. Therefore, VEGFR2 is crucial for a tumor development. VEGFR3 (Flt-4) regulates lymphatic endothelial cell functions. (Figure 26)

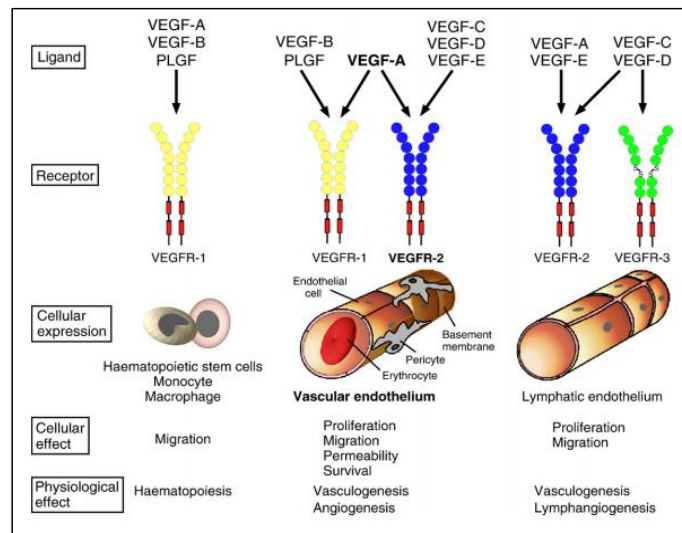


Figure 26. A schematic illustration of each vascular endothelial growth factor receptors (VEGFRs) with their growth factors (VEGF(A-E), PLGF) and their cellular and physiological effects.

⁶ Penn, J.S. *Retinal and Coroidal Angiogenesis* (1st ed.), Springer Netherlands, 2008, 119, ISBN 978-1-4020-6779-2.

⁷ Holmes, K.; Roberts, O.L.; Thomas, A.M.; Cross, M.J. *Cell Signal.*, **2007**, *19*, 2003 - 2012.

6.1. VEGFR2 tyrosin kinase

VEGFR2 TK (kinase insert domain receptor (KDR) or foetal liver kinase (Flk-1)) is a transmembrane tyrosine kinase receptor consisted of an extracellular region (composed of seven immunoglobuline (Ig)-like domains), a short transmembrane domain and an intracellular region (containing tyrosine kinase domain).⁸ (Figure 27)

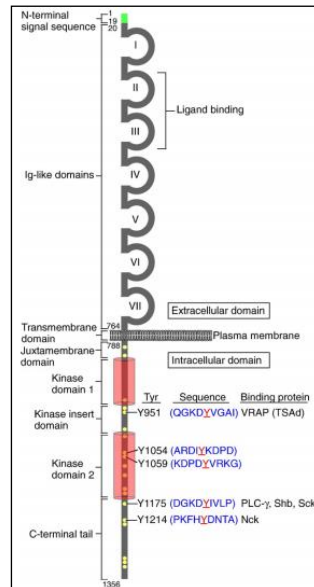


Figure 27. The structure of human VEGFR2 tyrosin kinase.

VEGFR2 TK is activated when a ligand (VEGF) binds to the extracellular domain of a receptor which leads to dimerization of a receptor with a neighboring receptor and stabilization of this complex. After that, multiple intracellular tyrosine residues of each receptor monomer are *trans* – phosphorylated by its partner receptor. Phosphorylation and activation of these two receptor proteins lead to an activation and initiation of various cellular responses and pathways.^{9,10} (Figure 28)

⁸ Sait, S.N.; Dougher-Vermazen, M.; Shows, T.B.; Terman, B.I.; *Cytogenet. Cell. Genet.*, **1995**, *70*, 145 - 146.

⁹ Lemmon, M.A.; Schlessinger, J. *Cell*, **2010**, *141*, 1117 - 1134.

¹⁰ www.tes.com (accessed May 23rd, 2020)

Vascular endothelial growth factor receptor (VEGFR)

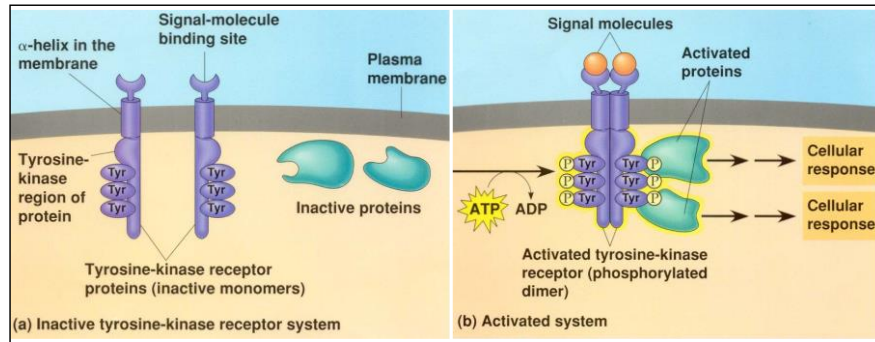


Figure 28. a) an inactive state of tyrosin kinase receptor b) an activated homodimeric tyrosin kinase receptor.

VEGFR2 expression in cancer cells is upregulated during tumor growth by environmental stimuli such as hypoxia or genetic mutations.¹¹ The hypoxia state promotes secretion of VEGF-A, which bind to VEGFR2 TK expressed on vascular endothelial cells. (Figure 29) Expression of VEGF-A is a prognostic marker in patients with variety of malignancies. Therefore, inhibition of angiogenesis with effective anti-angiogenic drugs may results in suppression of tumor growth.¹² These agents are divided into several classes according to mechanism of action.¹³ (Figure 29)

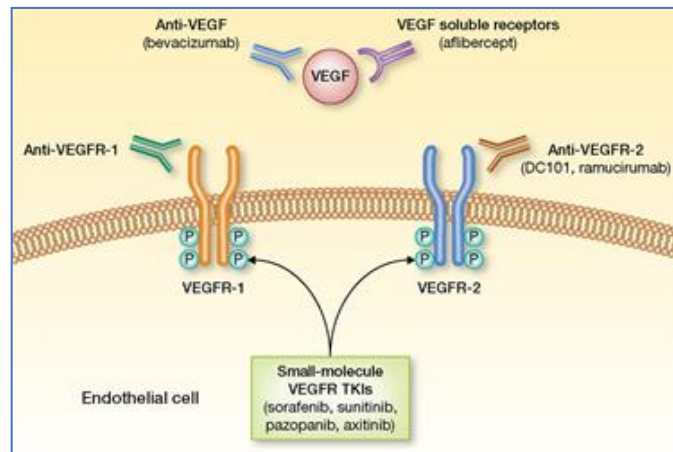


Figure 29. Inhibition of VEGFR2 TK by various pathways.

¹¹ Plate, K.H.; Breier, G.; Millauer, B.; Ullrich, A.; Risau, W. *Cancer Res.*, **1993**, *53*, 5822 - 5827.

¹² Folkman, J.; *N. Engl. J. Med.*, **1971**, *285*, 1182 - 1186.

¹³ Chau, C.H.; Figg, W.D. *Clin. Cancer Res.*, **2012**, *18*, 4868 - 4871.

6.2. Inhibitors of VEGF

Bevacizumab (trade name: Avastin) became the first angiogenesis inhibitor as a humanized recombinant monoclonal antibody. It binds to VEGF-A and blocks angiogenesis. Bevacizumab was first approved by FDA USA in 2004 for a treatment of colorectal cancer and later for other serious types of cancers such as lung, breast and brain tumor.¹⁴ The main side effects of bevacizumab are hypertension, nose bleeding, headache and rash. **Aflibercept** (trade names: Eylea and Zaltrap) is a medication primarily used to treat metastatic colorectal cancer and wet macular degeneration (a chronic eye disorder). It is a recombinant protein, that acts as a decoy receptor with characteristic high affinity toward VEGF and placental growth factor (PIGF).^{15,16} In 2014 aflibercept was indicated for the treatment of patient with visual diseases and in 2019 was approved by FDA for the treatment of diabetic retinopathy.¹⁷ **Ramucirumab** (trade name: Cyramza) is a human monoclonal antibody, that binds to the extracellular domain of VEGFR2 and blocks the binding of natural growth factors (VEGF-A, VEGF-C and VEGF-D).¹⁸ It was approved by FDA for treatment of advanced gastric cancer, non-small-cell lung carcinoma (NSCLC), colorectal cancer and in 2019 for hepatocellular carcinoma (HCC).¹⁹

6.3. Inhibitors of VEGFR2 TK

Imatinib (trade name Gleevec) is a competitive TK inhibitor used for treatment of acute lymphoblastic leukemia (FDA in 2013), rare gastrointestinal cancer (FDA in 2012) and gastrointestinal stromal tumor (GIST) (FDA in 2002). Imatinib occupies a TK active site of fused proteins *bcr* and *abl* (termed bcr-abl), which leads to locking of ATP-binding site and therefore inhibiting the enzyme activity of the bcr-abl kinase.²⁰ (Figure. 30) **Sunitinib** (marketed as Sutent by Pfizer) is a multiple receptor tyrosine kinase (RTK) inhibitor which was approved by FDA in 2006 for the treatment of renal cell carcinoma (RCC) and gastrointestinal stromal tumor (GIST). It inhibits also platelet-derived growth factor receptors

¹⁴ Ferrara, N.; Hillan, K.J.; Novotny, W.; *Biochem. Biophys. Res. Commun.*, **2005**, 333, 328 - 335.

¹⁵ Pandey, A.K.; Singhi, E.K.; Arroyo, J.P.; Ikizler, T.A.; Gould, E.R.; Brown, J.; Beckman, J.A.; Harrison, D.G.; Moslehi, J. *Hypertension*, **2018**, 71, e1 - e8.

¹⁶ <https://www.drugbank.ca/drugs/DB08885> (accessed April 15th, 2020).

¹⁷ <https://investor.regeneron.com/news-releases/news-release-details/fda-approves-eylear-aflibercept-injection-diabetic-retinopathy> (accessed April 15th, 2020).

¹⁸ Singh, A.D.; Parmar, S. *P. T.*, **2015**, 40, 430 - 434.

¹⁹ <https://www.fda.gov/drugs/resources-information-approved-drugs/fda-approves-ramucirumab-hepatocellular-carcinoma> (accessed April 15th, 2020).

²⁰ Pazdur, R.; Wagman, D.L.; Camphausen, K.A.; Hoskins, W.J. *Cancer Management: A Multidisciplinary Approach* (11th ed.), CMP United Business Media, USA, 2009, ISBN 9781891483622

(PDGF-Rs), CLKs and VEGFR receptors which play a role of both tumor angiogenesis and cell proliferation. Therefore, sunitinib was the first cancer drug simultaneously approved for two different indications.²¹ The main side effects are hand-foot syndrome (redness and pain on the hands and / or feet) and stomatitis (inflammation of the mouth and lips).²² **Sorafenib** (marketed as Nexavar by Bayer) is an inhibitor of several tyrosin kinases such as PDGFR, VEGFR and Raf family kinases (C-Raf, B-Raf).²³ In 2005 it was approved by FDA USA for the treatment of kidney cancer (advanced renal cell carcinoma), later in 2007 for hepatocellular carcinomas (HCC) and in 2013 for the treatment of thyroid carcinoma. Very effective and selective VEGFR2 TK inhibitor is **apatinib**, which was approved in 2014 for patient with late-stage gastric carcinoma in China.²⁴ Other active VEGFR2 TK inhibitors are **lenvatinib**, **vandetanib** and **cediranib**. (Figure. 30)

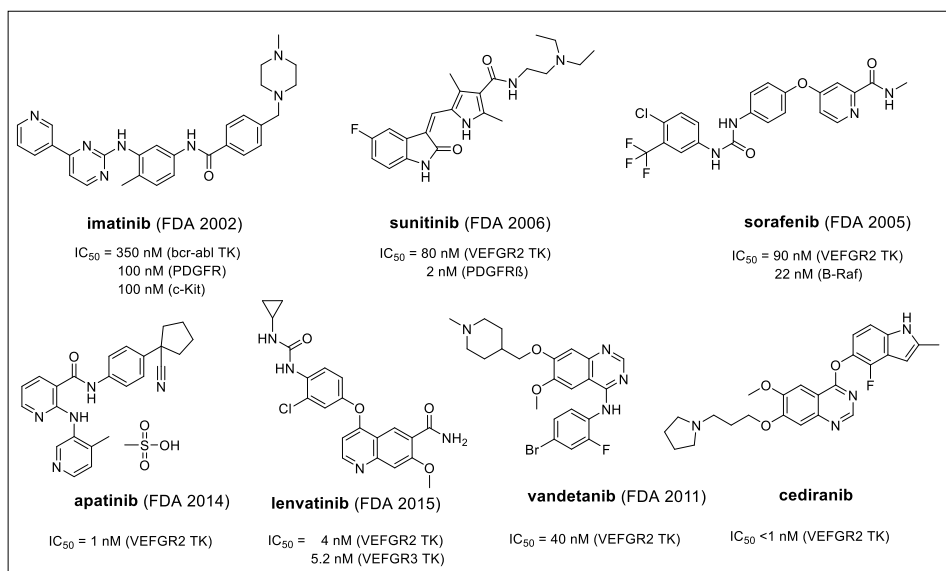


Figure. 30. Structures and activities of developed VEGFR2 tyrosin kinases inhibitors and years of the FDA first approval.

²¹ www.fda.gov (accessed April 25th, 2020)

²² Gan, H.L.; Seruga, B.; Knox, J.J. *Expert. Opin. Investig. Drugs*, **2009**, *18*, 821 - 834.

²³ Smalley, K.S.; Xiao, M.; Villanueva, J.; Nguyen, T.K.; Flaherty, K.T.; Letrero, R.; Van Belle, P.; Elder, D.E.; Wang, Y.; Nathanson, K.L.; Herlyn, M. *Oncogene*, **2009**, *28*, 85 - 94.

²⁴ www.cancer.gov (accessed April 25th, 2020)

6.4. Biological assay activity (VEGFR2 TK)

For investigation of the IC₅₀ activity of inhibitors, a radioactive *in vitro* kinase assay can be used. This method utilizes substrate, kinase and ³²P- or ³³P-labeled ATP (on gamma phosphate) to transfer a radioactive phosphate group to a tyrosine residues containing substrate. The product of the reaction is spotted on a phosphocellulose (P81) paper and washed, removing excess of radiolabeled ATP. The transferred phosphate group can be visualized and quantified using a phosphorimager.²⁵ (Figure 31)

Developed VEGFR2 TK inhibitors were assayed and their IC₅₀ values were determined by testing at 10 concentrations (1 x 10⁻⁴ M to 3 x 10⁻⁹ M) for each compound. All active compounds bound to VEGFR2 TK by concentration dependent manner. Biological assays were performed by ProQinase GmbH, Freiburg, Germany.²⁶

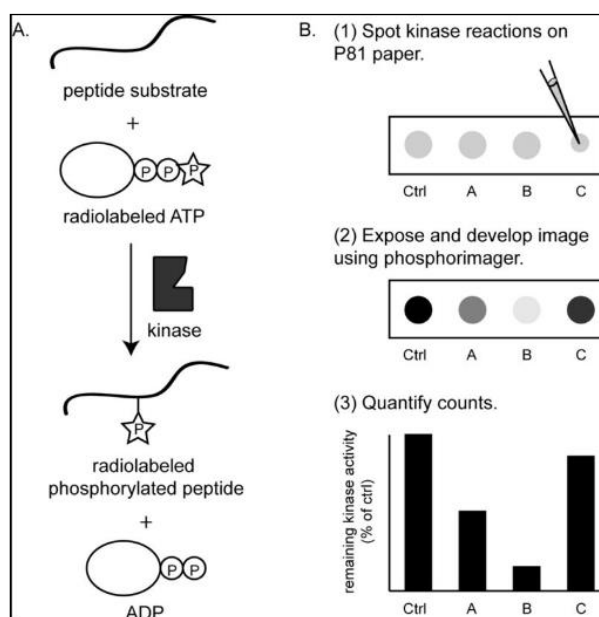


Figure 31. Schematic view of the radiometric kinase assay.

²⁵ Duong-Ly, K.C.; Peterson, J.R. *Methods Mol. Biol.*, **2016**, 1360, 87 - 95.

²⁶ Determination of enzymatic IC₅₀ activity on VEGFR2 TK was performed by ProQinase GmbH, Freiburg, Germany, <https://www.proqinase.com> (accessed August 21th, 2020).

Chapter 4. Synthesis of aminooxazole VEGFR2 TK inhibitors

7. Synthesis of aminooxazole VEGFR2 TK inhibitors

Diaryloxazole-2-amine moiety represents an interesting pharmacophoric fragment found in many biological active compounds such as antitumor, immunosuppressive and anti-inflammatory compounds. Among large number of heterocyclic compounds, an oxazole ring is characterized by various biological properties, such as antibacterial, hypoglycemic and anti-inflammatory activities.²⁷ There are two regioisomeric forms of aminooxazoles: 2,5-disubstituted aminooxazole and 2,4-disubstituted aminooxazole. (Figure 32)

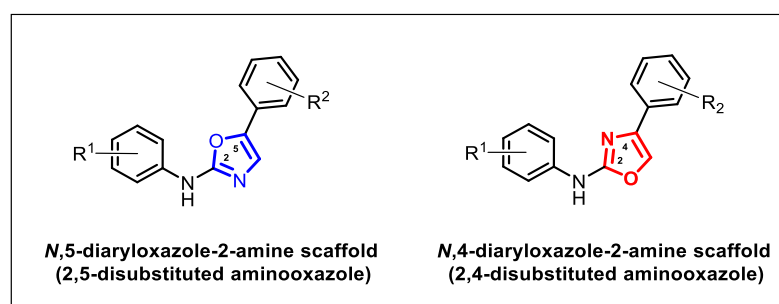


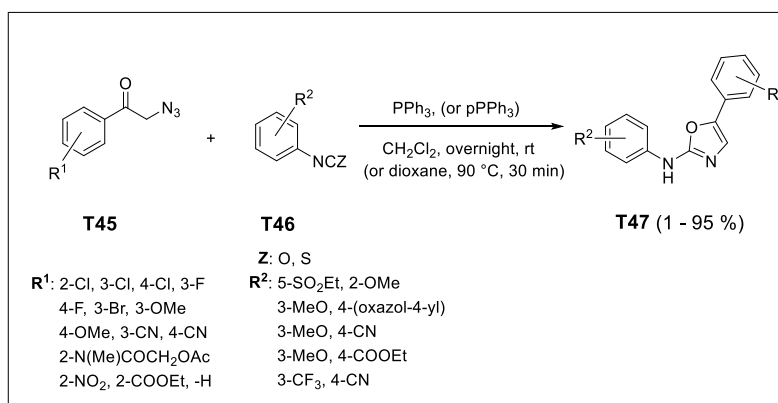
Figure 32. The structures of *N*,5-diaryloxazole-2-amine and *N*,4-diaryloxazole-2-amine scaffolds.

7.1. Synthesis of *N*,5-diaryloxazole-2-amines

The most common and efficient synthesis of the *N*,5-diaryloxazole-2-amine derivatives **T47** was described by Harris in 2005 by the reaction of various α -azidoketones **T45** and isocyanates or isothiocyanates **T46** in the presence of PPh₃ (or pPPh₃).²⁸ Authors described two conditions: overnight at room temperature in CH₂Cl₂ and 30 min heating at 90 °C in dioxane. (Scheme 5)

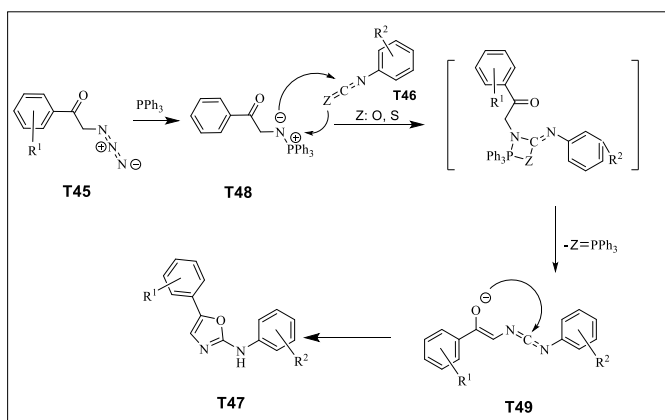
²⁷ Rauf, A.; Farshori, N.N. *Microwave-induced Synthesis of Aromatic Heterocycles* **2012** Springer, Dordrecht, Heidelberg, London, New York.

²⁸ Harris, A.P.; Cheung, M.; Hunter III, N.R.; Brown, L.M.; Veal, M.J.; Nolte, T.R.; Wang, L.; Liu, W.; Crosby, M.R.; Johnson, H.J.; Epperly, H.A.; Kumar, R.; Luttrell, K.D.; Stafford J. A. *J. Med. Chem.* **2005**, *48*, 1610 - 1619.



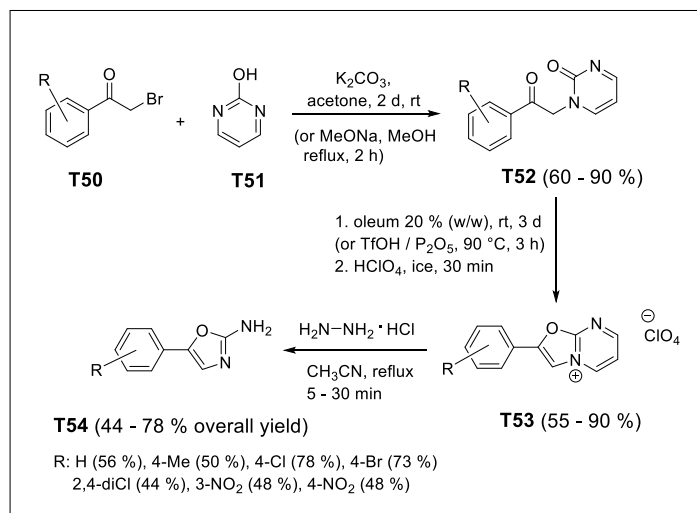
Scheme 5. Synthesis of *N*,5-diaryloxazole-2-amines **T47**.

The yields of desired oxazoles **T47** were recorded in very broad range (from 1 to 95 %) and depended on the structure of substrates and reaction conditions. The best yields of oxazoles **T47** were obtained with electron-donating substituents on α -azidoketones **T45**, whereas structure of isothiocyanates **T46** had weaker impact on the yield of products. Reactions in dioxane at 90 °C within 30 min also provided higher yields. A proposed mechanism of the oxazole-2-amine core formation is described below. (Scheme 6) In the first step, an azaylide **T48** is prepared by a reaction between α -azidoketone **T45** and PPh₃ analogically to the Staudinger reaction. Subsequently, obtained azaylid **T48** reacts with aryliothiocyanate (or arylisocyanate) **T46** and performs carbodiimide **T49**, which leads to oxazole **T47**. (Scheme 6)



Scheme 6. A mechanism of oxazol-2-amine core formation from an azide **T45**, PPh₃ and arylisocyanate or arylisothiocyanate **T46**.

Quite unusual preparation of 2,5-disubstituted aminooxazoles was performed by synthesis started from α -bromoacetophenones **T50** and 2-hydroxypyrimidine **T51**.²⁹ (Scheme 7)



Scheme 7. The synthesis of 2,5-disubstituted aminooxazoles **T54** from bromoacetophenone **T50** and 2-hydroxypyrimidine **T51**.

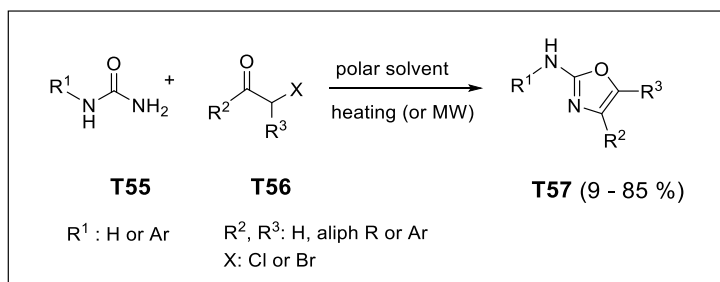
The first step of this methodology is an alkylation of the pyrimidine nitrogen of **T51** by α -bromoacetophenone **T50** in the presence of a base (K₂CO₃ or MeONa). Afterwards, protonation of the intermediate **T52** by a super acid (oleum or a mixture of TfOH / P₂O₅) gives 2-arylooxazolo[3,2-*a*]pyrimidin-4-ium sulfate (not shown), which is transferred by HClO₄ to a less soluble perchlorate **T53**. In the last step, hydrazine opens pyrimidinium ring in **T53** to form 5-arylooxazole-2-amines **T54** in 44 – 78 % overall yields.

Another preparation of trisubstituted aminooxazoles was described by the reaction of substituted urea **T55** and α -bromo (or α -chloro) carbonyls **T56** in various polar solvents (DMF, EtOH or H₂O) by heating or by microwave irradiation.^{30,31} (Scheme 8)

²⁹ Alifanov, V.L.; Babaev, E.V. *Synthesis*, **2007**, 263 - 270.

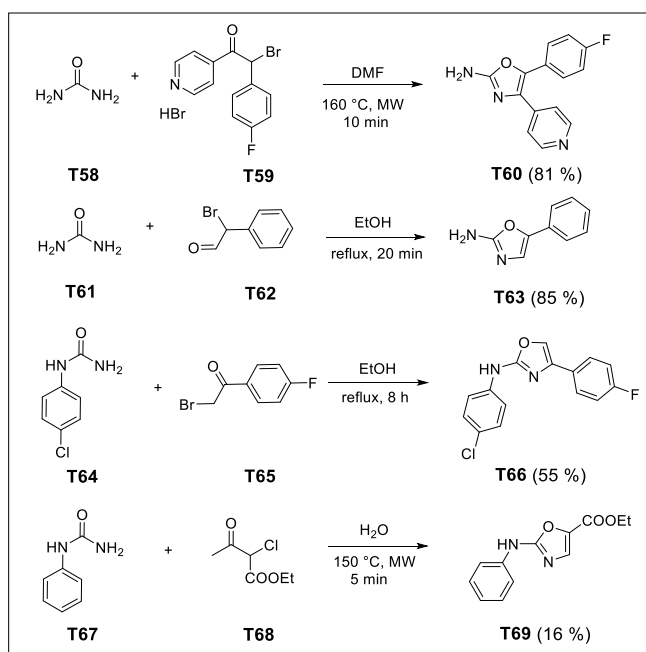
³⁰ Collins, J.L.; Blanchard, S.G.; Boswell, G.E.; Charifson, P.S.; Cobb, J.E.; Henke, B.R.; Hull-Ryde, E.A.; Kazmierski, W.M.; Lake, D.H.; Leesnitzer, L.M.; Lehmann, J.; Lenhard, J.M.; Orband-Miller, L.A.; Gray-Nunez, Y.; Parks, D.J.; Plunkett, K.D.; Tong, W.Q. *J. Med. Chem.*, **1998**, *41*, 5037 - 5054.

³¹ Kondrat'eva, G.Y.; Aitzhanova, M.A.; Bogdanov, V.S.; Stashina, G.A.; Sedishev, I.P. *Chem. Heterocycl. Comp.*, **2000**, *36*, 584 - 592.



Scheme 8. Synthesis of trisubstituted aminooxazoles **T57**.

By this method, a number of oxazolic compounds were prepared and even *N*,4-diaryloxazole-2-amine **T66** (a regioisomer of *N*,5-diaryloxazole-2-amine) was obtained in a moderate yield.^{32,33} (Scheme 9)



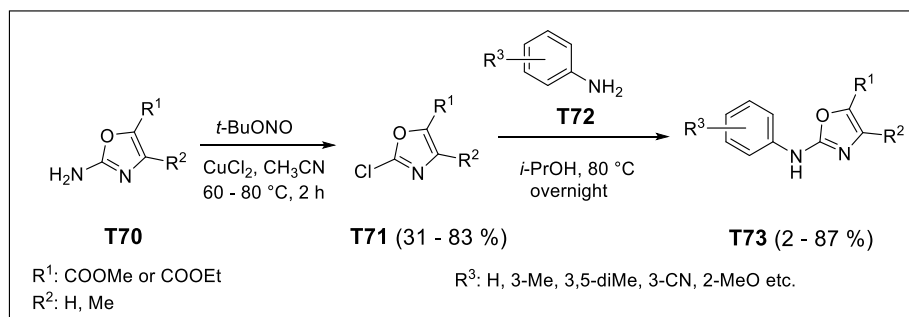
Scheme 9. Syntheses of various oxazolic compounds from ureas and α -bromo carbonyl compounds.

Another preparation of *N*-aryloxazole-2-amines **T73** was performed by two steps synthesis starting from 2-aminooxazole-5-carboxylates **T70**, which were transformed to corresponding

³² Yang, X.; Zhou, Z.A. Chinese Patent Appl. 102134224, **2011**, *Chem. Abstr.* 2011, 155, 271265.

³³ Koch, P.; Laufer, S. *J. Med. Chem.*, **2010**, 53, 4798 - 4802.

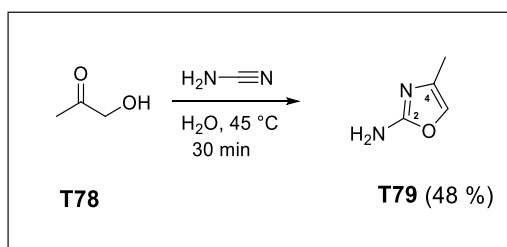
2-chlorooxazoles **T71** by *t*-BuONO / CuCl₂. Obtained 2-chlorooxazoles **T71** reacted with anilines **T72** to give *N*-aryloxazole-2-amines **T73** in 2 - 87 % yields.^{34,35} (Scheme 10)



Scheme 10. Synthesis of aminooxazoles **T73** via chlorooxazoles **T71**.

7.2. Synthesis of *N*,4-diaryloxazole-2-amines

Compared to previously discussed synthesis of *N*,5-diaryloxazole-2-amines, the preparation of their regioisomers e.g. *N*,4-diaryloxazole-2-amines is less described in the literature. Synthesis of *N*,4-diaryloxazole-2-amines by using cyanamide and hydroxyketone was carried out by Ohta et. al.³⁶ Desired aminooxazole was obtained in 48 % yield. (Scheme 11)



Scheme 11. Synthesis of 2,4-disubstituted aminooxazole **T79**.

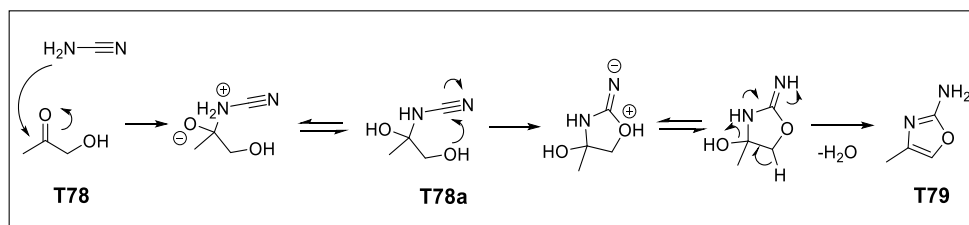
A reaction is initiated by a nucleophilic addition of cyanamide to a carbonyl of hydroxyketone and subsequent conversion of an intermediate **T78a** to an oxazole **T79** by a nucleophilic attack

³⁴ Dhar, T.G.M.; Shen, Z.; Guo, J.; Liu, C.; Watterson, S.H.; Gu, H.H.; Pitts, W.J.; Fleener, C.A.; Rouleau, K.A.; Sherbina, N.Z.; McIntyre, K.W.; Witmer, M.R.; Tredup, J.A.; Chen, B.C.; Yhao, R.; Bednarz, M.S.; Cheney, D.L.; MacMaster, J.F.; Miller, L.M.; Berry, K.K.; Harper, T.W.; Barrish, J.C.; Hollenbaugh, D.L.; Iwanowicz, E.J. *J. Med. Chem.*, **2002**, *45*, 2127 - 2130.

³⁵ Lintnerova, L.; Kováčiková, L.; Hanquet, G.; Boháč, A. *J. Heterocyclic. Chem.*, **2015**, *52*, 425 - 439.

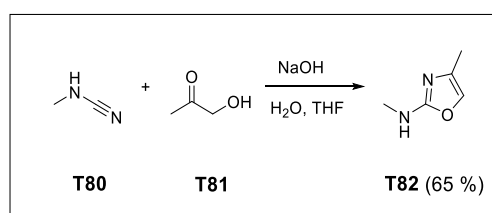
³⁶ Ohta, H.; Ishizaka, T.; Tatsuzuki, M.; Yoshinaga, M.; Iida, I.; Yamaguchi, T.; Tomishima, Y.; Futaki, N.; Toda, Y.; Saito, S. *Bioorg. Med. Chem.*, **2008**, *16*, 1111 - 1124.

of primary alcohol to the cyano group. Afterwards, a formation of oxazole **T79** occurs by elimination of water and tautomerization. (Scheme 12)



Scheme 12. A mechanism of the synthesis of aminooxazole **T79** from α -hydroxypropane-1-one **T78**.

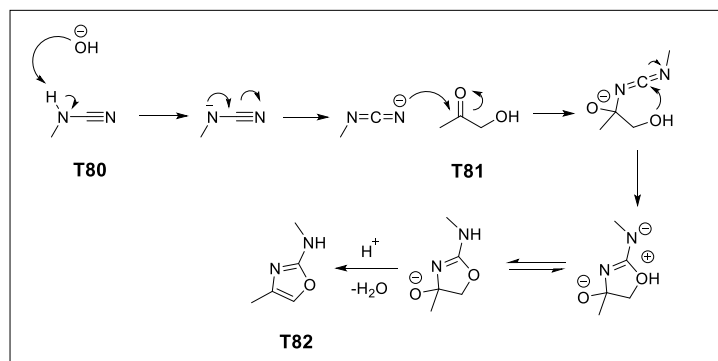
A 2,4-disubstituted aminooxazole was also obtained by a treating of *N*-methylcyanamide **T80** with hydroxyacetone **T81** in a water solution of NaOH and THF.³⁷ (Scheme 13)



Scheme 13. Synthesis of oxazole-2-amine **T82** from cyanamide **T80** and hydroxyacetone **T81**.

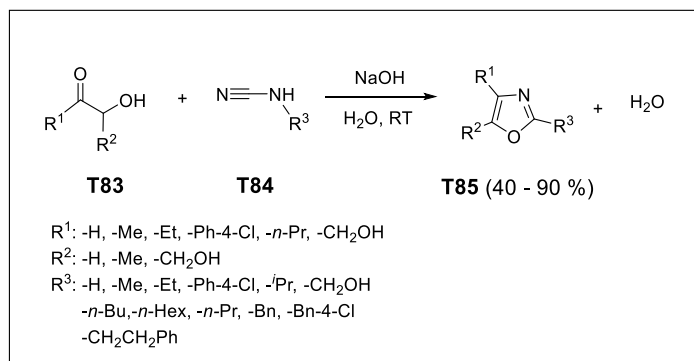
Mechanism of this reaction is slightly different compare to the previous case. After deprotonation of a cyanamide, resulting anion is tautomerized to terminal nitrogen and forms carbodiimide that attacks a carbonyl group of a hydroxyacetone **T81**. Then the mechanism is identical like in the previous case. (Scheme 14)

³⁷ Minassian, F. 2008. Methyl Cyanamide. e-EROS Encyclopedia of Reagents for Organic Synthesis, Grenoble, France



Scheme 14. The mechanism of synthesis of aminooxazole **T82** from *N*-methylcarbamide **T80**.

A similar study was described on various alkyl and aryl substituted hydroxyketones **T83** and cyanamides **T84**.³⁸ The yields of oxazoles **T85** were from 40 to 90 %. (Scheme 15)

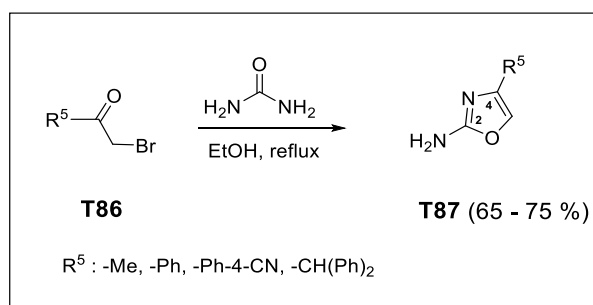


Scheme 15. Synthesis of various aminooxazoles **T85** carried out from hydroxyketones **T83** and cyanamides **T84**.

Another useful method for a preparation of 2,4-disubstituted oxazole-2-amines **T87** was published by Xiang et al.³⁹ Synthesis was carried out with α -bromoketone **T86** and urea. (Scheme 16)

³⁸ Cockerill, A.F.; Deacon, A.; Harrison, R.G. Osborne, D.J.; Prime, D.M.; Ross, W.J.; Todd, A.; Verge, J.P *Communications*, **1976**, 9, 591 - 593.

³⁹ Xiang, J.; Ipek, M.; Suri, V.; Massefski, W.; Pan, N.; Ge, Y.; Tam, M.; Xing, Y.; Tobin, J.F.; Xu, X.; Tam, S. *Bioorg. Med. Chem. Lett.*, **2005**, 15, 2865 - 2869.



Scheme 16. Synthesis of oxazole-2-amine **T87**.

Chapter 5. **Palladium-catalyzed cross-coupling reactions**

8. Palladium-catalyzed cross-coupling reactions

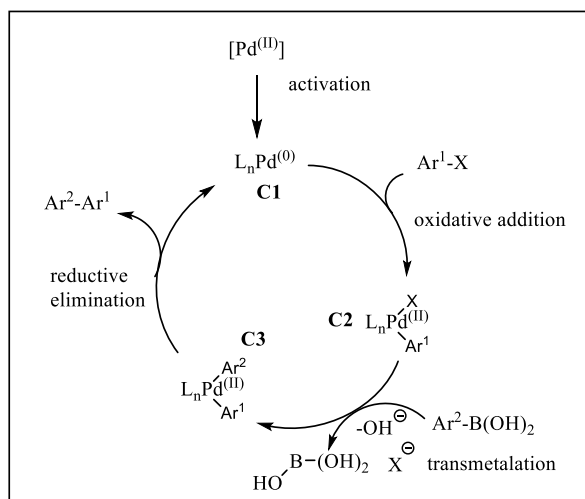
In organic chemistry, a palladium-catalyzed cross-coupling reaction is a process, where two fragments are joined together with catalysis of a transition metal-palladium.⁴⁰ This versatile reaction has become very popular in modern organic and medicinal chemistry owing to effective formation of carbon – carbon or carbon – heteroatom bonds. There are several types of cross-coupling reaction according to type of coupling reagents used in the reaction. Within this dissertation thesis, we used Suzuki-Miyaura and Stille coupling reactions for the synthesis of majority of designed VEGFR2 TK inhibitors. In general, all palladium-catalyzed reactions involves: 1) oxidative addition, 2) transmetallation and 3) reductive elimination.

8.1. Suzuki-Miyaura (SM) cross-coupling reaction

The Suzuki-Miyaura (SM) cross-coupling reaction was first described in 1979 by Prof. Akira Suzuki.⁴¹ It is widespread transition metal-catalyzed reaction, which utilizes organoboron compounds as a coupling partner. Popularity and broad application for this coupling arise from relatively stable, readily available and less toxic organoboron reagents relative to organotin or organozinc reagents. Mechanism of SM coupling reaction is described below. (Scheme 17)

⁴⁰ King, A.O.; Yasuda, N. *Organomet. Chem.*, **2004**, 6, 205 - 245.

⁴¹ Miyaura, N.; Suzuki, A. *J. Chem. Soc., Chem. Commun.* **1979**, 19, 866 - 867.



Scheme 17. Mechanism of SM cross-coupling reaction.

Oxidative addition

In the first step, the palladium⁽⁰⁾ catalyst **C1** is oxidized to palladium^(II) and coupled with an aryl halide to form organopalladium complex **C2**. A wide-variety of aryl halides in SM coupling are used, but bromides, iodides and “pseudohalids” triflates are most useful. Since oxidative addition is the rate determining step in the cycle, the reactivity decreases in the order of $I > OTf > Br > Cl$.⁴² Aryl halides are also activated by electron-withdrawing groups (EWD) in *ortho* and *para* position that increase their reactivity in oxidative addition.⁴³

Transmetalation

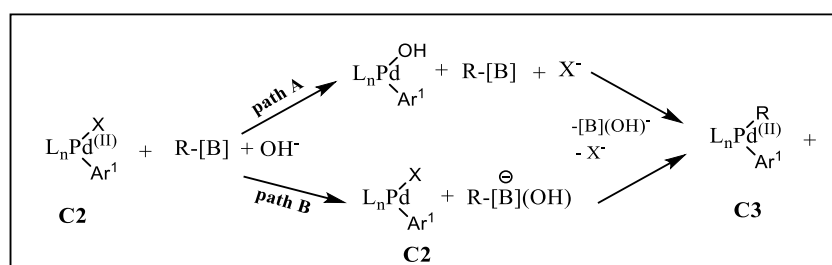
In transmetalation step, an organic group Ar^2 attached on boron species is transferred to the Pd^{II} complex **C2** to give a new Pd^{II} complex **C3**. The exact mechanism of transmetalation is still not clear and remains to be discovered. This step requires a presence of the base in order to increase electron density of boron atom. Lima et al. proposed two main pathways that explaining a role of the base in SM cross-coupling reaction.⁴⁴ The first pathway A: halogen or triflate is exchanged after oxidative addition with a nucleophilic species, which can be an anion of the used base or anion present in the solution. Resulting Pd^{II} -OR (alkoxy, hydroxy or acetoxy) complex is considered to be more reactive in transmetalation step relative toward

⁴² Aliprantis, A. O.; Canary, J. W. *J. Am. Chem. Soc.*, **1994**, *116*, 6985.

⁴³ ChemLer, S. R.; Trauner, D.; Danishefsky, S. J. *Angew. Chem. Int. Ed.*, **2001**, *40*, 4544.

⁴⁴ Lima, C.F.R.A.C.; Rodrigues, A.S.M.C.; Silva, V.L.M.; Silva, A.M.S.; Santos, L.M.N.B.F. *Chem. Cat. Chem.*, **2014**, *6*, 1291 - 1302.

$\text{Pd}^{\text{(II)}}\text{-X}$ complex. The second pathway B explains a role of the base differently. The base attacks a boron atom to get more electronic rich borate and increases its reactivity toward palladium in the **C2** complex. (Scheme 18) Commonly employed bases for this process are K_3PO_4 , K_2CO_3 , KOH or even fluoride anions could be used (KF). (Scheme 18)



Scheme 18. Two proposed pathways A and B of the base in SM cross-coupling reaction.

Reductive elimination

The final step is reductive elimination where a required product is eliminated from **C3** and palladium^(II) catalyst is regenerated to $\text{Pd}^{(0)}$ **C1**.

8.1.1. Types of boronic derivatives

Over the last decade, a wide range of boronic derivatives for SM cross-coupling reaction have been developed. Most common are arylboronic acids $\text{ArB}(\text{OH})_2$, aryl boronic esters $\text{ArB}(\text{OR})_2$, aryl trifluoroborate salts $[\text{ArBF}_3]^{(-)}$ or popular aryl boronic acid pinacol esters ArBpin . (Figure 33) The reactivity of borane in transmetalation depends on its Lewis acidity. Therefore, electron withdrawing substituents increase the reactivity of the borane, which suggests higher reactivity of boronic acids than esters.⁴⁵ In boronic esters, σ -donating ability of carbon leads to a stronger conjugation of oxygen lone pairs with a neighboring boron atom, which results to reduced Lewis acidity.⁴⁶ On the other hand, boronic esters exhibit stability toward column chromatography and liquid esters could be distilled.

⁴⁵ ChemLer, S. R.; Trauner, D.; Danishefsky, S. J. *Angew. Chem. Int. Ed.*, **2001**, *40*, 4544 - 4568.

⁴⁶ Lennox, A.J.J.; Lloyd-Jones, G.C.; *Chem. Soc. Rev.*, **2014**, *43*, 412 - 443.

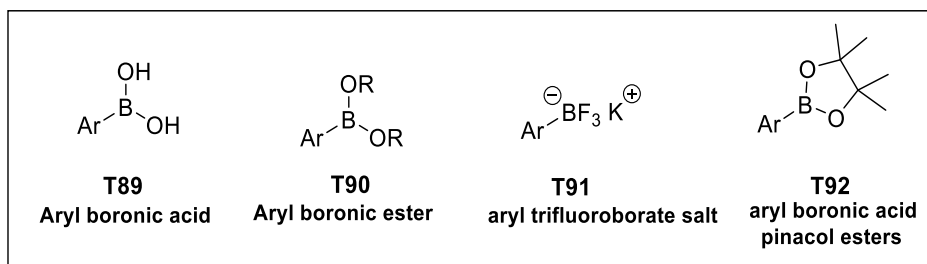


Figure 33. The structures of the most common aryl boronic derivatives used in SM cross-coupling reaction.

N-methyliminodiacetic acid (MIDA) boronates were developed by Burke for unstable boronic acids.⁴⁷ (Figure 34) In this type of compounds a boron atom forms two covalent bonds with an oxygen and one extra donating bond from nitrogen atom acting as a Lewis base. Resulting MIDA-boronates are characterised by general air and moisture stability and stability toward column chromatography as well.⁴⁸

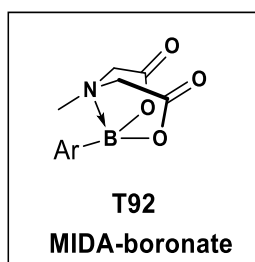


Figure 34. The general structure of aryl MIDA-boronate **T92**.

8.1.2. Ligands in SM-cross coupling reactions

Ligands play important role during the cross-coupling reactions due to their electron donating and bulky features, which can stabilize Pd⁽⁰⁾ catalyst and promote oxidative addition and reductive elimination.⁴⁹

Very effective and common are monodentate phosphine ligands, widely used in both laboratory and industry. Among them, triphenylphosphine (PPh₃) is characterised by high ability to donate electrons to the palladium⁽⁰⁾ and accelerate the reaction. In order to facilitate reactivity of the various coupling reactions, Netherton et al. proposed and replaced aromatic rings of PPh₃

⁴⁷ E. P. Gillis, M. D. Burke, *J. Am. Chem. Soc.*, **2007**, *129*, 6716 – 6717.

⁴⁸ E. P. Gillis, M. D. Burke, *J. Am. Chem. Soc.*, **2008**, *130*, 14084 - 14085.

⁴⁹ Miyaura, N.; Suzuki, A. *Chem. Rev.*, **1995**, *95*, 2457 - 2483.

with bulkier and more electron-rich alkyl groups, which result to a higher catalytic reactivity.⁵⁰ (Figure 35)

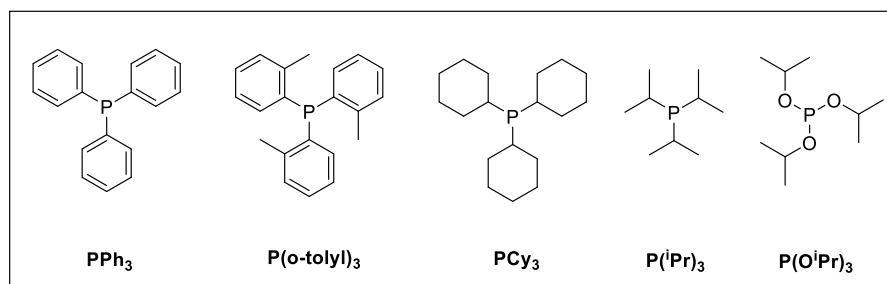


Figure 35. The most common phosphine ligands used in cross-coupling reactions.

Later, Buchwald et al. introduced a new generation of bulky and electron-rich dialkyl(biaryl) phosphine ligands, that are used to modulate the chemical reactivity of palladium or other transition-metal catalysts. These ligands possess various attributes such as air and thermal stability, commercial availability and application to all types of palladium cross-coupling reactions forming C-C or C-N bonds.⁵¹ Many traditional sources of Pd in cross-coupling reactions, such as Pd(PPh₃)₄ or Pd_n(dba)_m (e.g. Pd(dba)₂, Pd₂(dba)₃) have significant limitation (to substrate or temperature) or must be reduced *in situ* from Pd^(II) to Pd⁽⁰⁾ (e.g. Pd(OAc)₂ and PdCl₂). Developed electron-rich and bulky ligands mitigate these limitations and overallly improved properties of ligand.⁵² In the figure below, functions of all particular R-substituents at various position of a ligand are explained.⁵³ (Figure 36)

⁵⁰ Netherton, M. R.; Dia, C.; Neuschutz, K.; Fu, G. C. *J. Am. Soc. Chem.* **2001**, *123*, 10099.

⁵¹ Old, D. W.; Wolf, J. P.; Buchwald, S. L. *J. Am. Soc. Chem.* **1998**, *120*, 9722 - 9723.

⁵² Beletskaya, I. P.; Cheprakov, A. V. *J. Organomet. Chem.*, **2004**, *689*, 4055 - 4082.

⁵³ Martin, R.; Buchwald, S.L. *Account Chem. Res.* **2008**, *41*, 1461- 1473.

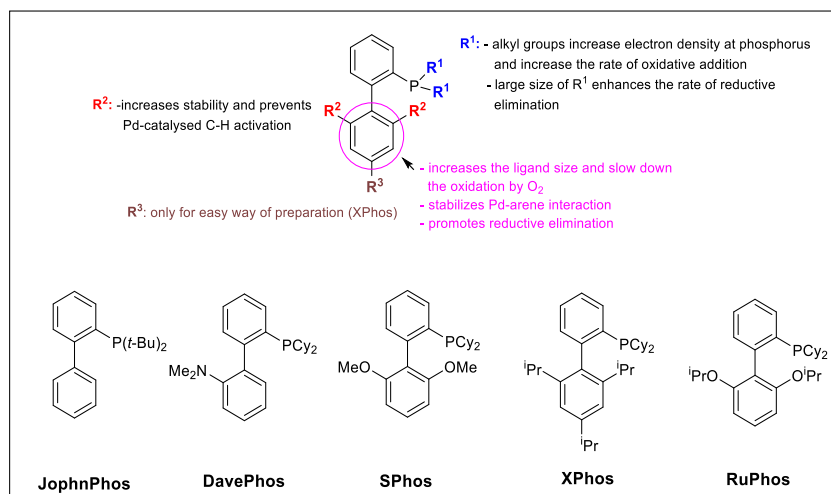


Figure 36. Structural and functional features of particular substituents attached on dialkylbiarylphosphine. The structures of the most utilized ligands are depicted as well.

Other very effective ligands belong to a bidentate class of phosphorus ligand, such as DPPF, DPPE or DPPP, which showed excellent ligand properties in SM cross-coupling reaction. (Figure 37)

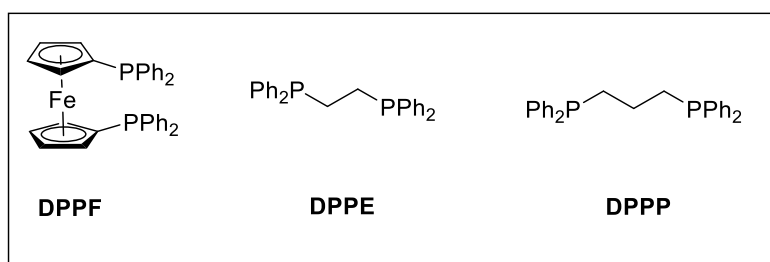


Figure 37. Structures of the most useful bidentate phosphorus ligands.

Very versatile catalysts widely used in various cross-coupling reaction are **PEPPSI** (**P**yridine-**E**nhanced **P**recatalyst **P**reparation **S**tabilization and **I**nitiation) compounds. (Figure 38) This group of palladium catalysts was introduced in 2005 by professor Mike Organ with his co-workers Dr. Chris O'Brien and Dr. Eric Kantchev.⁵⁴ They are characterized by extremely high air and moisture stability, good commercial availability and widespread application in the research and industry.

⁵⁴ Organ, M. G. Rational catalyst design and its application in sp³-sp³ couplings. Presented at the 230th National Meeting of the American Chemical Society, Washington, DC, **2005**; Abstract 308.

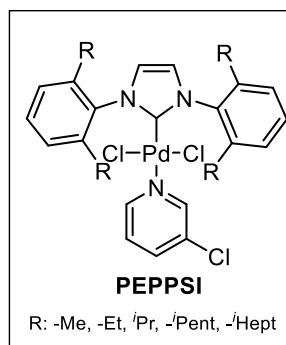
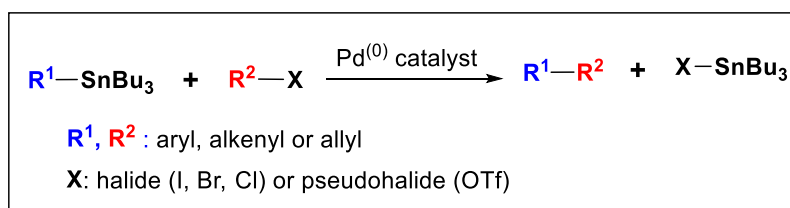


Figure 38. General structure of **PEPPSI** catalysts.

Pyridyl ligand in the structure provides additional stability and bulky -R substituents improve reductive elimination. Phenylimidazolium moiety binds the palladium more tightly than traditional phosphines and prevents metal dissociation.⁵⁵ PEPPSI-*i*Pr is very efficient in Negishi, Suzuki, Sonogashira or Kumada coupling as well as in Buchwald-Hartwig amination and Heck coupling.

8.2. Stille cross-coupling reaction

Another versatile cross-coupling reaction, widely used in organic synthesis, is Stille reaction. This type of coupling includes the same steps as SM cross-coupling, but organotin compounds (or organostannanes) instead of organoborones are used without basic activation.⁵⁶ (Scheme 19)



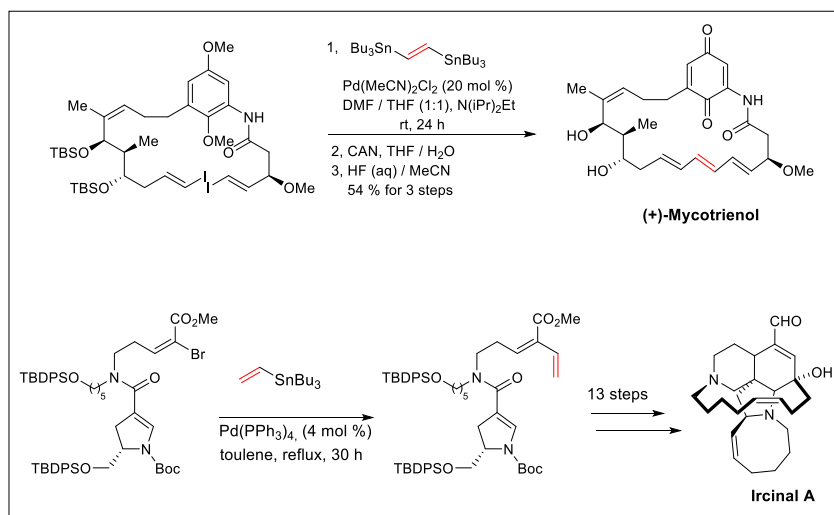
Scheme 19. General scheme of Stille coupling reaction.

The main drawback of all organotin compounds is their toxicity, which makes Stille coupling less popular than SM coupling reaction. The Stille coupling reaction has been used mainly in

⁵⁵ Organ, M.G.; Avola, S.; Dubovyk, I.; Hadei, N.; Kantchev, E.A.B.; O'Brien, Ch.J.; Valente, C. *Chem-Eur. J.*, **2006**, *12*, 4749-4755.

⁵⁶ Stille, J.K. *Angew. Chem. Int. Ed. Engl.*, **1986**, *25*, 508 - 524

the synthesis of natural products. Panek et al. described a total synthesis of antibiotic (+)-mycotrienol using Stille coupling in macrocyclization step.⁵⁷ Also, in a total synthesis of antitumor alkaloid Ircinal A includes a Stille reaction.⁵⁸ (Scheme 20)



Scheme 20. Application of Stille coupling reaction in total syntheses of natural products.

8.2.1. Additives in Stille coupling reactions

The most frequent additive to the Stille coupling reaction is copper^(I) which may enhance the rate of reaction by 10³-fold more.⁵⁹ In polar solvents stannane is exchange with copper, which results to organocuprate reagent readily transmetalated with palladium catalyst. (Scheme 21) Lithium chloride is another effective rate accelerant of Stille coupling reaction. It is believed that chloride anion either replace another halogen atom X on palladium leading to higher reactivity for transmetalation or coordinate Pd⁽⁰⁾ centre resulting to enhanced rate of oxidative addition. In addition, LiCl salts increase the polarity of solvents leading to easier leaving of anionic ligand (-Cl, -Br, -OTf etc.).⁶⁰ The same favorable effect is also attributed to fluoride

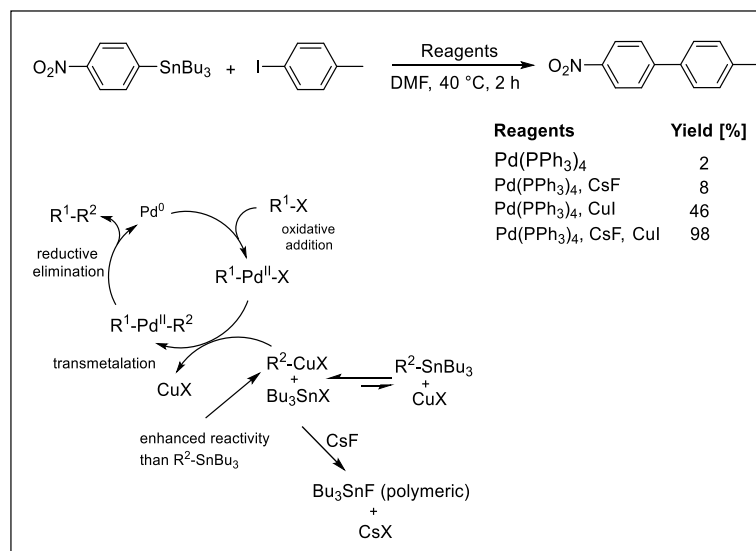
⁵⁷ Masse, C. E.; Yang, M.; Solomon, J.; Panek, J. S. *J. Am. Chem. Soc.*, **1998**, *120*, 4123 - 4134.

⁵⁸ Martin, S. F.; Humphrey, J. M.; Ali, A.; Hillier, M. C. *J. Am. Chem. Soc.*, **1999**, *121*, 866 - 867.

⁵⁹ Farina, V. *Pure Appl. Chem.*, **1996**, *68*, 73 - 78.

⁶⁰ Farina, V.; Kapadia, S.; Brishnan, B.; Wang, C.; Liebeskind, L. S. *J. Org. Chem.*, **1994**, *59*, 5905 - 5911.

anion (CsF), that could increase the rate of reaction. Moreover, fluoride anions could act as scavenger for stannane side products, making them easily to remove.⁶¹ (Scheme 21)



Scheme 21. An effect of copper⁽¹⁾ and fluoride anion in Stille coupling reaction.

Other type is **Negishi coupling** that utilizes reaction of organic halides or triflates with organozinc compounds forming new C-C bonds. Palladium is largely used as a catalyst, but in some cases also nickel could replace it.⁶² Negishi coupling was used in 2003 by Novartis in a synthesis of a phosphodiesterase inhibitor **PDE472**, considered as a leading structure for treatment of asthma.⁶³ The **Heck coupling** is another palladium-catalyzed reaction of aromatic / vinyl halide or triflate with an alkene in the presence of a base (e.g. synthesis of naproxen).^{64,65} Other useful reaction is **Sonogashira** cross-coupling (organohalide with alkyne) used in synthesis of an alkaloid (+)-(S)-laudanoline.⁶⁶ (Scheme 22)

⁶¹ Mee, S. P. H.; Lee, V.; Baldwin, J. E. *Angew. Chem. Int. Ed.*, **2004**, *43*, 1132 - 1136.

⁶² King, A.O.; Okukado, N.; Negishi, E. *J. Chem. Soc., Chem. Commun.*, **1977**, *19*, 683 - 684.

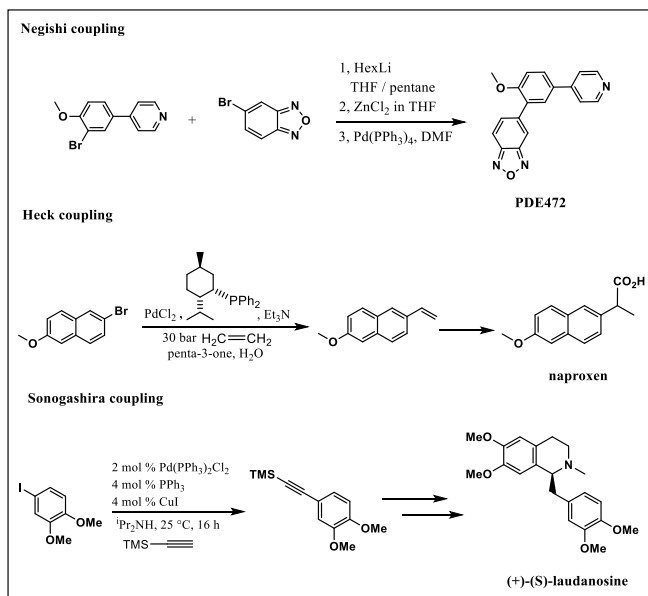
⁶³ Manley, P.W.; Acemoglu, M.; Marterer, W.; Pachinger, W. *Org. Proc. Res. Dev.*, **2003**, *7*, 436 - 445.

⁶⁴ Heck, R. F. *Org. React.*, **1982**, *27*, 345 - 390.

⁶⁵ De Vries, J.G. *Can. J. Chem.*, **2001**, *79*, 5 - 6.

⁶⁶ Mujahidin, D.; Doye, S. *Eur. J. Org. Chem.*, **2005**, *2005*, 2635 - 2848.

Palladium-catalyzed cross-coupling reactions



Scheme 22. Examples of Negishi, Heck and Sonogashira coupling reactions.

Chapter 6. Project 1. - Development of novel *N*,4-diaryloxazol-2-amine VEGFR2 TK inhibitors NBM(1-7)

9. Development of novel *N*,4-diaryloxazol-2-amine VEGFR2 TK inhibitors NBM(1-7)

In 2005 GlaxoSmithKline⁶⁷ developed *N*,5-diaryloxazole-2-amine VEGFR2 TK inhibitor **AAZ** (**BM6**), which exhibited strong VEGFR2 TK inhibitory activity ($IC_{50} = 22$ nM) and good pharmacokinetic properties.²⁸ According to a Biomagi proposal our group has developed other active aminooxazole derivatives **BM(1-5,7)**, containing various heterocyclic compounds in a *meta* position of an internal phenyl ring instead of pyridin-2-yl moiety present in **AAZ**.⁶⁸ (Figure 39)

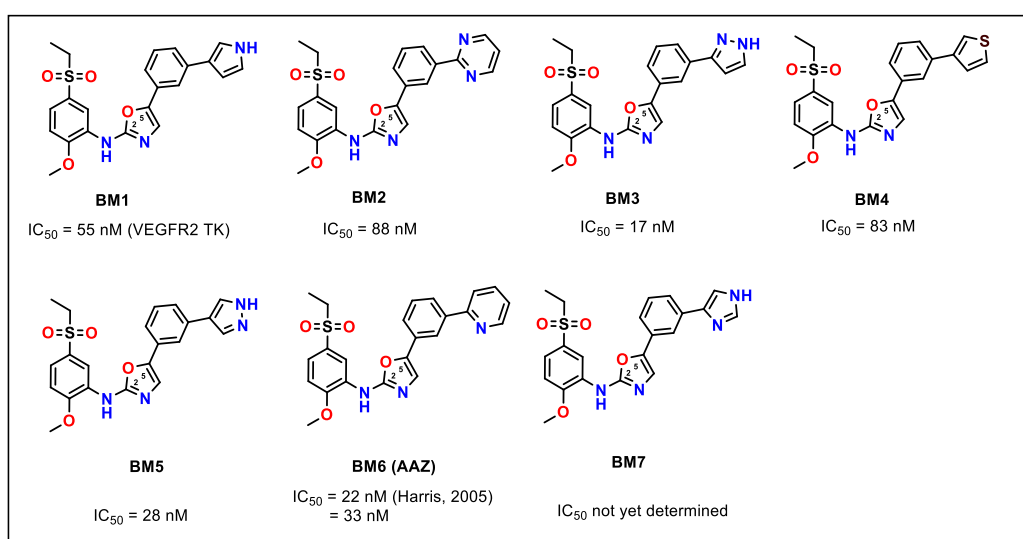


Figure 39. Structures of the most active *N*,5-disubstituted oxazole-2-amine VEGFR2 TK inhibitors **BM(1-7)** and their VEGFR2 Tk activities if determined.

All inhibitors **BM(1-7)** represent a class of *N*,5-disubstituted oxazole-2-amines (for simplification in our group we call them *O*-regioisomers). In this project we were focused on a development of their *N*-regioisomeric pairs (*N*,4-disubstituted oxazole-2-amines **NBM(1-7)**). (Figure 40) An oxygen in the 1,3-oxazolic ring is an isostere to an oxazolic nitrogen and *vice versa*. Therefore similar binding interactions with Cys917 from ATP-binding site is expected for both regioisomers. Proposed *N*-regioisomers are in an equilibrium: conformationally more favourable “L” shaped conformer in solution and induced “U” shaped conformation in an ATP binding site of VEGFR2 kinase. Therefore the Biomagi assumed that *N*-regioisomers (**NBM1-**

⁶⁷ GlaxoSmithKline, Five Moore Drive, Research Triangle Park, North Carolina 27709, USA.

⁶⁸ Šramel, P. *Dissertation Thesis* 2017, Comenius University in Bratislava, Slovakia and Université de Strasbourg, France.

7) may preserve the same “U” shaped conformation as *O*-regioisomers (BM1-7) in VEGFR2 TK. Their “L” conformation will lead to a loss of kinase inhibitory activity. (Figure 40)

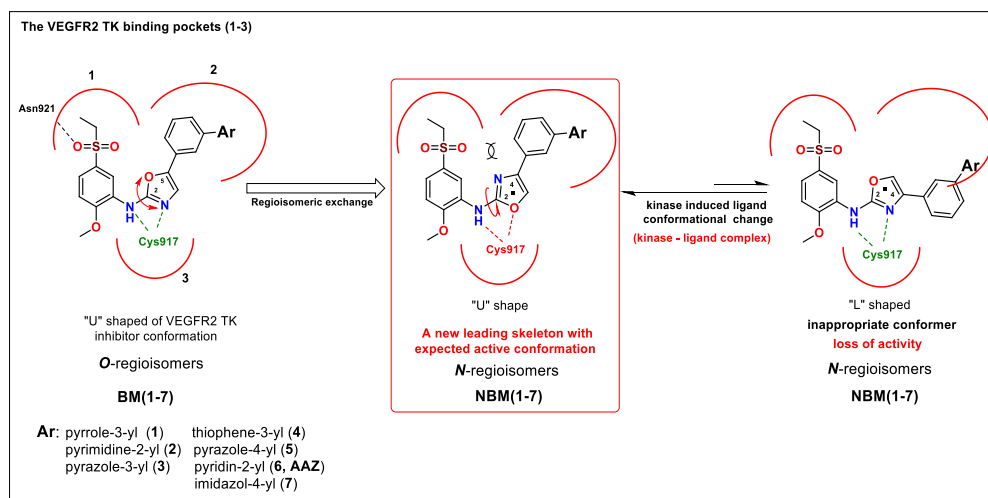


Figure 40. An illustration of the Biomagi concept of Regioisomeric Bioisostery (*RegBio*).

Regioisomers NBM(1-7) with expected “U” shaped conformation should be in principle regioisomeric bioisosters to BM(1-7). Thanks to this regioisomeric bioisostery (*RegBio*) hypothesis we have focused to prepare a novel leading skeleton for VEGFR2 TK inhibitors NBM(1-7) and to determine their inhibitory activity (IC₅₀, VEGFR2 TK) and compare them to BM(1-7) *O*-regioisomers. (Figure 41)

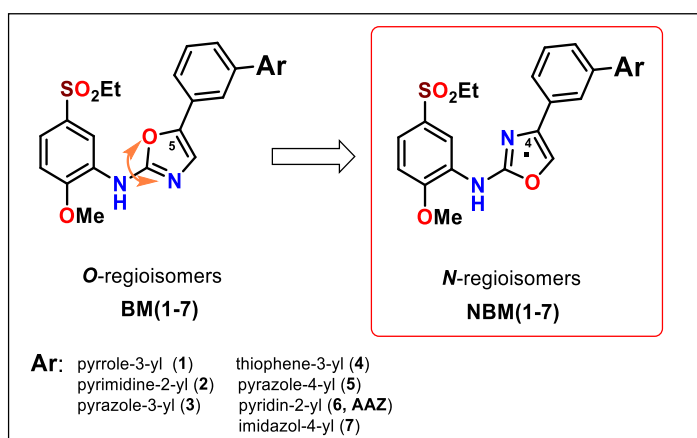
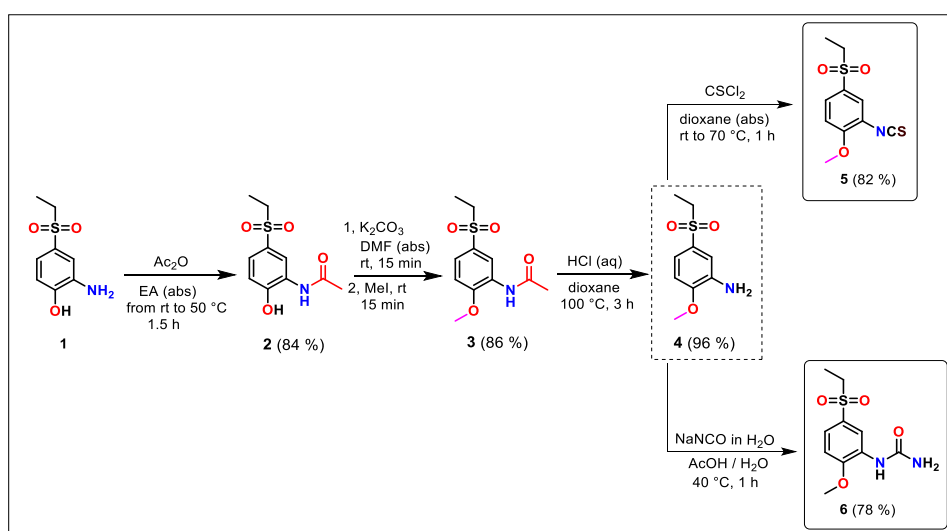


Figure 41. A general structure of *N*,4-disubstituted oxazole-2-amines NBM(1-7) proposed according to *N*,5-disubstituted oxazole-2-amines BM(1-7) possessing various heterocyclic substituents (Ar) in a meta position.

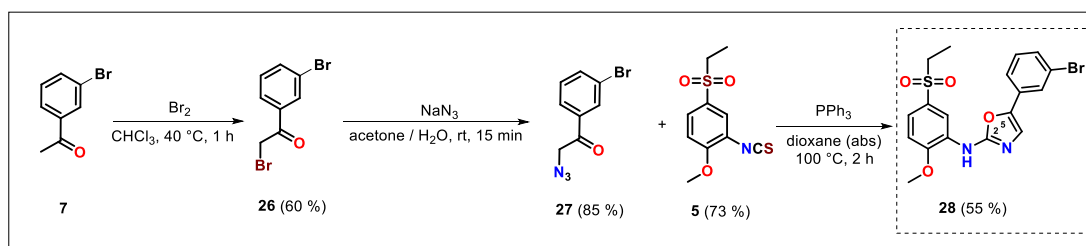
9.1. Synthesis of *N*,5-diaryloxazole-2-amine intermediate (**28**) and VEGFR2 TK inhibitor (**BM7**)

Based on the available literatures in both research databases (Reaxys, SciFinder) we selected a synthetic method for preparation of *O*-regioisomeric intermediate **28** and proposed VEGFR2 TK imidazole inhibitor **BM7**. Synthesis of *N*,5-disubstituted oxazole-2-amines **BM(1-6)** have already been performed and completely described in our group.⁶⁸ Synthesis of **BM7** started from commercially available aniline **1**, which was transformed to aniline **4** by three steps. Compound **4** is a useful joint intermediate for both regioisomers **BM(1-7)** and **NMB(1-7)**. Aniline **4** was converted to isothiocyanate **5** or urea **6** by CSCl_2 and NaNCO , resp. (Scheme 23)



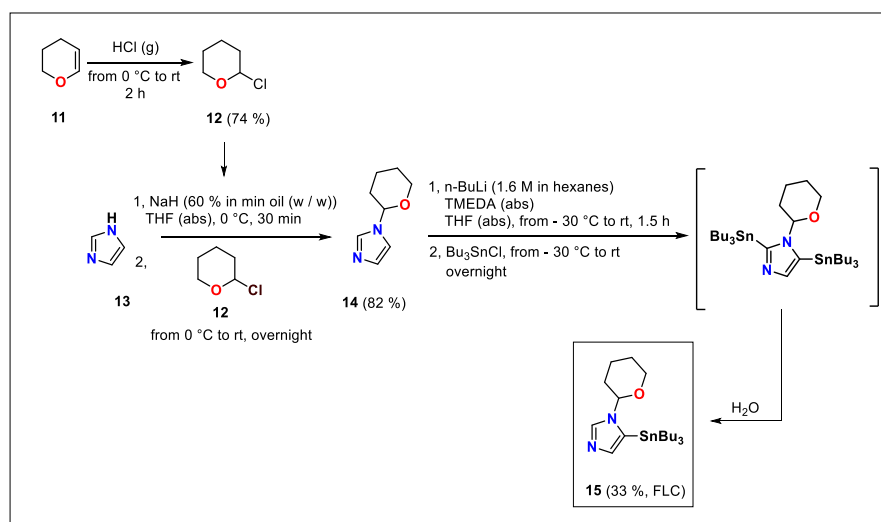
Scheme 23. Synthesis of intermediates: isothiocyanate **5** and urea **6**.

Preparation of oxazole **28** was carried out by cyclization of α -azidoacetophenone **27** and isothiocyanate **5** in a presence of PPh_3 . (Scheme 24) Yield of the last reaction varied from 30 to 90 % depending on substituents on a bromine substituted phenyl ring. In our case this method has become an effective way for preparation of other *N*,5-disubstituted oxazole-2-amine inhibitors **BM(1-7)**.



Scheme 24. Synthesis of *N*,5-disubstituted oxazole-2-amine precursor **28**.

The last step in the synthesis of **BM-7** was an introduction of a heterocyclic substituent instead of bromine in a *meta* position of **28** by palladium-catalyzed coupling reaction. Other inhibitors **BM(1-6)** were prepared in our group by Stille or Suzuki couplings using commercially available reagents. But in case of **BM-7** all imidazole-4-yl coupling reagents (pinacol boronic ester or boronate) were rarely available. Therefore, we have developed a three-step synthesis of tributylstannylimidazole **15**. (Scheme 25) We also tried to prepare a less toxic pinacol boronate reagent according to Primas *et al.*, but the synthesis was not efficient and provided very low yields. What more, subsequent Suzuki reaction with this reagent didn't work according to published procedure.⁶⁹

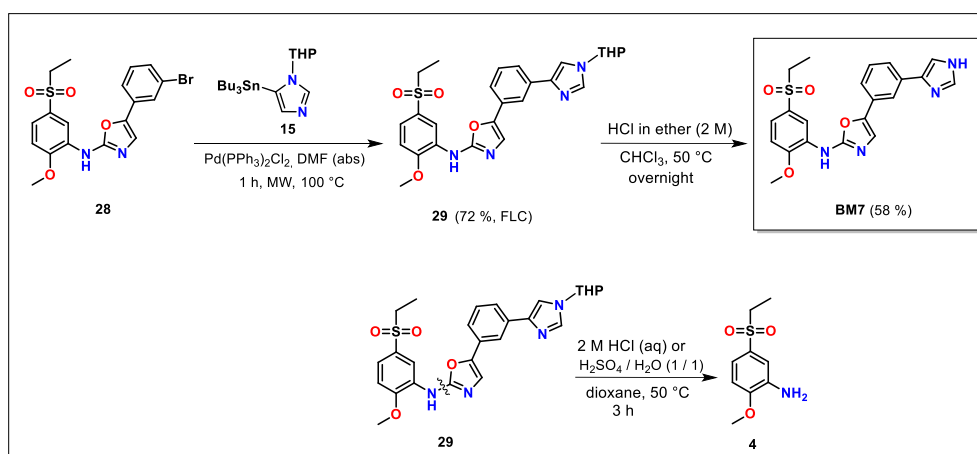


Scheme 25. Synthesis of tributylstannylimidazole **15** as a coupling reagent for a synthesis of **BM-7**.

Desired inhibitor **BM7** was synthesized from oxazole **28** by Stille coupling conditions, followed by an acidic hydrolysis of a THP protecting group in 72 and 58 % yield, resp. (Scheme 26)

⁶⁹ Primas, N.; Mahatsekake, C.; Bouillon, A.; Lancelot, J-Ch.; de Oliveira Santos, J.S.; Lohier, J-F.; Rault, S. *Tetrahedron*, **2008**, *64*, 4596 - 4601.

Acidic hydrolysis carried out in water led to a cleavage of an amino-oxazole bond and provided aniline **4**. Yield of the unsuccessful reaction was not determined. (Scheme 26)

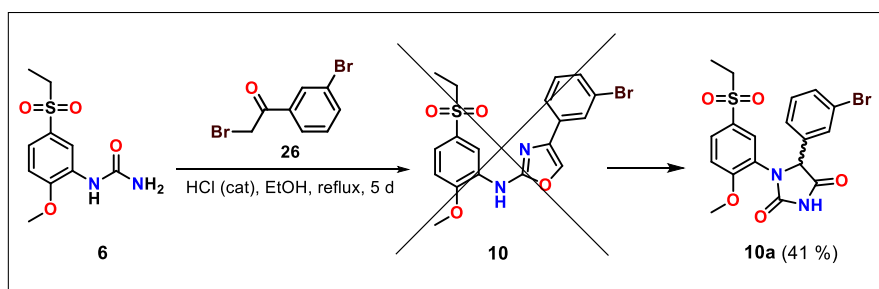


Scheme 26. Synthesis of VEGFR2 inhibitor **BM7** performed by Stille coupling reaction followed by acidic hydrolysis of a THP group.

9.2. Synthesis of *N*,4-diaryloxazole-2-amine precursor (10)

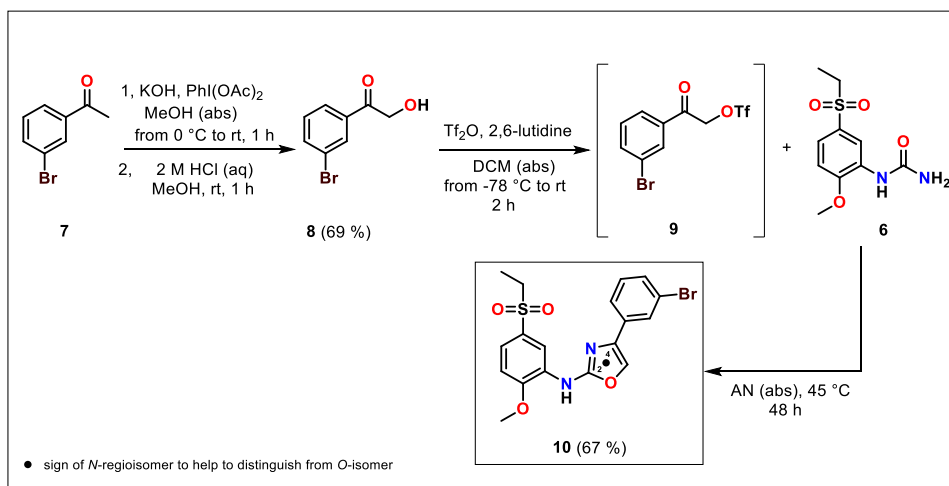
Based on available data from literature the most common procedure for preparation of *N*,4-diaryloxazole-2-amines is heterocyclization between α -bromoacetophenones and arylureas under various conditions (see in the chapter 4 of this dissertation thesis). Following the most promising described procedures, we were not able to prepare the desired *N*,4-diaryloxazole-2-amine **10**. Instead of that, our colleagues confirmed 1,5-diarylimidazoline-2,4-dione **10a** and so our group accidentally developed a novel synthesis of a hydatoxin compounds. The structure of **10a** has been confirmed also by an X-ray analysis.⁷⁰ (Scheme 27)

⁷⁰ Synthesis was developed by Maroš Smolíček and Peter Šramel. See in: Peter Šramel, *Dissertation Thesis 2017*, Comenius University in Bratislava, Slovakia and Université de Strasbourg, France.



Scheme 27. Unexpected formation of hydantoin **10a** instead of desired *N*,4-diaryloxazole-2-amine precursor **10**.

Based on the proposed mechanism we decided to replace an alpha bromine in **26** with a more reactive TfO- group. The better leaving group could favor formation of the oxazole **10** instead of the hydantoin **10a**. Our synthesis started from acetophenone **7**, which underwent α -oxidation with $\text{PhI}(\text{OAc})_2$ subsequently and hydrolysis to give **8** in 69 % yield. Reaction of **8** with triflic anhydride in a presence of 2,6-lutidine provided triflate **9**. Because of generally low stability of triflates, compound **9** was used in the next step without further purification. In addition, triflate **9** due to its instability had to be added portionwise to the reaction mixture at 45 °C every 12 h within 2 days. Resulting *N*,4-diaryloxazole-2-amine precursor **10** was obtained with 67 % yield and its structure was finally verified by an X-ray analysis. (Scheme 28 and Figure 42)



Scheme 28. Synthesis of general *N*,4-diaryloxazole-2-amine precursor **10** using triflate **9** and arylurea **6**.

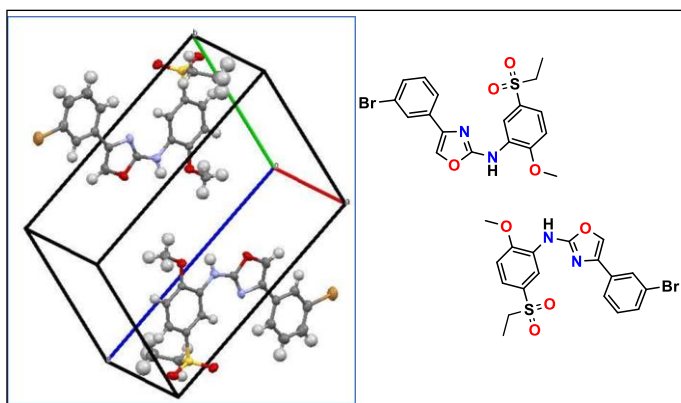
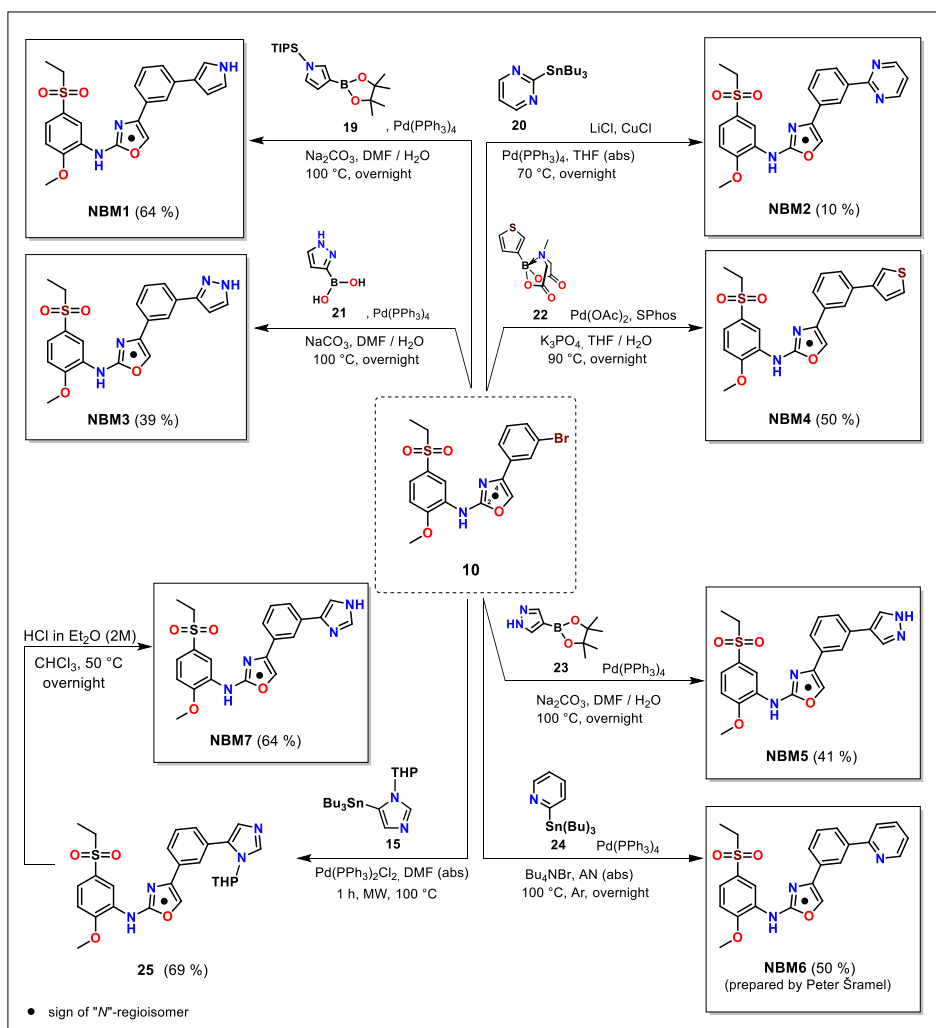


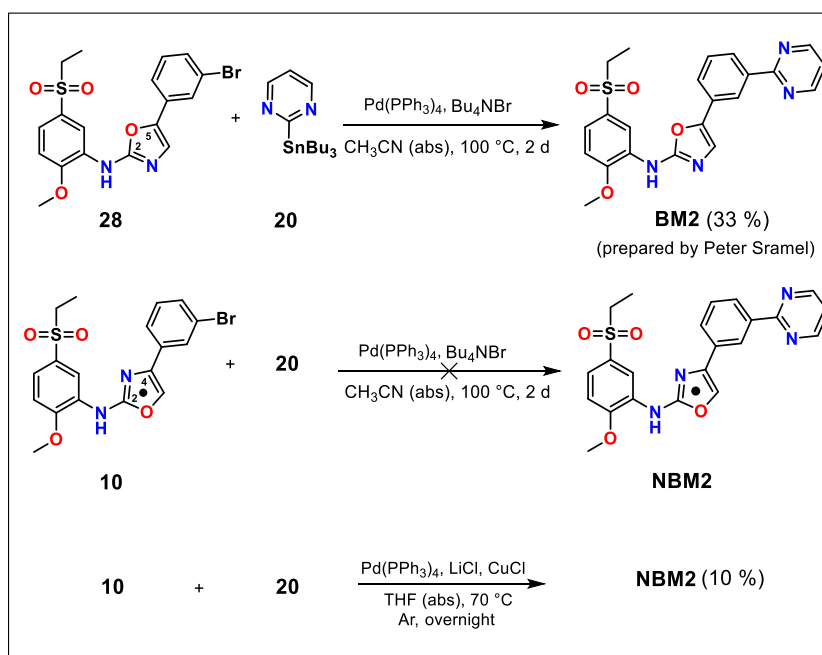
Figure 42. X-ray analysis of compound **10**.

The last part of **NMB(1-7)** preparation was successfully carried out by palladium-catalyzed coupling reactions. The obtained joint *N*,4-diaryloxazole-2-amine precursor **10** underwent Stille or Suzuki coupling reactions with particular boronic acid or ester reagent **19**, **21**, **22** and **23** or stannanes **15**, **20** and **24**. Each performed coupling reaction gave similar or slightly lower yield of products compare to their *O*-regioisomeric *N*,5-diaryloxazole-2-amines **BM(1,3-7)**.⁶⁸ (Figure 39 and Scheme 29)



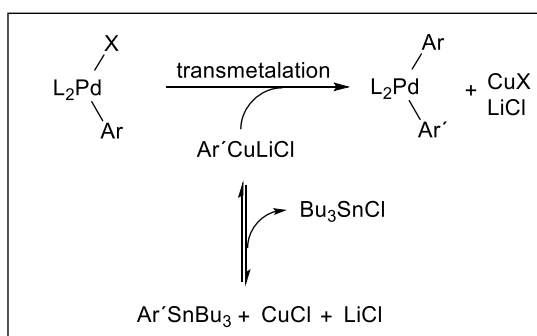
Scheme 29. Synthesis of *N*,4-diaryloxazol-2-amine VEGFR2 TK inhibitors **NBM(1-7)**.

Synthesis of the pyrimidine inhibitor **NBM2** with the same reaction conditions as in the synthesis of its regioisomeric compound **BM2** was the most problematic. Addition of cocatalysts CuCl / LiCl promoted the Stille coupling reaction and allowed to obtain **NBM2** in at least 10 % yield. (Scheme 30)



Scheme 30. Comparison of reactivity of both regioisomers **28** and **10** in Stille coupling reactions.

The function of CuCl / LiCl mixture as a promoter in Stille coupling reaction was described in the literature.⁷¹ Less reactive arylstannane is converted to a more reactive arylcopper(I) compound, that enters the transmetalation step. (Scheme 31)

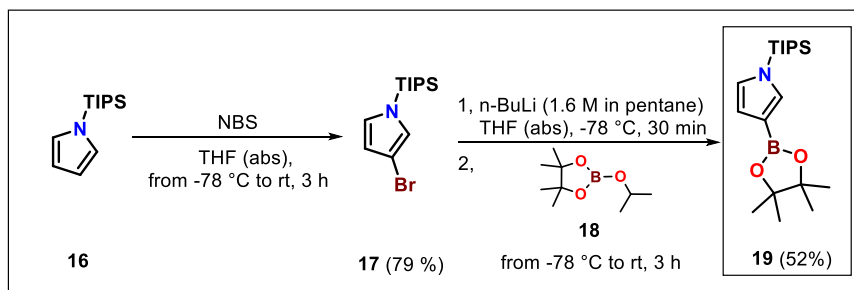


Scheme 31. The function of CuCl / LiCl mixture in Stille coupling.

All coupling reagents except of tributylstannylimidazole **15** and pyrrole pinacol boronic ester **19** were commercially available. Preparation of tributylstannylimidazole **15** was previously described on Scheme 25. Pyrrole pinacol boronic ester **19** was synthesized in two steps. In the first step, *N*-protected imidazole **16** was brominated with freshly crystalized NBS (1.00 mol eq) at -78 °C. Low temperature was required to avoid formation of its thermodynamically more

⁷¹ Han, X.; Stoltz, B.M.; Corey, E.J. *J. Am. Chem. Soc.*, **1999**, *121*, 7600 - 7605.

favourable α -brominated regioisomer. By this method, brominated imidazole **17** was obtained in 79 % yield together with traces of its regioisomer. In the next step, metalation of bromimidazole **17** with *n*-BuLi and subsequent reaction with boronic ester **18** afforded pinacol boronate **19** in 52 % yield. (Scheme 32)



Scheme 32. Synthesis of pyrrole pinacol boronate reagent **19**.

9.3. Determination of biological activity and evaluation of the project

Within this project I have successfully prepared inhibitor **BM7** and six *N*-regioisomeric pairs **NBM(1-5,7)** to the *N*,5-diaryloxazole-2-amine (*O*-regioisomeric) inhibitors **BM(1-7)**. We also determined the most of their *in vitro* IC₅₀ (VEGFR2 TK) activities.²⁶ Inhibitory activity of imidazole derivatives **BM7** and **NBM7** remain to be determined. All *N*,4-diaryloxazole-2-amine inhibitors **NBM(1-6)** exhibited lower inhibitory IC₅₀ activity (micromolar range) in comparison to their nM regioisomeric pairs **BM(1-7)**. (Figure 43) All VEGFR2 TK inhibitors **BM(1-7)** and **NBM(1-7)** are predicted to bind a kinase active pocket in their “U” shaped conformation compare to the expected more relaxed “L” shaped conformation in solution. Accordingly, for all inhibitors a conformation penalty is expected. In case of *N*-regioisomers the lower activity can be explained also by weaker H-bond between an oxygen from oxazole and Cys917 compare to H-bond of *O*-regioisomers between a nitrogen from an oxazole and the same backbone amino acids. Within this part the Biomagi hypothesis was confirmed and both regioisomers are VEGFR2 TK inhibitors.

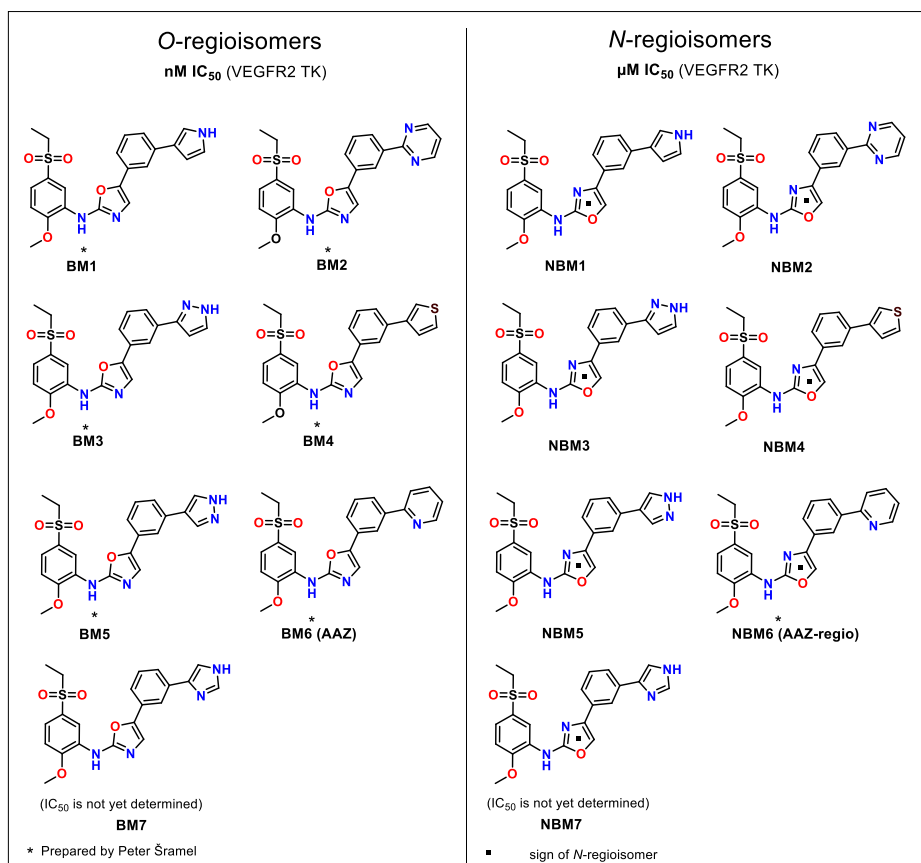
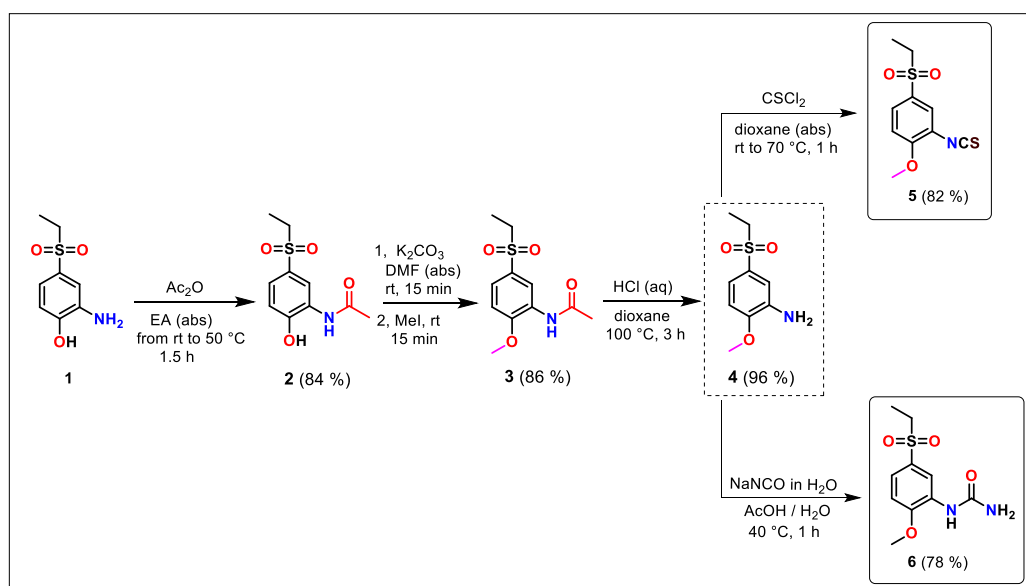


Figure 43. Comparison of structures and activities of *O*-regioisomers **BM(1-7)** with their regioisomeric partners **NBM(1-7)**.

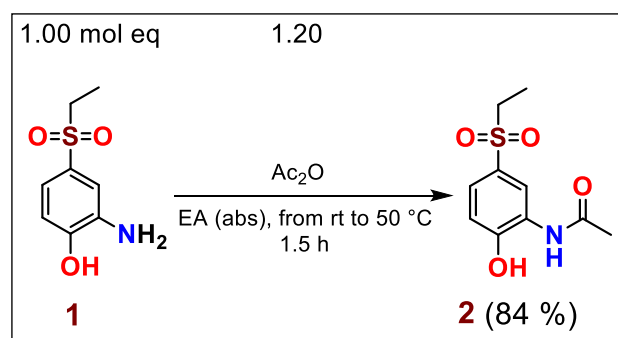
9.4. Experimental part

9.4.1. Synthesis of isothiocyanate (5) and urea (6)



Scheme 33. Synthesis of intermediates: isothiocyanate **5** and urea **6**.

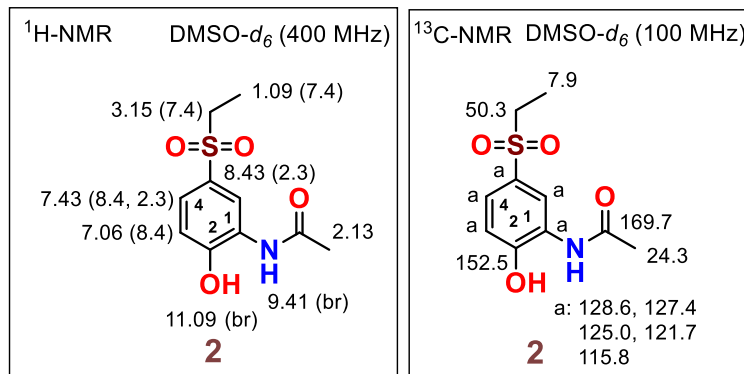
Synthesis of *N*-[5-(ethylsulfonyl)-2-hydroxyphenyl]acetamide (**2**)



To a solution of 3.00 g (14.9 mmol, 1.00 mol eq) 2-amino-4-(ethylsulfonyl)phenol (**1**) in 50 mL of EA (abs), acetic anhydride 1.69 mL (17.9 mmol, 1.20 mol eq) was added within 10 min under Ar. Then the mixture was stirred 1.5 h at 50 °C. Within this time grey solid material was precipitated. The mixture was cooled to rt and stirred in an ice bath for 20 min. Obtained solid material was filtered off, washed with H₂O and dried under reduced pressure to yield 3.05 g (12.5 mmol, 84 %) of desired aniline **2**.

Novelty: *N*-[5-(ethylsulfonyl)-2-hydroxyphenyl]acetamide (**2**) is not described in the literature.

M.p.: 237.9 - 240.2 °C [EA].



¹H-NMR (400 MHz, DMSO-*d*₆): δ 11.09 (br s, 1H, -OH), 9.41 (br s, 1H, -NH-), 8.43 (d, 1H, $J(4,6) = 2.3$ Hz, H-C(6)), 7.43 (dd, 1H, $J(3,4) = 8.4$ Hz, $J(4,6) = 2.3$ Hz, H-C(4)), 7.06 (d, 1H, $J(3,4) = 8.4$ Hz, H-C(3)), 3.15 (q, 2H, $J(\text{CH}_2, \text{CH}_3) = 7.4$ Hz, $\text{CH}_3\text{CH}_2\text{SO}_2^-$), 2.13 (s, 3H, $\text{CH}_3\text{CO}-$), 1.09 (t, 3H, $J(\text{CH}_2, \text{CH}_3) = 7.4$ Hz, $\text{CH}_3\text{CH}_2\text{SO}_2^-$).

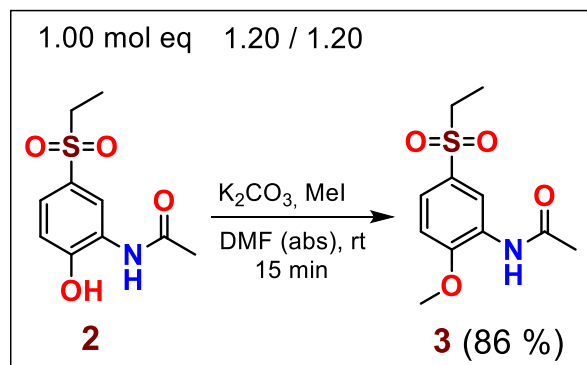
¹³C-NMR (100 MHz, DMSO-*d*₆): δ 169.7 ($\text{CH}_3\text{CO}-$), 152.5 C(2), 128.6, 127.4, 125.0, 121.7, 115.8, 50.3 ($\text{CH}_3\text{CH}_2\text{SO}_2^-$), 24.3 ($\text{CH}_3\text{CO}-$), 7.9 ($\text{CH}_3\text{CH}_2\text{SO}_2^-$).

FT-IR (solid, cm^{-1}): 3410 (w), 2855 (w), 2611 (w), 2112 (w), 1655 (m), 1581 (m), 1533 (m), 1418 (s), 1370 (m), 1276 (s), 1243 (m), 1143 (m), 1114 (s), 1079 (s), 1023 (m), 922 (w), 825 (w), 784 (m), 736 (s), 645 (m), 609 (s), 577 (m), 529 (s), 489 (s), 456 (m).

MS (ESI m/z): 242.0 $[\text{M}-\text{H}]^-$ (negative mode).

Anal. calcd for $\text{C}_{10}\text{H}_{13}\text{NO}_4\text{S}$ (243.28): C, 49.37; H, 5.39; N, 5.76; Found: C, 49.50; H, 5.48; N, 5.82.

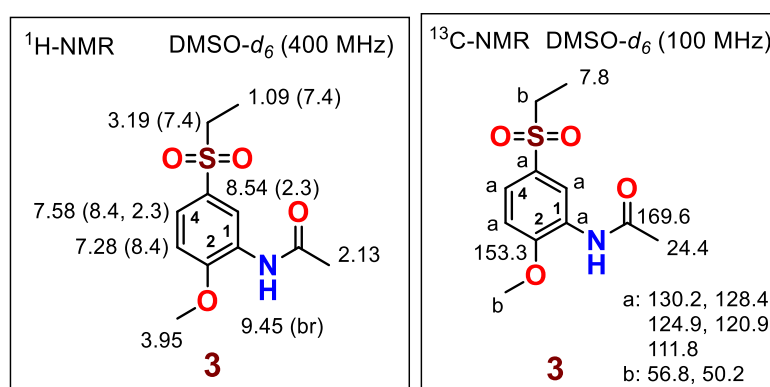
Synthesis of *N*-[5-(ethylsulfonyl)-2-methoxyphenyl]acetamide (**3**)



To a solution of 750 mg (3.09 mmol, 1.00 mol eq) acetamide **2** in 10 mL DMF (abs), 511 mg (3.70 mmol, 1.20 mol eq) of K_2CO_3 was added and the mixture stirred for 5 min at rt under Ar. Afterwards, 231 μ l (3.70 mmol, 1.20 mol eq) of MeI was added dropwise over 5 min and the mixture was stirred for another 10 min. Subsequently TLC analysis confirmed a presence of only one new spot. Then 50 mL of brine was added and the mixture extracted with EA (5 x 10 mL). Combined organic layer was dried over Na_2SO_4 , filtered and filtrate concentrated under vacuum to yield 682 mg (2.65 mmol, 86 %) of acetamide **3** in form of a dark solid material.

Novelty: *N*-[5-(ethylsulfonyl)-2-methoxyphenyl]acetamide (**3**) is not described in the literature.

M.p.: 140 - 150 °C [EA] (dec).



¹H-NMR (400 MHz, DMSO-*d*₆): δ 9.45 (br s, 1H, -NH-), 8.54 (d, 1H, $J(4,6) = 2.3$ Hz, H-C(6)), 7.58 (dd, 1H, $J(3,4) = 8.4$ Hz, $J(4,6) = 2.3$ Hz, H-C(4)), 7.28 (d, 1H, $J(3,4) = 8.4$ Hz, H-C(3)),

3.95 (s, 3H, CH₃O-), 3.19 (q, 2H, $J(\text{CH}_2, \text{CH}_3) = 7.4$ Hz, CH₃CH₂SO₂-), 2.13 (s, 3H, CH₃CO-), 1.09 (t, 3H, $J(\text{CH}_2, \text{CH}_3) = 7.4$ Hz, CH₃CH₂SO₂-).

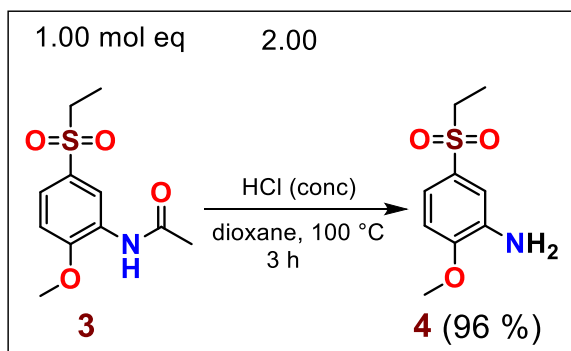
¹³C-NMR (100 MHz, DMSO-*d*₆): δ 169.6 (CH₃C=O-), 153.3 C(2), 130.2, 128.4, 124.9, 120.9, 111.8, 56.8, 50.2, 24.4 (CH₃CO-), 7.8 (CH₃CH₂SO₂-).

FT-IR (solid, cm⁻¹): 3405 (m), 3082 (w), 2985 (w), 2927 (w), 1890 (w), 1685 (s), 1592 (s), 1523 (s), 1468 (s), 1412 (s), 1366 (m), 1340 (w), 1298 (s), 1262 (s), 1241 (s), 1122 (s), 1079 (s), 1017 (s), 886 (m), 824 (m), 793 (m), 775 (s), 729 (s), 636 (m), 604 (s), 565 (s), 524 (s), 489 (s), 441 (m).

MS (ESI *m/z*): 256.0 [M-H]⁻ (negative mode).

Anal. calcd for C₁₁H₁₅NO₄S (257.30): C, 51.35; H, 5.88; N, 5.44; Found: C, 51.55; H, 6.15; N, 5.80.

Synthesis of 5-(ethylsulfonyl)-2-methoxyaniline (4)

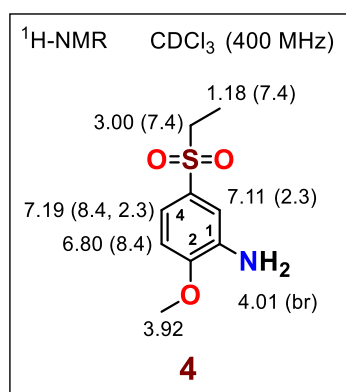


To a solution of 2.29 g (8.91 mmol, 1.00 mol eq) acetamide **3** in 50 mL of dioxane, 1.57 mL (17.8 mmol, 2.00 mol eq) of HCl (conc) was added dropwise by stirring for 3 h at 100 °C. Then the reaction mixture was cooled down and volatile parts evaporated by RVO. The obtained crude product was dissolved in 50 mL of EA and extracted with 1 % solution of NaHCO₃ (5 x 15 mL). Combined organic layer was dried over Na₂SO₄, filtered and the filtrate concentrated

under reduced pressure to yield 1.843 g (8.57 mmol, 96 %) of aniline **4** in form of a grey solid material.

Novelty: 5-(ethylsulfonyl)-2-methoxyaniline (**4**) is described in the literature by its M.p., ¹H-NMR, ¹³C-NMR, IR, MS and elemental analysis.⁷²

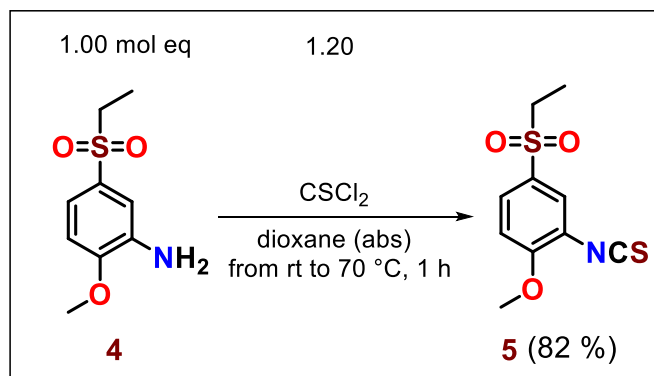
M.p.: 96.0 - 98.9 [EA] (lit.: 102.9 - 103.8 [MeOH]).⁷²



¹H-NMR (400 MHz, CDCl₃): δ 7.19 (dd, 1H, $J(3,4) = 8.4$ Hz, $J(4,6) = 2.3$ Hz, H-C(4)), 7.11 (d, 1H, $J(4,6) = 2.3$ Hz, H-C(6)), 6.80 (d, 1H, $J(3,4) = 8.4$ Hz, H-C(3)), 4.01 (br s, 2H, -NH₂), 3.92 (s, 3H, CH₃O-), 3.00 (q, 2H, $J(\text{CH}_2, \text{CH}_3) = 7.4$ Hz, CH₃CH₂SO₂-), 1.18 (t, 3H, $J(\text{CH}_2, \text{CH}_3) = 7.4$ Hz, CH₃CH₂SO₂-).

⁷² Murár, M.; Addová, G.; Boháč, A. *Beilstein J. Org. Chem.*, **2013**, 9, 173-179.

4-(Ethylsulfonyl)-2-isothiocyanato-1-methoxybenzene (5)

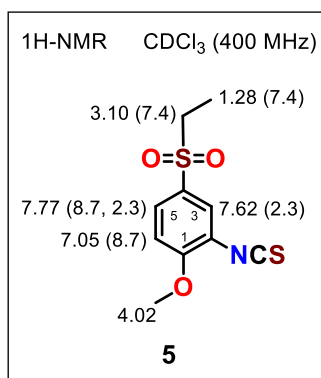


To a solution of 1.00 g (4.65 mmol, 1.00 mol eq) aniline **4** in 20 mL dioxane (abs), 428 μL (5.58 mmol, 1.20 mol eq) of thiophosgene (CSCI_2) was added dropwise within 30 min. Then the reaction mixture was stirred 1 h at 70 $^\circ\text{C}$. After complete consumption of aniline **4**, the reaction mixture was cooled down, 20 mL of NaHCO_3 (saturated aq solution) was added and stirred for 5 min. Subsequently, dioxane and volatile parts were evaporated and 40 mL of EA added. The obtained solution was extracted with 3 x 15 mL of NaHCO_3 (saturated aq solution) and brine (3 x 15 mL). The organic layer was separated, dried over Na_2SO_4 , filtered and concentrated under reduced pressure. Resulted oily crude product was stored in a refrigerator to provide 980 mg (3.81 mmol, 82 %) of 4-(ethylsulfonyl)-2-isothiocyanato-1-methoxybenzene (**5**) in the form of a grey solid compound.

Novelty: 4-(ethylsulfonyl)-2-isothiocyanato-1-methoxybenzene (**5**) is described in the literature by its M.p., $^1\text{H-NMR}$, $^{13}\text{C-NMR}$, IR, MS and elemental analysis.⁷³

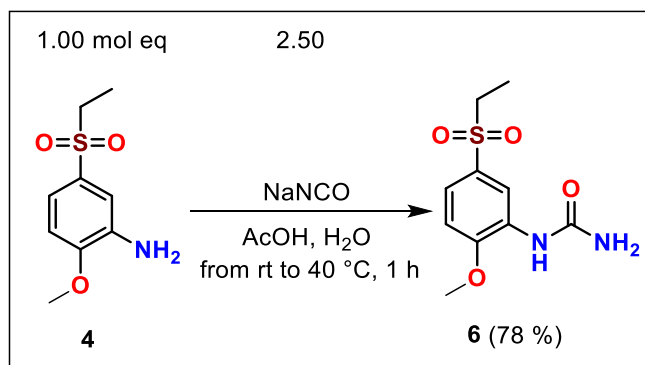
M.p.: 106.5 - 109.8 $^\circ\text{C}$ [H / EA] (lit.: 108.0 – 110.0 [H / EA]).⁷³

⁷³ Murár, M.; Dobiaš, J.; Šramel, P.; Addová, G.; Hanquet, G.; Boháč, A. *Eur. J. Med. Chem.*, **2017**, *126*, 754 - 761.



¹H-NMR (400 MHz, CDCl₃): δ 7.77 (dd, 1H, $J(5,6) = 8.7$ Hz, $J(3,5) = 2.3$ Hz, H-C(5)), 7.62 (d, 1H, $J(3,5) = 2.3$ Hz, H-C(3)), 7.05 (d, 1H, $J(5,6) = 8.7$ Hz, H-C(6)), 4.02 (s, 3H, -OCH₃), 3.10 (q, 2H, $J(\text{CH}_2, \text{CH}_3) = 7.4$ Hz, -COOCH₂CH₃), 1.28 (t, 3H, $J(\text{CH}_2, \text{CH}_3) = 7.4$ Hz, -COOCH₂CH₃).

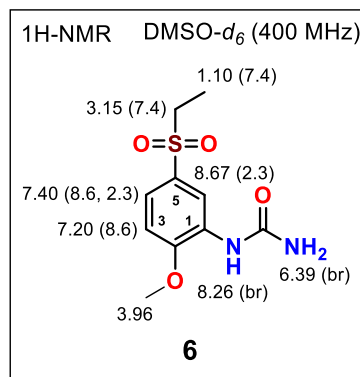
1-[5-(Ethylsulfonyl)-2-methoxyphenyl]urea (6)



To 2.00 g (9.30 mmol, 1.00 mol eq) of aniline **4**, dissolved in a mixture of 20 mL CH₃COOH and 15 mL of H₂O, a solution of 1.51 g (23.2, 2.50 mol eq) NaNCO in 10 mL of H₂O was slowly added and the mixture was heated at 40 °C for 1 h. The reaction was diluted with H₂O, placed into an ice bath while the formation of precipitate occurred. Resulted precipitate was filtered, washed with water and dried under reduced pressure yielding 1.88 g (7.29 mmol, 78 %) of 1-(5-(ethylsulfonyl)-2-methoxyphenyl)urea **6** as a grey solid material.

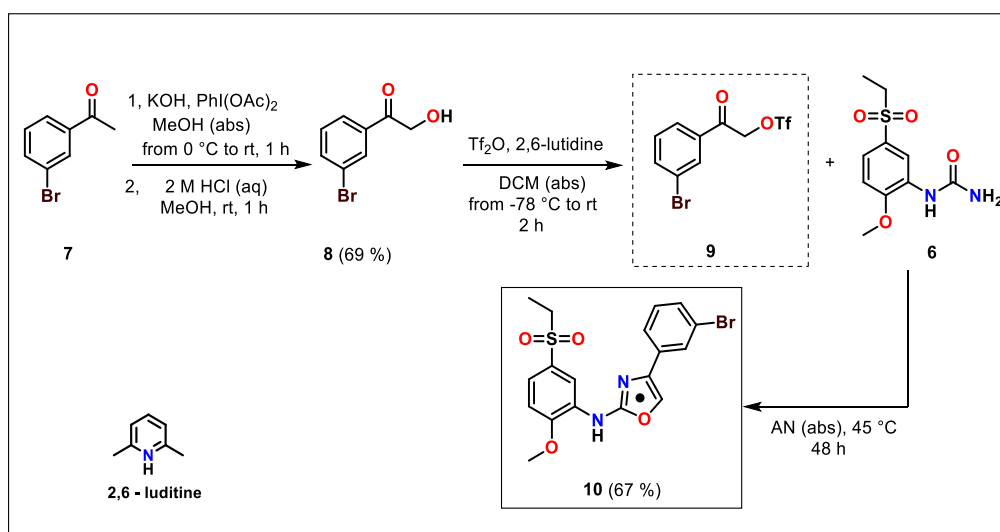
Novelty: 1-[5-(ethylsulfonyl)-2-methoxyphenyl]urea (**6**) is described in the literature by its ^1H -NMR, ^{13}C -NMR, IR spectra and elemental analysis.⁷⁴

M.p.: 196.0 - 197.0 °C [$\text{H}_2\text{O} / \text{H}^+$]. (lit. 198 - 199 °C [EA]).⁷⁴



^1H -NMR (400 MHz, DMSO- d_6): δ 8.67 (d, 1H, $J(4,6) = 2.3$ Hz, H-C(6)), 8.26 (br s, 1H, -NHCONH $_2$), 7.40 (dd, 1H, $J(3,4) = 8.6$ Hz, $J(4,6) = 2.3$ Hz, H-C(4)), 7.20 (d, 1H, $J(3,4) = 8.6$ Hz, H-C(3)), 6.39 (br s, 2H, -NHCONH $_2$), 3.96 (s, 3H, -OCH $_3$), 3.15 (q, 2H, $J(\text{CH}_2, \text{CH}_3) = 7.4$ Hz, -COOCH $_2$ CH $_3$), 1.10 (t, 3H, $J(\text{CH}_2, \text{CH}_3) = 7.4$ Hz, -COOCH $_2$ CH $_3$).

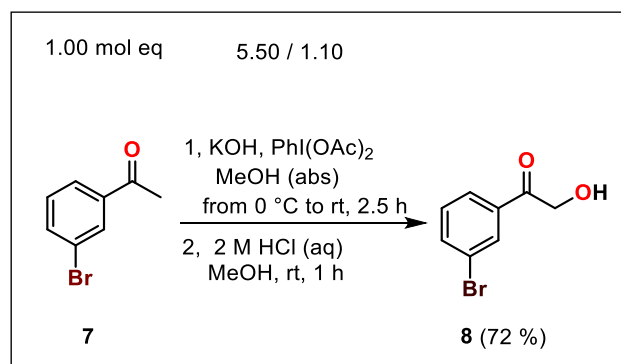
8.4.2. Synthesis of *N*,4-diaryloxazole-2-amine general intermediate (**10**)



Scheme 34. Synthesis of *N*,4-diaryloxazole-2-amine general intermediate **10**.

⁷⁴ Lintnerová, L.; Kováčiková, L.; Hanquet, G.; Boháč, A. *J. Heterocyclic. Chem.* **2015**, *52*, 425 – 439.

Synthesis of 1-(3-bromophenyl)-2-hydroxyethan-1-one (8)

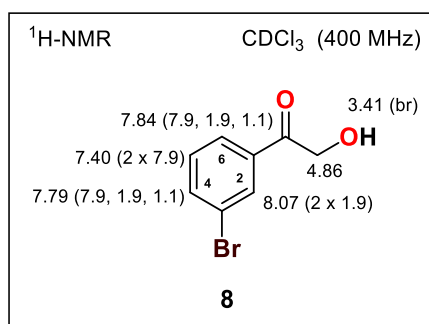


To a solution of 4.64 g (82.7 mmol, 5.50 mol eq) KOH in 40 mL of MeOH (abs), 3.00 g (15.1 mmol, 1.00 mol eq) of acetophenone **7**, dissolved in ca 50 mL of MeOH (abs), was added and cooled to 0 °C. Afterwards, 5.34 g (16.6 mmol, 1.10 mol eq) of PhI(OAc)₂ was added portionwise within 10 min and stirred for another 10 min at the same temperature. After 2.5 h of stirring at rt, TLC analysis confirmed presence of a new product with traces of two side products. Reaction mixture was evaporated with RVE, resulting solid material was diluted in 70 mL of EA and 20 mL of H₂O and subsequently extracted with H₂O (3 x 40 mL). Obtained crude oil was dissolved in 20 mL of MeOH and 15 mL of 2 M HCl (aq) was added. After 30 min of stirring at rt, yellow precipitate was obtained and mixture was stirred for another 30 min in an ice bath. Yellow precipitate was filtered off and washed with cHex to yield 2.34 g (10.8 mmol, 72 %) of hydroxyketone **8** as a white solid material.

Novelty: 1-(3-bromophenyl)-2-hydroxyethan-1-one (**8**) is described in literature together with its M.p., ¹H-NMR, ¹³C-NMR, IR, HRMS, ESI and LCMS spectra.⁷⁵

M.p.: 104.2 - 107.1 °C [MeOH], (lit. 104 - 106 °C).⁷⁵

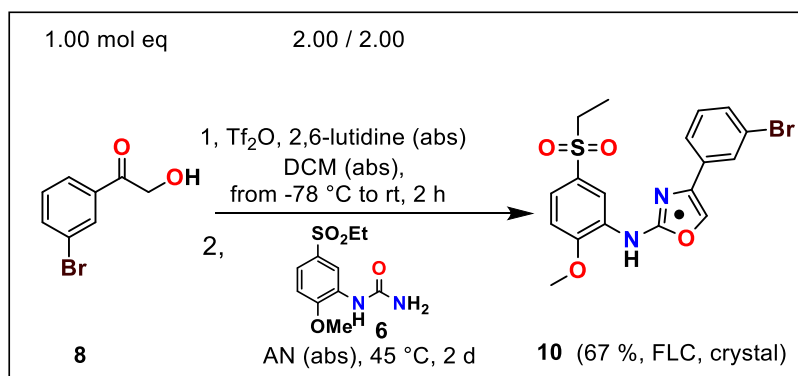
⁷⁵ Demir, A.S.; Ayhan, P.; Igdır, A.C.; Duygu, A.N. *Tetrahedron*, **2004**, *60*, 6509 - 6512.



¹H-NMR (400 MHz, CDCl₃): δ 8.07 (dd, 1H, $J(2,4) = J(2,6) = 1.9$ Hz, H-C(2)), 7.84 (ddd, 1H, $J(5,6) = 7.9$ Hz, $J(2,6) = 1.9$ Hz, $J(4,6) = 1.1$ Hz, H-C(6)), 7.79 (ddd, 1H, $J(4,5) = 7.9$ Hz, $J(2,4) = 1.9$ Hz, $J(4,6) = 1.1$ Hz, H-C(4)), 7.40 (dd, 1H, $J(4,5) = J(5,6) = 7.9$ Hz, H-C(5)), 4.86 (s, 2H, -COCH₂OH), 3.41 (br s, 1H, -OH)

Synthesis of 4-(3-bromophenyl)-*N*-[5-(ethylsulfonyl)-2-methoxyphenyl]oxazol-2-amine

(10)



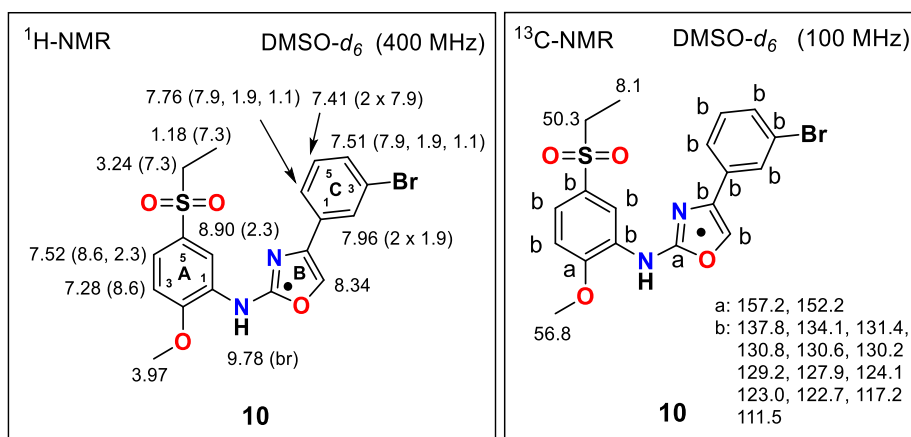
1st step: Acetophenone **8** 1.50 g (6.98 mmol, 1.00 mol eq) was dissolved in 50 mL of DCM (abs) and cooled to - 78 °C. At this temperature 1.62 mL (13.96 mmol, 2.00 mol eq) of 2,6-lutidine was added with subsequent dropwise addition of 2.35 mL (13.96 mmol, 2.00 mol eq) of Tf₂O. Reaction mixture was stirred for 2 h while its temperature rose up to rt. Afterwards, volatile parts were evaporated with RVE and obtained crude intermediate used in the next step without further purification.

2nd step: Urea **6** 500 mg (1.95 mmol, 1.00 mol eq) was dissolved in 40 mL of AN (abs). Previously prepared intermediate (triflate, not shown) was added portionwise every 12 h within

2 days. After that, TLC analysis confirmed presence of a new product, traces of hydroxyketone **8**, starting urea **6** and two side products. Desired oxazole **10** was purified by FLC (SiO₂, EA / cHex = 1 / 1) and by crystallization (EA / cHex) to yield 570 mg (1.30 mmol, 67 %) of oxazole **10**.

Novelty: 4-(3-bromophenyl)-*N*-[5-(ethylsulfonyl)-2-methoxyphenyl]oxazol-2-amine (**10**) is not yet described in the literature.

M.p.: 135.0 - 139.1 °C [EA / cHex].



¹H-NMR (400 MHz, DMSO-*d*₆): δ 9.78 (br s, 1H, -NH-), 8.90 (d, 1H, *J*(A₄,A₆) = 2.3 Hz, H-C_A(6)), 8.34 (s, 1H, H-C_B(5)), 7.96 (dd, 1H, *J*(C₂,C₄) = *J*(C₂,C₆) = 1.9 Hz, H-C_C(2)), 7.76 (ddd, 1H, *J*(C₅,C₆) = 7.9 Hz, *J*(C₂,C₆) = 1.9 Hz, *J*(C₄,C₆) = 1.1 Hz, H-C_C(6)), 7.52 (dd, 1H, *J*(A₃,A₄) = 8.6 Hz, *J*(A₄,A₆) = 2.3 Hz, H-C_A(4)), 7.51 (ddd, 1H, *J*(C₄,C₅) = 7.9 Hz, *J*(C₂,C₄) = 1.9 Hz, *J*(C₄,C₆) = 1.1 Hz, H-C_C(4)), 7.41 (dd, 1H, *J*(C₄,C₅) = *J*(C₅,C₆) = 7.9 Hz, H-C_C(5)), 7.28 (d, 1H, *J*(A₃,A₄) = 8.6 Hz, H-C_A(3)), 3.97 (s, 3H, CH₃O-), 3.24 (q, 2H, *J*(CH₂,CH₃) = 7.3 Hz, CH₃CH₂SO₂-), 1.18 (t, 3H, *J*(CH₂,CH₃) = 7.3 Hz, CH₃CH₂SO₂-).

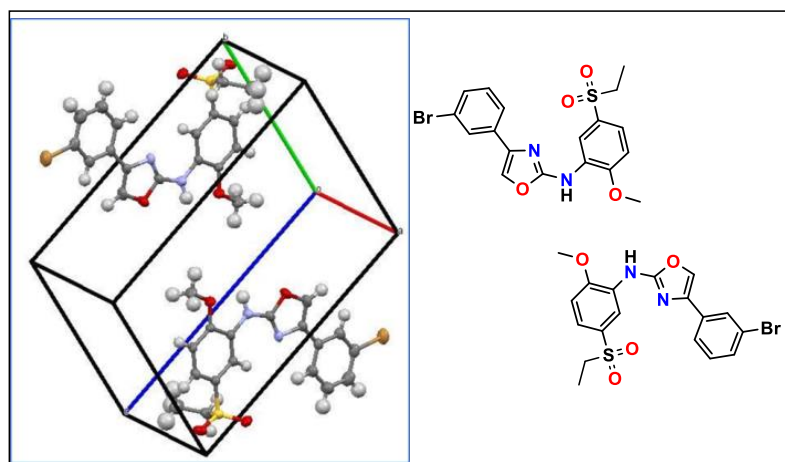
¹³C-NMR (100 MHz, DMSO-*d*₆): δ 157.2, 152.2, 137.8, 134.1, 131.4, 130.8, 130.6, 130.2, 129.2, 127.9, 124.1, 123.0, 122.7, 117.2, 111.5, 56.8 (CH₃O-), 50.3 (CH₃CH₂SO₂-), 8.1 (CH₃CH₂SO₂-).

FT-IR (solid, cm^{-1}): 3327 (m), 2936 (w), 2842 (w), 1624 (m), 1598 (m), 1577 (s), 1532 (s), 1492 (m), 1460 (m), 1426 (m), 1347 (w), 1300 (s), 1265 (s), 1224 (m), 1124 (s), 1080 (m), 1021 (m), 928 (w), 883 (m), 817 (m), 771 (w), 720 (s), 650 (w), 615 (w), 564 (m), 499 (s), 459 (m), 436 (m).

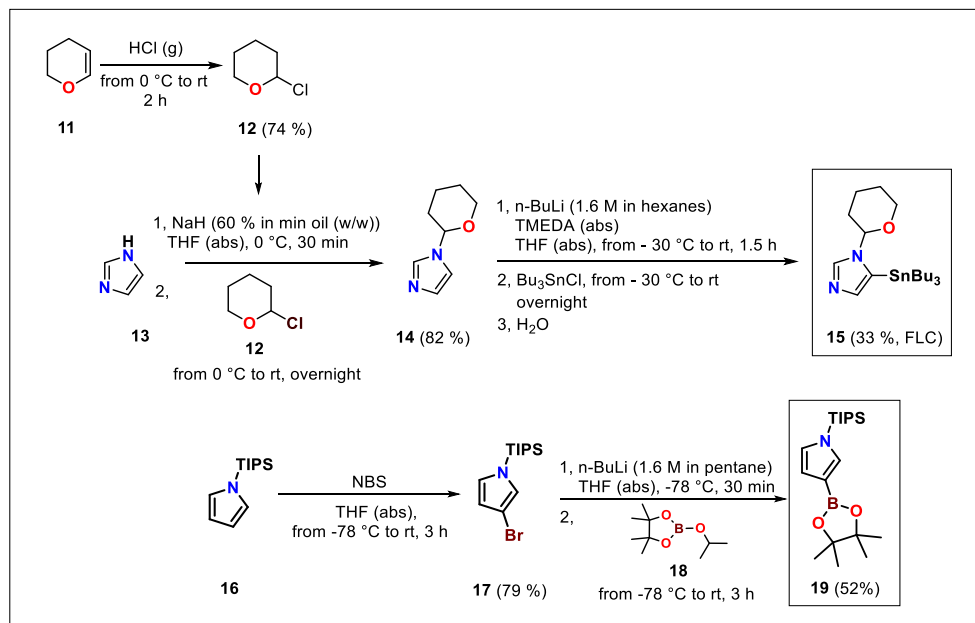
MS (ESI m/z): 437.0 (100 % for Br^{79}) $[\text{M}+\text{H}]^+$, 439.0 (85 % for Br^{81}) $[\text{M}+\text{H}]^+$ (positive mode).

Anal. calcd for $\text{C}_{18}\text{H}_{17}\text{BrN}_2\text{O}_4\text{S}$ (437.31): C, 49.44; H, 3.92; N, 6.41; Found: C, 49.56; H, 4.01; N, 6.60.

X-ray analysis:

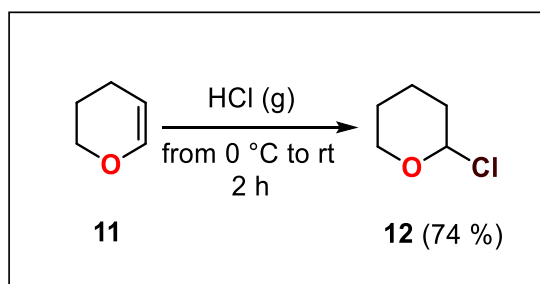


9.4.2. Synthesis of tributylstannylimidazole (15) and pyrrol pinacol boronic ester (19) coupling partners



Scheme 35. Synthesis of tributylstannylimidazole **15** and pyrrole pinacol boronate **19** as coupling intermediates.

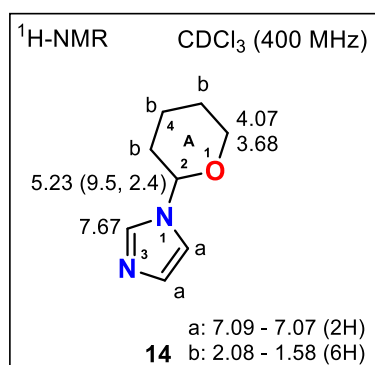
Synthesis of 2-chlorotetrahydro-2H-pyran (**12**)



In the first step gaseous HCl was generated *in situ* by adding conc. H₂SO₄ dropwise to sodium chloride in a two-neck round-bottom flask. Generated gas was bubbled through a stirred solution of 7.00 g (83.3 mmol) of 3,4-dihydro-2H-pyran (DHP, **11**) in a sealed tube at 0 °C for 1 h and another 1 h at room temperature. Resulting dark brown solution was distilled under reduced pressure (50 °C at 23 mbar) yielding 7.40 g (61.7 mmol, 74 %,) of 2-chlorotetrahydro-2H-pyran **12** as colorless liquid. Obtained compound is unstable and was used directly in a next step.

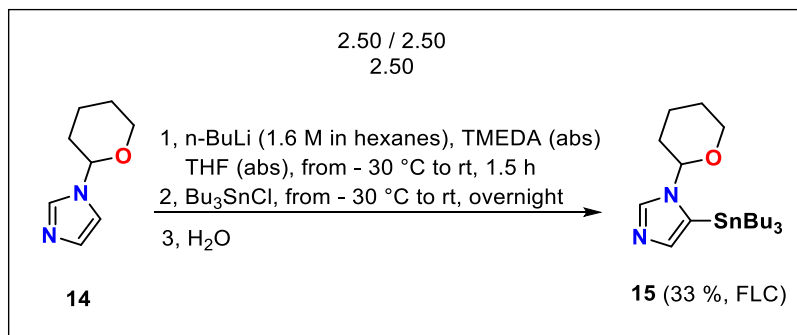
the reaction mixture at 0 °C and stirred overnight at rt. The reaction was quenched with ice at 0 °C, extracted with Et₂O (3 x 15 mL), dried over Na₂SO₄, filtered and concentrated under reduced pressure. An obtained red oily product was purified by vacuum distillation (130 °C at 1 mbar) to provide 4.27 g (2.81 mmol, 82 %) of protected imidazole **14** as a white waxen compound.

Novelty: 1-(tetrahydro-2*H*-pyran-2-yl)-1*H*-imidazole (**14**) is described in the literature by its ¹H-NMR, ¹³C-NMR and IR.⁷⁹



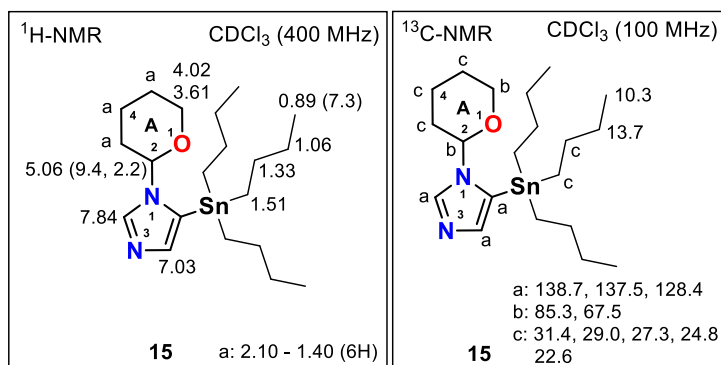
¹H-NMR (400 MHz, CDCl₃): δ 7.67 (s, 1H, H-C(2)), 7.09 – 7.07 (m, 2H, H-C(4 and 5)), 5.23 (dd, 1H, $J(A_2, A_3) = 9.5$ Hz, $J(A_2, A_3) = 2.4$ Hz, H-C_A(2)), 4.07 and 3.68 (2 x m, 2 x 1H, 2 x H-C_A(6)), 2.08 - 1.58 (m, 6H, 3 x -CH₂- from C_A(3)-C_A(5)).

⁷⁹ Primas, N.; Mahatsekake, C.; Bouillon, A.; Lancelot, J-Ch.; de Oliveira Santos, J.S.; Lohier, J-F.; Rault, S. *Tetrahedron*, **2008**, *64*, 4596 - 4601.

Synthesis of 1-(tetrahydro-2*H*-pyran-2-yl)-5-(tributylstannyl)-1*H*-imidazole (15)

A solution of imidazole **14** (900 mg, 5.92 mmol, 1.00 mol eq) in 10 mL of THF (abs) was added slowly at - 30 °C to a mixture of 9.25 mL (14.8 mmol, 2.50 mol eq) n-BuLi (1.6 M in hexanes) and 2.21 mL (14.8 mmol, 2.50 mol eq) of TMEDA (abs) in 15 mL of THF (abs). The reaction mixture was stirred for 30 min at the same temperature and 1 h at rt. Subsequently, reaction mixture was cooled down to - 30 °C and 4.00 mL (14.8 mmol, 2.50 mol eq) of Bu₃SnCl in 10 mL of THF (abs) was added dropwise and stirred for 20 min at the same temperature and overnight at rt. Then, the mixture was quenched with H₂O (30 mL) and extracted with EA (3 x 20 mL). Combined organic layer was washed with brine (3 x 15 mL), dried over Na₂SO₄, filtered and concentrated under reduced pressure. A crude product was purified by FLC (EA / cHex: gradient from 1 / 1 to 4 / 1) to afford 850 mg (1.93 mmol, 33 %) of imidazole **15** as a red oily material.

Novelty: 1-(tetrahydro-2*H*-pyran-2-yl)-5-(tributylstannyl)-1*H*-imidazole (**15**) is not described in the literature.



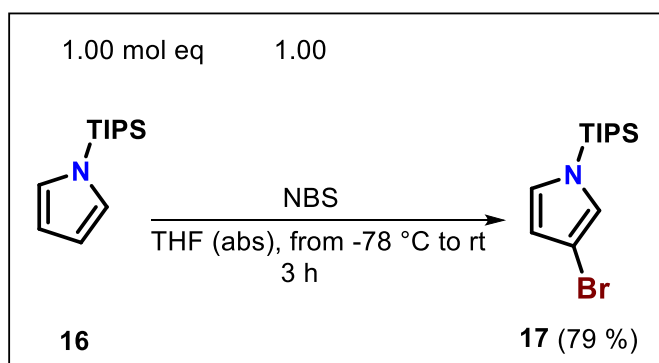
¹H-NMR (400 MHz, CDCl₃): δ 7.84 (s, 1H, H-C(2)), 7.03 (s, 1H, H-C(4)), 5.06 (dd, 1H, $J(A_2,A_3) = 9.5$ Hz, $J(A_2,A_3) = 2.4$ Hz, H-C_A(2)), 4.02 and 3.61 (2 x m, 2 x 1H, 2 x H-C_A(6)),

2.10 - 1.40 (m, 6H, 3 x -CH₂- from H-C_A(3)-C_A(5)), 1.51 (m, 2H, -SnCH₂CH₂-), 1.33 (m, 2H, -SnCH₂CH₂-), 1.06 (m, 2H, -CH₂CH₃), 0.89 (t, 3H, *J*(CH₂,CH₃) = 7.3 Hz, -CH₂CH₃).

¹³C-NMR (100 MHz, CDCl₃): 138.7, 137.5, 128.4, 85.3, 67.5, 31.4, 29.0, 27.3, 24.8, 22.6, 13.7 (-CH₂CH₃), 10.3 (-CH₂CH₃).

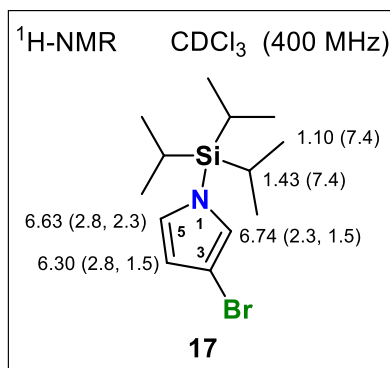
FT-IR (solid, cm⁻¹): 2954 (m), 2923 (s), 2852 (m), 1506 (w), 1464 (m), 1376 (w), 1357 (w), 1259 (w), 1240 (w), 1204 (w), 1177 (w), 1111 (w), 1083 (s), 1044 (s), 997 (m), 911 (m), 876 (m), 825 (m), 769 (w), 661 (s), 595 (m), 550 (w), 506 (w), 458 (w).

Synthesis of 3-bromo-1-(triisopropylsilyl)-1*H*-pyrrole (17)



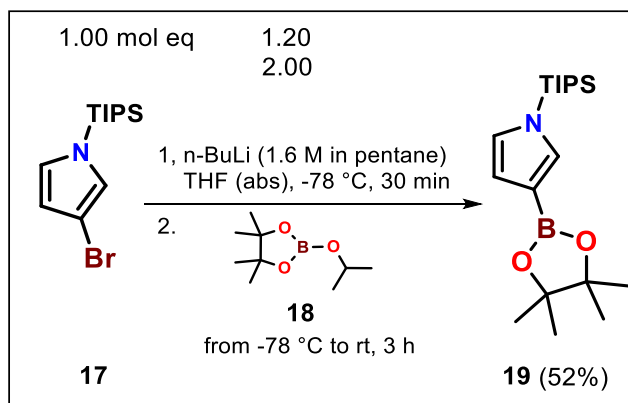
A solution of 1.00 g (4.48 mmol, 1.00 mol eq) of pyrrole **16** in 15 mL of THF (abs) was cooled to -78 °C. Subsequently 797 mg (4.48 mmol, 1.00 mol eq) of freshly crystallized NBS was added portionwise to the reaction mixture. Resulting solution was stirred for 1.5 h at the same temperature and another 1.5 h at room temperature. Afterwards, the reaction was quenched with NaHCO₃ (sat aq solution), extracted with Et₂O (3 x 15 mL), combined organic layer washed with brine, dried over Na₂SO₄, filtered and concentrated under reduced pressure. Obtained oily product was filtered through a thin layer of silica gel (cHex / EA = 30 / 1) yielding 1075 mg (3.56 mmol, 79 %) of pyrrole **17** with traces of its α-isomer as colorless oil.

Novelty: 3-bromo-1-(triisopropylsilyl)-1*H*-pyrrole (**17**) is described in the literature by its ¹H-NMR, ¹³C-NMR and IR.⁸⁰



¹H-NMR (400 MHz, CDCl₃): 6.74 (dd, 1H, $J(2,5) = 2.3$ Hz, $J(2,4) = 1.5$ Hz, H-C(2)), 6.63 (dd, 1H, $J(4,5) = 2.8$ Hz, $J(2,5) = 2.3$ Hz, H-C(5)), 6.30 (dd, 1H, $J(4,5) = 2.8$ Hz, $J(2,4) = 1.5$ Hz, H-C(4)), 1.43 (sep, 3H, $J(\text{CH},(\text{CH}_3)_2) = 7.4$ Hz, 3 x (CH₃)₂CHSi-), 1.10 (d, 18H, $J(\text{CH},(\text{CH}_3)_2) = 7.4$ Hz, 3 x (CH₃)₂CHSi-).

Synthesis of 3-(4,4,5,5-tetramethyl-1,3,2-dioxaborolan-2-yl)-1-(triisopropylsilyl)-1*H*-pyrrole (**19**)



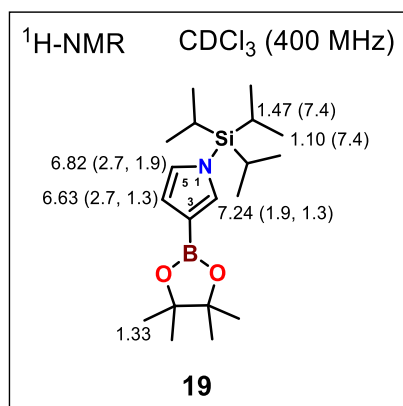
A solution of 550 mg (1.82 mmol, 1.00 mol eq) pyrrole **17** in 15 mL of THF (abs) was cooled to -78 °C and 1.37 mL (2.18 mmol, 1.20 mol eq) of n-BuLi (1.6 M in pentane) was added dropwise. Resulting mixture was stirred for 30 min at the same temperature. Subsequently 677 mg (3.64 mmol, 2.00 mol eq) of pinacol boronate **18** was added to the mixture and stirred 1 h

⁸⁰ Kotoku, N.; Fuijoka, S.; Nakata, C.; Yamada, M.; Sumii, Y.; Kawachi, T.; Arai, M.; Kobayashi, M. *Tetrahedron*, **2011**, *67*, 6673 - 6678.

at - 78 °C and 2 h at rt. Afterwards, the reaction was quenched with 20 mL of NH₄Cl (sat aq solution), extracted with Et₂O (3 x 15 mL), dried over Na₂SO₄, filtered and concentrated under reduced pressure. Crude oily product was purified by FLC (cHex / EA = 30 / 1) yielding 330 mg (0.95 mmol, 52 %) of pinacol boronate **19** as a colorless oil, which solidified in a refrigerator.

Novelty: 3-(4,4,5,5-tetramethyl-1,3,2-dioxaborolan-2-yl)-1-(triisopropylsilyl)-1*H*-pyrrole (**19**) is described in the literature by its ¹H-NMR, ¹³C-NMR, M.P, IR and elemental analysis.⁸¹

M.p.: 56.0 - 59.0 °C [cHex / EA], lit: 59 °C.⁸¹



¹H-NMR (400 MHz, CDCl₃): 7.24 (dd, 1H, $J(2,5) = 1.9$ Hz, $J(2,4) = 1.3$ Hz, H-C(2)), 6.82 (dd, 1H, $J(4,5) = 2.7$ Hz, $J(2,5) = 1.3$ Hz, H-C(5)), 6.63 (dd, 1H, $J(4,5) = 2.7$ Hz, $J(2,4) = 1.3$ Hz, H-C(4)), 1.47 (sept, 3H, $J(\text{CH},(\text{CH}_3)_2) = 7.4$ Hz, 3 x (CH₃)₂CHSi-), 1.33 (s, 12H, 4 x -Me from pinacol ester group), 1.10 (d, 18H, $J(\text{CH},(\text{CH}_3)_2) = 7.4$ Hz, 3 x (CH₃)₂CHSi-).

⁸¹ Buchwald, S.L.; Billingsley, K. *J. Am. Chem. Soc.*, **2007**, *11*, 3358 - 3366.

9.4.3. Synthesis of *N*,4-diaryloxazole-2-amine VEGFR2 TK inhibitors NBM(1-7)

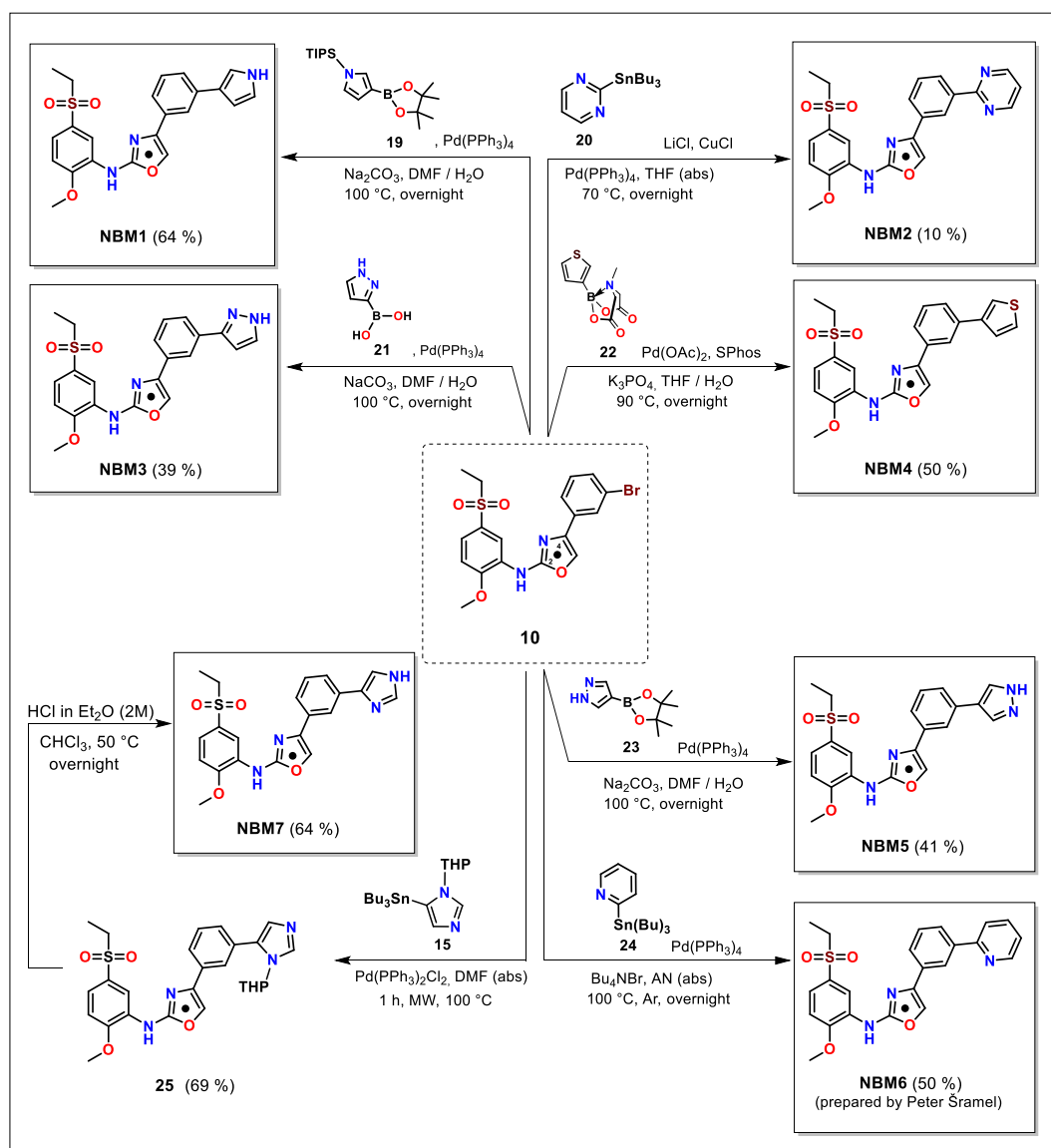
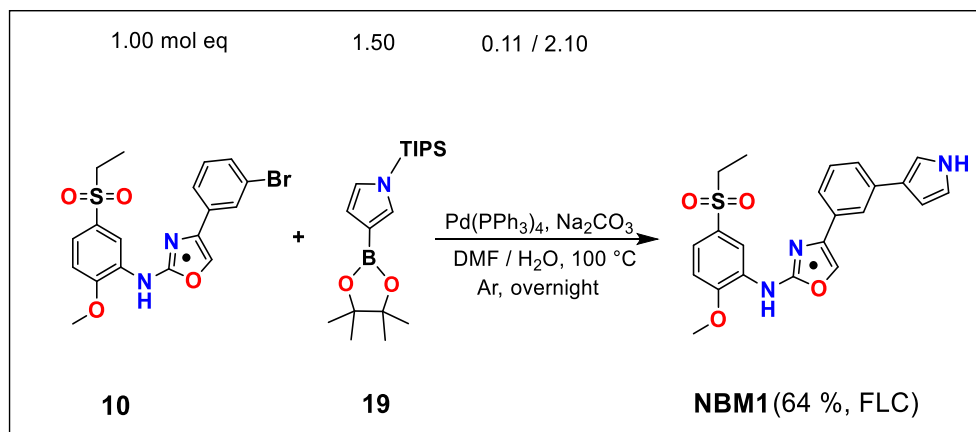


Figure 44. Synthesis of *N*,4-diaryloxazole-2-amine VEGFR2 TK inhibitors NBM(1-7).

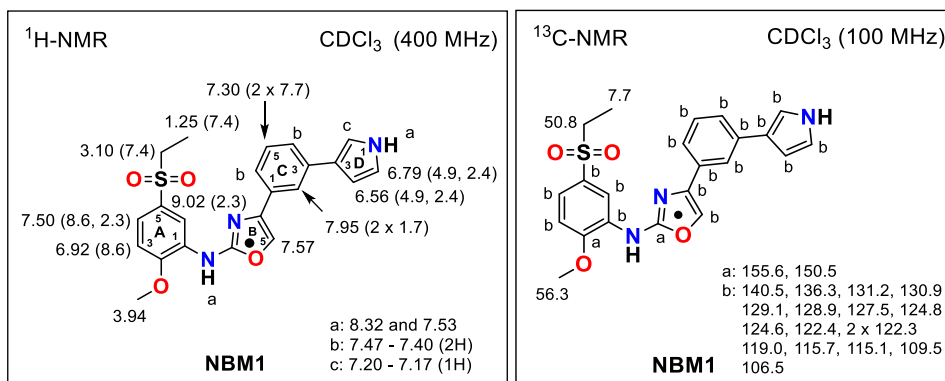
Synthesis of 4-[3-(1*H*-pyrrol-3-yl)phenyl]-*N*-[5-(ethylsulfonyl)-2-methoxyphenyl]oxazol-2-amine (NBM1)



A mixture of 50.0 mg (0.11 mmol, 1.00 mol eq) of oxazole **10**, 60.0 mg (0.17 mmol, 1.50 mol eq) of pinacol boronate **19** and 13.2 mg (0.01 mmol, 0.11 mol eq) of Pd(PPh₃)₄ in 3 mL of DMF (abs) was bubbled by Ar for 10 min. A solution of 24.0 mg (0.23 mmol, 2.10 mol eq) Na₂CO₃ in 1 mL of H₂O was bubbled by Ar for 10 min and added to the reaction mixture. Resulting mixture was sealed and stirred overnight at 100 °C. Then TLC analysis confirmed a presence of a new compound with traces of two side compounds, the reaction was cooled down, diluted with 10 mL of EA and washed with brine (3 x 15 mL). The separated organic layer was dried over Na₂SO₄, filtered and concentrated under reduced pressure. The crude product was purified by FLC (EA / cHex = 1 / 1) and obtained oily material triturated with EA / cHex yielding 31.0 mg (0.07 mmol, 64 %) of desired oxazole **NBM1** as a white solid compound.

Novelty: 4-[3-(1*H*-pyrrol-3-yl)phenyl]-*N*-[5-(ethylsulfonyl)-2-methoxyphenyl]oxazol-2-amine (**NBM1**) is not described in the literature.

M.p.: 163.0 - 180.0 °C (dec) [EA / cHex].



¹H-NMR (400 MHz, CDCl₃): δ 9.02 (d, 1H, $J(A_4, A_6) = 2.3$ Hz, H-C_A(6)), 8.32 and 7.53 (2 x br s, 2 x 1H, 2 x -NH-), 7.95 (dd, 1H, $J(C_2, C_4$ and $C_2, C_6) = 2.2$ and 1.7 Hz, H-C_C(2)), 7.57 (s, 1H, H-C_B(5)), 7.50 (dd, 1H, $J(A_3, A_4) = 8.6$ Hz, $J(A_4, A_6) = 2.3$ Hz, H-C_A(4)), 7.47 - 7.40 (m, 2 x 1H, H-C_C(4 and 6)), 7.30 (dd, 1H, $J(C_4, C_5$ and $C_5, C_6) = 8.1$ and 7.7 Hz, H-C_C(5)), 7.20 - 7.17 (m, 1H, H-C_D(2)), 6.92 (d, 1H, $J(A_3, A_4) = 8.6$ Hz, H-C_A(3)), 6.79 (dd, 1H, $J(D_4, D_5) = 4.9$ Hz, $J(D_2, D_5) = 2.4$ Hz, H-C_D(5)), 6.56 (dd, 1H, $J(D_4, D_5) = 4.9$ Hz, $J(D_2, D_4) = 2.4$ Hz, H-C_D(4)), 3.94 (s, 3H, CH₃O-), 3.10 (q, 2H, $J(\text{CH}_2, \text{CH}_3) = 7.4$ Hz, CH₃CH₂SO₂-), 1.25 (t, 3H, $J(\text{CH}_2, \text{CH}_3) = 7.4$ Hz, CH₃CH₂SO₂-).

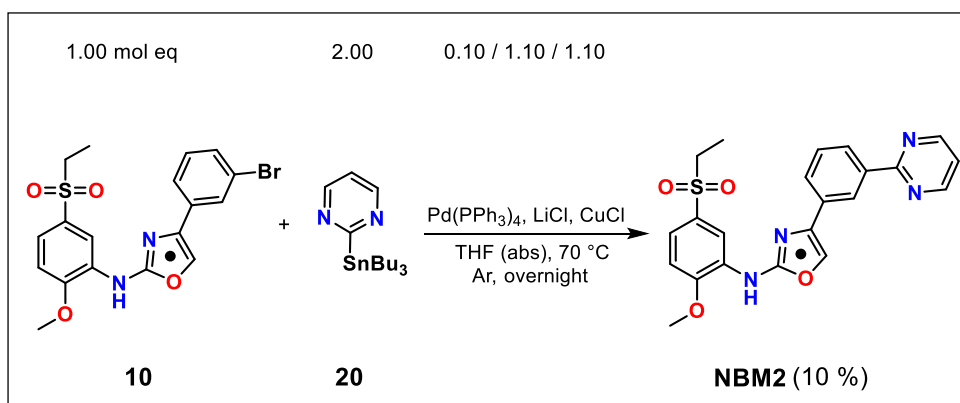
¹³C-NMR (100 MHz, CDCl₃): δ 155.6, 150.5, 140.5, 136.3, 131.2, 130.9, 129.1, 128.9, 127.5, 124.8, 124.6, 122.4, 2 x 122.3, 119.0, 115.7, 109.5, 106.5, 56.3 (CH₃O-), 50.8 (CH₃CH₂SO₂-), 7.7 (CH₃CH₂SO₂-).

FT-IR (solid, cm⁻¹): 3427 (w), 3334 (m), 3263 (w), 2980 (w), 2929 (w), 2343 (w), 2113 (w), 1728 (w), 1632 (s), 1597 (m), 1573 (s), 1534 (s), 1490 (m), 1349 (w), 1301 (m), 1286 (s), 1223 (m), 1181 (w), 1143 (m), 1119 (s), 1069 (s), 1024 (m), 912 (m), 847 (w), 811 (m), 782 (s), 640 (m), 593 (s), 574 (s), 540 (m), 499 (s), 446 (s).

MS (ESI m/z): 424.1 (100 %) [M+H]⁺, 446.11 (55 %) [M+Na]⁺, 462 (35 %) [M+K]⁺ (positive mode).

Anal. calcd for C₂₂H₂₁N₃O₄S (423.49): C, 62.40; H, 5.00; N, 9.92; Found: C, 62.75; H, 5.34; N, 10.26.

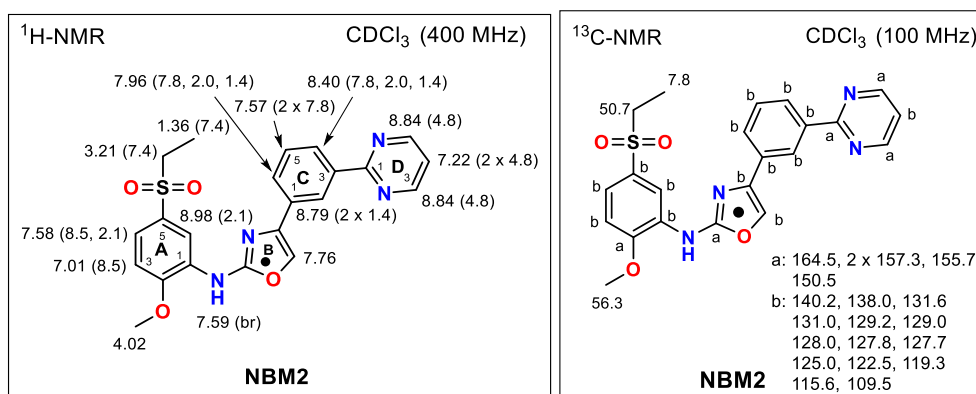
Synthesis of *N*-[5-(ethylsulfonyl)-2-methoxyphenyl]-4-[3-(pyrimidin-2-yl)phenyl]oxazol-2-amine (NBM2)



A mixture of 150 mg (0.34 mmol, 1.00 mol eq) oxazole **10**, 39.6 mg (0.03 mmol, 0.10 mol eq) of Pd(PPh₃)₄, 15.7 mg (0.37 mmol, 1.10 mol eq) of LiCl and 37.0 mg (0.37, 1.10 mol eq) of CuCl in 10 mL of THF (abs) was purged by Ar for 10 min. Subsequently 252 mg (0.68 mmol, 2.00 mol eq) of tributylstannane **20** was added and the mixture was sealed and stirred at 70 °C overnight. Then the reaction was cooled down and filtered through a thin layer of silicagel. Afterwards, the solution was diluted with 10 mL of EA, quenched with 10 mL of KF (sat aq solution) and stirred for 4 h. The organic layer was separated, washed with 10 mL of H₂O, dried over Na₂SO₄, filtered and evaporated under reduced pressure. The crude product was purified by FLC (Hex / EA = 1 / 2) and crystallized with Hex / EA yielding 10.0 mg (0.03 mmol, 10 %) of desired oxazole **NBM2**.

Novelty: *N*-[5-(ethylsulfonyl)-2-methoxyphenyl]-4-[3-(pyrimidin-2-yl)phenyl]oxazol-2-amine (**NBM2**) is not described in the literature.

M.p.: 150 - 170 °C (dec).



¹H-NMR (400 MHz, CDCl₃): δ, 8.98 (d, 1H, *J*(A₄,A₆) = 2.1 Hz, H-C_A(6)), 8.84 (2 x d, 2 x 1H, *J*(D₃,D₄) = *J*(D₄,D₅) = 4.8 Hz, H-C_D(3 and 6)), 8.79 (dd, 1H, *J*(C₂,C₆) = *J*(C₂,C₄) = 1.4 Hz, H-C_C(2)), 8.40 (ddd, 1H, *J*(C₄,C₅) = 7.8 Hz, *J*(C₄,C₆) = 2.0 Hz, *J*(C₂,C₄) = 1.4 Hz, H-C_C(4)), 7.96 (ddd, 1H, *J*(C₅,C₆) = 7.8 Hz, *J*(C₄,C₆) = 2.0 Hz, *J*(C₂,C₆) = 1.4 Hz, H-C_C(6)), 7.76 (s, 1H, H-C_B(5)), 7.59 (br s, 1H, -NH-), 7.58 (dd, 1H, *J*(A₃,A₄) = 8.5 Hz, *J*(A₄,A₆) = 2.1 Hz, H-C_A(4)), 7.57 (dd, 1H, *J*(C₄,C₅) = *J*(C₅,C₆) = 7.8 Hz, H-C_C(5)), 7.22 (t, 1H, *J*(D₃,D₄) = 4.8 Hz, H-C_D(4)), 7.01 (d, 1H, *J*(A₃,A₄) = 8.5 Hz, H-C_A(3)), 4.02 (s, 3H, CH₃O-), 3.21 (q, 2H, *J*(CH₂,CH₃) = 7.4 Hz, CH₃CH₂SO₂-), 1.36 (t, 3H, *J*(CH₂,CH₃) = 7.4 Hz, CH₃CH₂SO₂-).

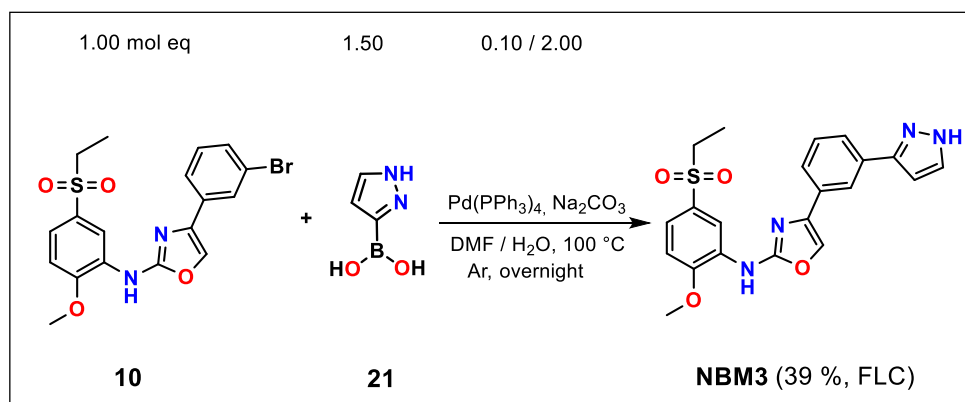
¹³C-NMR (100 MHz, CDCl₃): δ 164.5, 2 x 157.3, 155.7, 150.5, 140.2, 138.0, 131.6, 131.0, 129.2, 129.0, 128.0, 127.8, 127.7, 125.0, 122.5, 119.3, 115.6, 109.5, 56.3 (CH₃O-), 50.7 (CH₃CH₂SO₂-), 7.8 (CH₃CH₂SO₂-).

FT-IR (solid, cm⁻¹) 3399 (w), 2917 (w), 2848 (w), 2343 (w), 1629 (m), 1585 (m), 1566 (m), 1529 (m), 1486 (m), 1458 (w), 1408 (s), 1350 (w), 1298 (m), 1261 (s), 1224 (w), 1184 (w), 1122 (s), 1072 (m), 1009 (w), 929 (w), 812 (m), 787 (m), 718 (s), 687 (m), 575 (m), 523 (m), 492 (m), 465 (w).

MS (ESI *m/z*): 437.2 (100 %) [M+H]⁺, 459.1 (35 %) [M+Na]⁺, 475.1 (10 %) [M+K]⁺ (positive mode).

Anal. calcd for C₂₂H₂₀N₄O₄S (436.49): C, 60.54; H, 4.62; N, 12.84; Found: C, 60.66; H, 4.70; N, 12.99.

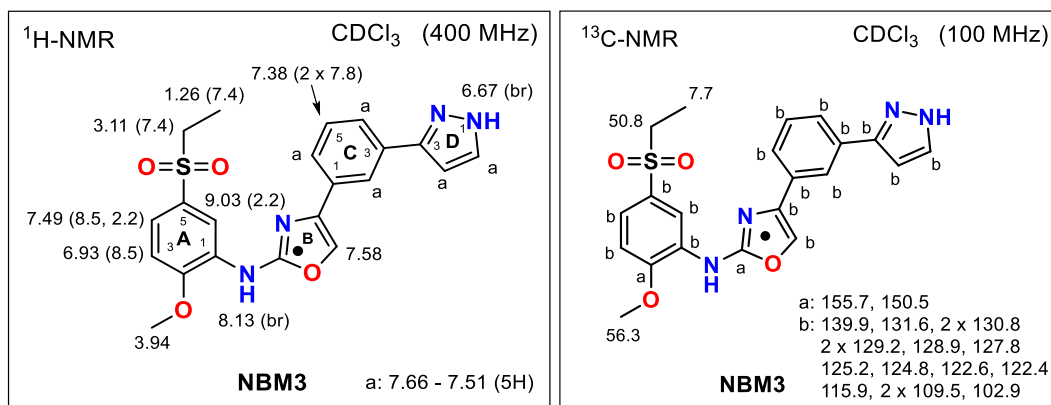
Synthesis of 4-[3-(1*H*-pyrazol-3-yl)phenyl]-*N*-[5-(ethylsulfonyl)-2-methoxyphenyl]oxazol-2-amine (NBM3)



A mixture of 60.0 mg (0.14 mmol, 1.00 mol eq) oxazole **10**, 23.0 mg (0.21 mmol, 1.50 mol eq) of boronic acid **21** and 15.9 mg (0.01 mmol, 0.10 mol eq) of Pd(PPh₃)₄ in 3 mL of DMF (abs) was bubbled by Ar for 10 min. A solution of 29.5 mg (0.28 mmol, 2.00 mol eq) Na₂CO₃ in 1.0 mL of H₂O was bubbled by Ar for 10 min and added to the reaction. Resulting mixture was sealed and stirred overnight at 100 °C. Then TLC analysis confirmed a presence only a new product with traces of a side product. The reaction was cooled down, diluted with 10 mL of EA and washed with brine (3 x 15 mL). The separated organic layer was dried over Na₂SO₄, filtered and evaporated under reduced pressure. The crude product was purified by FLC (DCM / MeOH = 50 / 1) and resulting material triturated with EA / cHex yielding 23.0 mg (0.05 mmol, 39 %) of desired oxazole **NBM3** as a white solid compound.

Novelty: 4-[3-(1*H*-pyrazol-3-yl)phenyl]-*N*-[5-(ethylsulfonyl)-2-methoxyphenyl]oxazol-2-amine (**NBM3**) is not described in the literature.

M.p.: 88.0 - 114.0 °C (dec) [DCM / MeOH].



¹H-NMR (400 MHz, CDCl₃): δ 9.03 (d, 1H, *J*(A₄,A₆) = 2.2 Hz, H-C_A(6)), 8.13 (br s, 1H, ArNH-), 6.67 (br s, 1H, -NH-(D)), 7.66 - 7.51 (m, 5 x 1H, H-C_C(2,4 and 6) and H-C_D(4 and 5)), 7.58 (s, 1H, H-C_B(5)), 7.49 (dd, 1H, *J*(A₃,A₄) = 8.5 Hz, *J*(A₄,A₆) = 2.2 Hz, H-C_A(4)), 7.38 (dd, 1H, *J*(C₄,C₅) = *J*(C₅,C₆) = 7.8 Hz, H-C_C(5)), 6.93 (d, 1H, *J*(A₃,A₄) = 8.5 Hz, H-C_A(3)), 3.94 (s, 3H, CH₃O-), 3.11 (q, 2H, *J*(CH₂,CH₃) = 7.4 Hz, CH₃CH₂SO₂-), 1.26 (t, 3H, *J*(CH₂,CH₃) = 7.4 Hz, CH₃CH₂SO₂-).

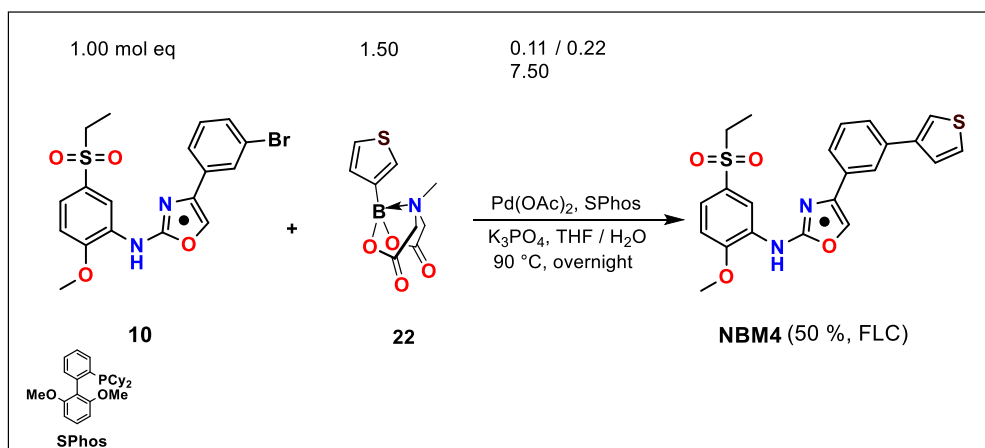
¹³C-NMR (100 MHz, CDCl₃, MH-21-17): δ 155.7, 150.5, 139.9, 131.6, 2 x 130.8, 2 x 129.2, 128.9, 127.8, 125.2, 124.8, 122.6, 122.4, 115.9, 2 x 109.5, 102.9, 56.3 (CH₃O-), 50.8 (CH₃CH₂SO₂-), 7.7 (CH₃CH₂SO₂-).

FT-IR (solid, cm⁻¹): 3304 (w), 2938 (w), 2117 (w), 1725 (w), 1630 (m), 1576 (m), 1532 (m), 1498 (m), 1354 (w), 1301 (m), 1282 (s), 1227 (w), 1180 (w), 1122 (s), 1072 (m), 1091 (m), 924 (w), 808 (w), 771 (m), 733 (s), 659 (w), 596 (m), 575 (m), 526 (m), 494 (m), 448 (w).

MS (ESI *m/z*): 425.1 (100 %) [M+H]⁺, 447.11 (60 %) [M+Na]⁺, 463.1 (15 %) [M+K]⁺ (positive mode).

Anal. calcd for C₂₁H₂₀N₄O₄S (424.48): C, 59.42; H, 4.75; N, 13.20; Found: C, 59.78; H, 5.05; N, 13.57.

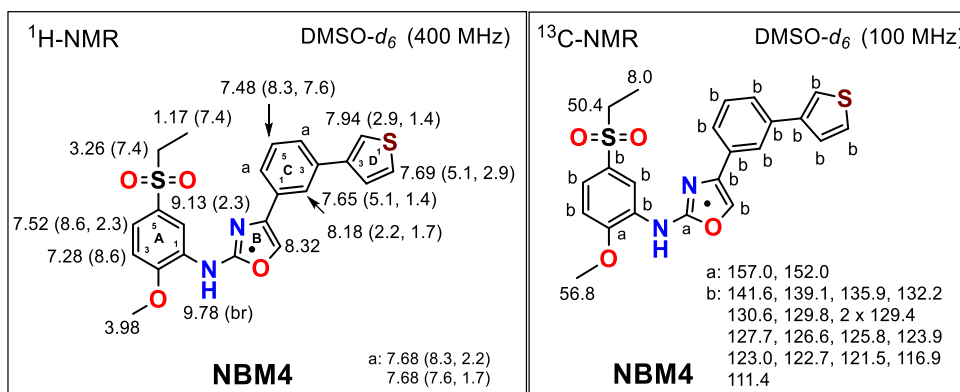
Synthesis of *N*-[5-(ethylsulfonyl)-2-methoxyphenyl]-4-[3-(thiophen-3-yl)phenyl]oxazol-2-amine (NBM4)



A suspension of 50.0 mg (0.11 mmol, 1.00 mol eq) of oxazole **10**, 41.0 mg (0.17 mmol, 1.50 mol eq) of MIDA-boronate **22**, 2.60 mg (0.01 mmol, 0.11 mol eq) of Pd(OAc)₂ and 9.40 mg (0.02 mmol, 0.22 mol eq) of SPhos in 5 mL of THF (abs) was bubbled by Ar for 10 min. Then the solution of 175 mg (0.82 mmol, 7.50 mol eq) K₃PO₄ in 1 mL of H₂O was also bubbled by Ar for 10 min and added to the reaction mixture. Resulting mixture was sealed and stirred overnight at 90 °C. The reaction was cooled down, diluted with 20 mL of EA and washed with brine (3 x 15 mL). The organic layer was dried over Na₂SO₄, filtered and a solution concentrated under reduced pressure. The crude product was purified by FLC (EA / cHex = 1 / 1) to yield 25.3 mg (0.06 mmol, 50 %) of desired oxazole **NBM4** as a red solid compound.

Novelty: *N*-[5-(ethylsulfonyl)-2-methoxyphenyl]-4-[3-(thiophen-3-yl)phenyl]oxazol-2-amine (**NBM4**) is not described in the literature.

M.p.: 155.1 - 160.4 °C [EA / cHex].



¹H-NMR (400 MHz, DMSO-*d*₆): δ 9.78 (br s, 1H, -NH-), 9.13 (d, 1H, *J*(A₄,A₆) = 2.3 Hz, H-C_A(6)), 8.32 (s, 1H, H-C_B(5)), 8.18 (dd, 1H, *J*(C₂,C₄ or C₂,C₆) = 2.2 or 1.7 Hz, H-C_C(2)), 7.94 (dd, 1H, *J*(D₂,D₅) = 2.9 Hz, *J*(D₂,D₄) = 1.4 Hz, H-C_D(2)), 7.69 (dd, 1H, *J*(D₄,D₅) = 5.1 Hz, *J*(D₂,D₅) = 2.9 Hz, H-C_D(5)), 2 x 7.68 (dd, 1H, *J*(C₄,C₅ or C₅,C₆) = 8.3 or 7.6 Hz, *J*(C₂,C₄ or C₂,C₆) = 2.2 or 1.7 Hz, H-C_C(4 and 6)), 7.65 (dd, 1H, *J*(D₄,D₅) = 5.1 Hz, *J*(D₂,D₄) = 1.4 Hz, H-C_D(4)), 7.52 (dd, 1H, *J*(A₃,A₄) = 8.6 Hz, *J*(A₄,A₆) = 2.3 Hz, H-C_A(4)), 7.48 (dd, 1H, *J*(C₄,C₅ or C₅,C₆) = 8.3 or 7.6 Hz, H-C_C(5)), 7.28 (d, 1H, *J*(A₃,A₄) = 8.6 Hz, H-C_A(3)), 3.98 (s, 3H, CH₃O-), 3.26 (q, 2H, *J*(CH₂,CH₃) = 7.4 Hz, CH₃CH₂SO₂-), 1.17 (t, 3H, *J*(CH₂,CH₃) = 7.4 Hz, CH₃CH₂SO₂-).

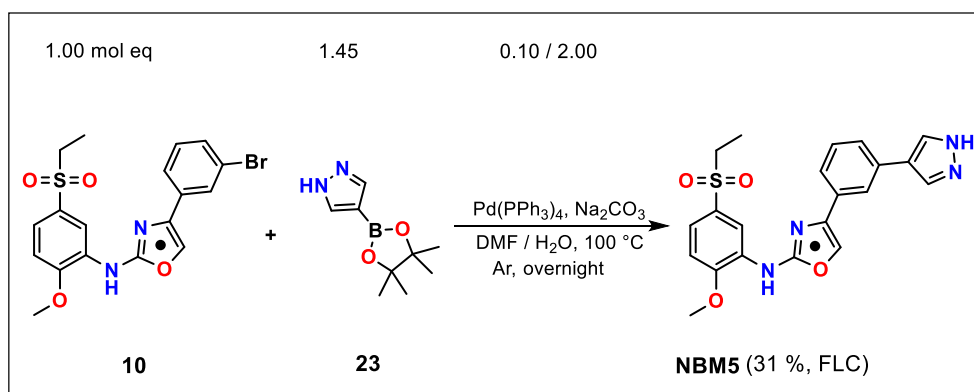
¹³C-NMR (100 MHz, DMSO-*d*₆): δ 157.0, 152.0, 141.6, 139.1, 135.9, 132.2, 130.6, 129.8, 2 x 129.4, 127.7, 126.6, 125.8, 123.9, 123.0, 122.7, 121.5, 116.9, 111.4, 56.8 (CH₃O-), 8.0 (CH₃CH₂SO₂-).

FT-IR (solid, cm⁻¹): 3432 (w), 3304 (w), 3094 (w), 2938 (w), 2343 (w), 2112 (w), 1730 (w), 1624 (m), 1597 (m), 1570 (s), 1529 (s), 1480 (m), 1422 (s), 1299 (s), 1258 (s), 1217 (m), 1177 (w), 1143 (m), 1121 (s), 1073 (s), 1045 (m), 1019 (m), 933 (w), 895 (m), 808 (m), 776 (s), 714 (s), 675 (w), 573 (s), 539 (s), 495 (s), 490 (m).

MS (ESI *m/z*): 441.1 (100 %) [M+H]⁺, 463.1 (90 %) [M+Na]⁺, 479.1 (90 %) [M+K]⁺ (positive mode).

Anal. calcd for C₂₂H₂₀N₂O₄S₂ (440.53): C, 59.98; H, 4.58; N, 6.36; Found: C, 59.68; H, 4.39; N, 6.15.

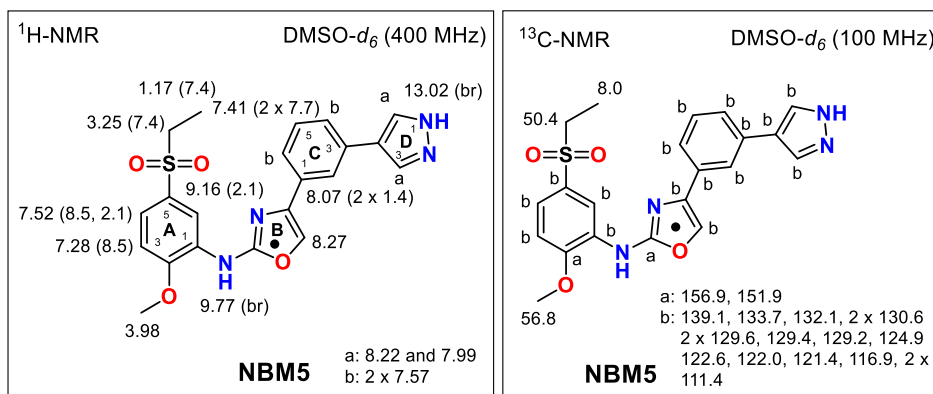
Synthesis of 4-[3-(1*H*-pyrazol-4-yl)phenyl]-*N*-[5-(ethylsulfonyl)-2-methoxyphenyl]oxazol-2-amine (NBM5)



A suspension of 50.0 mg (0.11 mmol, 1.00 mol eq) of oxazole **10**, 32.0 mg (0.16 mmol, 1.45 mol eq) of pinacol boronate **23** and 12.7 mg (0.01 mmol, 0.10 mol eq) of Pd(PPh₃)₄ in 2 mL of DMF (abs) was bubbled by Ar for 10 min. A solution of 23.3 mg (0.22 mmol, 2.00 mol eq) Na₂CO₃ in 1 mL of H₂O was bubbled by Ar for 10 min and added to the reaction mixture. Resulting mixture was sealed and stirred overnight at 100 °C. After that TLC analysis confirmed a presence of a new product with traces of the starting compound **10**. The reaction was cooled down, diluted with 10 mL of EA and washed with brine (3 x 15 mL). The separated organic layer was dried over Na₂SO₄, filtered and concentrated under reduced pressure. The crude product was purified by FLC (DCM / MeOH = 30 / 1), resulting material triturated with Et₂O / cHex and dried under reduced pressure yielding 15.0 mg (0.04 mmol, 31 %) of oxazole **NBM5** as a white solid compound.

Novelty: 4-[3-(1*H*-pyrazol-4-yl)phenyl]-*N*-[5-(ethylsulfonyl)-2-methoxyphenyl]oxazol-2-amine (**NBM5**) is not described in the literature.

M.p.: 209 - 222 °C (dec) [DCM / MeOH].



¹H-NMR (400 MHz, DMSO-*d*₆): δ 13.02 (br s, 1H, H-N_D(1)), 9.77 (br s, 1H, -NH-), 9.16 (d, 1H, $J(A_4, A_6) = 2.1$ Hz, H-C_A(6)), 8.27 (s, 1H, H-C_B(5)), 8.22 and 7.99 (2 x br, 2 x 1H, H-C_D(3 and 5)), 8.07 (dd, 1H, $J(C_2, C_4) = J(C_2, C_6) = 1.4$ Hz, H-C_C(2)), 2 x 7.57 (2 x dd, 2 x 1H, $J(C_4, C_5) = J(C_5, C_6) = 7.7$ Hz, $J(C_2, C_4) = (C_2, C_6) = 1.4$ Hz, H-C_C(4 and 6)), 7.52 (dd, 1H, $J(A_3, A_4) = 8.5$ Hz, $J(A_4, A_6) = 2.1$ Hz, H-C_A(4)), 7.41 (dd, 1H, $J(C_4, C_5) = J(C_5, C_6) = 7.7$ Hz, H-C_C(5)), 7.28 (d, 1H, $J(A_3, A_4) = 8.5$ Hz, H-C_A(3)), 3.98 (s, 3H, CH₃O-), 3.25 (q, 2H, $J(\text{CH}_2, \text{CH}_3) = 7.4$ Hz, CH₃CH₂SO₂-), 1.17 (t, 3H, $J(\text{CH}_2, \text{CH}_3) = 7.4$ Hz, CH₃CH₂SO₂-).

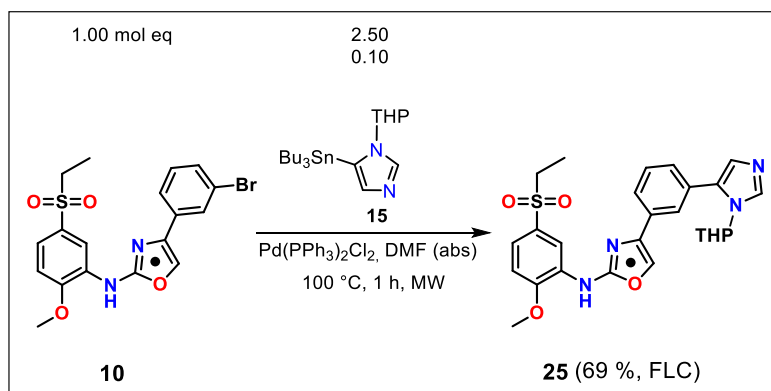
¹³C-NMR (100 MHz, DMSO-*d*₆): δ 156.9, 151.9, 139.1, 133.7, 132.1, 2 x 130.6, 2 x 129.6, 129.4, 129.2, 124.9, 122.6, 122.0, 121.4, 116.9, 2 x 111.4, 56.8 (CH₃O-), 50.4 (CH₃CH₂SO₂-), 8.0 (CH₃CH₂SO₂-).

FT-IR (solid, cm⁻¹) 3350 (m), 2962 (w), 2112 (w), 1629 (s), 1556 (m), 1488 (w), 1418 (m), 1348 (w), 1304 (m), 1264 (s), 1230 (m), 1179 (w), 1143 (m), 1072 (s), 1039 (m), 1019 (m), 949 (m), 926 (w), 892 (w), 865 (w), 796 (s), 637 (m), 611 (s), 595 (s), 524 (s).

MS (ESI *m/z*): 425.1 (80 %) [M+H]⁺, 447.1 (100 %) [M+Na]⁺, 463.1 (20 %) [M+K]⁺ (positive mode).

Anal. calcd for C₂₁H₂₀N₄O₄S (424.48): C, 59.42; H, 4.75; N, 13.20; Found: C, 59.65; H, 5.12; N, 13.43.

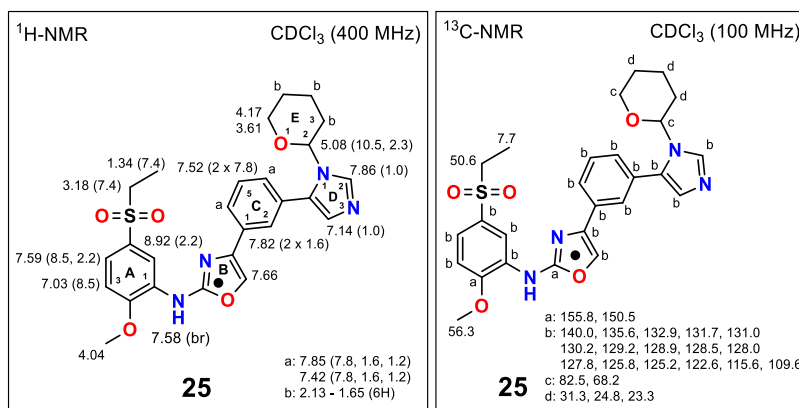
Synthesis of *N*-[5-(ethylsulfonyl)-2-methoxyphenyl]-4-{3-[1-(tetrahydro-2*H*-pyran-2-yl)-1*H*-imidazol-5-yl]phenyl}oxazol-2-amine (25**)**



A solution of 100 mg (0.23 mmol, 1.00 mol eq) oxazole **10** and 16.0 mg (22.8 μ mol, 0.10 mol eq) of Pd(PPh₃)₂Cl₂ in 4 mL of DMF (abs) was bubbled in by Ar for 10 min. Afterwards 252 mg (0.57 mmol, 2.50 mol eq) of tributylstannane **15** was added to the reaction mixture and stirred at 100 °C in a microwave reactor for 1 h. After that TLC analysis confirmed a presence of a new product without **10** and side products. The reaction was cooled down, diluted with 50 mL of brine and resulting mixture was extracted with EA (3 x 15 mL). Combined organic layer was washed with brine (4 x 15 mL), dried over Na₂SO₄, filtered and concentrated under reduced pressure. Obtained oily product was diluted in CH₃CN, extracted with *n*-hexane (3 x 15 mL) and concentrated with RVE. The crude product was purified by FLC (SiO₂, from 100 % of EA to EA / MeOH : 20 / 1) yielding 80.2 mg (0.16 mmol, 69 %) of desired oxazole **25** as an orange solid compound.

Novelty: *N*-[5-(ethylsulfonyl)-2-methoxyphenyl]-4-{3-[1-(tetrahydro-2*H*-pyran-2-yl)-1*H*-imidazol-5-yl]phenyl}oxazol-2-amine (**25**) is not described in the literature.

M.p.: 84.0 - 89.0 °C [EA / MeOH].



¹H-NMR (400 MHz, CDCl₃): δ 8.92 (d, 1H, *J*(A₄,A₆) = 2.2 Hz, H-C_A(6)), 7.86 (d, 1H, *J*(D₂,D₄) = 1.0 Hz, H-C_D(2)), 7.85 and 7.42 (2 x ddd, 2 x 1H, 2 x *J*(C₅,C₆ or C₄,C₅) = 7.8 Hz, *J*(C₂,C₆ or C₂,C₄) = 1.6 Hz, *J*(2 x C₄,C₆) = 1.2 Hz, H-C_C(4 and 6)), 7.82 (dd, 1H, *J*(C₂,C₄ and C₂,C₆) = 1.6 Hz, H-C_C(2)), 7.66 (s, 1H, H-C_B(4)), 7.58 (br s, 1H, -NH-) 7.52 (dd, 1H, *J*(C₄,C₅) = *J*(C₅,C₆) = 7.8 Hz, H-C_C(5)), 7.59 (dd, 1H, *J*(A₃,A₄) = 8.5 Hz, *J*(A₄,A₆) = 2.2 Hz, H-C_A(4)), 7.14 (d, 1H, *J*(D₂,D₄) = 1.0 Hz, H-C_D(4)), 7.03 (d, 1H, *J*(A₃,A₄) = 8.5 Hz, H-C_A(3)), 5.08 (dd, 1H, *J*(E₂,E₃) = 10.5 Hz, *J*(E₂,E₃) = 2.3 Hz, H-C_E(2)), 4.17 and 3.61 (2 x m, 2 x 1H, 2 x H-C_E(6)), 4.04 (s, 3H, CH₃O-), 3.18 (q, 2H, *J*(CH₂,CH₃) = 7.4 Hz, CH₃CH₂SO₂-), 2.13 - 1.65 (m, 6H, H-C_E(3-5)), 1.34 (t, 3H, *J*(CH₂,CH₃) = 7.4 Hz, CH₃CH₂SO₂-).

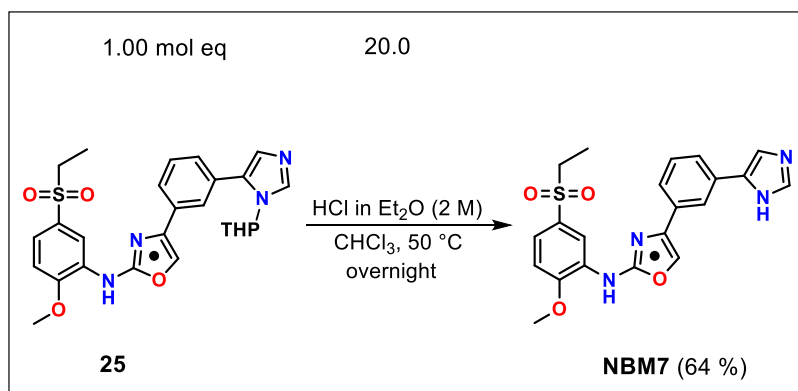
¹³C-NMR (100 MHz, CDCl₃): δ 155.8, 150.5, 140.0, 135.6, 132.9, 131.7, 131.0, 130.2, 129.2, 128.9, 128.5, 128.0, 127.8, 125.8, 125.2, 122.6, 115.6, 109.6, 82.5, 68.2, 56.3 (CH₃O-), 50.6 (CH₃CH₂SO₂-), 31.3, 24.8, 23.3, 7.7 (CH₃CH₂SO₂-).

FT-IR (solid, cm⁻¹): 2942 (w), 1732 (w), 1629 (s), 1597 (m), 1583 (m), 1535 (w), 1487 (w), 1462 (w), 1422 (m), 1375 (w), 1345 (w), 1307 (s), 1263 (s), 1228 (w), 1180 (w), 1144 (w), 1125 (s), 1080 (s), 1059 (w), 1041 (s), 1021 (w), 1001 (w), 958 (w), 910 (s), 878 (w), 808 (m), 734 (s), 658 (m), 494 (m).

MS (ESI *m/z*): 425.24 (100 %) [M-THP+2H]⁺ (positive mode).

Anal. calcd for C₂₆H₂₈N₄O₅S (508.18): C, 61.40; H, 5.55; N, 11.02; Found: C, 61.78; H, 5.43; N, 11.25.

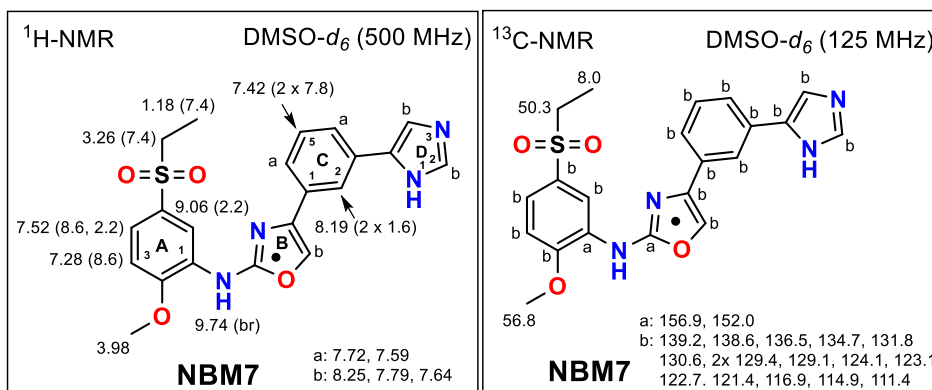
Synthesis of 4-[3-(1*H*-imidazol-5-yl)phenyl]-*N*-[5-(ethylsulfonyl)-2-methoxyphenyl]oxazol-2-amine (NBM7)



To a solution of 60.0 mg (0.20 mmol, 1.00 mol eq) oxazole **25** in 20 mL of CHCl₃, 2.00 mL (4.00 mmol, 20 mol eq) of HCl (2M in Et₂O) was added and the mixture stirred at 50 °C overnight. Resulting imidazolium salt (white precipitate) was filtered off, obtained solid triturated with a mixture of cHex / EA and subsequently dissolved in 50 mL of H₂O. After addition of 50 mL of NaHCO₃ (sat aq solution) the mixture was extracted with EA (3 x 20 mL). Combined organic layer was extracted with saturated aq solution of NaHCO₃ (3 x 15 mL) and brine (3 x 15 mL), dried over Na₂SO₄, filtered and concentrated under reduced pressure yielding 32.0 mg (0.08 mmol, 64 %) of oxazole **NBM7** as a yellow-white powder.

Novelty: 4-[3-(1*H*-imidazol-5-yl)phenyl]-*N*-[5-(ethylsulfonyl)-2-methoxyphenyl]oxazol-2-amine (**NBM7**) is not described in the literature.

M.p.: 191.0 - 194.0 [EA].



¹H-NMR (500 MHz, DMSO-*d*₆): δ 9.74 (br s, 1H, -NH-), 9.06 (d, 1H, *J*(A₄,A₆) = 2.2 Hz, H-C_A(6)), 8.25, 7.79 and 7.64 (3 x br s, 3 x 1H, H-C_B(5) and H-C_D(2 and 4)), 8.19 (dd, 1H, *J*(C₂,C₄ and C₂,C₆) = 1.6 Hz, H-C_C(2)), 7.72 and 7.59 (2 x dd, 2 x 1H, *J*(C₄,C₅ and C₅,C₆) = 7.8 Hz, *J*(C₂,C₄ and C₂,C₆) = 1.6 Hz, H-C_C(4 and 6)), 7.52 (dd, 1H, *J*(A₃,A₄) = 8.6 Hz, *J*(A₄,A₆) = 2.2 Hz, H-C_A(4)), 7.42 (dd, 1H, *J*(C₄,C₅) = *J*(C₅,C₆) = 7.8 Hz, H-C_C(5)), 7.28 (d, 1H, *J*(A₃,A₄) = 8.6 Hz, H-C_A(3)), 3.98 (s, 3H, CH₃O-), 3.26 (q, 2H, *J*(CH₂,CH₃) = 7.4 Hz, CH₃CH₂SO₂-), 1.18 (t, 3H, *J*(CH₂,CH₃) = 7.4 Hz, CH₃CH₂SO₂-).

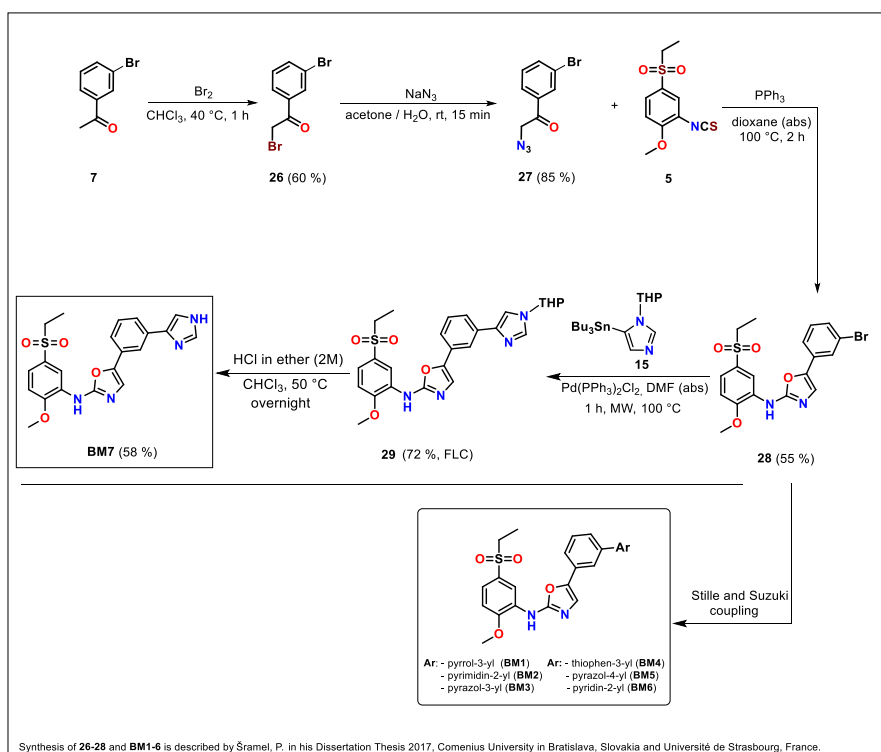
¹³C-NMR (125 MHz, DMSO-*d*₆): δ 156.9, 152.0, 139.2, 138.6, 136.5, 134.7, 131.8, 130.6, 2 x 129.4, 129.1, 124.1, 123.1, 122.7, 121.4, 116.9, 114.9, 111.4, 56.8 (CH₃O-), 50.3 (CH₃CH₂SO₂-), 8.0 (CH₃CH₂SO₂-).

FT-IR (solid, cm⁻¹): 3432 (w), 2920 (w), 2847 (w), 1636 (m), 1597 (m), 1578 (m), 1535 (m), 1487 (m), 1457 (w), 1426 (m), 1300 (m), 1261 (s), 1226 (w), 1181 (w), 1120 (s), 1075 (m), 1022 (w), 971 (w), 930 (w), 879 (w), 795 (m), 774 (m), 726 (s), 699 (m), 658 (w), 626 (m), 599 (w), 560 (w), 525 (m), 488 (m), 427 (m).

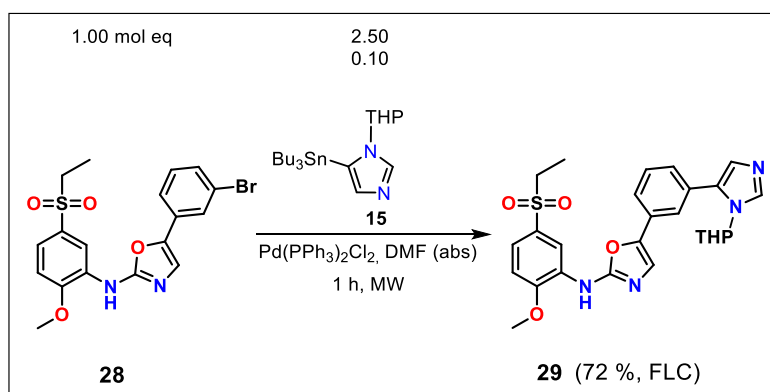
MS (ESI *m/z*): 425.2 (100 %) [M+H]⁺, 447.1 (15 %) [M+Na]⁺ (positive mode).

Anal. calcd for C₂₁H₂₀N₄O₄S (424.48): C, 59.42; H, 4.75; N, 13.20; Found: C, 59.72; H, 4.43; N, 13.45.

9.4.4. Synthesis of 5-[3-(1*H*-imidazol-5-yl)phenyl]-*N*-[5-(ethylsulfonyl)-2-methoxyphenyl]oxazol-2-amine (BM7)



Synthesis of *N*-[5-(ethylsulfonyl)-2-methoxyphenyl]-5-[3-[1-(tetrahydro-2*H*-pyran-2-yl)-1*H*-imidazol-5-yl]phenyl]oxazol-2-amine (29)

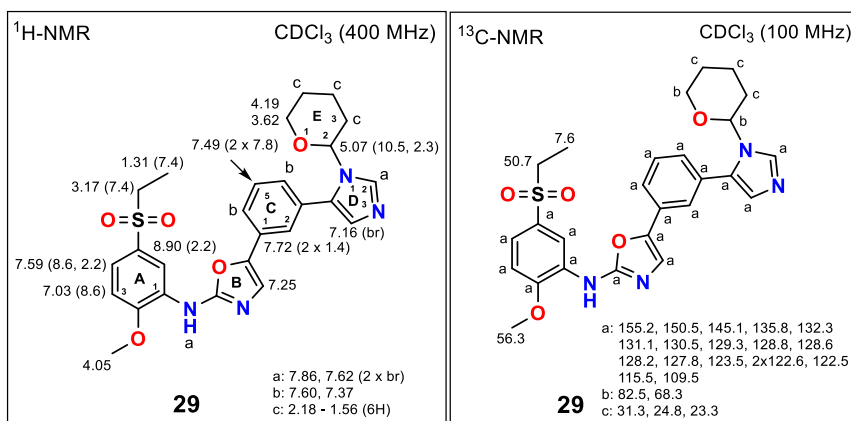


A solution of 150 mg (0.35 mmol, 1.00 mol eq) oxazole **28** and 24.0 mg (34.2 μ mol, 0.10 mol eq) of Pd(PPh₃)₂Cl₂ in 4 mL of DMF (abs) was bubbled by Ar for 10 min. Afterwards 378 mg (0.86 mmol, 2.50 mol eq) of tributylstannane **15** was added and the reaction stirred at 100 °C and MW irradiated for 1 h. After that TLC analysis confirmed a presence of a new product

without **28** and side products. The reaction mixture was cooled down, diluted with 50 mL of brine and extracted with EA (3 x 15 mL). Combined organic layer was washed with brine (4 x 15 mL), dried over Na₂SO₄, filtered and concentrated under reduced pressure. Obtained oily product was diluted in CH₃CN, extracted with n-hexane (3 x 15 mL) and separated organic layer evaporated with RVE. The crude product was purified by FLC (SiO₂, from 100 % of EA to EA / MeOH : 20 / 1) yielding 125 mg (0.25 mmol, 72 %) of oxazole **29** as an orange solid compound.

Novelty: *N*-[5-(ethylsulfonyl)-2-methoxyphenyl]-5-{3-[1-(tetrahydro-2*H*-pyran-2-yl)-1*H*-imidazol-5-yl]phenyl}oxazol-2-amine (**29**) is not described in the literature.

M.p.: 125.0 - 130.0 °C [EA / MeOH].



¹H-NMR (400 MHz, CDCl₃): δ 8.90 (d, 1H, *J*(A₄,A₆) = 2.2 Hz, H-C_A(6)), 7.86 and 7.62 (2 x br s, 2 x 1H, -NH- and H-C_D(2)), 7.72 (dd, 1H, *J*(C₂,C₄) = (C₂,C₆) = 1.4 Hz, H-C_C(2)), 7.60 and 7.37 (2 x dd, 2 x 1H, *J*(C₄,C₅ or C₅,C₆) = 7.8 Hz, *J*(C₂,C₄ or C₂,C₆) = 1.4 Hz, H-C_C(4 and 6)), 7.59 (dd, 1H, *J*(A₃,A₄) = 8.6 Hz, *J*(A₄,A₆) = 2.2 Hz, H-C_A(4)), 7.49 (dd, 1H, *J*(C₄,C₅) = *J*(C₅,C₆) = 7.8 Hz, H-C_C(5)), 7.16 (br s, 1H, H-C_D(4)), 7.03 (d, 1H, *J*(A₃,A₄) = 8.6 Hz, H-C_A(3)), 5.07 (dd, 1H, *J*(E₂,E₃) = 10.5 Hz, *J*(E₂,E₃) = 2.3 Hz, H-C_E(2)), 4.19 and 3.62 (2 x m, 2 x 1H, 2 x H-C_E(6)), 4.05 (s, 3H, CH₃O-), 3.17 (q, 2H, *J*(CH₂,CH₃) = 7.4 Hz, CH₃CH₂SO₂-), 2.18 - 1.56 (m, 6H, H-C_E(3-5)), 1.31 (t, 3H, *J*(CH₂,CH₃) = 7.4 Hz, CH₃CH₂SO₂-).

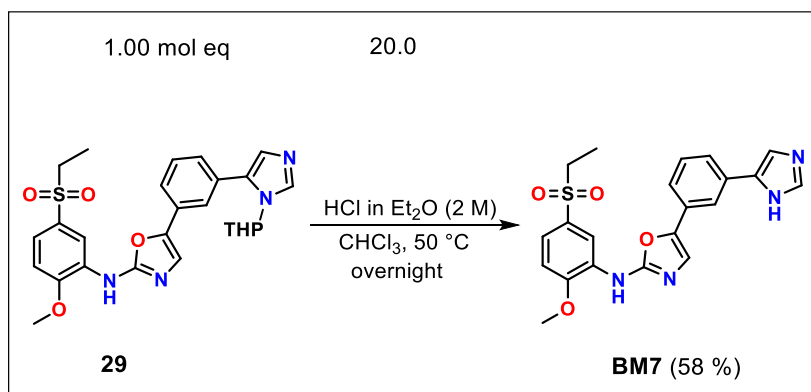
¹³C-NMR (100 MHz, CDCl₃) 155.2, 150.5, 145.1, 135.8, 132.3, 131.1, 130.5, 129.3, 128.8, 128.6, 128.2, 127.8, 123.5, 2 x 122.6, 122.5, 115.5, 109.5, 82.5, 68.3, 56.3 (CH₃O-), 50.7 (CH₃CH₂SO₂-), 31.3, 24.8, 23.3, 7.6 (CH₃CH₂SO₂-).

FT-IR (solid, cm⁻¹): 2940 (w), 1612 (m), 1574 (s), 1486 (w), 1422 (w), 1306 (m), 1263 (m), 1140 (s), 1122 (s), 1081 (m), 1041(m), 1020 (w), 999 (w), 911 (m), 878 (w), 794 (m), 736 (m), 719 (m), 698 (m), 657 (m), 597 (w), 575 (m), 554 (w), 525 (w), 493 (m).

MS (ESI m/z): 425.24 [M-THP+2H]⁺.

Anal. calcd for C₂₆H₂₈N₄O₅S (508.18): C, 61.40; H, 5.55; N, 11.02; Found: C, 61.60; H, 5.66; N, 11.28.

Synthesis of 5-[3-(1*H*-imidazol-5-yl)phenyl]-*N*-[5-(ethylsulfonyl)-2-methoxyphenyl]oxazol-2-amine (BM7)

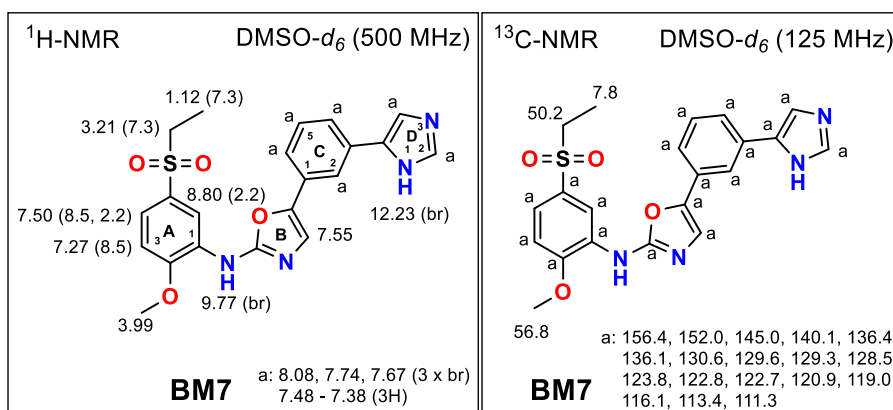


To a solution of 125 mg (0.25 mmol, 1.00 mol eq) oxazole **29** in 40 mL of CHCl₃, 4.00 mL (4.00 mmol, 20 mol eq) of HCl (2 M solution in Et₂O) was added and the mixture stirred at 50 °C overnight. Resulting imidazolium salt (white precipitate) was filtered off, triturated with a mixture of cHex / EA and subsequently dissolved in 50 mL of H₂O. After addition of 50 mL of saturated aq solution of NaHCO₃ the obtained mixture was extracted with EA (3 x 20 mL). Combined organic layer was washed again with saturated aq solution of NaHCO₃ (3 x 15 mL)

and brine (3 x 15 mL), dried over Na₂SO₄, filtered and concentrated under reduced pressure to yield 60 mg (0.14 mmol, 58 %) of oxazole **BM7** as a white powder.

Novelty: 5-[3-(1*H*-imidazol-5-yl)phenyl]-*N*-[5-(ethylsulfonyl)-2-methoxyphenyl]oxazol-2-amine (**BM7**) is not described in the literature.

M.p.: 210.0 - 213.0 °C [EA].



¹H-NMR (500 MHz, DMSO-*d*₆): δ 12.23 (br s, 1H, -N_DH), 9.77 (br s, 1H, -NH-), 8.80 (d, 1H, *J*(A₄,A₆) = 2.2 Hz, H-C_A(6)), 8.08, 7.74, 7.67 and 7.48 - 7.38 (3 x br and 1 x m, 6 x 1H, H-C_C(2 and 4-6), H-C_D(2 and 4), 7.50 (dd, 1H, *J*(A₃,A₄) = 8.5 Hz, *J*(A₄,A₆) = 2.2 Hz, H-C_A(4)), 7.27 (d, 1H, *J*(A₃,A₄) = 8.5 Hz, H-C_A(3)), 3.99 (s, 3H, CH₃O-), 3.21 (q, 2H, *J*(CH₂,CH₃) = 7.3 Hz, CH₃CH₂SO₂-), 1.12 (t, 3H, *J*(CH₂,CH₃) = 7.3 Hz, CH₃CH₂SO₂-).

¹³C-NMR (125 MHz, DMSO-*d*₆): 156.4, 152.0, 145.0, 140.1, 136.4, 136.1, 130.6, 129.6, 129.3, 128.5, 123.8, 122.8, 122.7, 120.9, 119.0, 116.1, 113.4, 111.3, 56.8 (CH₃O-), 50.2 (CH₃CH₂SO₂-), 7.8 (CH₃CH₂SO₂-).

FT-IR (solid, cm⁻¹): 3360 (m), 1597 (m), 1574 (s), 1530 (m), 1488 (m), 1427 (s), 1352 (w), 1308 (s), 1263 (s), 1141 (s), 1116 (s), 1101 (s), 1082 (s), 1054 (w), 1025 (m), 964 (w), 906 (w), 795 (m), 763 (m), 735 (s), 717 (s), 687 (s), 555 (m), 519 (m), 487 (s).

MS (ESI *m/z*): 425.1 (100 %) [M+H]⁺, 447.1 (10 %) [M+Na]⁺ (positive mode).

Anal. calcd for C₂₁H₂₀N₄O₄S (424.48): C, 59.42; H, 4.75; N, 13.20; Found: C, 59.68; H, 4.63; N, 13.55.

**Chapter 7. Project 2. Development of three-point interacting
SBCP VEGFR2 TK inhibitors BM(8-16)**

10. Development of three-point interacting SBCP VEGFR2 TK inhibitors BM(8-16)

Next project of the dissertation thesis was also dedicated to VEGFR2 TK with an aim to find more active inhibitors with more interactions in the active site of the kinase. Recently, the SBCP pocket in some VEGFR2-TKs (PDB: 1Y6A, 1Y6B) was discovered by the Biomagi. Apart from **AAZ** (described in the previous project) Harris et al. developed several efficient *para* substituted aminooxazole VEGFR2 TK inhibitors.²⁸ Among them, compounds **60** and **61**, with *p*-CN and *p*-CONH₂ group on a terminal phenyl ring, exhibited high inhibitory activity with IC₅₀ = 51.0 nM and 18.0 nM (VEGFR2 TK), resp. No interaction analyses of these inhibitors had been noted before and according to our docking study (PDB: 1Y6A) we developed more active carboxylic acid analogue **62** with IC₅₀ = 13.2 nM (VEGFR2 TK). (Figure 45)

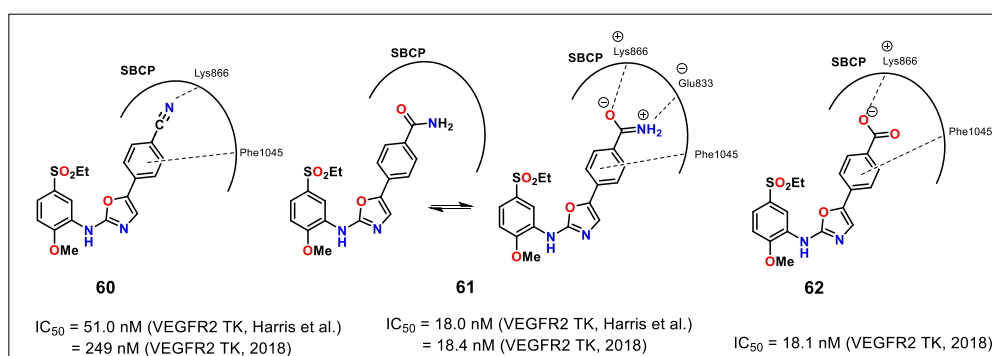


Figure 45. The structures of the most active *p*-substituted VEGFR2 TK inhibitors **60-62** with their position and proposed interactions within the SBCP pocket of VEGFR2 TK (PDB: 1Y6A). IC₅₀ activities in upper row are from lit. and in the last row are measured by us in ProQinase.

As was mentioned in the previous project, our group developed several *meta* substituted aminooxazoles as powerful VEGFR2 TK inhibitors. Pyrrole and pyrazole derivatives **BM1**, **BM3** exhibited similar IC₅₀ values than **AAZ** and their activity is attributed to an extra H-bond interaction of their heterocyclic -NH- group with Val912 or Glu883 from the SBCP, not present in **AAZ**. (Figure 46)

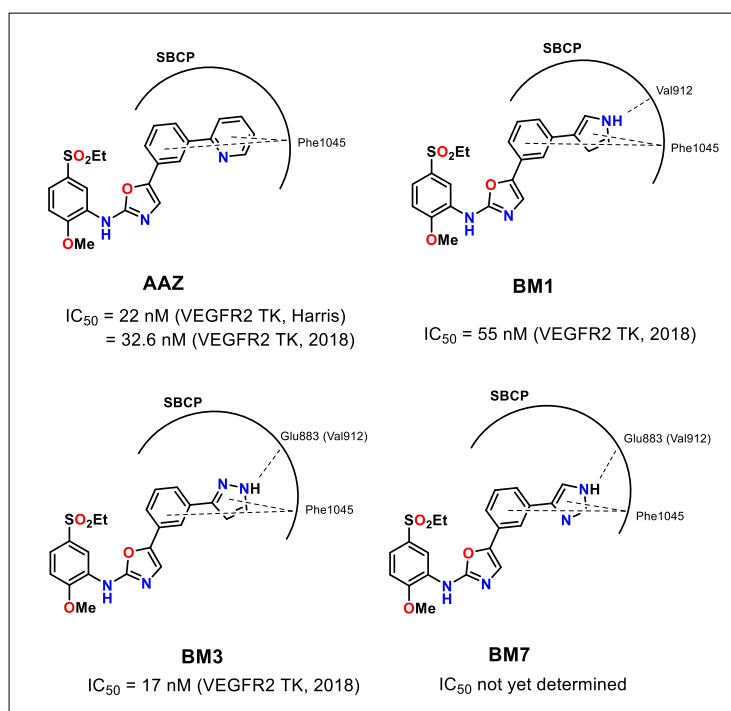


Figure 46. The structures of meta substituted aminooxazoles **BM1**, **BM3** and **BM7** in comparison to **AAZ**.

When we prepared the analogue **63**, which was formed as a combination of *p*-CN derivative **60** and *meta* substituted compound **AAZ**, an improved activity with $IC_{50} = 26 \text{ nM}$ (VEGFR2 TK) was observed. (Figure 47)

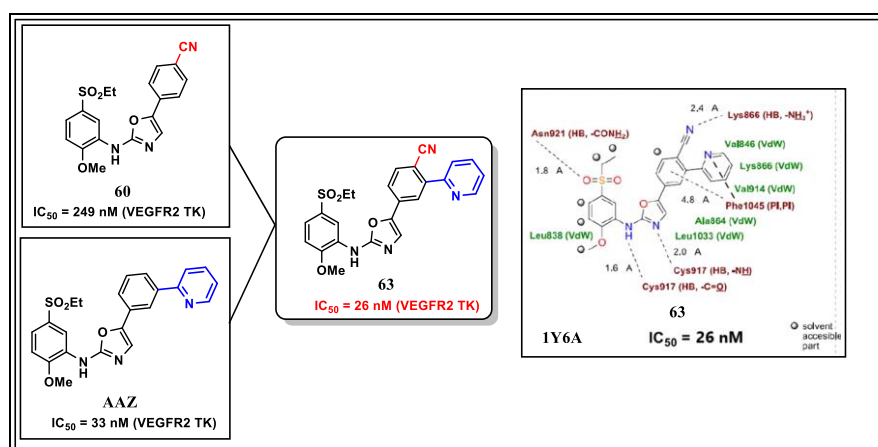


Figure 47. A synergic effect of disubstituted aminooxazole **63** on VEGFR2 TK inhibitory activity.

Based on expected synergy effect novel disubstituted oxazole compounds **BM(8-16)** were designed. These compounds can possess **three-point interactions within the recently uncovered SBCP pocket**:

- 1) *para* interaction mediated by -CN, -CONH₂ or -COOH group with Lys866 from the SBCP
- 2) H-bond of pyrrole, pyrazole or imidazole with Glu883 or Val912 from the SBCP
- 3) π - π interaction with Phe1045 from the SBCP (Figure 48)

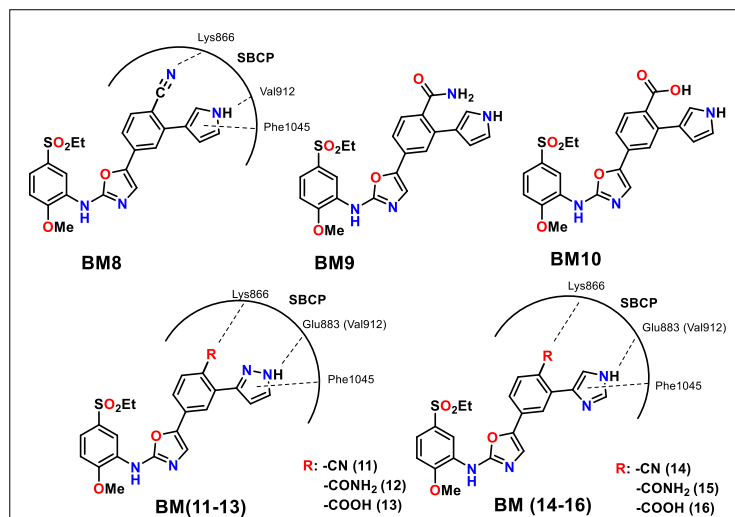


Figure 48. Structures of the 2nd generation inhibitors **BM(8-16)** with proposed three-point interaction with the SBCP.

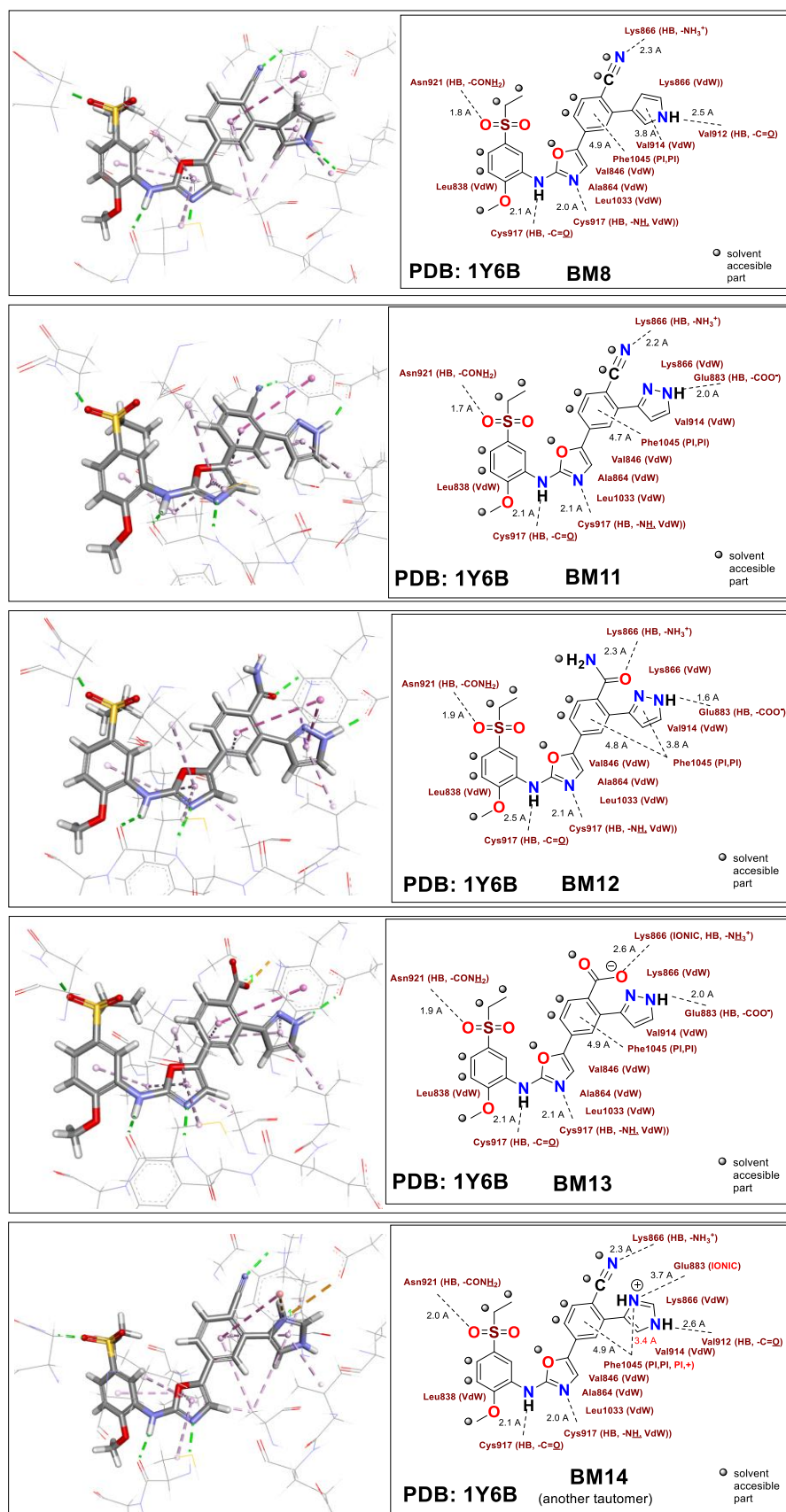
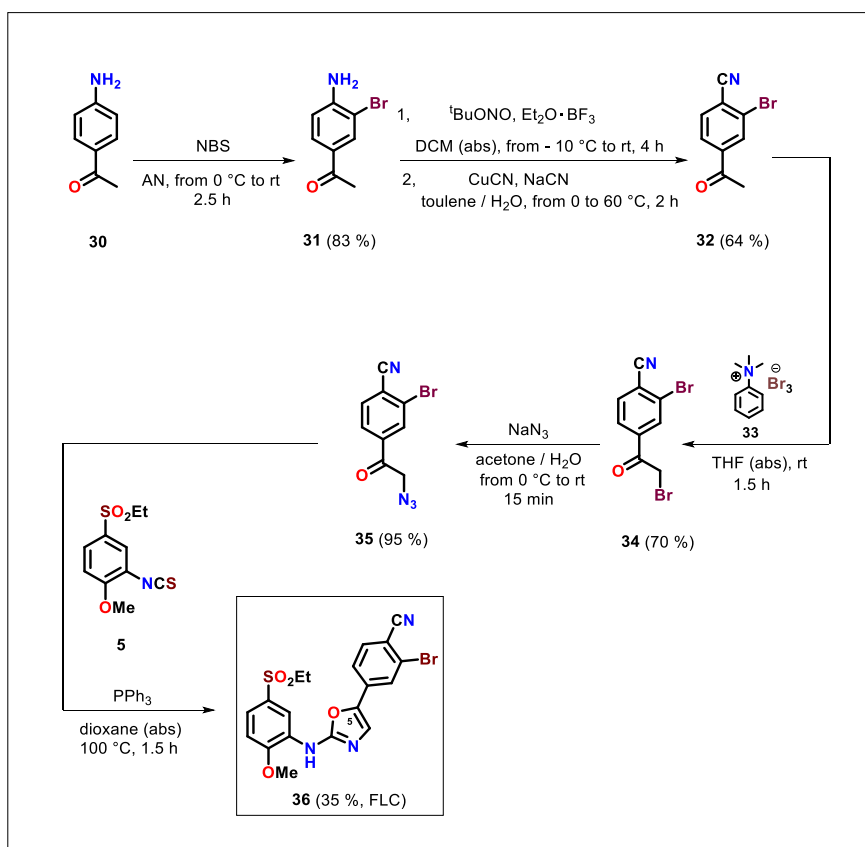


Figure 49. Predicted interacting poses of some three-point interacting VEGFR2 TK inhibitors BM(8 and 11-14).

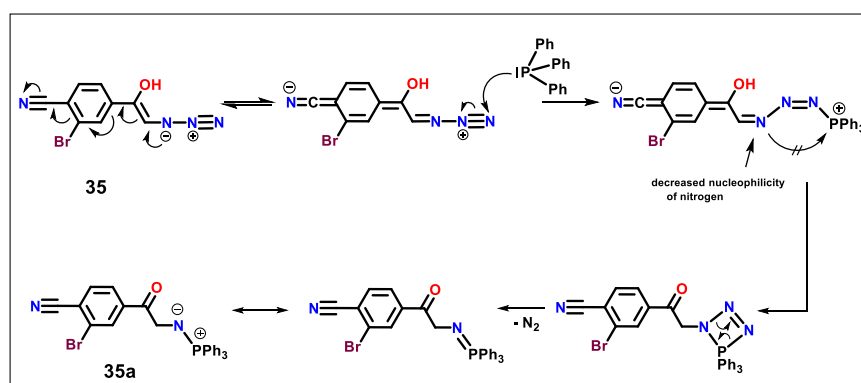
10.1. Synthesis of the general intermediate *N*,5-diaryloxazol-2-amine (36)

The synthesis of inhibitors **BM(8-16)** started by preparation of their joint intermediate **36**. Synthesis was initiated by treating of *p*-aminoacetophenone **30** with NBS to form brominated acetophenone **31**. Next step was a conversion of an amino group of **31** to a cyano group by Sandmeyer reaction with ^tBuONO and Et₂O · BF₃ to form diazonium salt. Subsequent slow addition of a mixture of CuCN / NaCN below 5 °C followed by stirring at 60 °C afforded benzonitrile **32** in 64 % yield. Alpha brominated derivative **34** was obtained within 1.5 h by treating of **32** with trimethylphenylammonium tribromide (**33**). Traces of bisbrominated side product was removed by trituration with a mixutre of EA / Hex. Nuclephilic substitution of bromine on aliphatic chain in **34** by NaN₃ afforded azide **35** in 95 % yield. The last reaction step was a formation of an oxazole ring by reaction of azide **35**, isothiocyanate **5** and PPh₃ in refluxing dioxane. (Scheme 36)



Scheme 36. Synthesis of the joint intermediate **36**.

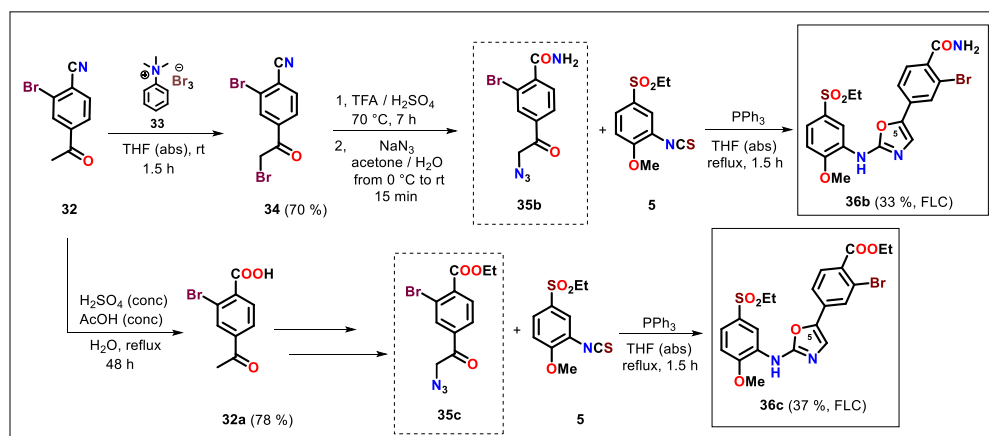
A formation of an oxazole ring was the most problematic step of the synthesis. According to experience in our research group, this type of reaction provides a product from 50 to 85 % yield after FLC. The reason of relatively low 35 % yield of the required oxazole **36** was probably caused by low reactivity of azide **35** toward PPh₃. In the first step of the synthesis (Staudinger reaction) PPh₃ attacks terminal nitrogen of an azide group which leads to another nucleophilic attacking to form four-membered ring. (Scheme 37) After releasing of N₂ an aza-ylide compound **35a** is formed. Complete reaction mechanism is described in the chapter 3 of this thesis in the Scheme 5. In our case, presence of *para* -CN substituted as a strong electron withdrawing group decreases a nucleophilicity of first nitrogen of an azide group leading to formation of other side product rather than **35a**. The scope of this type of reaction was investigated in our research group.⁸²



Scheme 37. Proposed mechanism of decreased reactivity of azide **35** in performed Staudinger reaction.

We also prepared the amide and ester derivatives **36b** (33 %) and **36c** (37 %) in order to verify low yield of an oxazole ring formation due to a presence of an electron withdrawing group in *para* position of acetophenone **35b,c**. As expected, the products **36b** and **36c** were formed in a similar low yield as **36**. (Scheme 38)

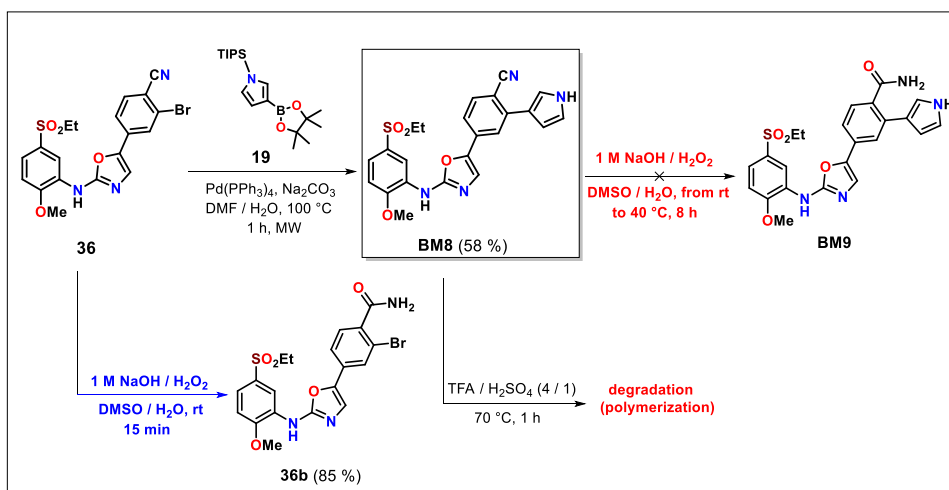
⁸² Almásy, A.; Šramel, P.; Almášiová, K.; Addova, G.; Hanquet, G.; Boháč, A (unpublished results)



Scheme 38. Synthesis of amide and carboxylic acid aminooxazoles **36b** and **36c**.

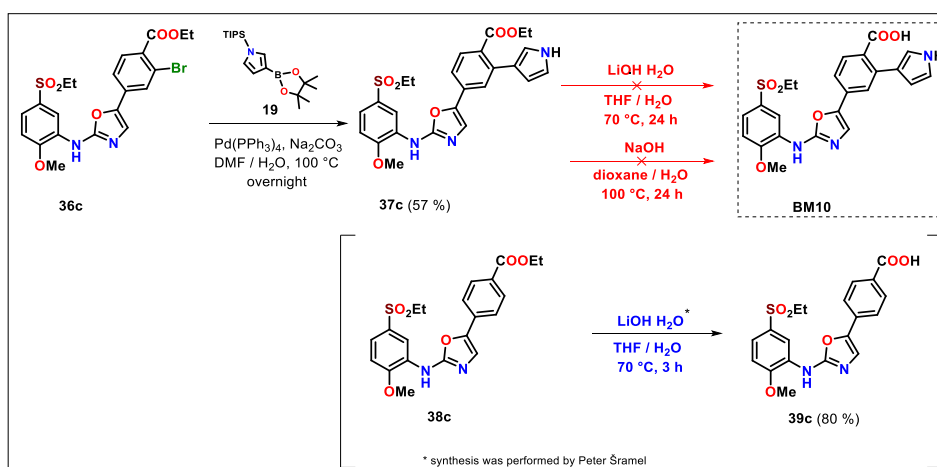
Synthesis of the first designed inhibitor **BM8** started from **36**. Bromooxazole **36** underwent Suzuki coupling reaction with previously prepared pyrrole pinacol boronate **19** to give **BM8** in 58 % yield. (Scheme 39) We also tried to prepare the amidic pyrrole containing inhibitor **BM9** by hydrolysis of a cyano group according to our previously published procedure.⁸³ Unfortunately, in this case hydrolysis was unsuccessful. When we applied the same reaction conditions to the intermediate **36** we successfully obtained amide **36b** within 15 min in 85 % yield. (Scheme 39) We have seen that pyrrole anion, formed in a basic conditions, disrupts reactivity of a cyano group toward nucleophilic attack. Since the pyrrole is an unstable heterocyclic compound in acidic conditions, hydrolysis performed in a mixture of TFA / H₂SO₄ caused polymerization of the starting compound **BM8**. (Scheme 39)

⁸³ Dobiaš, J.; Ondruš, M.; Hlaváč, M.; Murár, M.; Kóňa, J.; Addová, G.; Boháč, A. *Chem. Papers*, **2019**, *73*, 71 - 84.



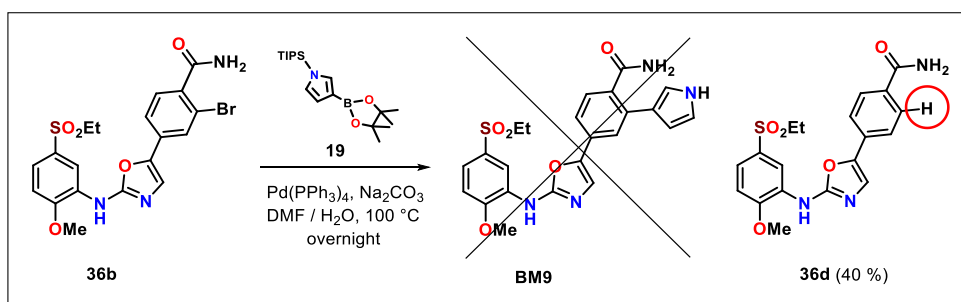
Scheme 39. Synthesis of required cyano derivative **BM8** and attempt to prepare the designed amide analogue **BM9**.

Similar results were observed by basic hydrolysis of an ester group of the pyrrole containing compound **37c**. Basic hydrolysis of a cyano group in **37c** did not provide the desired product **BM10**, but the same reaction condition applied to unsubstituted ester **38c** afforded the carboxylic acid **39c** in 80 % yield. (Scheme 40)



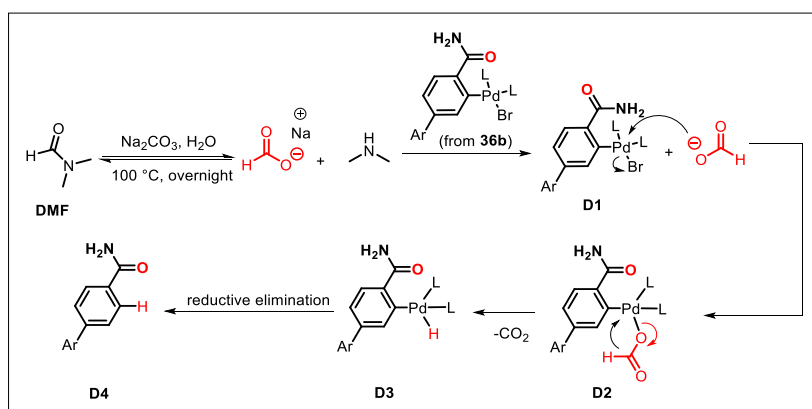
Scheme 40. Unsuccessful basic hydrolysis of an ester group on pyrrole derivative **37c**.

According to the above results we decided to perform hydrolysis of a cyano group first and then carry out a coupling reaction. Unfortunately, Suzuki coupling reaction with the amide derivative **36b** provided the dehalogenation product **36d** instead of the desired product **BM9**. (Scheme 41)



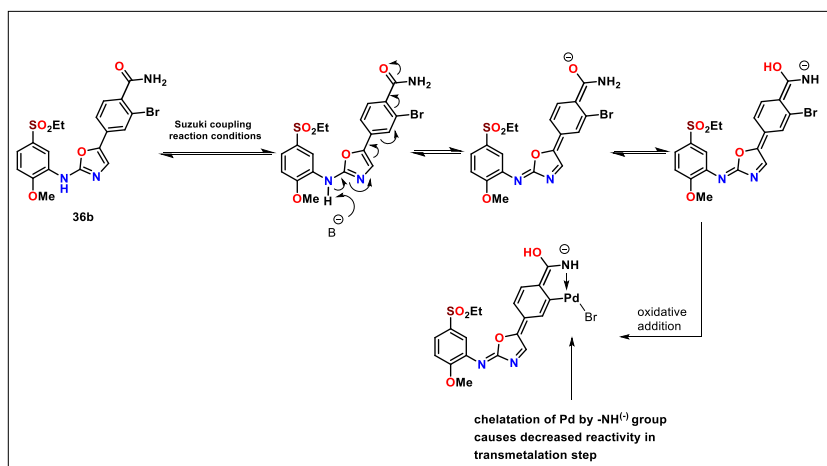
Scheme 41. Unexpected preparation of **36d** by dehalogenation of starting compound **36b**.

We proposed a mechanism of dehalogenation, which was initiated by hydrolysis of dimethylformamide (DMF) in a basic solution at 100 °C. Formed sodium formate attacks palladium^(II) in **D1** intermediate and releases a bromide anion to form intermediate **D2**. Subsequently, a hydride anion from formate moiety is transferred to Pd^(II) with simultaneous releasing of CO₂. Subsequent reductive elimination gives a product **D4**. (Scheme 42)



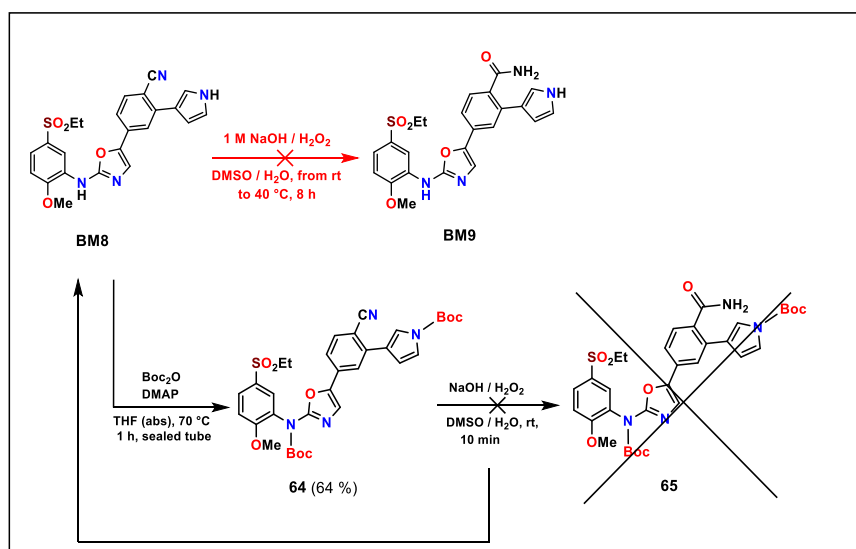
Scheme 42. A proposed mechanism of debromination of **36b** by decomposition products of DMF.

Therefore we decided to use dimethylacetamide (DMA) as a solvent, which does not contain hydrogen as in DMF. But in this case after 16 h at 100 °C we observed only a starting compound **36b**. The obvious reason of non-reactivity of **36b** is a presence of an amide group. In basic conditions of Suzuki coupling reaction an internal amine group of **36d** is deprotonated, which leads to delocalization of an anion and form more nucleophilic amide group, which could either disrupt Pd⁽⁰⁾ oxidative addition or favour Pd^(II) chelation. (Scheme 43)



Scheme 43. A proposed mechanism of non-reactivity of **36b** by Suzuki coupling reaction.

Since a pyrrole formed anion in **BM8** did not allow to prepare the amide product **BM9**, we decided to protect -NH- groups in **BM8** in order to hydrolyse an *ortho* -CN moiety. Reaction of **BM8** with Boc_2O and DMAP in THF (abs) provided bis Boc-protected oxazole **64** within 1 h. Even though resulting intermediate **64** should have been stable in basic environment, hydrolysis did not performed and only starting compound **BM8** was recovered. (Scheme 44)

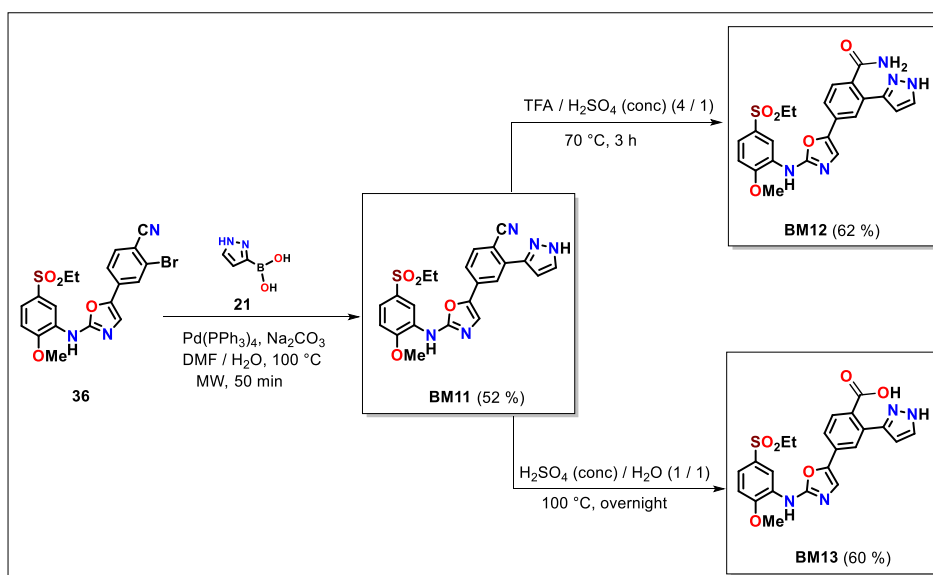


Scheme 44. Protection of a **BM8** and its unsuccessful hydrolysis.

According to unsatisfactory results we decided not to continue with preparation of three-point interacting pyrrole derivatives **BM9** and **BM10**.

10.2. Synthesis of pyrazole inhibitors BM(11-13)

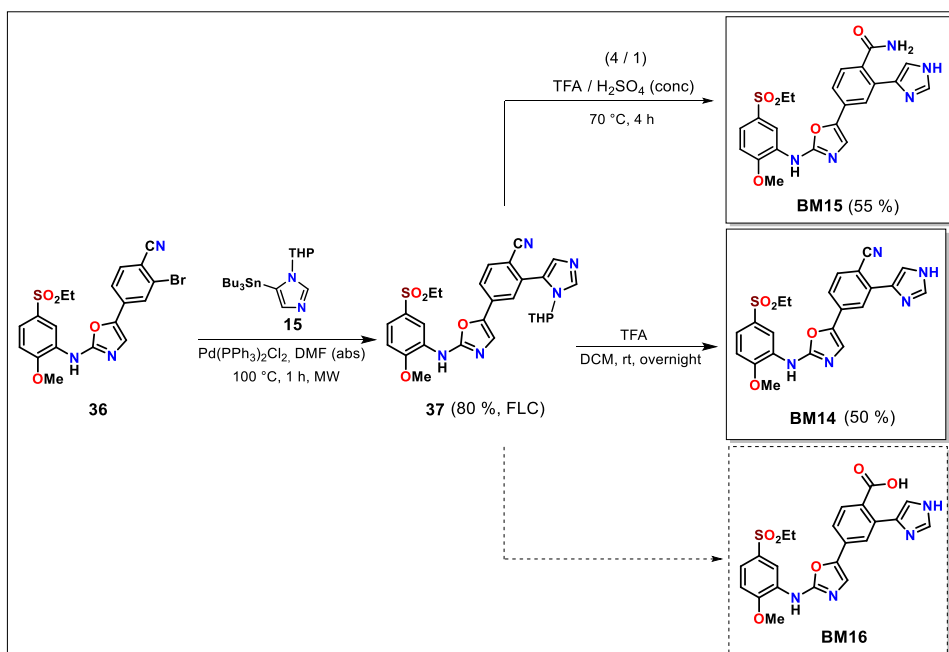
The pyrazole derivate **BM11** was prepared by Suzuki coupling reaction from the joint intermediate **36** and pyrazole boronic acid **21** in DMF / H₂O at 100 °C within 50 min under microwave irradiation. In a basic catalysed synthesis of amidic and carboxylic acid derivatives **BM(12-13)** we expected similar reduced reactivity of -CN group in a presence of a pyrazole anion. Much higher stability of pyrazole in acidic conditions compare to pyrrole analogue allowed us to successfully perform acidic hydrolysis of **BM11**. Partial hydrolysis of a cyano group by a mixture of TFA / H₂SO₄ (conc) (4 / 1) at 70 °C within 3 h gave an amidic inhibitor **BM12** in 62 % yield. Harder hydrolysis carried out in an aqueous solution of H₂SO₄ at 100 °C (overnight) provided a carboxylic acid derivative **BM13** in 60 % yield. (Scheme 45)



Scheme 45. Preparation of required pyrazole inhibitors **BM(11-13)**.

10.3. Synthesis of imidazole inhibitors BM(14-16)

Synthesis of proposed imidazole inhibitor **BM14** was initiated by Suzuki reaction from aminooxazole **36** and previously prepared tributylstannylimidazole **15** under microwave irradiation. THP-protected imidazole intermediate **37** was hydrolysed by TFA to get required compound **BM14** in 50 % yield. Synthesis of amide derivative **BM(15)** was also performed by partial acidic hydrolysis with a mixture of TFA / H₂SO₄. (Scheme 46) Derivative **BM16** has not been synthesized yet.



Scheme 46. Synthesis of the imidazole inhibitors **BM(14-16)**.

10.4. Synthesis of *N*,4-diaryloxazole-2-amine precursor (69)

Part of this project represents a development of *N*,5-regioisomers to the previously mentioned three-point interacting inhibitors **BM(8 and 11-16)**. Biomagi proposed *N*,4-disubstituted oxazole-2-amines **NBM(8 and 11-16)**, which may preserve the same binding position in the active site of VEGFR2 as **BM8 and BM(11-16)**. (Figure 50)

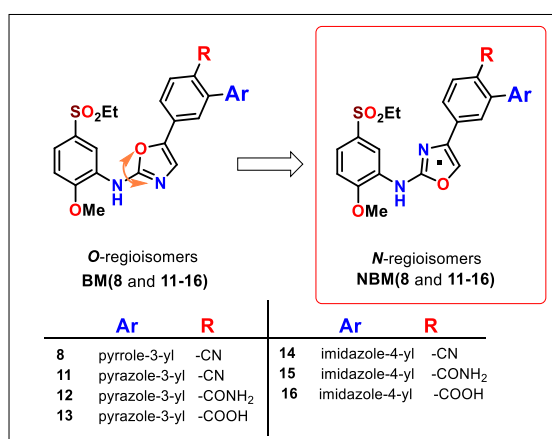
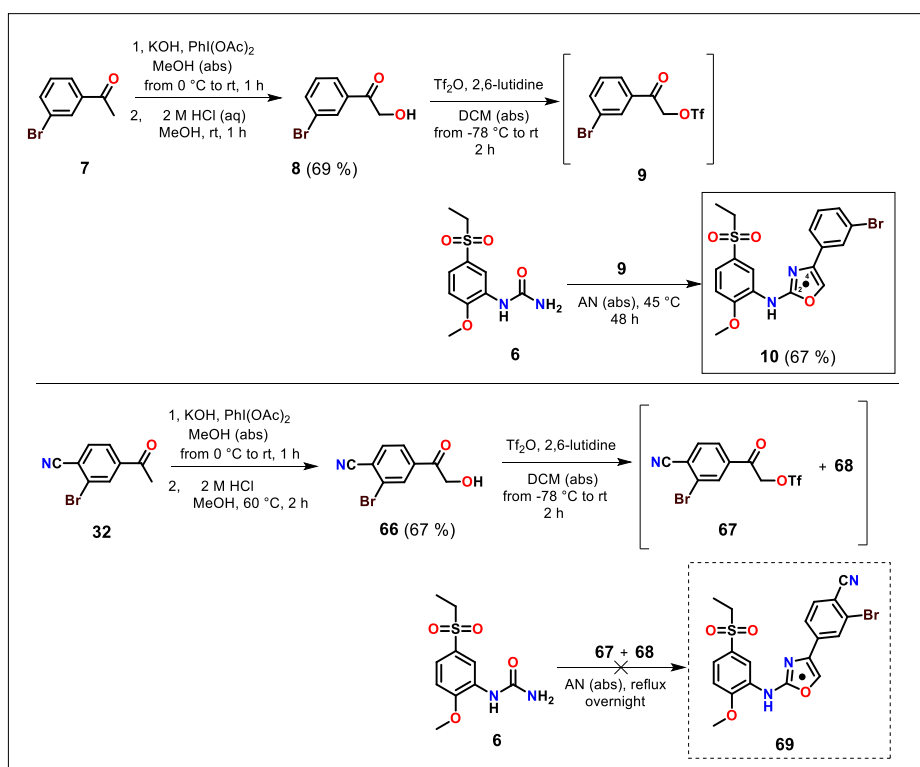


Figure 50. Structures of *N*,5-disubstituted oxazole-2-amines **BM(8 and 11-16)** and their regioisomers **NBM(8 and 11-16)**.

We used the same synthetic pathway for **69** as was successfully applied for the intermediate **10**. (Scheme 34) Synthesis started from benzonitrile **32**, which underwent α -oxidation with $\text{PhI}(\text{OAc})_2$ and subsequent hydrolysis yielding **66** in 75 % yield. Reaction of benzonitrile **66** with triflic anhydride in a presence of 2,6-lutidine provided a mixture of two major products **67** and **68** (based on TLC analysis), which was used in the next step without further purification. According to analogues of *N*-oxazole intermediate **10** (67 %), the mixture (**67** + **68**) had to be added portionwise to the urea **6** for 2 days at 45 °C. In this case no product **69** was obtained, even after increased temperature to reflux overnight. (Scheme 47)



Scheme 47. Unsuccessful preparation of *N*-regioisomeric intermediate **69** in comparison to the synthesis of less substituted compound **10**.

These unsatisfactory results forced us to analyse the crude mixture **67**+**68** (containing expected triflate **67**). Despite general low stability of triflates we performed an extraction and subsequent $^1\text{H-NMR}$ analyses of both crude products **9** and **67**+**68** in order to verify the formation of triflate during the transformation **8** or **66**. Obtained analyses revealed a presence of two products with very similar $^1\text{H-NMR}$ shifts but with different ratios depending on a analyzed reaction. (Figure 51)

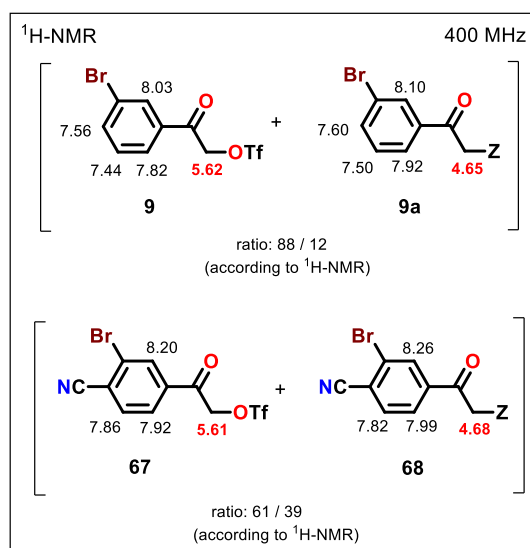
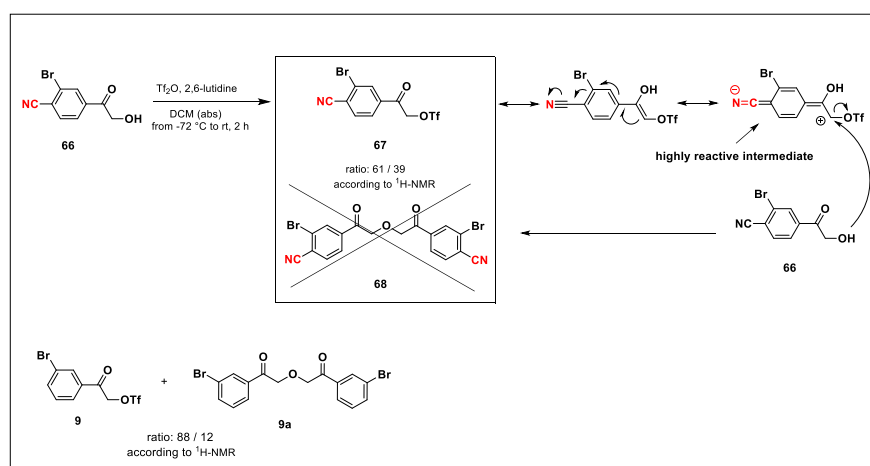


Figure 51. $^1\text{H-NMR}$ diagram of two crude mixtures (**9+9a**) and (**67+68**) with assigned chemical shifts.

According to described $^1\text{H-NMR}$ chemical shifts for α -trifluoromethanesulfonyl acetophenone from the literature, we assigned the products **9** and **67** to desired triflate reagents.⁸⁴ Then we suggested that side products **9a** and **68** could be dimers, formed from triflates **9** and **67** and their hydroxyethanone compounds **8** and **66**, resp. Presence of *p*-cyano substituent in **67** as a strong electron-withdrawing group may have caused formation of dimer **68** (61 : 39) in different ratio than the compound **9**. (Figure 51 and Scheme 48)



Scheme 48. A proposed mechanism of a dimer **68** formation.

Our hypothesis was also supported by fact, that proposed dimer **68** was easily separated by FLC on SiO_2 compare to relative low stability of triflates. On the other hand, $^{19}\text{F-NMR}$ and IR spectra

⁸⁴ Vedejs, E.; Engler, D.A.; Mullins, M.J. *J. Org. Chem.*, **1977**, *42*, 3109 - 3113.

confirmed a presence of unexpected $-\text{SO}_2\text{CF}_3$ group and obtained MS spectrum did not correspond directly with a structure of dimer **68**. Based on a proved presence of $-\text{SO}_2\text{CF}_3$ group in the structure **68** and markedly lower chemical shift of its α -methylene group in ^1H - and mainly ^{13}C -NMR in comparison to starting compound **66** (65.9 vs 45.2 ppm), we also proposed benzonitrile **70**. (Figure 52) Comparable spectral analyses and reaction of similar trifluoromethanesulfonyl compounds in the literatures also supported our hypothesis.^{85,86,87}

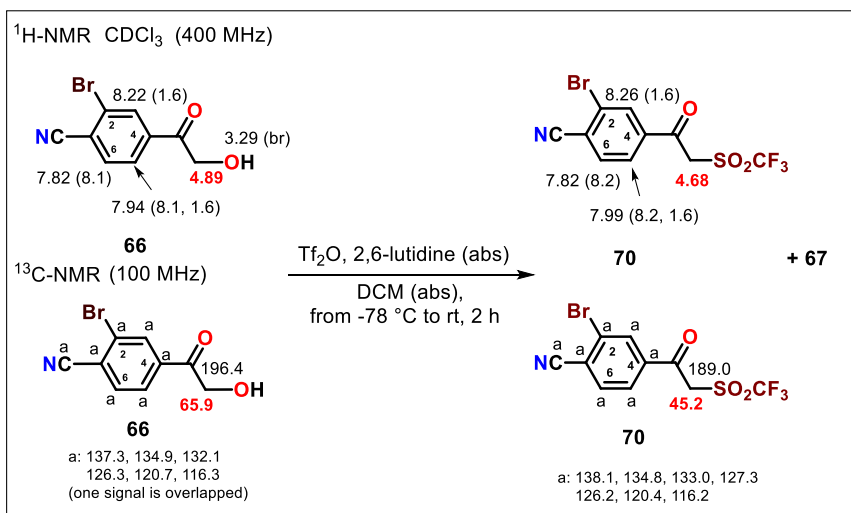


Figure 52. Comparison of NMR shifts of starting compound **66** and proposed product **70**.

Nevertheless, MS spectrum of **68** did not directly support **70** from our hypothesis. Therefore a structure of both side products **9a** and **68** remains unknown and other supporting analyses are planned to be performed

Another and more important problem in the synthesis of required intermediate **69** is low reactivity of crude triflate **67**, containing $-\text{CN}$ group compare to less substituted triflate **9**, whose structure was proved by next reaction product **10**. Despite various stronger reaction conditions (extended reaction time, higher temperature or microwave irradiation) we were not able to prepare the desired aminooxazole **69** from **67** and only starting material **6** and some decomposed products were present.

⁸⁵ Il Kong, H.; Crichton, J.E.; Manthorpe, J.M. *Tetrahedron Lett.*, **2011**, 52, 3714 - 3717.

⁸⁶ Hanack, M.; Wilhelm, B.; Subramanian, L.R. *Synthesis*, **1988**, 8, 592 - 595.

⁸⁷ Caldwell, Ch.; Chapman, K.; Hale, J.; Kim, D.; Lynch, Ch.; Maccoss, M.; Mills, S.G.; Willoughby, Ch.; Berk, S.; Kim, R.M. Assignee Merck and Co., Inc., USA, WO 2000059498, **2000**, A1

10.5. Evaluation of biological activity

In this project we have prepared proposed SBCP interacting inhibitors **BM(8 and 11-15)**, containing pyrrole-3-yl, pyrazole-3-yl and imidazole-4-yl moieties. (Figure 53) Synthesis of inhibitor **BM(16)** is still in progress. Pyrrole inhibitor **BM8** with *p*-cyano group exhibited nanomolar IC_{50} activity. Meanwhile we also determined an inhibitory activity of *N*-regioisomer **NBM1**, containing pyrrole-3-yl heterocycle in *meta* position (described in the Project 1). It exhibited $> 100 \mu M$ IC_{50} activity in comparison to its regioisomeric pair **BM1** possessing nanomolar IC_{50} activity. This unexpected results did not correspond with our aim to find the most appropriate heterocycle for both *N*- and *O*-regioisomers and planned synthesis of two pyrrole derivatives **BM(9-10)** was discontinued. Inhibitory activities of derivatives **BM(11-15)** will be determined.

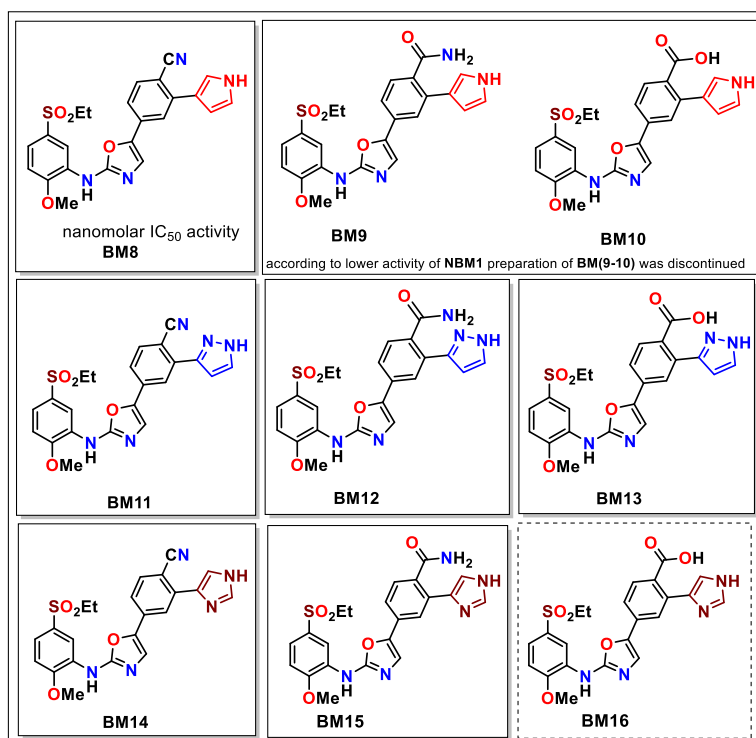
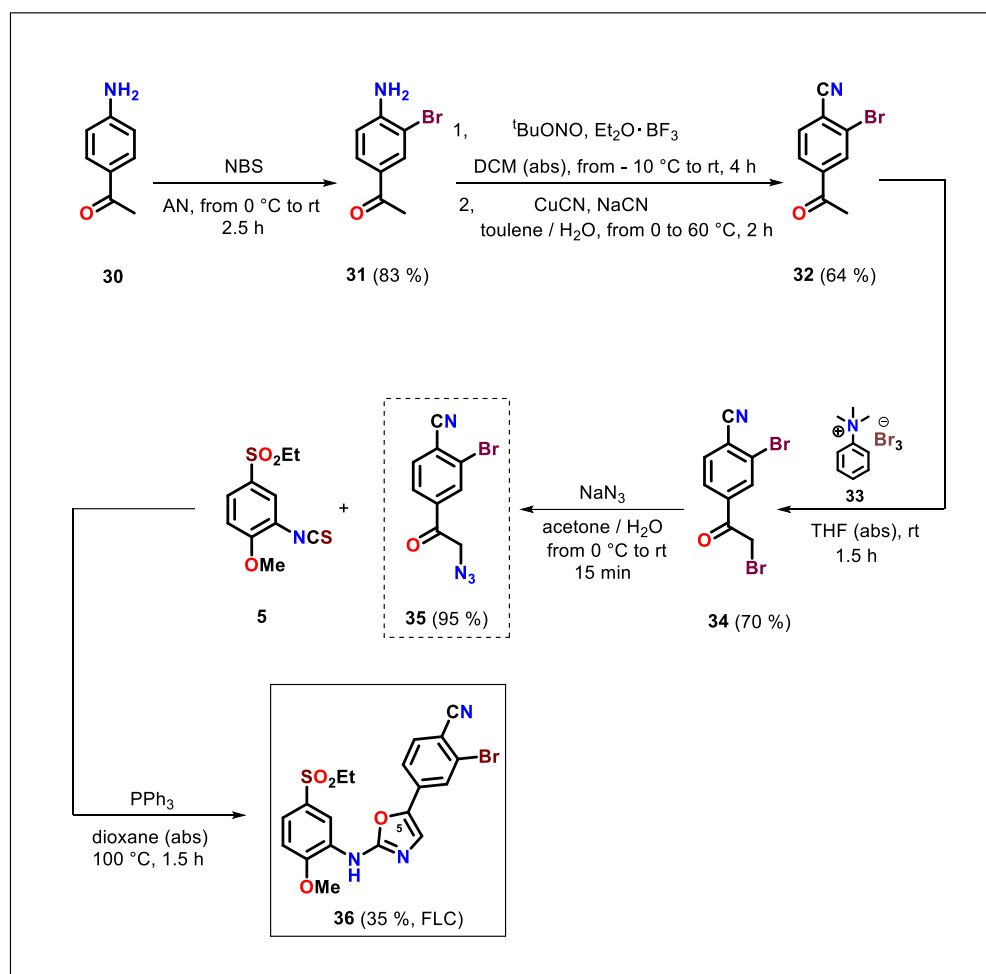


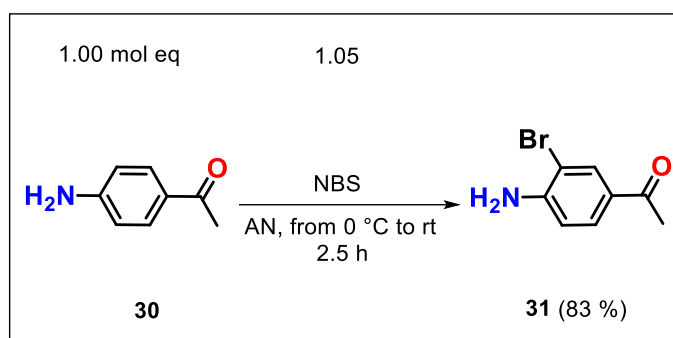
Figure 53. Structures of prepared three-point SBCP interacting inhibitors **BM(8 and 11-14)** and other planned **BM(15-16)** derivatives.

10.6. Experimental part

10.6.1. Synthesis of a general intermediate *N*,5-diaryloxazol-2-amine (36)

Scheme 49. Synthesis of a general intermediate 36.

Synthesis of 1-(4-amino-3-bromophenyl)ethanone (31)



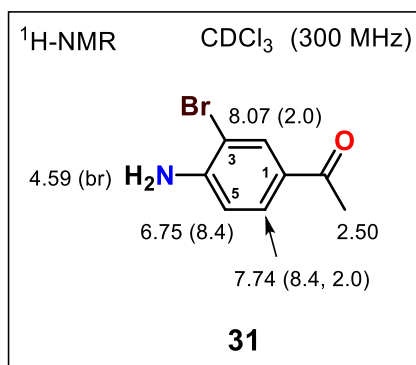
A solution of 500 mg (3.70 mmol, 1.00 mol eq) acetophenone **30** in 10 mL of AN was cooled down to 0 °C. Subsequently 692 mg (3.89 mmol, 1.05 mol eq) of NBS in 5 mL of AN was added dropwise and stirred 30 min at 0 °C and 2 h at rt. After complete consumption of starting material **30**, TLC analysis confirmed only a presence of a one product. Reaction mixture was evaporated, obtained solid residue dissolved in 20 mL of EA and extracted with NaHCO₃ (sat aq solution) (3 x 20 mL) and brine (3 x 20 mL). Combined organic layer was dried over Na₂SO₄, filtered and concentrated under reduced pressure yielding 658 mg (3.07 mmol, 83 %) of acetophenone **31** as brown oil, which solidified in a refrigerator.

Novelty: 1-(4-amino-3-bromophenyl)ethanone **31** is described in the literature by its M.p., ¹H-NMR, ¹³C-NMR and MS spectra.⁸⁸

M.p.: 59.0 - 62.0 °C [EA] (lit. M.p.: 52 °C [CH₂Cl₂]).⁸⁹

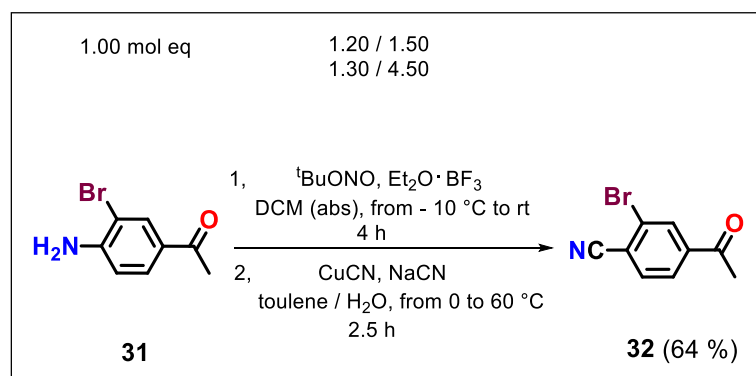
⁸⁸ Nery, M.S.; Azevedo, M.S.; Cardoso, J.N.; Slana, G.B.C.; Lopes, R.S.C.; Lopes, C.C. *Synthesis* **2007**, *10*, 1471 - 1474.

⁸⁹ Sartorius, F.; Trebing, M.; Brückner, C.; Brückner, R. *Chem. Eur. J.*, **2017**, *23*, 17463 - 17468.



$^1\text{H-NMR}$ (300 MHz, CDCl_3): δ 8.07 (d, 1H, $J(2,6) = 2.0$ Hz, H-C(2)), 7.74 (dd, 1H, $J(5,6) = 8.4$ Hz, $J(2,6) = 2.0$ Hz, H-C(6)), 6.75 (d, 1H, $J(5,6) = 8.4$ Hz, H-C(5)), 4.59 (br s, 2H, $-\text{NH}_2$), 2.50 (s, 3H, $-\text{COCH}_3$).

Synthesis of 4-acetyl-2-bromobenzonitrile (**32**)

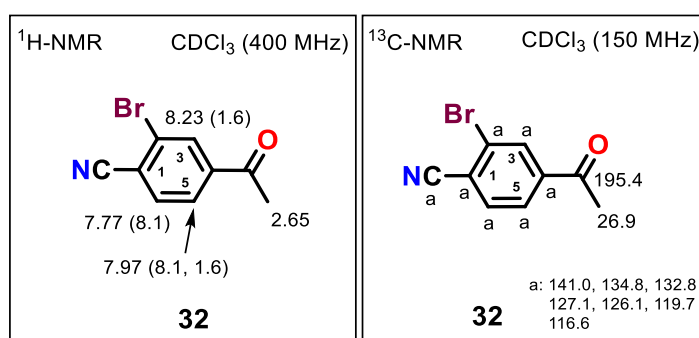


A solution of 3.50 g (16.4 mmol, 1.00 mol eq) acetofenone **31** in 30 mL of DCM (abs) was cooled down to -10 °C under Ar. Then, 2.33 mL (19.6 mmol, 1.20 mol eq) of $^t\text{BuONO}$ and 3.03 mL (24.5 mmol, 1.50 mol eq) of $\text{Et}_2\text{O} \cdot \text{BF}_3$ were added dropwise and the resulting mixture stirred at rt for 4 h. After precipitation of diazonium salt, the mixture was diluted with 30 mL of Et_2O , the precipitate filtered off, washed with Et_2O and dried by HV. Obtained salt was suspended in 40 mL of toluene and cooled to -5 °C. After that, the solution of 1.90 g (21.3 mmol, 1.30 mol eq) CuCN and 3.60 g (73.6 mmol, 4.50 mol eq) NaCN in 60 mL of H_2O was added dropwise while the temperature was kept below 5 °C. When addition was completed, the mixture was stirred at 0 °C for 30 min, warmed to 60 °C and stirred another 2 h. After cooling down to rt, 40 mL of EA was added, extracted with H_2O (3 x 20 mL) and brine (3 x 20).

Combined organic layer was dried over Na₂SO₄, filtered and concentrated with RVE to approx. 30 mL of its volume. Resulting solution was crystallized in a refrigerator to yield 2.34 g (10.4 mmol, 64 %) of **32** in form of brown-red crystals.

Novelty: 4-acetyl-2-bromobenzonitrile (**32**) is described in the literature by its ¹H-NMR, M.p. and IR spectra.⁹⁰

M.p.: 125.0 - 127.0 °C [Hex / EA] (lit. M.p.: 129 - 130 °C [EA]).⁹⁰

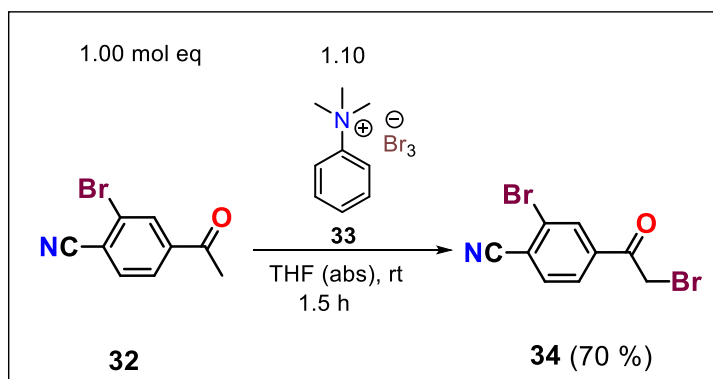


¹H-NMR (400 MHz, CDCl₃): δ 8.23 (d, 1H, $J(3,5) = 1.6$ Hz, H-C(3)), 7.97 (dd, 1H, $J(5,6) = 8.1$ Hz, $J(3,5) = 1.6$ Hz, H-C(5)), 7.77 (d, 1H, $J(5,6) = 8.1$ Hz, H-C(6)), 2.65 (s, 3H, -COCH₃).

¹³C-NMR (150 MHz, CDCl₃): δ 195.4 (-C(=O)CH₃), 141.0, 134.8, 132.8, 127.1, 126.1, 119.7, 116.6, 26.9 (-C(=O)CH₃).

⁹⁰ Tagawa, H.; Kubo, S. *Chem. Pharm. Bull.*, **1984**, 32, 3047 - 3052.

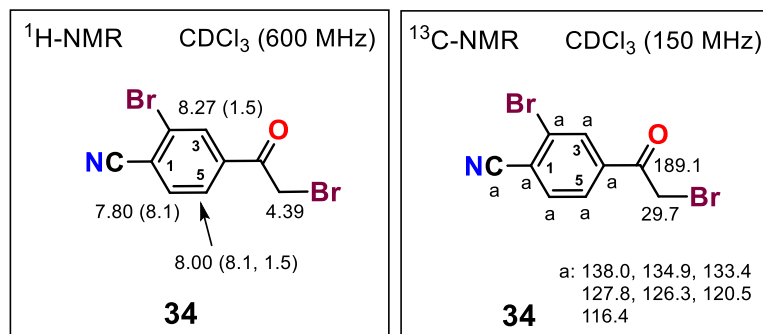
Synthesis of 2-bromo-4-(2-bromoacetyl)benzonitrile (**34**)



A solution of trimethylphenylammonium tribromide **33** (460 mg, 1.23 mmol, 1.10 mol eq) in 15 mL of THF (abs) was added dropwise to the solution of 250 mg (1.12 mmol, 1.00 mol eq) benzonitrile **32** in 15 mL of THF (abs) at rt within 30 min. After that, the reaction mixture was stirred another 1 h at the same temperature. Then the reaction mixture was evaporated, an obtained solid material dissolved in 30 mL of EA, extracted with H₂O (3 x 20 mL) and brine (3 x 10). The organic layer was dried over Na₂SO₄, filtered and evaporated under reduced pressure. The crude product was purified by trituration with Hex / EA yielding 236 mg (0.78 mmol, 70 %) of benzonitrile **34** as a red solid material.

Novelty: 2-bromo-4-(2-bromoacetyl)benzonitrile (**34**) is not described in the literature.

M.p.: 93.0 - 95.0 °C [Hex / EA].



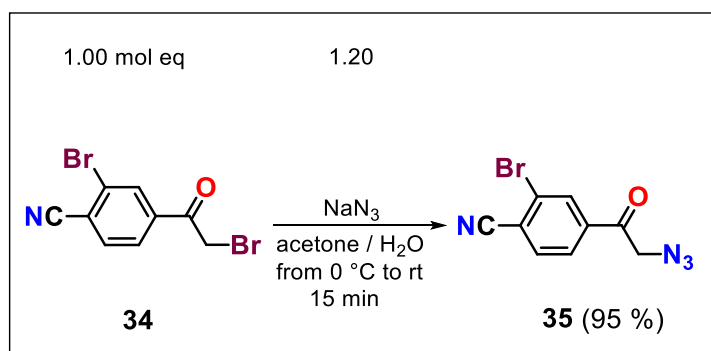
¹H-NMR (600 MHz, CDCl₃): δ 8.27 (d, 1H, *J*(3,5) = 1.5 Hz, H-C(3)), 8.00 (dd, 1H, *J*(5,6) = 8.1 Hz, *J*(3,5) = 1.5 Hz, H-C(5)), 7.80 (d, 1H, *J*(5,6) = 8.1 Hz, H-C(6)), 4.39 (s, 2H, -COCH₂Br).

¹³C-NMR (150 MHz, CDCl₃, PS-36-18): δ 189.1 (-COCH₂Br), 138.0, 134.9, 133.4, 127.8, 126.3, 120.5, 116.4, 29.7 (-COCH₂Br).

FT IR (solid, cm⁻¹): 3085 (w), 2943 (w), 2230 (w), 2083 (w), 1806 (w), 1709 (s), 1590 (w), 1546 (w), 1388 (s), 1274 (m), 1185 (s), 1141 (m), 1043 (m), 1015 (m), 927 (w), 887 (w), 832 (s), 750 (w), 687 (m), 668 (s), 600 (m), 549 (m), 460 (m).

Anal. calcd for C₉H₅Br₂NO (302.95): C, 35.68; H, 1.66; N, 4.62; found: 35.77; H: 1.90; N, 4.88.

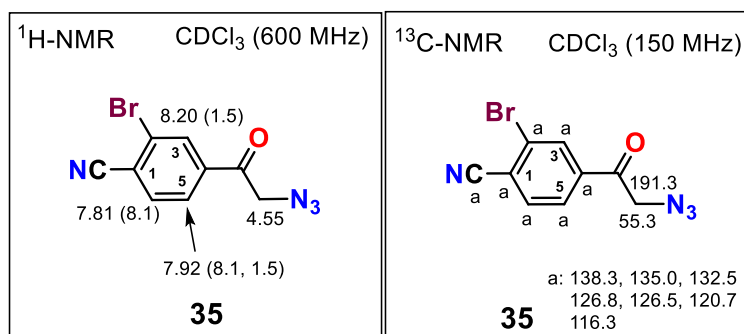
Synthesis of 4-(2-azidoacetyl)-2-bromobenzonitrile (**35**)



A solution of 500 mg (1.65 mmol, 1.00 mol eq) benzonitrile **34** in 15 mL of acetone was cooled down to 0 °C. Then, 127 mg (1.98 mmol, 1.20 mol eq) of NaN₃ dissolved in 2 mL of H₂O was added dropwise at 0 °C and resulting mixture stirred for 15 min at rt. Subsequently, acetone was evaporated with RVE, remaining material was dissolved in 15 mL of EA, washed with H₂O (2 x 20 mL) and brine (2 x 15 mL). Separated organic layer was dried over Na₂SO₄, filtered and concentrated under reduced pressure. The obtained oily product was purified by trituration with Hex / EA yielding 415 mg (1.57 mmol, 95 %) of benzonitrile **35** as a red solid compound.

Novelty: 4-(2-azidoacetyl)-2-bromobenzonitrile (**35**) is not described in the literature.

M.p.: 89.0 - 101.0 °C [Hex / EA] (dec).



¹H-NMR (600 MHz, CDCl₃): δ 8.20 (d, 1H, $J(3,5) = 1.5$ Hz, H-C(3)), 7.92 (dd, 1H, $J(5,6) = 8.1$ Hz, $J(3,5) = 1.5$ Hz, H-C(5)), 7.81 (d, 1H, $J(5,6) = 8.1$ Hz, H-C(6)), 4.55 (s, 2H, -COCH₂N₃).

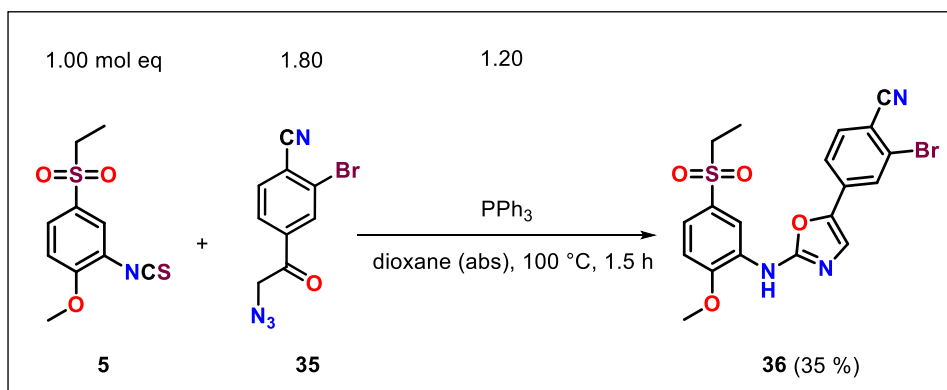
¹³C-NMR (150 MHz, CDCl₃): δ 191.3 (-C=O), 138.3 (C(4)), 135.0, 132.5, 126.8, 126.5, 120.7, 116.3, 55.3 (-COCH₂N₃).

FT IR (solid, cm⁻¹): 3378 (w), 2962 (w), 2906 (w), 2231 (w), 2203 (w), 2101 (s), 2007 (w), 1793 (w), 1702 (s), 1595 (w), 1548 (w), 1477 (w), 1388 (m), 1344 (w), 1267 (m), 1231 (m), 1199 (s), 1042 (m), 1023 (m), 982 (w), 919 (m), 828 (m), 771 (w), 674 (m), 655 (m), 603 (m), 555 (m), 524 (w), 453 (w).

MS (ESI m/z): 234.9 (60 % for Br⁷⁹) [M-N₂-e]⁻, 236.9 (60 % for Br⁸¹) [M-N₂-e]⁻ (unstable compound; negative mode).

Anal. calcd for C₉H₅BrN₄O (265.07): C, 40.78; H, 1.90; N, 21.14; found: 40.65; H, 1.78; N, 21.35

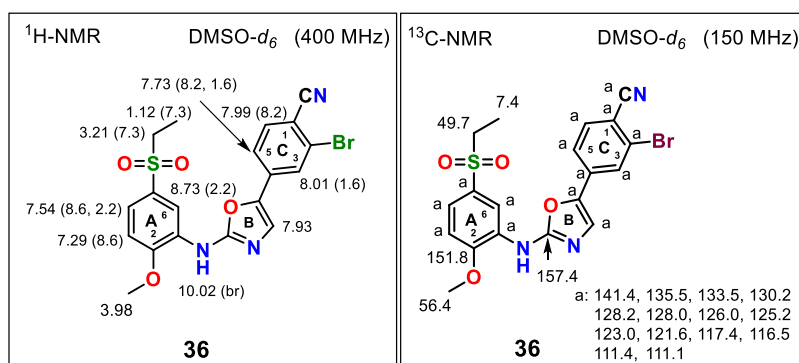
Synthesis of 2-bromo-4-{2-[5-(ethylsulfonyl)-2-methoxyphenylamino]oxazol-5-yl}benzonitrile (36)



A solution of 100 mg (0.39 mmol, 1.00 mol eq) isothiocyanate **5** and 122 mg (1.17 mmol, 1.20 mol eq) of PPh_3 in 10 mL of dioxane (abs) was placed into a $100\text{ }^\circ\text{C}$ preheated bath. Then, 185 mg (0.70 mmol, 1.80 mol eq) of azide **35** dissolved in 20 mL of dioxane (abs) was dropwise added to the mixture within 30 min. Then, the reaction mixture was stirred another 1 h at the same temperature. After that, the solvent was evaporated and the crude product purified by FLC (EA / cHex: gradient from 50 % to 100 % of EA). Subsequent trituration of the obtained product with benzene (to remove traces of $\text{PPh}_3=\text{S}$) provided 63.0 mg (0.14 mmol, 35 %) of aminooxazole **36** as a red solid material.

Novelty: 2-bromo-4-{2-[5-(ethylsulfonyl)-2-methoxyphenylamino]oxazol-5-yl}benzonitrile (**36**) is not described in the literature.

M.p.: $253.0 - 256.0\text{ }^\circ\text{C}$ (dec.) [Hex / EA].



¹H-NMR (400 MHz, DMSO-*d*₆): δ 10.02 (br s, 1H, -NH-), 8.73 (d, 1H, $J(4,6) = 2.2$ Hz, H-C_A(6)), 8.01 (d, 1H, $J(3,5) = 1.6$ Hz, H-C_C(3)), 7.99 (d, 1H, $J(5,6) = 8.2$ Hz, H-C_C(6)), 7.93 (s, 1H, H-C_B(4)), 7.73 (dd, 1H, $J(5,6) = 8.2$ Hz, $J(3,5) = 1.6$ Hz, H-C_C(5)), 7.54 (dd, 1H, $J(3,4) = 8.6$ Hz, $J(4,6) = 2.2$ Hz, H-C_A(4)), 7.29 (d, 1H, $J(3,4) = 8.6$ Hz, H-C_A(3)), 3.98 (s, 3H, -OCH₃), 3.21 (q, 2H, $J(\text{CH}_2, \text{CH}_3) = 7.3$ Hz, -SO₂CH₂CH₃), 1.12 (t, 3H, $J(\text{CH}_2, \text{CH}_3) = 7.3$ Hz, -SO₂CH₂CH₃).

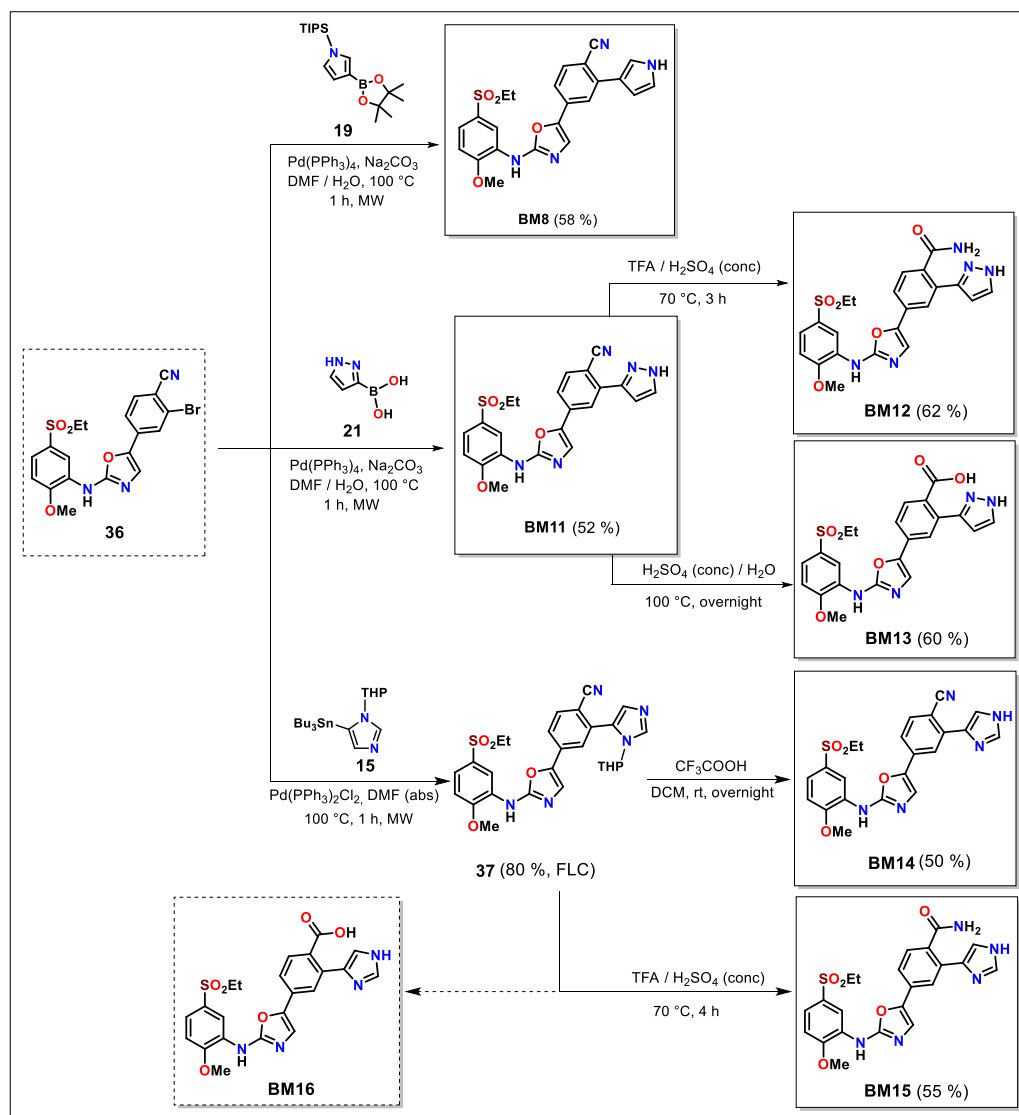
¹³C-NMR (150 MHz, DMSO-*d*₆): δ 157.4 (C_B(2)), 151.8 (C_A(2)), 141.4, 135.5, 133.5, 130.2, 128.2, 128.0, 126.0, 125.2, 123.0, 121.6, 117.4, 116.5, 111.4, 111.1, 56.4 (-OCH₃), 49.7 (-SO₂CH₂CH₃), 7.4 (-SO₂CH₂CH₃).

FT IR (solid, cm⁻¹): 2227 (w), 1602 (m), 1572 (s), 1520 (w), 1482 (w), 1424 (w), 1306 (m), 1264 (m), 1141 (m), 1122 (s), 1084 (m), 1016 (m), 887 (w), 825 (m), 795 (m), 719 (s), 640 (w), 575 (w), 552 (w), 525 (m), 478 (m), 422 (m), 411 (m).

MS (ESI *m/z*): 462.1 (100 % for Br⁷⁹) [M+H]⁺, 464.1 (98 % for Br⁸¹) [M+H]⁺ (positive mode).

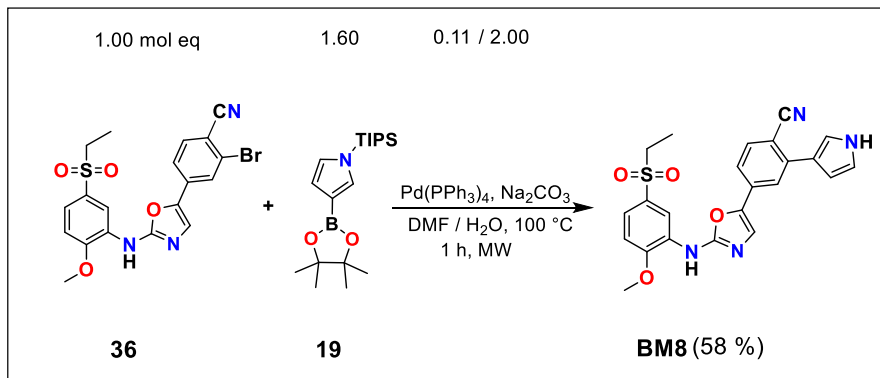
Anal. calcd for C₁₉H₁₆BrN₃O₄S (462.32): C, 49.36; H, 3.49; N, 9.09; found: C, 49.46; H, 3.58; N, 9.25.

10.6.2. Synthesis of *N*,5-diaryloxazol-2-amine VEGFR2 TK inhibitors BM(8-16)



Scheme 50. Synthesis of *N*,5-diaryloxazol-2-amine VEGFR2 TK inhibitors BM(8-16).

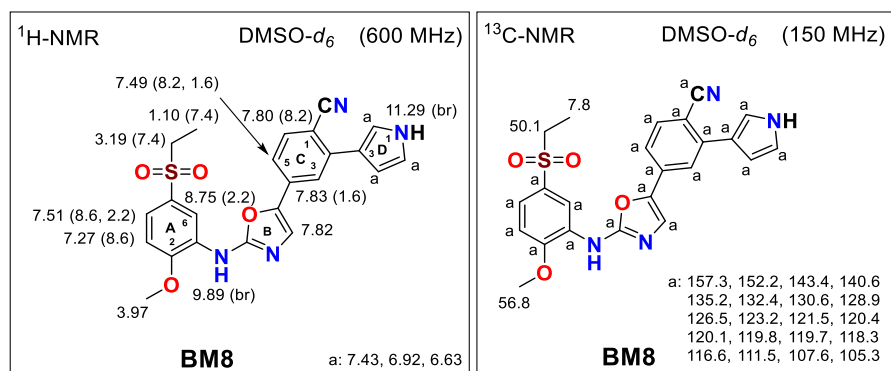
Synthesis of 4-{2-{[5-(ethylsulfonyl)-2-methoxyphenyl]amino}oxazol-4-yl}-2-(1*H*-pyrrol-3-yl)benzotrile (BM8)



A mixture of 25.0 mg (0.05 mmol, 1.00 mol eq) oxazole **36**, 28.3 mg (0.08 mmol, 1.60 mol eq) of pinacol boronate **19** and 6.26 mg (5.42 μmol, 0.11 mol eq) of Pd(PPh₃)₄ in 4 mL of DMF placed in a microwave vial was purged by Ar for 10 min. Then the solution of 11.0 mg (0.10 mmol, 2.00 mol eq) Na₂CO₃ in 1 mL of H₂O was also purged by Ar for 10 min and added to the reaction. Resulting mixture was stirred and heated in a microwave reactor at 100 °C for 1 h. After that TLC analysis confirmed a presence of only one new compound with traces of one side product. The reaction was cooled down, diluted with 10 mL of EA and washed with brine (5 x 15 mL). The organic layer was dried over Na₂SO₄, filtered and concentrated under reduced pressure. The crude product was purified by FLC (EA / Hex = 1 / 1) and crystallized from EA yielding 14.0 mg (0.03 mmol, 58 %) of desired oxazole **BM8** as a red solid material.

Novelty: 4-{2-{[5-(ethylsulfonyl)-2-methoxyphenyl]amino}oxazol-4-yl}-2-(1*H*-pyrrol-3-yl)benzotrile (**BM8**) is not described in the literature.

M.p.: 236.0 - 253.0 °C [EA/H] (dec).



¹H-NMR (600 MHz, DMSO-*d*₆): δ 11.29 (br s, 1H, H-N_D(1)), 9.89 (br s, 1H, -NH-), 8.75 (d, 1H, *J*(A₄,A₆) = 2.2 Hz, H-C_A(6)), 7.43, 6.92 and 6.63 (3 x br s, 3 x 1H, H-C_D(2,4 and 5)), 7.83 (d, 1H, *J*(C₃,C₅) = 1.6 Hz, H-C_C(3)), 7.82 (s, 1H, H-C_B(4)), 7.80 (d, 1H, *J*(C₅,C₆) = 8.2 Hz, H-C_C(6)), 7.51 (dd, 1H, *J*(A₃,A₄) = 8.6 Hz, *J*(A₄,A₆) = 2.2 Hz, H-C_A(4)), 7.49 (dd, 1H, *J*(C₄,C₅) = 8.2 Hz, *J*(C₃,C₅) = 1.6 Hz, H-C_C(5)), 7.27 (d, 1H, *J*(A₃,A₄) = 8.6 Hz, H-C_A(3)), 3.97 (s, 3H, CH₃O-), 3.19 (q, 2H, *J*(CH₂,CH₃) = 7.4 Hz, CH₃CH₂SO₂-), 1.10 (t, 3H, *J*(CH₂,CH₃) = 7.4 Hz, CH₃CH₂SO₂-).

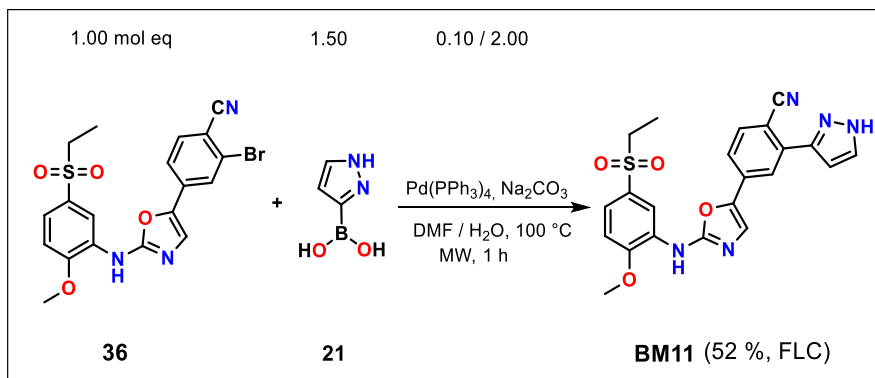
¹³C-NMR (150 MHz, DMSO-*d*₆): δ 157.3, 152.2, 143.4, 140.6, 135.2, 132.4, 130.6, 128.9, 126.5, 123.2, 121.5, 120.4, 120.1, 119.8, 119.7, 118.3, 116.6, 111.5, 107.6, 105.3, 56.8 (CH₃O-), 50.1 (CH₃CH₂SO₂-), 7.8 (CH₃CH₂SO₂-).

FT-IR (solid, cm⁻¹): 3405 (m), 2358 (w), 2340 (w), 2218 (w), 1721 (m), 1603 (s), 1572 (s), 1528 (s), 1486 (m), 1424 (s), 1372 (w), 1302 (m), 1264 (s), 1118 (s), 1084 (w), 1045 (w), 911 (m), 894 (m), 809 (s), 718 (s), 643 (w), 592 (s), 482 (s).

MS (ESI m/z): 447.1 (100 %) [M-H]⁻ (negative mode).

Anal. calcd for C₂₃H₂₀N₄O₄S (448.50): C, 61.60; H, 4.50; N, 12.49; Found: C, 61.95; H, 4.90; N, 12.82.

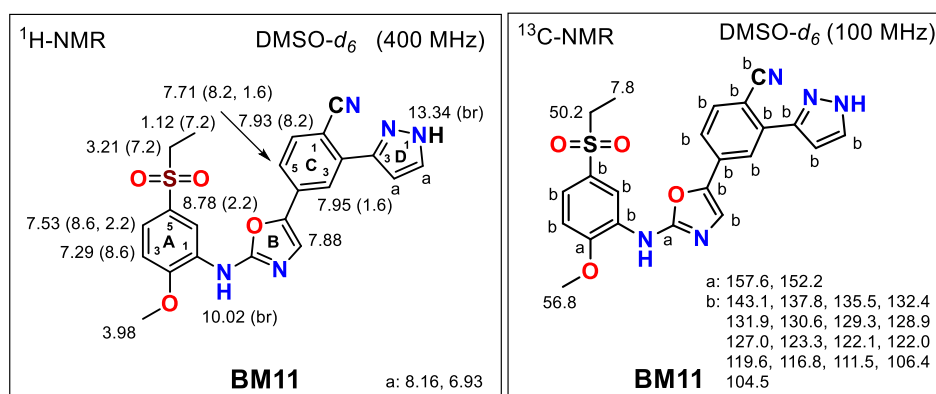
Synthesis of 4-{2-[[5-(ethylsulfonyl)-2-methoxyphenyl]amino]oxazol-4-yl}-2-(1H-pyrazol-3-yl)benzonitrile (BM11)



A mixture of 120 mg (0.26 mmol, 1.00 mol eq) oxazole **36**, 44.0 mg (0.39 mmol, 1.50 mol eq) of boronic acid **21** and 30.0 mg (0.03 mmol, 0.10 mol eq) of Pd(PPh₃)₄ in 4 mL of DMF (abs) was purged by Ar for 10 min. A solution of 55.0 mg (0.52 mmol, 2.00 mol eq) Na₂CO₃ in 1 mL of H₂O was purged by Ar for 10 min, subsequently added to the reaction mixture and stirred and irradiated at 100 °C in a microwave reactor for 1 h. Then TLC analysis confirmed a presence of a new product without **36** and some traces of two side products. The reaction was cooled down, diluted with 20 mL of H₂O and 5 mL of 2 M HCl (aq) was added. Resulting mixture was extracted with EA (3 x 15 mL) and organic layer washed with brine (3 x 15 mL). The separated organic layer dried over Na₂SO₄, filtered and concentrated under reduced pressure. The crude product was purified by FLC (DCM / MeOH = 50 / 1) yielding 63.0 mg (0.14 mmol, 52 %) of desired oxazole **BM11** as a gray solid compound.

Novelty: 4-{2-[[5-(ethylsulfonyl)-2-methoxyphenyl]amino]oxazol-4-yl}-2-(1H-pyrazol-3-yl)benzonitrile (**BM11**) is not described in the literature.

M.p.: 238.5 - 242.5 °C (dec) [DCM / MeOH].



¹H-NMR (400 MHz, DMSO-*d*₆): δ 13.34 (br s, 1H, H-N_D(1)), 10.02 (br s, 1H, -NH-), 8.78 (d, 1H, $J(A_4, A_6) = 2.2$ Hz, H-C_A(6)), 8.16 and 6.93 (2 x br s, 2 x 1H, H-C_D(4 and 5)), 7.95 (d, 1H, $J(C_3, C_5) = 1.6$ Hz, H-C_C(3)), 7.93 (d, 1H, $J(C_5, C_6) = 8.2$ Hz, H-C_C(6)), 7.88 (s, 1H, H-C_B(4)), 7.71 (dd, 1H, $J(C_5, C_6) = 8.2$ Hz, $J(C_3, C_5) = 1.6$ Hz, H-C_C(5)), 7.53 (dd, 1H, $J(A_3, A_4) = 8.6$ Hz, $J(A_4, A_6) = 2.2$ Hz, H-C_A(4)), 7.29 (d, 1H, $J(A_3, A_4) = 8.6$ Hz, H-C_A(3)), 3.98 (s, 3H, CH₃O-), 3.21 (q, 2H, $J(\text{CH}_2, \text{CH}_3) = 7.2$ Hz, CH₃CH₂SO₂-), 1.12 (t, 3H, $J(\text{CH}_2, \text{CH}_3) = 7.2$ Hz, CH₃CH₂SO₂-).

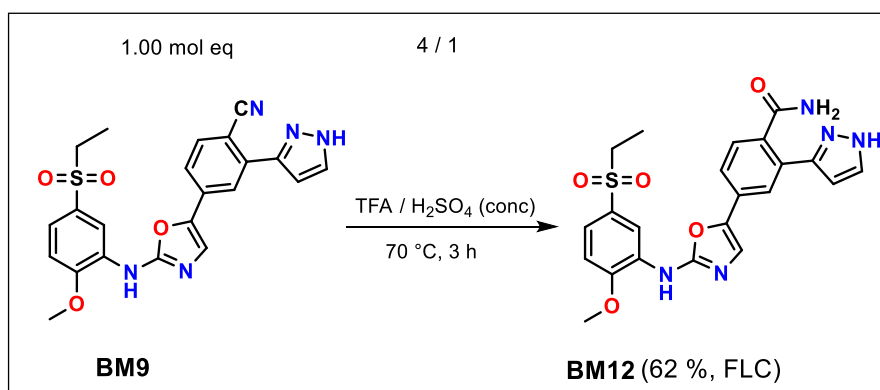
¹³C-NMR (100 MHz, DMSO-*d*₆): δ 157.6, 152.2, 143.1, 137.8, 135.5, 132.4, 131.9, 130.6, 129.3, 128.9, 127.0, 123.3, 122.1, 122.0, 119.6, 116.8, 111.5, 106.4, 104.5, 56.8 (CH₃O-), 50.2 (CH₃CH₂SO₂-), 7.8 (CH₃CH₂SO₂-).

FT-IR (solid, cm⁻¹): 3415 (w), 3285 (w), 2921 (w), 2215.1 (m), 1735 (w), 1601 (m), 1574 (s), 1503 (m), 1432 (m), 1299 (m), 1263 (s), 1185 (w), 1143 (s), 1123 (s), 1025 (m), 922 (m), 877 (m), 826 (m), 776 (s), 716 (s), 598 (m), 525 (m), 491 (s), 450 (m).

MS (ESI m/z): 448.1 (100 %) [M-H]⁺ (negative mode).

Anal. calcd for C₂₂H₁₉N₅O₄S (449.49): C, 58.79; H, 4.26; N, 15.58; Found: C, 58.95; H, 4.44; N, 15.48.

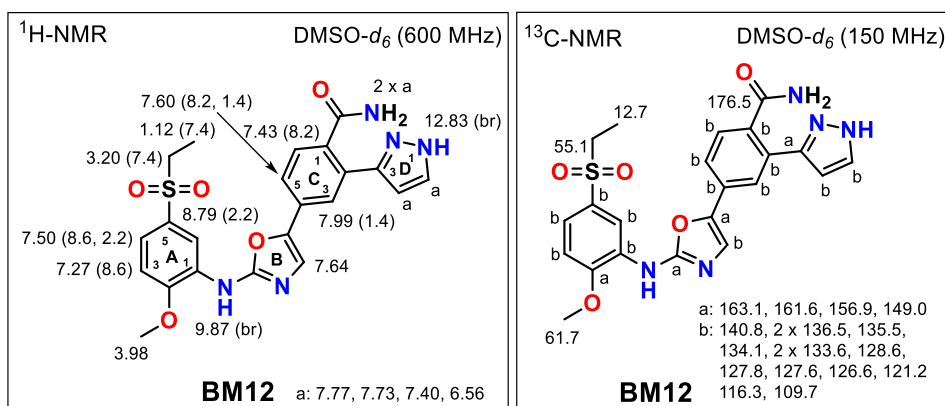
Synthesis of 4-(2-((5-(ethylsulfonyl)-2-methoxyphenyl)amino)oxazol-4-yl)-2-(1H-pyrazol-3-yl)benzamide (BM12)



A mixture of 50.0 mg (0.11 mmol, 1.00 mol eq) oxazole **BM9** in 2 mL of CF₃COOH (TFA) (conc) and 0.5 mL of H₂SO₄ (conc) was stirred at 70 °C for 3 h. Then TLC analysis confirmed a presence of a new product without **BM9** and some traces of side products. The reaction was cooled down, 100 mL of H₂O added and extracted with DCM (3 x 15 mL). Combined organic layer was extracted with saturated solution of NaHCO₃ (3 x 15 mL) and brine (2 x 15 mL), dried over Na₂SO₄, filtered and concentrated under reduced pressure. The crude product was triturated with cHex / EA to provide 32.0 mg (0.07 mmol, 62 %) of desired oxazole **BM12** as a white solid compound.

Novelty: 4-(2-((5-(ethylsulfonyl)-2-methoxyphenyl)amino)oxazol-4-yl)-2-(1H-pyrazol-3-yl)benzamide (**BM12**) is not described in the literature.

M.p.: 144.0 - 150.0 °C (dec) [DCM].



¹H-NMR (600 MHz, DMSO-*d*₆): δ 12.83 (br s, 1H, H-N_D(1)), 9.87 (br s, 1H, -NH-), 8.79 (d, 1H, $J(A_4, A_6) = 2.2$ Hz, H-C_A(6)), 7.99 (d, 1H, $J(C_3, C_5) = 1.4$ Hz, H-C_C(3)), 7.77, 7.73, 7.40 and 6.56 (4 x br s, 4 x 1H, H-C_D(4 and 5) and -CONH₂), 7.64 (s, 1H, H-C_B(4)), 7.60 (dd, 1H, $J(C_5, C_6) = 8.2$ Hz, $J(C_3, C_5) = 1.4$ Hz, H-C_C(5)), 7.50 (dd, 1H, $J(A_3, A_4) = 8.6$ Hz, $J(A_4, A_6) = 2.2$ Hz, H-C_A(4)), 7.43 (d, 1H, $J(C_5, C_6) = 8.2$ Hz, H-C_C(6)), 7.27 (d, 1H, $J(A_3, A_4) = 8.6$ Hz, H-C_A(3)), 3.98 (s, 3H, CH₃O-), 3.20 (q, 2H, $J(CH_2, CH_3) = 7.4$ Hz, CH₃CH₂SO₂-), 1.12 (t, 3H, $J(CH_2, CH_3) = 7.4$ Hz, CH₃CH₂SO₂-).

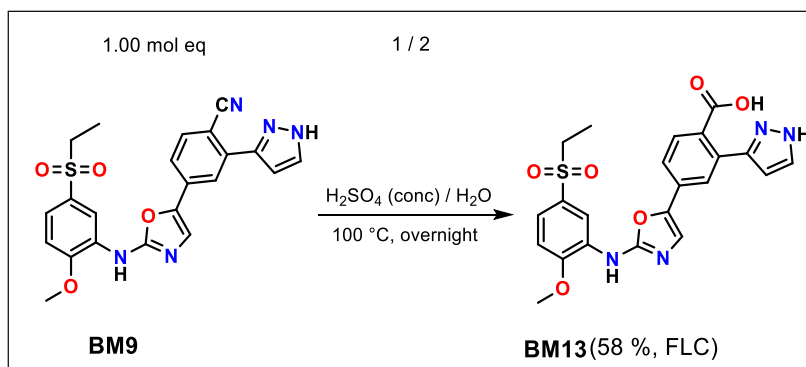
¹³C-NMR (150 MHz, DMSO-*d*₆): δ 176.5 (CONH₂), 163.1, 161.6, 156.9, 149.0, 140.8, 2 x 136.5, 135.5, 134.1, 2 x 133.6, 128.6, 127.6, 126.6, 121.2, 116.3, 109.7, 61.7 (CH₃O-), 55.1 (CH₃CH₂SO₂-), 12.7 (CH₃CH₂SO₂-).

FT-IR (solid, cm⁻¹): 3177 (m), 2962 (w), 2924 (w), 2363 (w), 2342 (w), 2117 (w), 1607 (m), 1572 (s), 1527 (m), 1506 (w), 1457 (w), 1421 (w), 1404 (w), 1301 (m), 1261 (s), 1200 (m), 1179 (w), 1139 (m), 1120 (s), 1086 (m), 1044 (m), 1016 (m), 923 (w), 792 (s), 719 (s), 490 (s).

MS (ESI m/z): 468.1 (100 %) [M+H]⁺, 490.0 (80 %) [M+Na]⁺, 506.0 (25 %) [M+K]⁺ (positive mode).

Anal. calcd for C₂₂H₂₁N₅O₅S (467.50): C, 56.52; H, 4.53; N, 14.98; Found: C, 56.85; H, 5.74; N, 15.16.

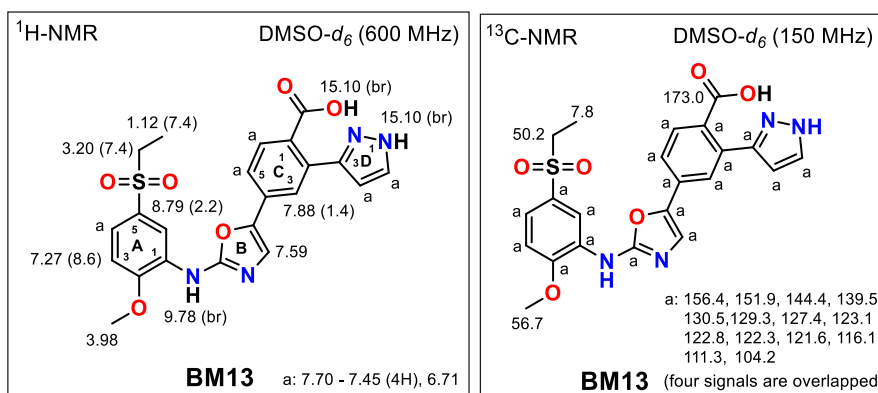
Synthesis of 4-{2-[(5-(ethylsulfonyl)-2-methoxyphenyl)amino]oxazol-4-yl}-2-(1H-pyrazol-3-yl)benzoic acid (BM13)



A mixture of 50.0 mg (0.11 mmol, 1.00 mol eq) oxazole **BM9** in 2 mL of H_2O and 1 mL of H_2SO_4 (conc) was stirred at $100\text{ }^\circ\text{C}$ overnight. Then TLC analysis confirmed a presence of a new product with traces of the amidic intermediate **BM12**. (also present after prolonged reaction time) The reaction was cooled down, 100 mL of H_2O was added, extracted with DCM (3 x 15 mL) and a combined organic layer washed with brine (3 x 15 mL). The crude product was purified by FLC (MeOH / EA = 1 / 10) yielding 30.0 mg (0.06 mmol, 58 %) of carboxylic acid **BM13** as a white solid compound.

Novelty: 4-{2-[(5-(ethylsulfonyl)-2-methoxyphenyl)amino]oxazol-4-yl}-2-(1H-pyrazol-3-yl)benzoic acid (**BM13**) is not described in the literature.

M.p.: $200 - 270\text{ }^\circ\text{C}$ (dec) [MeOH / EA].



$^1\text{H-NMR}$ (600 MHz, $\text{DMSO-}d_6$): δ 2 x 15.10 (2 x br s, 2 x 1H, -COOH and H- $\text{N}_D(1)$), 9.78 (br s, 1H, -NH-), 8.79 (d, 1H, $J(\text{A}_4, \text{A}_6) = 2.2\text{ Hz}$, H- $\text{C}_A(6)$), 7.88 (d, 1H, $J(\text{C}_3, \text{C}_5) = 1.4\text{ Hz}$, H-

Project 2. Development of three-point interacting SBCP VEGFR2 TK inhibitors BM(8-16)

$C_C(3)$), 7.70 - 7.45 and 6.71 (m and s, 5H, H- $C_D(4$ and 5), H- $C_C(5$ and 6) and H- $C_A(4)$), 7.59 (s, 1H, H- $C_B(4)$), 7.27 (d, 1H, $J(A_3,A_4) = 8.6$ Hz, H- $C_A(3)$), 3.98 (s, 3H, CH_3O^-), 3.20 (q, 2H, $J(CH_2,CH_3) = 7.4$ Hz, $CH_3CH_2SO_2^-$), 1.12 (t, 3H, $J(CH_2,CH_3) = 7.4$ Hz, $CH_3CH_2SO_2^-$).

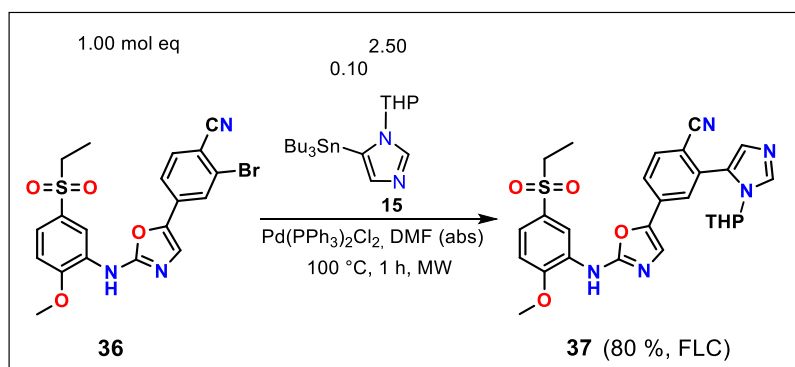
$^{13}C-NMR$ (150 MHz, DMSO- d_6 , MH-168B-19): δ 173.0 (COOH), 156.4, 151.9, 144.4, 139.5, 130.5, 129.3, 127.4, 123.1, 122.8, 122.3, 121.6, 116.1, 111.3, 104.2, 56.7 (CH_3O^-), 50.2 ($CH_3CH_2SO_2^-$), 7.8 ($CH_3CH_2SO_2^-$). Four signals are overlapped.

FT-IR (solid, cm^{-1}): 3132 (w), 2926 (w), 2852 (w), 2117 (w), 1998 (w), 1575 (s), 1507 (m), 1386 (m), 1302 (m), 1265 (m), 1141 (m), 1122 (s), 1047 (w), 1018 (w), 981 (w), 926 (m), 883 (w), 844 (w), 796 (m), 719 (m), 596 (w), 576 (w), 518 (w), 492 (m), 450 (w).

MS (ESI m/z): 467.1 (100 %) $[M-H]^+$ (negative mode).

Anal. calcd for $C_{22}H_{20}N_4O_6S$ (468.48): C, 56.40; H, 4.30; N, 11.96; Found: C, 56.75; H, 4.15; N, 12.10.

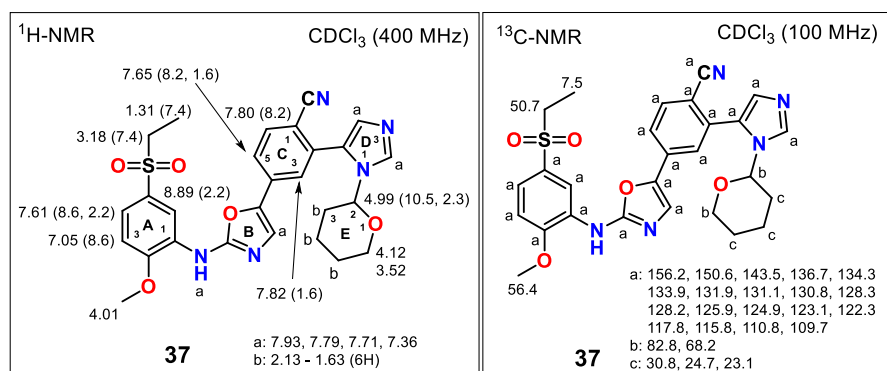
Synthesis of 4-{2-[[5-(ethylsulfonyl)-2-methoxyphenyl]amino]oxazol-5-yl}-2-[1-(tetrahydro-2H-pyran-2-yl)-1H-imidazol-5-yl]benzotrile (37)



A solution of 70.0 mg (0.15 mmol, 1.00 mol eq) oxazole **36** and 10.5 mg (14.9 μ mol, 0.10 mol eq) of Pd(PPh₃)₂Cl₂ in 3 mL of DMF (abs) was purged by Ar for 10 min. Afterwards 165 mg (0.37 mmol, 2.50 mol eq) of imidazole **15** was added to the reaction and the mixture stirred and irradiated at 100 °C in a microwave reactor for 1 h. Then TLC analysis confirmed a presence of a new product without **36** together with some traces of side products. The reaction was cooled down, diluted with 20 mL of EA and resulting mixture extracted with EA (3 x 15 mL). Separated organic layer was washed with brine (4 x 15 mL), dried over Na₂SO₄, filtered and concentrated under reduced pressure. Obtained oily product was diluted in CH₃CN, extracted with n-hexane (3 x 15 mL) and separated CH₃CN layer evaporated with RVE. The crude product **37** was purified by FLC (EA / cHex: gradient from 2 / 1 to 100 % of EA) to yield 65.0 mg (0.12 mmol, 80 %) of desired oxazole **37** as an orange solid compound.

Novelty: 4-{2-[[5-(ethylsulfonyl)-2-methoxyphenyl]amino]oxazol-5-yl}-2-[1-(tetrahydro-2H-pyran-2-yl)-1H-imidazol-5-yl]benzotrile (**37**) is not described in the literature.

M.p.: 144.0 - 148.0 [EA].



¹H-NMR (400 MHz, CDCl₃, MH-182-19): δ 8.89 (d, 1H, *J*(A₄,A₆) = 2.2 Hz, H-C_A(6)), 7.93, 7.79, 7.71 and 7.36 (4 x br s, 4 x 1H, H-C_D(2 and 4), H-C_B(4) and -NH-), 7.82 (d, 1H, *J*(C₃,C₅) = 1.6 Hz, H-C_C(3)), 7.80 (d, 1H, *J*(C₅,C₆) = 8.2 Hz, H-C_c(6)), 7.65 (dd, 1H, *J*(C₅,C₆) = 8.2 Hz, *J*(C₃,C₅) = 1.6 Hz, H-C_C(5)), 7.61 (dd, 1H, *J*(A₃,A₄) = 8.6 Hz, *J*(A₄,A₆) = 2.2 Hz, H-C_A(4)), 7.05 (d, 1H, *J*(A₃,A₄) = 8.6 Hz, H-C_A(3)), 4.99 (dd, *J*(E₂,E₃) = 10.5 Hz, *J*(E₂,E₃) = 2.3 Hz, H-C_E(2)), 4.12 and 3.52 (2 x m, 2 x 1H, 2 x H-C_E(6)), 4.01 (s, 3H, CH₃O-), 3.18 (q, 2H, *J*(CH₂,CH₃) = 7.4 Hz, CH₃CH₂SO₂-), 2.13 - 1.63 (m, 6H, H-C_E(3-5)), 1.31 (t, 3H, *J*(CH₂,CH₃) = 7.4 Hz, CH₃CH₂SO₂-).

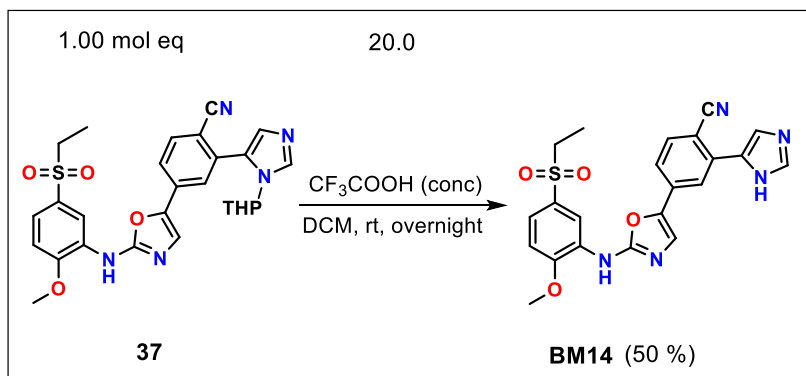
¹³C-NMR (100 MHz, CDCl₃, MH-179C-19): δ 156.2, 150.6, 143.5, 136.7, 134.3, 133.9, 131.9, 131.1, 130.8, 128.3, 128.2, 125.9, 124.9, 123.1, 122.3, 117.8, 115.8, 110.8, 109.7, 82.8, 68.2, 56.4 (CH₃O-), 50.7 (CH₃CH₂SO₂-), 30.8, 24.7, 23.1, 7.8 (CH₃CH₂SO₂-).

FT-IR (solid, cm⁻¹): 2942 (m), 2221 (w), 1603 (-CN, m), 1571 (s), 1487 (w), 1422 (w), 1344 (w), 1307 (w), 1263 (m), 1229 (w), 1207 (w), 1142 (m), 1122 (s), 1082 (m), 1042 (m), 1018 (w), 910 (m), 823 (m), 794 (m), 720 (s), 657 (m), 626 (w), 598 (w), 553 (w), 526 (m), 491 (m).

MS (ESI m/z): 450.11 (100 %) [M-THP+2H]⁺, 534.13 (10 %) [M+H]⁺ (positive mode).

Anal. calcd for C₂₇H₂₇N₅O₅S (533.60): C, 60.77; H, 5.10; N, 13.12; Found: C, 60.88; H, 5.43; N, 13.26.

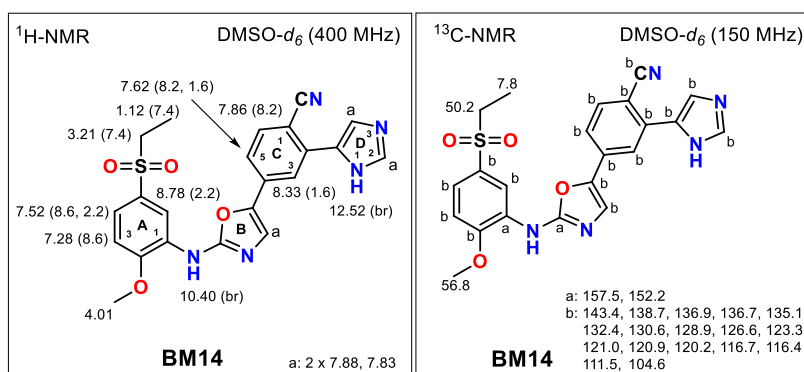
Synthesis of 4-{2-[[5-(ethylsulfonyl)-2-methoxyphenyl]amino]oxazol-5-yl}-2-(1H-imidazol-5-yl)benzonitrile (BM14)



To the solution of 70.0 mg (0.13 mmol, 1.00 mol eq) oxazol **37** dissolved in 6 mL of DCM, 1.70 mL (2.60 mmol, 20.0 mol eq) of CF₃COOH (conc) was added and the mixture stirred at rt overnight. Then, solvent and CF₃COOH volatile parts were evaporated with RVE and resulting oil dissolved in DCM. Obtained solution was extracted with NaHCO₃ (saturated aq solution) (2 x 15 mL) while a formation of precipitate was observed. Resulting suspension was evaporated to a half of its volume and put to a refrigerator overnight. After 16 h an obtained solid product was filtered off, washed with small amount of cold water and dried by HV to provide 30.0 mg (0.07 mmol, 50 %) of oxazole **BM14** as a white solid compound.

Novelty: 4-{2-[[5-(ethylsulfonyl)-2-methoxyphenyl]amino]oxazol-5-yl}-2-(1H-imidazol-5-yl)benzonitrile (**BM14**) is not described in the literature.

M.p.: 255.0 - 257.5 [DCM].



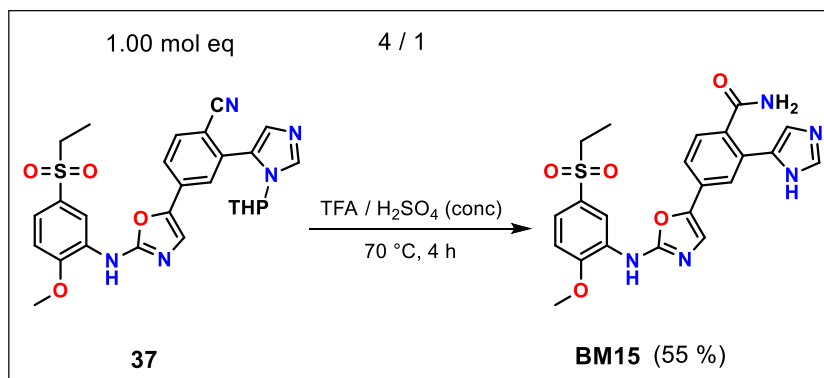
¹H-NMR (400 MHz, DMSO-*d*₆, MH-185-19): δ 12.52 (br s, 1H, H-N_D(1)), 10.40 (br s, 1H, -NH-), 8.78 (d, 1H, $J(A_4, A_6) = 2.2$ Hz, H-C_A(6)), 8.33 (d, 1H, $J(C_3, C_5) = 1.6$ Hz, H-C_C(3)), 2 x 7.88 and 7.83 (3 x br s, 3 x 1H, H-C_D(2 and 4) and H-C_B(4)), 7.86 (d, 1H, $J(C_5, C_6) = 8.2$ Hz, H-C_C(6)), 7.62 (dd, 1H, $J(C_5, C_6) = 8.2$ Hz, $J(C_3, C_5) = 1.6$ Hz, H-C_C(5)), 7.52 (dd, 1H, $J(A_3, A_4) = 8.6$ Hz, $J(A_4, A_6) = 2.2$ Hz, H-C_A(4)), 7.28 (d, 1H, $J(A_3, A_4) = 8.6$ Hz, H-C_A(3)), 4.01 (s, 3H, CH₃O-), 3.21 (q, 2H, $J(CH_2, CH_3) = 7.4$ Hz, CH₃CH₂SO₂-), 1.12 (t, 3H, $J(CH_2, CH_3) = 7.4$ Hz, CH₃CH₂SO₂-).

¹³C-NMR (150 MHz, DMSO-*d*₆, MH-185E-19): δ 157.5, 152.2, 143.4, 138.7, 136.9, 136.7, 135.1, 132.4, 130.6, 128.9, 126.6, 123.3, 121.0, 120.9, 120.2, 116.7, 116.4, 111.5, 104.6, 56.8 (CH₃O-), 50.2 (CH₃CH₂SO₂-), 7.8 (CH₃CH₂SO₂-).

FT-IR (solid, cm⁻¹): 3322 (m), 2216 (-CN, m), 1606 (s), 1575 (s), 1525 (m), 1492 (w), 1429 (s), 1349 (w), 1306 (s), 1261 (s), 1131 (s), 1112 (s), 1083 (m), 1084 (s), 1060 (m), 1028 (m), 968 (w), 918 (w), 888 (w), 857 (w), 818 (m), 793 (s), 733 (s), 718 (s), 685 (w), 634 (w), 618 (s), 597 (w), 581 (w), 514 (s), 499 (s), 490 (s).

MS (ESI m/z): 450.07 (100 %) [M+H]⁺ (positive mode).

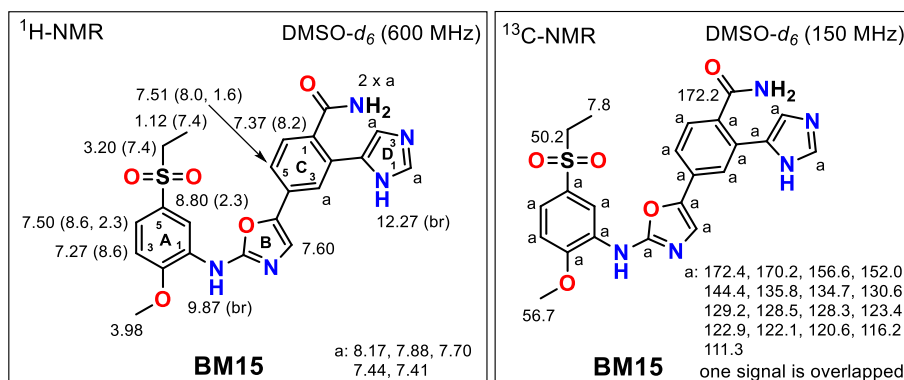
Anal. calcd for C₂₂H₁₉N₅O₄S (449.49): C, 58.79; H, 4.26; N, 15.58; Found: C, 58.84; H, 4.33; N, 15.46.

Synthesis of 4-(2-((5-(ethylsulfonyl)-2-methoxyphenyl)amino)oxazol-5-yl)-2-(1H-imidazol-5-yl)benzamide BM15

A mixture of 40.0 mg (0.08 mmol, 1.00 mol eq) oxazole **37** in 1 mL of CF₃COOH (TFA) (conc) and 0.25 mL of H₂SO₄ (conc) was stirred at 70 °C for 4 h. Then TLC analysis confirmed a presence of a new product without **37** and some traces of side products. The reaction was cooled down, 100 mL of H₂O added and extracted with DCM (3 x 15 mL). Combined organic layer was extracted with saturated solution of NaHCO₃ (3 x 15 mL) and brine (2 x 15 mL), dried over Na₂SO₄, filtered and concentrated under reduced pressure. The crude product was triturated with MeOH / DMSO to provide 19.0 mg (0.07 mmol, 55 %) of desired oxazole **BM15** as a white solid compound.

Novelty: 4-(2-((5-(ethylsulfonyl)-2-methoxyphenyl)amino)oxazol-5-yl)-2-(1H-imidazol-5-yl)benzamide (**BM15**) is not described in the literature.

M.p.: 227 - 245 °C (dec) [DCM].



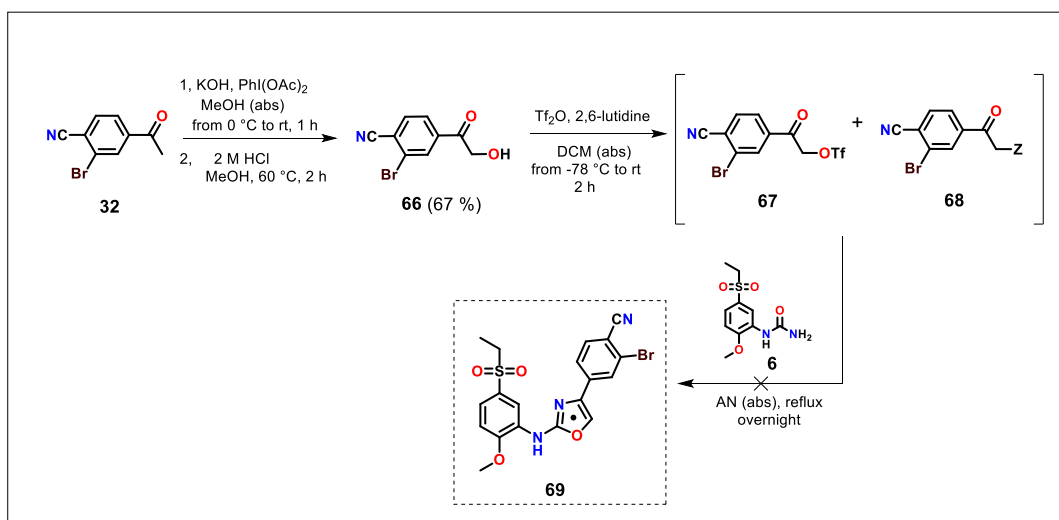
¹H-NMR (600 MHz, DMSO-*d*₆): δ 12.27 (br s, 1H, H-N_D(1)), 9.87 (br s, 1H, -NH-), 8.80 (d, 1H, $J(A_4, A_6) = 2.3$ Hz, H-C_A(6)), 8.17, 7.88, 7.70, 7.44 and 7.41 (5 x br s, 5 x 1H, H-C_D(1 and 4), H-C_C and -CONH₂), 7.60 (s, 1H, H-C_B(4)), 7.51 (dd, 1H, $J(C_5, C_6) = 8.0$ Hz, $J(C_3, C_5) = 1.6$ Hz, H-C_C(5)), 7.50 (dd, 1H, $J(A_3, A_4) = 8.6$ Hz, $J(A_4, A_6) = 2.3$ Hz, H-C_A(4)), 7.37 (d, 1H, $J(C_5, C_6) = 8.2$ Hz, H-C_C(6)), 7.27 (d, 1H, $J(A_3, A_4) = 8.6$ Hz, H-C_A(3)), 3.98 (s, 3H, CH₃O-), 3.20 (q, 2H, $J(CH_2, CH_3) = 7.4$ Hz, CH₃CH₂SO₂-), 1.12 (t, 3H, $J(CH_2, CH_3) = 7.4$ Hz, CH₃CH₂SO₂-).

¹³C-NMR (150 MHz, DMSO-*d*₆): δ 172.4, 172.2 (CONH₂), 170.2, 156.6, 152.0, 144.4, 135.8, 134.7, 130.6, 129.2, 128.5, 128.3, 123.4, 122.9, 122.1, 120.6, 116.2, 111.3 56.7 (CH₃O-), 50.2 (CH₃CH₂SO₂-), 7.8 (CH₃CH₂SO₂-).

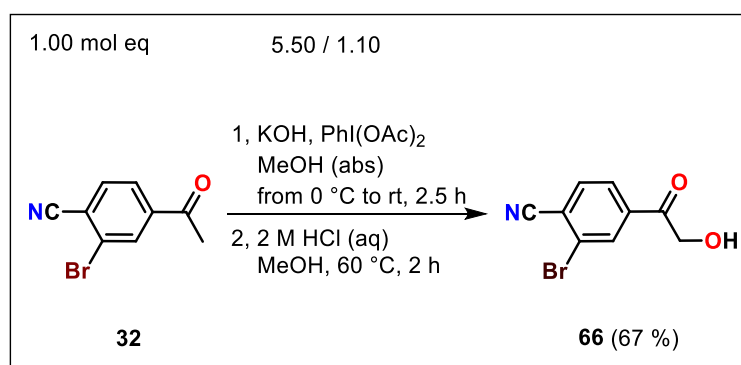
FT-IR (solid, cm⁻¹): 3266 (m), 2922 (m), 2853 (m), 1662 (w), 1611 (s), 1575 (s), 1497 (w), 1408 (w), 1383 (w), 1298 (m), 1267 (s), 1192 (s), 1083 (m), 1066 (m), 1032 (m), 898 (w), 794 (s), 613 (m), 514 (w), 490 (s).

MS (ESI m/z): 468.1 (100 %) [M+H]⁺, 490.0 (10 %) [M+Na]⁺ (positive mode).

Anal. calcd for C₂₂H₂₁N₅O₅S (467.50): C, 56.52; H, 4.53; N, 14.98; Found: C, 56.75; H, 5.76; N, 15.23.

10.6.3. Synthesis of *N*,4-diaryloxazole-2-amine precursor (69)

Synthesis of 2-bromo-4-(2-hydroxyacetyl)benzonitrile (66)

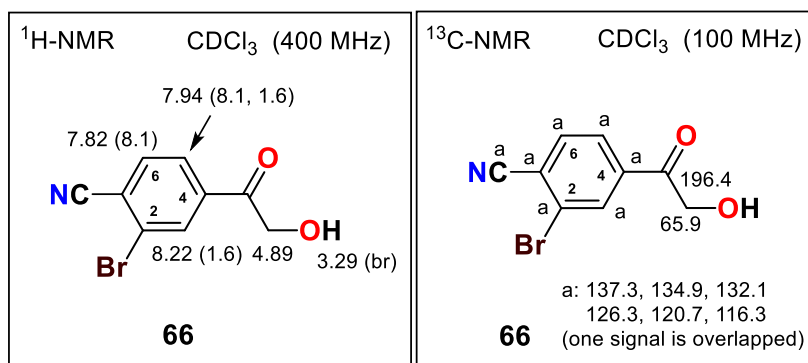


To a solution of 687 mg (12.3 mmol, 5.50 mol eq) KOH in 30 mL of MeOH (abs), 500 mg (2.23 mmol, 1.00 mol eq) of benzonitrile **32**, suspended in ca 40 mL of MeOH (abs), was added and cooled to 0 °C. Afterwards, 791 mg (2.46 mmol, 1.10 mol eq) of PhI(OAc)₂ was added portionwise within 10 min and stirred for another 10 min at the same temperature. After 2.5 h of stirring at rt, reaction mixture was evaporated by RVE, resulting solid material diluted in 50 mL of EA and extracted with H₂O (3 x 30 mL) and brine (3 x 30 mL). Obtained oil was dissolved in 20 mL of MeOH and 15 mL of 2 M HCl (aq) was added. After 2 h of stirring at 60 °C, TLC analysis confirmed a presence of one product with traces of two side products. Afterwards, reaction mixture was evaporated by RVE, diluted in 50 mL of EA and extracted with H₂O (3 x 30 mL) and brine (3 x 30 mL). Combined organic layer was dried over Na₂SO₄,

filtered and evaporated under reduced pressure. Crude product was triturated with a mixture of cHex / EA to yield 360 mg (1.50 mmol, 67 %) of benzonitrile **66** as a brown solid compound.

Novelty: 2-bromo-4-(2-hydroxyacetyl)benzonitrile (**66**) is not described in the literature.

M.p.: 120.0 - 124.0 [EA].



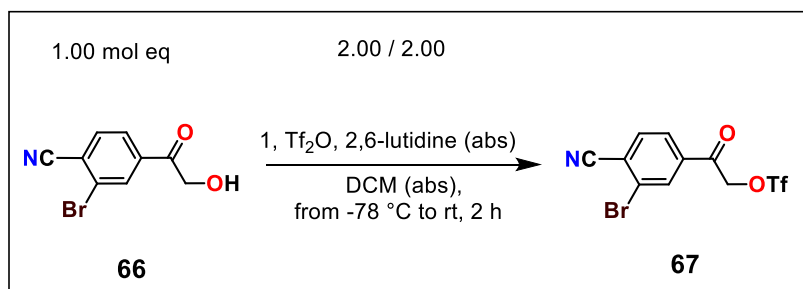
¹H-NMR (400 MHz, CDCl₃): δ 8.22 (d, 1H, $J(3,5) = 1.6$ Hz, H-C(3)), 7.94 (dd, 1H, $J(5,6) = 8.1$ Hz, $J(3,5) = 1.6$ Hz, H-C(5)), 7.82 (d, 1H, $J(5,6) = 8.1$ Hz, H-C(6)), 4.89 (s, 2H, -COCH₂OH), 3.29 (br s, 1H, -OH).

¹³C-NMR (100 MHz, CDCl₃): δ 196.4 (-COCH₂OH), 137.3, 134.9, 132.1, 126.3, 120.7, 116.3, 65.9 (-COCH₂OH).

FT-IR (solid, cm⁻¹): 3256 (m), 2988 (w), 2230 (w, -CN), 1702 (s), 1550 (m), 1373 (m), 1271 (m), 1224 (s), 1099 (m), 1042 (m), 985 (s), 892 (w), 844 (s), 761 (m), 675 (m), 608 (m).

MS (ESI m/z): 238.1 (100 % for Br⁷⁹) [M-H]⁻, 240.1 (100 % for Br⁸¹) [M-H]⁻ (negative mode).

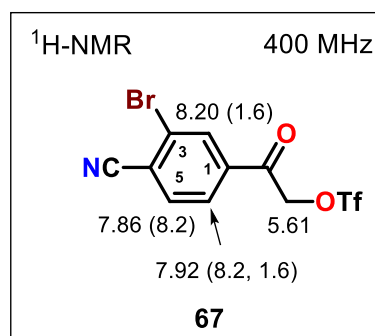
Synthesis of 2-(3-bromo-4-cyanophenyl)-2-oxoethyl trifluoromethanesulfonate (67)



Benzonitrile **66** 120 mg (0.50 mmol, 1.00 mol eq) was dissolved in 30 mL of DCM (abs) and cooled to -78 °C. At this temperature 120 µl (108 mg, 1.00 mmol, 2.00 mol eq) of 2,6-lutidine was added with subsequent dropwise addition of 168 µl (284 mg, 1.00 mmol, 2.00 mol eq) of Tf₂O. Reaction mixture was stirred for 2 h while its temperature went to rt. Afterwards, volatile parts were evaporated by RVE, obtained crude product dissolved in 30 mL of EA and extracted with H₂O (1 x 30 mL) and brine (1 x 30 mL). Combined organic layer was dried over Na₂SO₄, filtered and concentrated under reduced pressure to yield 150 mg of a mixture of two products. Due to expected low stability of triflates, desired product **67** was not separated from side product **68** and was used as a mixture (**67** / **68** : 61 / 39 % according to ¹H-NMR) for a next reaction.

Novelty: 2-(3-bromo-4-cyanophenyl)-2-oxoethyl trifluoromethanesulfonate (**67**) is not described in the literature.

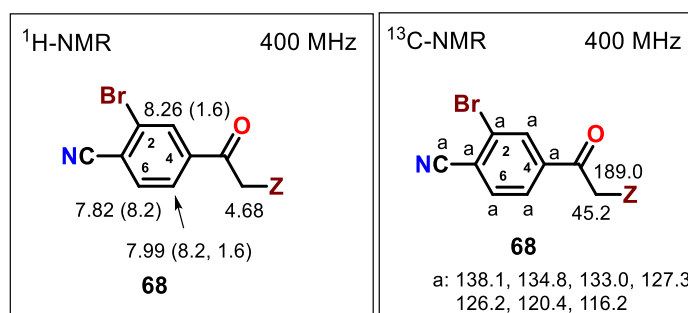
¹H-NMR analysis (determined from a mixed ¹H-NMR spectrum):



¹H-NMR (400 MHz, CDCl₃): δ 8.20 (d, 1H, $J(3,5) = 1.6$ Hz, H-C(3)), 7.92 (dd, 1H, $J(5,6) = 8.2$ Hz, $J(3,5) = 1.6$ Hz, H-C(5)), 7.86 (d, 1H, $J(5,6) = 8.2$ Hz, H-C(6)), 5.61 (s, 2H, -COCH₂OTf).

Due to instability, other characteristics for **67** were not determined. Side product **68** revealed high stability on SiO₂, therefore we separated it from a mixture by FLC (SiO₂, eluent: cHex / EA : 3 / 1) and performed spectral analysis. Unfortunately, its structure has not been exactly determined yet.

M.p.: 100.0 - 126.0 [cHex / EA] (dec).



¹H-NMR (400 MHz, CDCl₃): δ 8.26 (d, 1H, $J(3,5) = 1.6$ Hz, H-C(3)), 7.99 (dd, 1H, $J(5,6) = 8.2$ Hz, $J(3,5) = 1.6$ Hz, H-C(5)), 7.82 (d, 1H, $J(5,6) = 8.2$ Hz, H-C(6)), 4.68 (s, 2H, -COCH₂Z).

¹³C-NMR (100 MHz, CDCl₃): δ 189.0 (-COCH₂R), 138.1, 134.8, 133.0, 127.3, 126.2, 120.4, 116.2, 45.2 (-COCH₂R).

¹⁹F-NMR (376.6 MHz, CDCl₃): δ 74.4.

FT-IR (solid, cm⁻¹): 3086 (w), 2230 (m), 2230 (w, -CN), 1713 (s), 1547(m), 1393 (m), 1311 (w), 1279 (w), 1269 (w), 1195 (s, -S=O), 1142 (m), 1043 (w), 1020 (w), 904 (w), 838 (s), 794 (s), 722 (s), 672 (s), 604 (w), 582 (w), 554 (m), 460 (m).

MS (ESI m/z): 479.3 (100 %), 477.2 (45 %), 415.3 (15 %), 372.1 (35 %), 345.2 (45%), 240.2 (25 %); in negative mode 258.1 (70 %), 256.1 (55 %), 149.1 (100 %), 133.1 (60 %).

Chapter 8. Aldose reductase (ALR2) in diabetes mellitus

11. Aldose reductase (ALR2) in diabetes mellitus

The second part of this dissertation thesis is dedicated to another serious and well-known disease diabetes mellitus (DM). The most important factor implicated in DM and its related diseases is blood sugar. **Glucose** is a hexose sugar, which circulates in the blood of human. It is an important source of energy for cells and it is also stored as polymer glycogen in a liver.⁹¹ In the normal aerobic circumstances (non-diabetic conditions), *D*-glucose is phosphorylated by hexokinase and subsequently metabolized through several metabolic steps to CO₂ and water. This cascade produces energy mostly in the form of energetically rich molecules like NADH and ATP (adenosine triphosphate).⁹²

Glycolysis is a metabolic pathway that converts glucose into pyruvate and the free energy is released in a form of ATP and NADH.⁹³ Produced pyruvate molecules are then transported into the mitochondrial matrix, where they are oxidized by coenzyme A to form CO₂, acetyl-CoA and NADH.⁹⁴ Resulted acetyl-CoA molecules enter to citric acid cycle (or Krebs cycle) and by the series of reactions are oxidized to CO₂ and produce energy-rich ATP.⁹⁵ The cycle also reduces NAD⁺ to NADH, which is utilised in the oxidative phosphorylation (electron transport) pathway to generate energy-rich ATP. The theoretical yield of ATP through oxidation of one molecule of the *D*-glucose in glycolysis, Krebs cycle and oxidative phosphorylation is 36 molecules of ATP.⁹⁶ (Scheme 51)

⁹¹ Ponomarev, V.V.; Migarskaya, L.B. *Russ. J. Phys. Chem.* **1960**, *34*, 1182 - 1183.

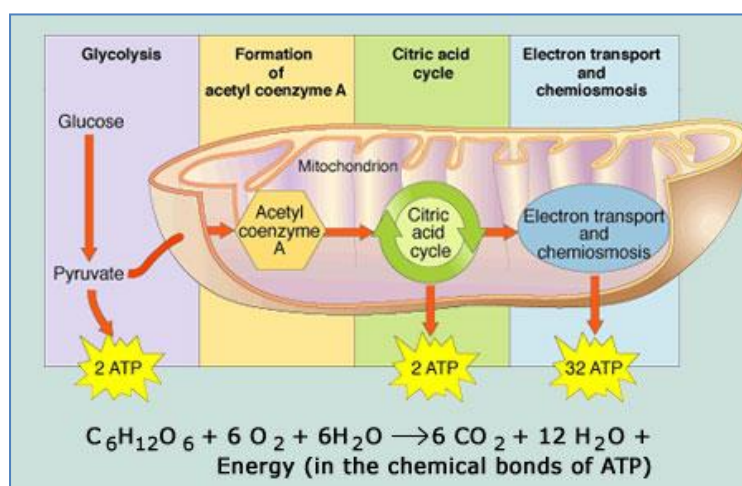
⁹² Fairclough, S.H.; Houston, K. *Biol. Psychol.* **2004**, *2*, 177 - 190.

⁹³ www.thoughtco.com (accessed April 17th, 2020)

⁹⁴ Voet, D.; Voet, J.G.; Pratt, C.W. *Fundamental of Biochemistry* (2nd ed.), John Wiley & Sons, Inc. USA, 2006, 547-556, ISBN: 0-471-21495-7.

⁹⁵ Wagner, A. *Arrival of the Fittest* (1th ed.), Penguin Group, New York, 2014, p 100, ISBN: 9781591846468.

⁹⁶ Porter, P.K.; Brand, M.D. *Biochem. J.* **1995**, *2*, 379 - 382.



Scheme 51. An overview of metabolism of the *D*-glucose.

However, if large amounts of glucose are present under hyperglycemic conditions, hexokinase becomes saturated and around 33 % of overall glucose is metabolized through a polyol pathway. While most of the cells require the action of insulin for glucose to gain entry into the cell, the cells of retina, kidney and nervous tissues are insulin-independent, so glucose moves across the cell membrane, regardless of the action of insulin. The cells will use glucose for energy as usually, and excess of glucose will enter **the polyol pathway**.⁹⁷

11.1. The polyol pathway

The polyol pathway is a two-step process which converts the glucose to the fructose. It uses an **aldose reductase (ALR2)** and a sorbitol dehydrogenase as catalysts.⁹⁸ (Figure 54) The polyol pathway reduces *D*-glucose and oxidizes NADPH to NADP⁺. Subsequently sorbitol dehydrogenase oxidizes sorbitol to fructose, which produces NADH from NAD⁺.⁹⁷ NADPH promotes glutathione production *via* the polyol pathway and deficiency of NADPH (e.g. its consumption *via* the polyol pathway) causes oxidative stress and hemolysis. NADPH is important to prevent accumulation of reactive oxygen species (ROS) and damaging of cells. Furthermore, produced fructose causes glycation of proteins and fats and enhances formation of **advanced glycation end products (AGEs)**, which production causes oxidative stress and

⁹⁷ Brownlee, M. *Nature*, **2001**, *414*, 813 - 820.

⁹⁸ Bonnefont-Rousselot, D. *Curr .Opin .Clin. Nutr.* **2002**, *5*, 561 - 568.

inflammation.⁹⁹ What more, the sorbitol is highly polar compound and hardly penetrates through the cell membranes. Its accumulation causes cell swelling leading to osmotic imbalances and causes various diabetic complications such as cataract, retinopathy, neuropathy and nephropathy.¹⁰⁰

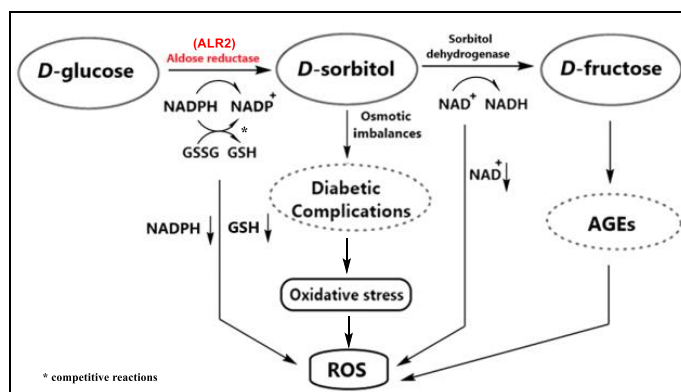


Figure 54. An illustration of the polyol pathway and its implication in the diabetic complications.

11.2. Diabetes mellitus (DM) and diabetic complications

Diabetes mellitus type I is a metabolic disorder of a pancreas, an organ that produces the hormone insulin. Insuline is peptide hormone, which plays a key role in the regulation of variety of biomacromolecules, especially a blood glucose level. Normally, when the glucose level is high, the beta cells of the pancreas secrete the insulin and release it into the blood stream. Then, the glucose is absorbed into the cell thanks to glucose transporter activated by a complex of insuline with its receptor and glucose can be converted directly to energy or to energy storages: either glycogen *via* glycogenesis or fats *via* lipogenesis.¹⁰¹ (Figure 55)

⁹⁹ Vistoli, G.; De Maddis, D.; Cipak, A.; Zarkovic, N.; Carini, M.; Aldini, G. *Free Radic. Res.* **2013**, *47*, 3 - 27.

¹⁰⁰ Kinoshita, J.H. *Invest. Opth. Vis. Sci.* **1974**, *10*, 713 - 724.

¹⁰¹ Stryer, L. *Biochemistry* (4th ed.), W.H. Freeman and Company, New York, **1995**, 773-774, ISBN: 0-7167-2009-4.

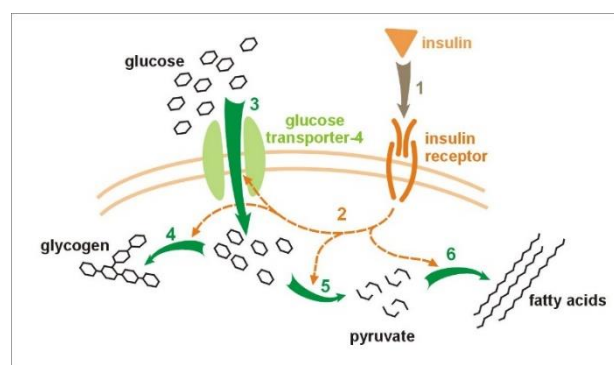


Figure 55. Transport du glucose à travers une membrane cellulaire médiée par l'insuline.

People with diabetes mellitus (DM) have either a lack of secretion of insulin (DM type I) or insulin can't be used properly (DM type II), which lead to the high level of blood sugar that causes a variety of pathology conditions (diabetic cataract, neuropathy and nephropathy). It can damage the tiny vessels in kidneys, heart, eyes or nervous system.¹⁰² All these diabetic pathological complications are associated with a **polyol pathway**, which in the first step converts glucose to sorbitol by an enzyme aldose reductase. Therefore, inhibition of ALR2 activity, which can prevent the abnormal accumulation of sorbitol and indirectly suppresses oxidative stress of cell, became **promising way to avoid or slow down late diabetic complications**.

11.3. Properties and function of ALR2

Aldose reductase (ALR2) is a first enzyme of a polyol pathway and belongs to the aldo-keto reductase enzyme superfamily. It catalyses NADPH-dependent reduction of a wide variety of carbonyl compounds, e.g. glucose.¹⁰³ The enzyme is a single polypeptide domain composed of 315 amino acid residues folded into a β/α -barrel structural motif containing eight parallel β strands.¹⁰⁴ The active site is located in a large cavity in the C-terminal end of the β barrel and the NADPH cofactor is situated at the top of the β/α -barrel with the nicotinamide ring stands out in the center of the barrel.

¹⁰² www.webmd.com (accessed August 8th, 2020)

¹⁰³ Kao, Y.L.; Donaghue, K.; Chan, A.; Knight, J.; Silink, M. *Diabetes*, **1999**, *48*, 1338 - 1340.

¹⁰⁴ Oleg, A.B.; Kenneth, H.G.; Kurt, M.B. *Genomics*, **1999**, *60*, 188 - 198.

11.4. An active site of ALR2

According to analysis of crystal structures of ALR2, the structure of its active site has been proposed. The first binding pocket of the ALR2 active site consists of a rigid **anion binding pocket**, composed of Trp20, Trp111, Tyr48, His110 amino acid side chains and amide group of NADP⁺. The second is a **specificity pocket**, consisted of Leu 300, Cys298, Cys303, Trp111 and Phe122.¹⁰⁵ This pocket is characteristic for its high degree of flexibility and the amino acid residues lining this pocket are not present in other aldo-keto reductases such as aldehyde reductase e.g. ALR1. The third is a **hydrophobic pocket** formed from Phe122, Trp219, Trp20 and Trp111 residues.¹⁰⁶ (Figure 56)

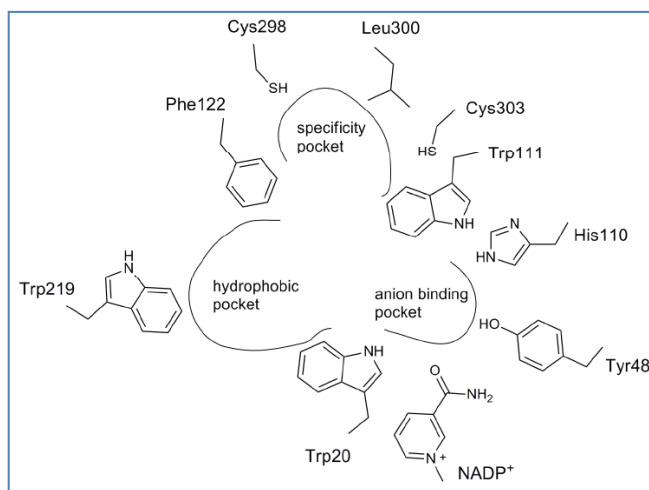


Figure 56. The structure of the active site of ALR2 enzyme.

11.5. Aldehyde reductase

Aldehyde reductase (ALR1) is another oxidoreductase closely related to the aldose reductase (ALR2). Both enzymes share 65 % of structural homology and these similarities play important role in a common inhibitor non-selectivity. The co-inhibition of related oxidoreductases may create undesirable side effects.¹⁰⁷ A main role of the ALR1 is a detoxification, because it specifically metabolises toxic aldehydes such as 3-deoxyglucosone (3DG), hydroxynonenal (HNE), which may arise from consequences connected with oxidative stress in

¹⁰⁵ Oates, P.J. *Curr. Drug. Targets*, **2008**, *9*, 14-36.

¹⁰⁶ El-Kabbani, O.; Darmanin, C.; Schneider, T.R.; Hazemann, I.; Ruiz, F.; Oka, M.; Joachimiak, A.; Schulze-Briese, C.; Tomizaki, T.; Mitschler, A.; Podjarny, A. *Proteins*, **2004**, *55*, 805 - 813.

¹⁰⁷ El-Kabbani, O.; Wilson, D. K.; Petrash, J. M.; Quiocho, F. A. *Mol. Vis.* **1998**, *4*, 19 - 25.

hyperglycemia.¹⁰⁸ In addition, it is responsible also for ascorbic acid synthesis in animals by reduction of *D*-glucuronate to *D*-gulonate.¹⁰⁹ Therefore ALR1 is an antitarget compare to an important antidiabetic target ALR2.

11.6. Inhibitors of ALR2

Over the last 40 years, numerous of ALR2 inhibitors have been developed, but only an **epalrestat** is available as a drug in Japan, China and India.¹¹⁰ Most of structurally different ARIs have been refused in the clinical trials mainly for their low *in vivo* efficacies, pharmacokinetic drawbacks and side effects affected by non-selective inhibition of aldehyde reductase (ALR1).

11.6.1. Carboxylic acid derivatives

Carboxylic acids are the most important and the largest class of ARIs, because carboxylic anion group of the inhibitor occupies an anion binding pocket of the active site of ALR2. On the other hand, low pK_A values hinder membrane permeability in physiological pH conditions and lead to a poor pharmacokinetic profile of such ARIs. **Epalrestat** is a noncompetitive and reversibile ALR2 inhibitor (containing rhodanine ring) used for treatment of diabetic neuropathy.¹¹¹ It was developed in 1983 and approved in Japan, China and India for the improvement of subjective neuropathy symptoms and abnormal changes in heart beat associated with a diabetic peripheral neuropathy. (Figure 57)

¹⁰⁸ Carper, D.A.; Wistow, G.; Nishimura, C.; Graham, C.; Watanabe, K.; Fujii, Y.; Hayashi, H.; Hayashi, O.A. *Exp. Eye. Res.* **1989**, *49*, 377 - 388.

¹⁰⁹ Linster, C.L.; Van Schaftingen, E.; *Febs J.* **2007**, *274*, 1 - 22.

¹¹⁰ Vyas, B.; Choudhary, S.; Singh, P.K.; Kumar, M.; Verma, H.; Singh, M.; Malik, A.K.; Silakari, O *Bioorg. Chem.*, **2020**, *96*, 103570.

¹¹¹ Terashima, H.; Hama, K. *J. Pharamacol. Exp. Ther.* **1984**, *229*, 226 - 230.

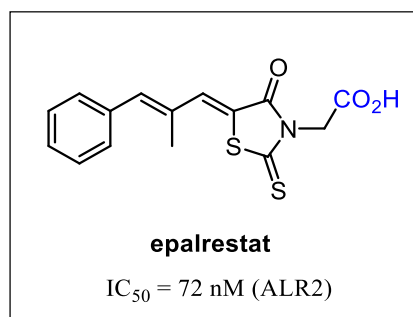


Figure 57. Structure and activity of the epalrestat.

Second very important ALR2 inhibitor is **tolrestat**, a potential drug for a treatment of diabetic complications, which was approved for several markets, but in 1997 withdrawn due to its liver toxicity in 3rd phase of a clinical trial and finally never received FDA approval.¹¹² (Figure 58) **Zenarestat** is a potential drug for a treatment of cataract, diabetic retinopathy and neuropathy. **Zenarestat** together with **zopolrestat** proceeded into clinical trials. In the 2nd phase of clinical study they showed beneficial effect on nerve conduction velocity, but the 3rd phase of trials showed that **zenarestat** therapy was linked with renal toxicity in a small number of patients. Its structurally similar inhibitor **ponalrestat** also failed in clinical trials due to the lack of efficacy. (Figure 58)

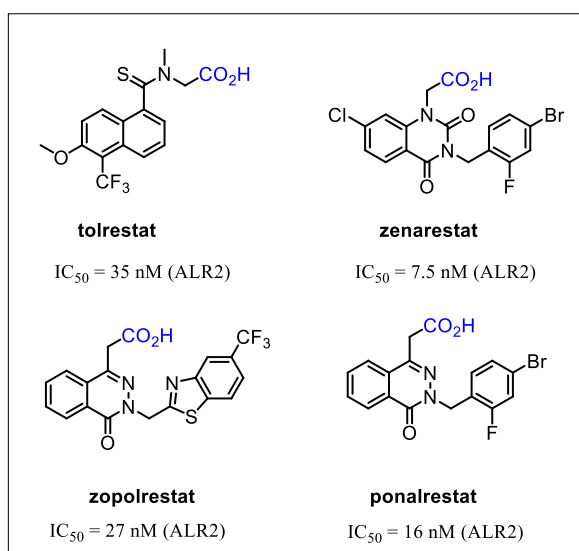


Figure 58. Structures of the most developed ARIs possessing carboxylic functionality.

¹¹² Kador, P.F.; Kinoshita, J.H.; Sharpless, N.E. *J. Med. Chem.* **1985**, *7*, 841 - 849.

11.6.2. Spirohydantoin and spirosuccinimide derivatives

The second important class of ALR2 inhibitors includes spirohydantoin derivatives, where the hydantoin group occupies the anion binding pocket similarly as occupies anion group of carboxylic derivatives.¹¹³ **Sorbinil**, a strong ALR2 inhibitor with chromane substructure, has been shown to be an excellent inhibitor of ALR2 for both *in vivo* and *in vitro* assays. Unfortunately, in clinical trials sorbinil was found, that increase a risk for developing of hypersensitivity such as skin rash, fever and myalgia (muscle pain).¹¹⁴ These adverse reactions may be attributed to the poor selectivity of sorbinil with aldehyde reductase (ALR1).¹¹⁵ Based on the structure of the sorbinil, several spirohydantoin inhibitors have been developed. Addition of a carbamoyl or methyl group at the sorbinil skeleton resulted in **fidarestat** and **M79175**, resp. Replacement of chromane ring with isoquinoline-1,3(2*H*,4*H*)-dione and introduction the spirosuccinimide ring produced **minalrestat**. Another similar inhibitor is **ranirestat**, which was developed for treatment of diabetic neuropathy¹¹⁶ and now it is in the 3rd phase of a clinical trial in Japan. **Imirestat**, containing planar fluorene ring, was also in the 3rd phase of clinical trial and later withdrawn due to its toxicity. (Figure 59)

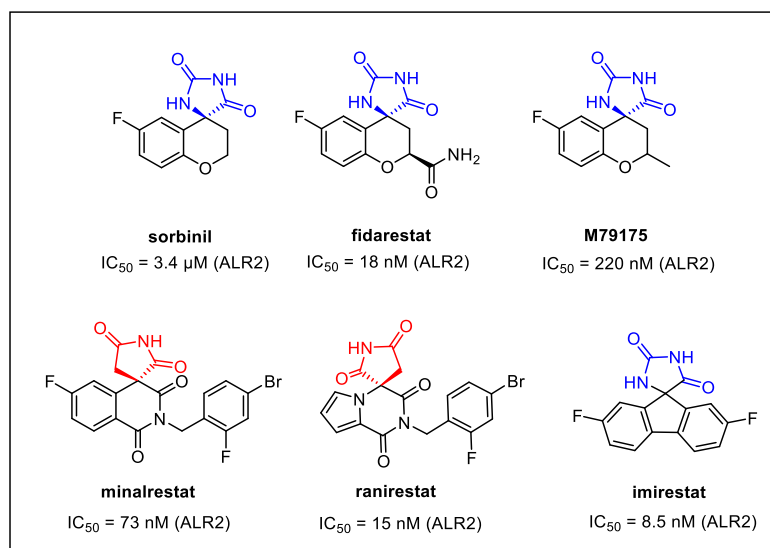


Figure 59. Structures and activities of the most important ALR2 spirohydantoin inhibitors.

¹¹³ Fukushi, S.; Merola, L.O.; Kinoshita, J.H. *Invest. Ophthalm. Vis. Sci.*, **1980**, 3, 313 - 315.

¹¹⁴ Jaspan, J.B.; Herold, K.; Bartkus, C. *Am. J. Med.* **1985**, 5, 24 - 37.

¹¹⁵ Barski, O.A.; Gabbay, K.H.; Grimshaw, C.E.; Bohren, K.M. *Biochemistry*, **1995**, 35, 11264 - 11275.

¹¹⁶ Negoro, T.; Murata, M.; Ueda, S.; Fujitani, B.; Ono, Y.; Kuromiya, A.; Komiya, M.; Suzuki, K. *J. Med. Chem.*, **1998**, 21, 4118 - 4129.

None of these carboxylic acids as well as spirohydantoin derivatives as ALR2 inhibitors are approved by FDA. Therefore, in the recent search for better ARIs, the focus has been shifted towards novel leading skeletons.

11.6.3. Discovery of the indole-1-acetic acid ALR2 inhibitor (CMTI)

Substituted indole-1-acetic acids represent another leading skeleton of ARIs.¹¹⁷ **Lidorestat** was a promising candidate for clinical studies, but it was withdrawn due to its side effects.¹¹⁸ (Figure 60)

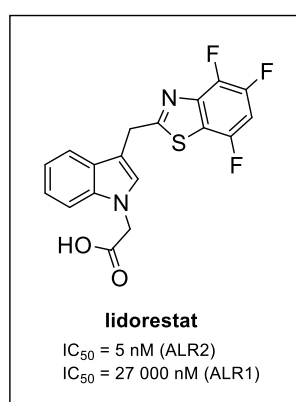


Figure 60. The structure of lidorestat.

Based on **lidorestat**, scientists from the Slovak Academy of Sciences proposed fifteen compounds possessing indole-1-acetic acid moiety.¹¹⁹ These structures were evaluated for their potential to inhibit reduction of *D,L*-glyceraldehyd by isolated ALR2 enzyme from rat lenses. Among them, 3-merkpto-5*H*-1,2,4-triazino[5,6-*b*]-indole-5-acetic acid, named **cemtirestat** (**CMTI**), exhibited the highest biological activity both at the level of isolated enzyme with IC₅₀ = 97 nM (ALR2) and also at an organ level. For determination of selectivity, closely related detoxification enzyme aldehyde reductase (ALR1) from a rat kidney was used. The enzyme ALR1 is considered to be an antitarget. **CMTI** showed moderate inhibition for the reduction of

¹¹⁷ Van Zandt, M.C.; Doan, B.; Sawicki, D.R.; Sredy, J.; Podjarny, A.D. *Bioorg. Med. Chem. Lett.*, **2009**, 7, 2006 - 2008.

¹¹⁸ Van Zandt, M.C.; Jones, M.L.; Gunn, D.E.; Geraci, L.S.; Jones, J.H.; Sawicki, D.R.; Sredy, J.; Jacot, J.L.; Dicioccio, A.T.; Petrova, T.; Mitschler, A.; Podjarny, A.D. *J. Med. Chem.* **2005**, 48, 3141 - 3152.

¹¹⁹ Stefek, M.; Prnova, M.S.; Majekova, M.; Rechlin, C.; Heine, A.; Klebe, G. *J. Med. Chem.*, **2015**, 58, 2649 - 2657.

the *D*-glucuronate by ALR1 ($IC_{50} = 41 \mu\text{M}$) and selectivity factor $SF(IC_{50} \text{ ALR1} / IC_{50} \text{ ALR2}) = 400$. (Figure 61)

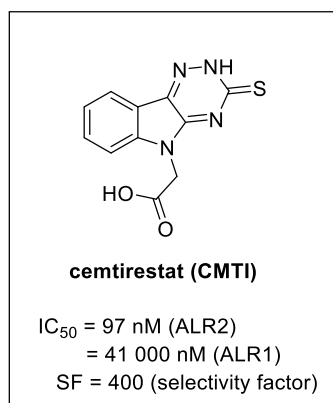


Figure 61. Structure, activity and selectivity of centiirestat (CMTI).

For the better understanding of interactions of **CMTI** with an active site of ALR2, a crystal structure of ALR2 in complex with **CMTI** was investigated. Two molecules of the **CMTI** inhibitor are present in a complex. First one as expected in the binding pocket and the second one in a neighbourhood of the entrance of the ALR2 active site. (Figure 62) A carboxylate group well occupies the anion binding pocket with interactions to His110, Tyr48 and Trp111. A sulfur atom of **CMTI** forms a crucial H-bond with Leu300 and the remaining interactions have hydrophobic character. (Figure 62)

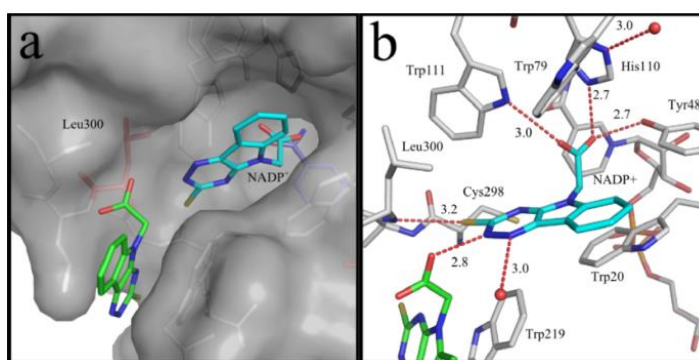


Figure 62. The crystal structure of CMTI in a complex with ALR2. a) Two molecules of CMTI are located in the complex. b) Binding mode of the deep buried molecule of CMTI in the ALR2 complex.

The molecule of **CMTI** positioned at the entrance to ALR2 active site makes hydrogen bond with the first **CMTI** *via* an oxygen of the carboxylate group and H-N(2) of a triazine ring of

the deep buried **CMTI** molecule. Furthermore, the second carboxylate oxygen forms a H-bond to the backbone -NH- group of Ser302 and an aromatic skeleton makes face to face π -stacking to Trp 219. (Figure 63)

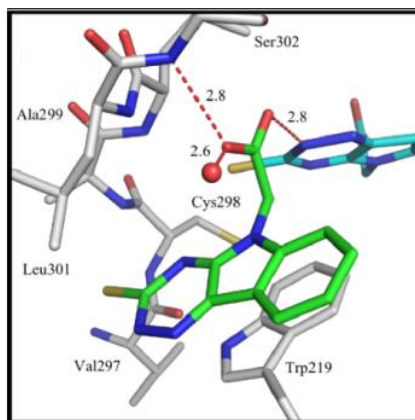


Figure 63. Binding mode of **CMTI** positioned at the entrance to the ALR2 active site.

Thanks to the high activity and selectivity of **CMTI**, excellent drug-like properties (Lipinski rules of five)¹²⁰ and water solubility, **CMTI** appears to be a promising lead compound suitable for further drug development.

11.7. Biological assay activity (ALR2)

Ability of ALR2 inhibitor to inhibit reduction of *D,L*-glyceraldehyde is a significant marker for an investigation of a remaining ALR2 activity. A partially purified ALR2 enzyme from rat eye lenses is used for an *in vitro* test. It is exhibiting 85 % sequence homology to human lens ALR2, while the catalytic active site of both enzymes is considered identical. Inhibitors are usually prepared in H₂O or DMSO with the final concentration no more than 1 % of DMSO. The reaction mixture for assay contains ALR2, sodium phosphate buffer, NADPH, substrate (*D,L*-glyceraldehyde) and ALR2 inhibitor at different concentrations. ALR2 activity is monitored spectrophotometrically by measuring the decrease in absorption of NADPH at 340 nm after addition of substrate. From obtained numbers a concentration of inhibitor giving 50 %

¹²⁰ Lipinski, C.A.; Lombardo, F.; Dominy B.W.; Feeney, P.J. *Adv. Drug Deliv. Rev.*, **2001**, *46*, 3 - 26.

inhibition of enzyme activity (IC_{50}) is calculated. For selectivity test, an aldehyde reductase (ALR1) isolated from a rat kidney is used.¹²¹

¹²¹ Kim, T.H.; Kim, J.K.; Kang, Y-H.; Lee, J-Y.; Kang, I.J, Lim, S.S. *Biomed. Res. Int.*, **2013**, 2013, 1 - 8.

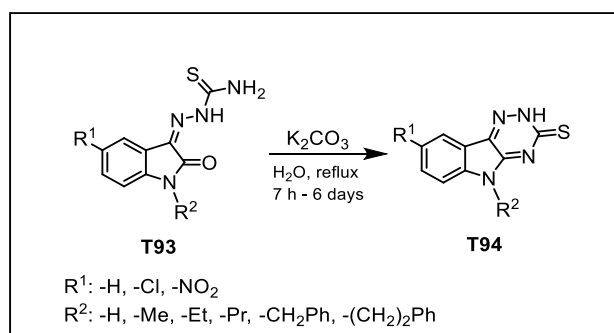
Chapter 9. Synthesis of ALR2 inhibitors possessing triazinoindole scaffold

12. Synthesis of ALR2 inhibitors possessing triazinoindole scaffold

In the previous chapter we described development of the effective ALR2 inhibitor **CMTI**, which possesses triazinoindole scaffold and its structure has become promising and suitable for further development. In the second part of this dissertation thesis we proceeded with optimization of **CMTI** skeleton and its analogues and therefore this chapter is devoted to the preparation of triazinoindole compounds.

12.1. Preparation of a 1,2,4-triazine-3-(2H)-thione catalysed by base

In 1972, Gladych et al. described the synthesis and biological importance of 5*H*-triazino[5,6-*b*]indole derivatives **T94** containing a 1,2,4-triazine-3(2*H*)-thione ring.^{122,123} Substituted isatin-3-thiosemicarbazones **T93** were cyclised to 5*H*-triazino[5,6-*b*]indole-3-thiones by heating in an aqueous solution of K₂CO₃. (Scheme 52)



Scheme 52. The synthesis of 5*H*-triazino[5,6-*b*]indole-3-thiones **T94** from thiosemicarbazone **T93**.

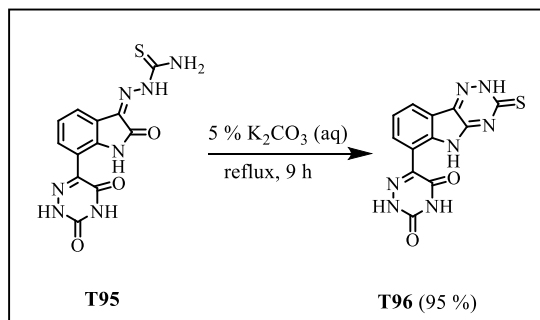
Steric factors markedly affected the rate of triazinethione cyclization. When R²: -CH₂Ph the rate of reaction required 6 days at reflux, but in case R²: -(CH₂)₂Ph the reaction required 10 h and with R²: -CH₃ the transformation was completed within 7 h. The yields of reactions were not stated. (Scheme 52)

In 2000, the preparation of the 1,2,4-triazine-3-(2*H*)-thione **T96** was also described

¹²² Gladych, J.M.Z.; Hornby, R.; Hunt, J.H.; Jack, D. *J. Med. Chem.* **1972**, *15*, 277 - 281.

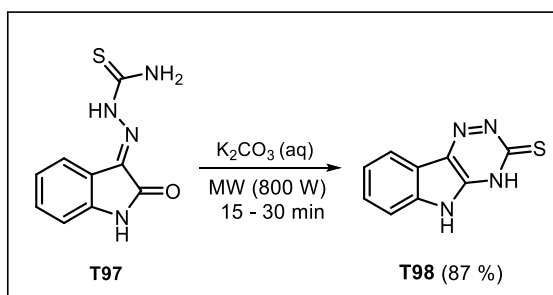
¹²³ Kgocong, J.L.; Smith, P.P.; Matsabisa, G.M. *Bioorg. Med. Chem.* **2005**, *13*, 2935 - 2942.

using basic conditions.¹²⁴ Synthesis started from 7-(6-azauracil-5-yl)isatine thiosemicarbazone **T95**, which was refluxed in 5 % aqueous solution of K_2CO_3 yielding 5*H*-triazino[5,6-*b*]indole **T96** in 95 %. (Scheme 53)



Scheme 53. Synthesis of the 5*H*-triazino[5,6-*b*]indole-3-thione **T96** from thiosemicarbazone **T95**.

El Ashry et al. in 2004 described the synthesis of another 1,2,4-triazine-3-thione **T98** by microwave irradiation from thiosemicarbazone **T97** in an aqueous solution of K_2CO_3 .¹²⁵ (Scheme 54)



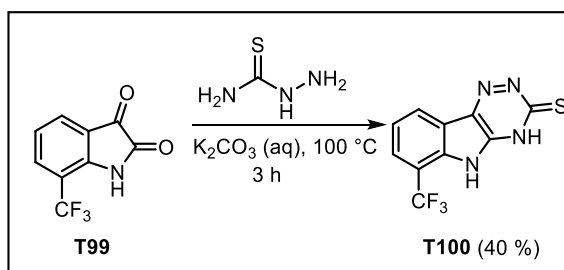
Scheme 54. The preparation of the 4,5-dihydro-3*H*-[1,2,4]triazino[5,6-*b*]indole-3-thione **T98** from thiosemicarbazone **T97**.

Similar results were obtained by refluxing of 7-trifluoromethylisatine **T99** in aqueous solution of K_2CO_3 within 3 h.¹²⁶ (Scheme 55)

¹²⁴ Hlaváč, J.; Slouka, J.; Hradil, P.; Lemr, K. *J. Heterocyclic Chem.*, **2000**, *37*, 115 - 118.

¹²⁵ El Ashry, E.S.H.; El Sayed, R.; Hamid, A.; Hagar, M.; *Synlett.*, **2004**, *4*, 723 - 725.

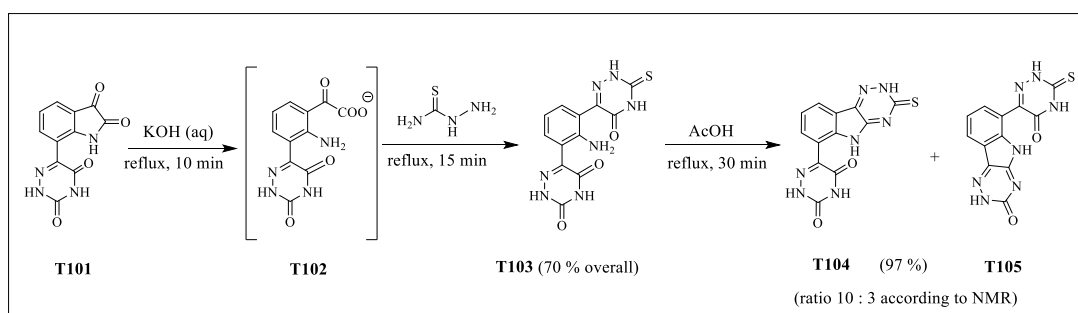
¹²⁶ Kgokong, J.L.; Smith, P.P.; Matsabisa, G.M. *Bioorg. Med. Chem.*, **2005**, *13*, 2935 - 2942.



Scheme 55. Preparation of the 4,5-dihydro-3H-[1,2,4]triazino[5,6-b]indole-3-thione **T100**.

12.2. Preparation of the 1,2,4-triazine-3-(2H)thione catalysed by HOAc or NaOAc / HOAc

An alternative way for the synthesis of 1,2,4-triazine-3-thione in acidic conditions was described in 2000 by J. Hlaváč et al.¹²⁴ The anion of the acid **T102** obtained from isatine **T101** was treated with thiosemicarbazide to give aniline **T103** in 70 % overall yield. The final reaction step from **T103** to **T104** was performed at refluxing AcOH. Based on ¹H-NMR spectrum the ratio of obtained isomers **T104** to **T105** was 10 : 3. (Scheme 56)

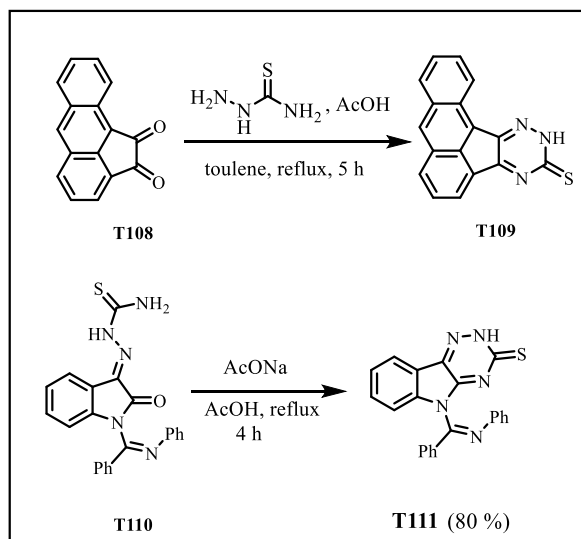


Scheme 56. Preparation of isomers **T104** and **T105** from isatine **T101**.

Another preparation of 1,2,4-triazine-3(2H)-thiones **T109** and **T111** were described on aceanthrylene-1,2-dione **T108** in acid-catalysed reaction¹²⁷ as well as on substituted thiosemicarbazone **T110** catalysed by AcONa in AcOH at reflux.¹²⁸ (Scheme 57)

¹²⁷ Amer, A.M.; El-Mobayed, M.; Ateya, A.M.; Muhdi, T.S. *Monatsh. Chem.* **2002**, *133*, 79 - 88.

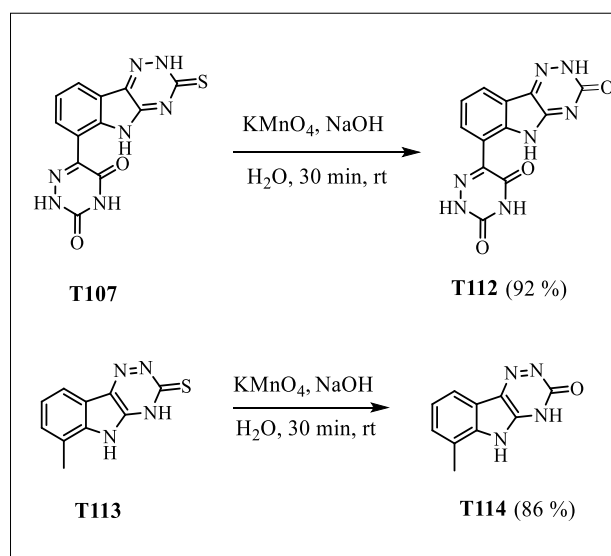
¹²⁸ Saad, H.A.; Moustafa, A.H. *J. Chem. Res.*, **2006**, *2006*, 318 - 323.



Scheme 57. Formation of 1,2,4-triazine-3(2H)-thione **T109** and **T111** from aceanthrylene-1,2-dione **T108** or substituted thiosemicarbazone **T110**.

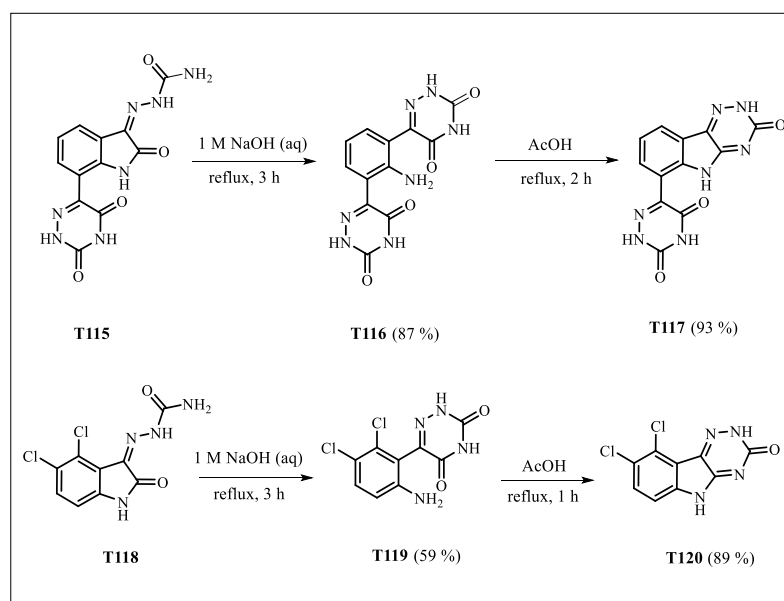
12.3. Formation of the 1,2,4-triazin-3(2H)-one

Oxidation of a sulfur atom in 1,2,4-triazine-3(2H)-thione **T107** is an effective way for the preparation of its isostere **T112**. In 2000 J. Hlaváč et al. described the synthesis of substituted 1,2,4-triazino[5,6-*b*]indole-3-ones **T112** and **T114** from 1,2,4-triazino[5,6-*b*]indole-3-thiones **T107** and **T113** by the oxidation of sulfur with KMnO_4 in an aqueous solution of NaOH .¹²⁴ (Scheme 58)



Scheme 58. Synthesis of the substituted 1,2,4-triazino[5,6-*b*]indole-3-one derivatives **T112** and **T114** by the sulphur oxidative substitution from **T107** and **T113**, resp.

Another effective way for the synthesis of 1,2,4-triazine-3(2*H*)-one was described on substituted isatines **T115** or **T118** via formation of 1,2,4-triazine-3,5(2*H*,4*H*)-diones **T116** or **T119**.^{129,130} These transformations include base-catalysed formation of 1,2,4-triazinediones **T116** or **T119** and their subsequent indole ring reconstitution in **T117** or **T120**. (Scheme 59)



Scheme 59. Synthesis of 1,2,4-triazine-3(2*H*)-ones **T117** and **T120** performed via formation of 1,2,4-triazine-3,5(2*H*,4*H*)-diones **T116** and **T119**.

¹²⁹ Hlaváč, J.; Slouka, J. *J. Heterocyclic Chem.* **1997**, *34*, 917 - 918.

¹³⁰ Hlaváč, J.; Buchtík, R.; Slouka, J.; Hradil, P.; Wiedermanova, I. *Arkivoc*, **2003**, *1*, 22 - 28.

Chapter 10. Project 3. - Isosteric sulphur/oxygen replacement in the ALR2 inhibitor centirestat (CMTI)

13. Project 3 - Isosteric sulphur/oxygen replacement in the ALR2 inhibitor cemtirestat (CMTI)

In the second part of the thesis we were focused on the development of aldose reductase (ALR2) inhibitors, implicated in various chronic diabetic complications. In 2015 Štefek *et al.* identified thioxotriazinoindoles as an effective ALR2 inhibitors.¹¹⁹ Cemtirestat (CMTI) exhibited high inhibitory activity and selectivity together with excellent lead-like properties.¹¹⁹ (Figure 64)

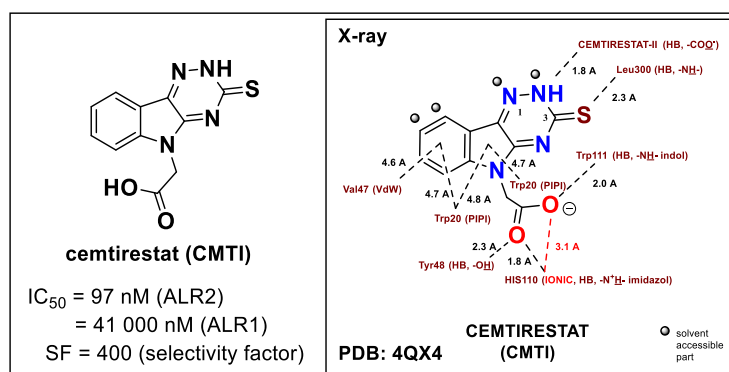


Figure 64. The structure and interaction analysis of novel ALR2 inhibitor cemtirestat (CMTI).

In our project we proceeded to optimize the CMTI thioxotriazinoindole scaffold by replacement of sulfur with oxygen. Based on prediction results several oxotriazinoindole derivatives OTI and OTI-(1-5) were developed and their inhibitory activity, selectivity and antioxidant properties determined. (Figure 65)

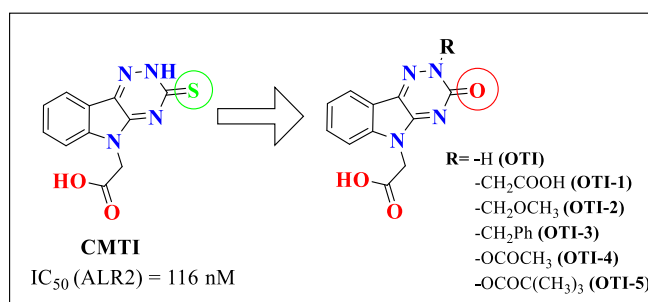
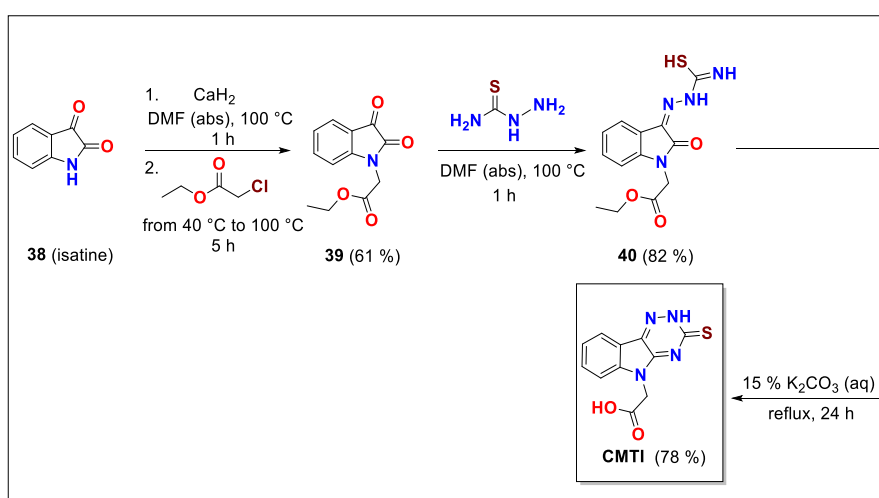


Figure 65. Bioisosteric replacement of sulfur with oxygen in CMTI and the structure of OTI and its proposed derivatives OTI-(1-5).

13.1. Synthesis of centirestat (CMTI)

Despite of known structure of **CMTI** in the SciFinder database, its preparation had not been described. Therefore we developed three-step synthesis, starting from commercially available isatine **38**. In the first step, isatine **38** was alkylated to **39** by calcium hydride, followed by ethyl chloroacetate in DMF at 100 °C within 5 h. Resulting ester **39** underwent condensation with thiosemicarbazide in DMF at 100 °C yielding thiosemicarbazone **40** in 82 %. Finally, the intermediate **40** was refluxed in 15 % aqueous solution of K₂CO₃ within 24 h to give centirestat (**CMTI**) in 78 % yield. (Scheme 60)

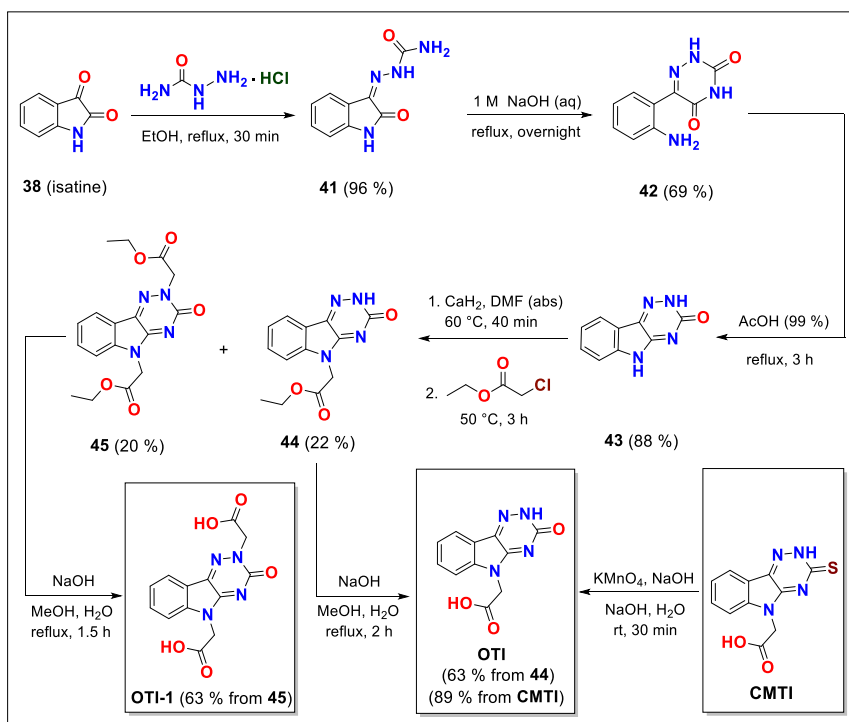


Scheme 60. Developed synthesis of centirestat (**CMTI**).

13.2. Synthesis of an oxo CMTI isostere (OTI) and its dicarboxylic derivative (OTI-1)

By synthesis of **OTI** we followed the procedures developed for preparation of **CMTI**. (Scheme 60) Due to a different reactivity of semicarbazone intermediate (a HO-analogue of **40**, the structure is not given) in cyclization step, we could not follow the synthetic pathway for **CMTI**. Therefore **OTI** and its dicarboxylic derivative **OTI-1** were prepared differently. In this case, isatine **38** was refluxed with semicarbazide hydrochloride in ethanol to give semicarbazone **41** in 96 % yield, that upon reflux in an aqueous solution of NaOH (1.0 M) led to triazinedione **42** in 69 % yield. Acidic treatment of **42** followed by ethyl chloroacetate alkylation of the resulting triazinoindole **43** afforded a mixture of **44** / **45** / **43** (in ratio: 2.0 / 2.5 / 1.0) After separation by FLC we obtained products **44** and **45** in relatively low yields 22 and 20 %, resp. Hydrolysis of **44** and **45** under basic conditions delivered **OTI** and **OTI-1** both in 63 % yield. In addition, the

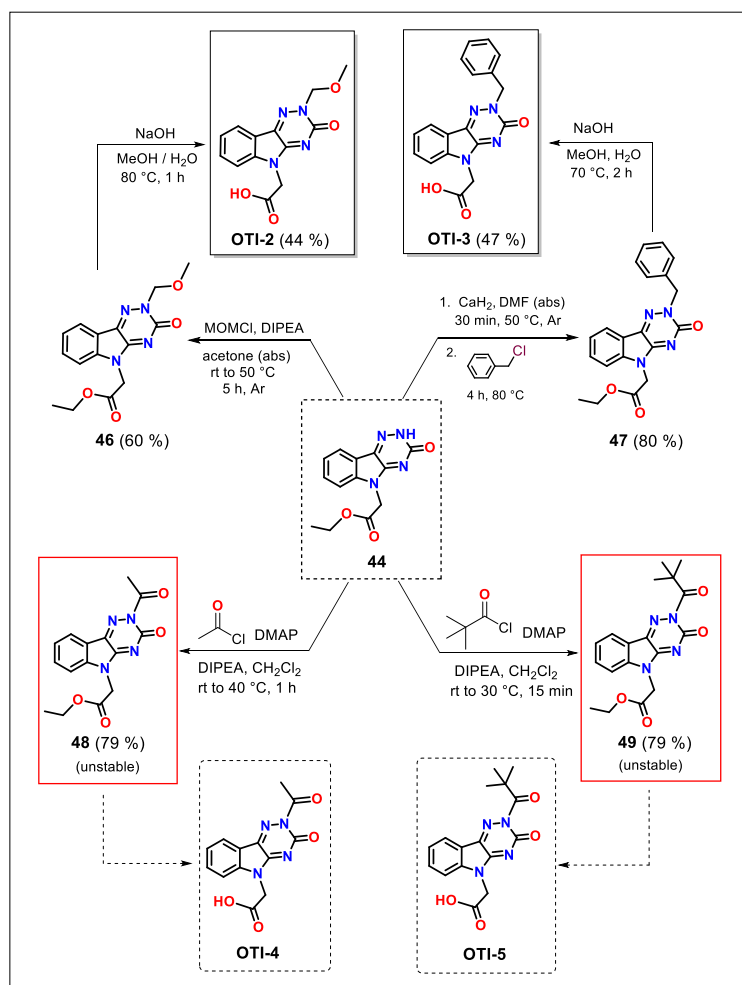
overall yield of the target inhibitor **OTI** was largely improved (35 % vs 8 %) by direct oxidative-hydrolysis of **CMTI** by KMnO_4 in an aqueous solution of NaOH at rt within 30 min. Compound **44** represents an important intermediate for the synthesis of other predicted inhibitors **OTI**-(2-5). (Scheme 61)



Scheme 61. Synthesis of ALR2 inhibitors **OTI** and **OTI-1**.

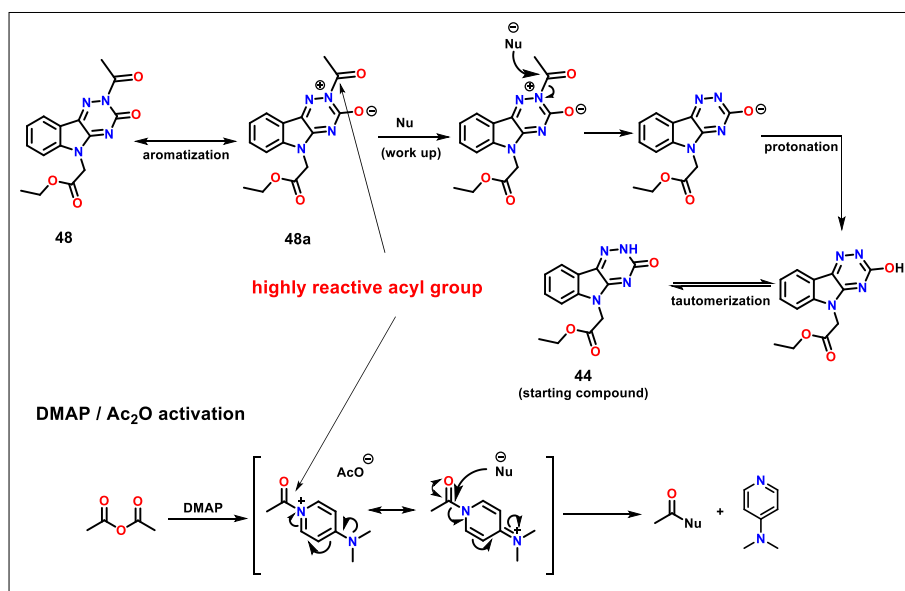
13.3. Synthesis of other OTI derivatives OTI-(2-5)

Synthesis of predicted methoxymethyl **OTI-2** and benzyl **OTI-3** derivatives was performed from ester **44** by *N*-alkylation to corresponding *N*-MOM and *N*-benzyl derivatives **46** and **47**, resp. Subsequent hydrolysis of **46** and **47** under basic conditions afforded compounds **OTI-2** and **OTI-3**, resp. (Scheme 62) Inhibitors **OTI-4** and **OTI-5** were thought to prepare from ester **44** by *N*-acylation to get precursors **48** and **49**, resp. Unfortunately, both compounds **OTI-4** and **OTI-5** were unstable due to their labile acyl group bounded on a partially aromatic 1,2,4-triazine-3-one ring and easily decomposed by deacylation even in a freezer. Therefore, we were not able to support required compounds **48** and **49** for biological screening.



Scheme 62. Synthesis of predicted oxotriazineindoles OTI-(2-5).

Proposed mechanism of OTI-(4-5) deacylation is similar to a known DMAP / Ac₂O activation. Aromatization of **48** leads to an intermediate **48a** with highly reactive acyl group, similarly as in case of DMAP activation depicted in Scheme 87 below. After work up any nucleophile present in a solution could attack the labile acyl group, which resulted to formation of starting compound **44**. Similar instability was observed also by acyl derivative **49**. (Scheme 63)



Scheme 63. Proposed mechanism explaining instability of compound 48.

13.4. Evaluation of OTIs ALR2 inhibition and selectivity

All inhibitors **CMTI**, **OTI** and **OTI-(1-3)** were assayed for their ability to inhibit *in vitro* enzymatic reduction of *D,L*-glyceraldehyde by NADPH and ALR2. ALR2 was isolated from rat eye lenses. For evaluation of selectivity we used aldehyd reductase (ALR1) as an antitarget, characterized by 65 % structural homology with ALR2. Biological assay revealed the highest inhibitory activity for unsubstituted derivative **OTI** ($IC_{50} = 42$ nM (ALR2)) that was compared with its isostere **CMTI** ($IC_{50} = 116$ nM). (Figure 66) Other *N*-substituted derivatives **OTI-(1-3)** were 2 - 10 times less active. The second most active inhibitor was methoxymetyl derivative **OTI-2** with $IC_{50} = 85$ nM. Derivatives **OTI-1** and **OTI-3** exhibited lower inhibitory activity with $IC_{50} = 120$ and 434 nM, resp. (Figure 66)

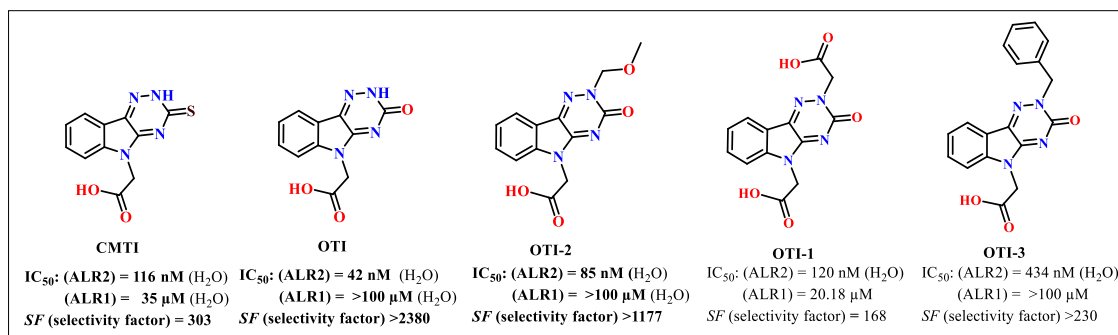


Figure 66. Biological activity and selectivity of **CMTI**, **OTI** and **OTI-(1-3)**.

Additionally to a high ALR2 inhibitory activity of **OTI**, it has importantly very low activity against ALR1, causing significantly high selectivity factor with $SF > 2380$ ($SF = IC_{50} (ALR1) / IC_{50} (ALR2)$) compare to **CMTI** ($SF = 303$). The reason of enormous increase of SF in **OTI** is due to different predicted pose of **CMTI** in an active site of ALR1 in contrast to weaker bounded **OTI** bioisostere. (Figure 67)

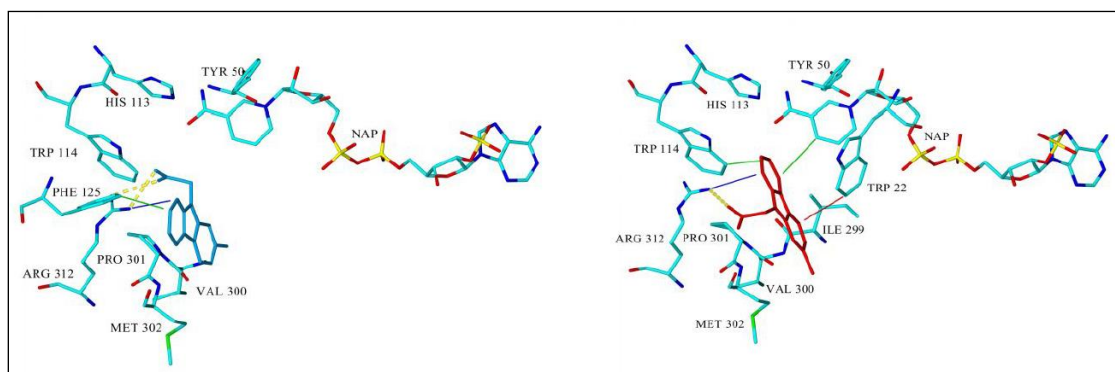


Figure 67. Comparison of intermolecular interactions of **OTI** (left) and its sulphur isostere **CMTI** (right) in an active site of AKR1A1 (ALR1) (PDB: 3FX4) containing NADP⁺.

For determination of an antioxidant activity, the 2,2-diphenyl-1-picrylhydrazyl (**DPPH**) test was employed to evaluate a radical scavenging efficacy of **CMTI**, **OTI** and **OTI-2**. Considerably decreased antioxidant activity of **OTI** ($SF > 2300$) and **OTI-2** ($SF > 1177$) was recorded in comparison to **CMTI** ($SF > 303$). Nevertheless, higher scavenging activity of both inhibitors **OTI** and **OTI-2** was observed relative to a standard melatonin.

In addition, we also determined an activity of **CMTI** and **OTI** on human recombinant aldose reductase AKR1B1. Human small intestine aldose reductase AKR1B10 was used as an antitarget, characterized by 71 % structural homology to AKR1B1. Also in this assay **OTI** ($IC_{50} = 66$ nM and $SF = 1000$) exhibited higher inhibitory activity and selectivity than **CMTI** ($IC_{50} = 102$ nM and $SF = 200$). (Figure 68)

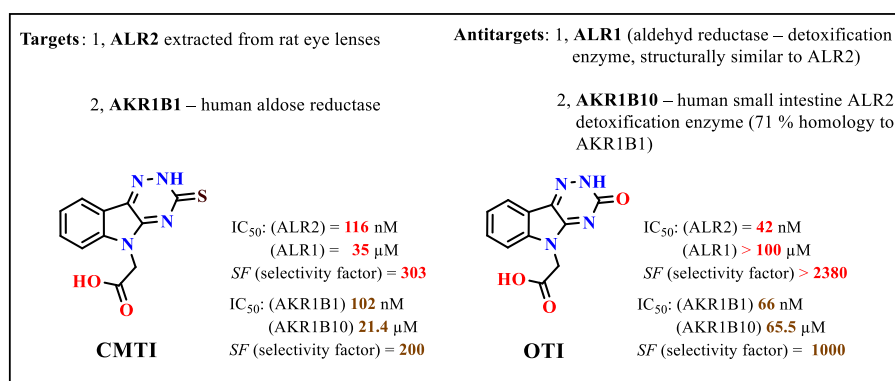


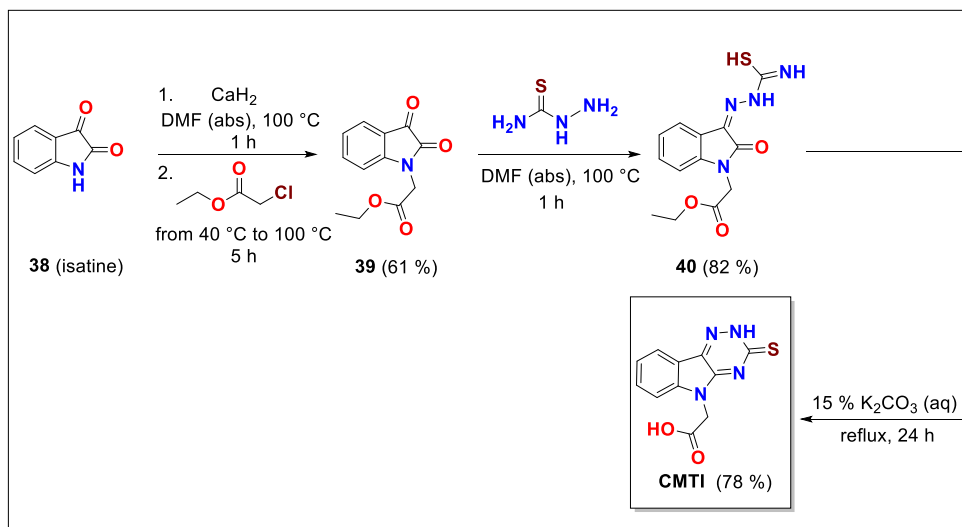
Figure 68. Comparison of determined inhibitory activity and selectivity of **CMTI** and **OTI**.

To conclude, **OTI** revealed 3-fold higher inhibitory activity on a rat ALR2 and 1.5-fold higher activity on human AKR1B1 compare to **CMTI**. What more, **OTI** exhibited 8-fold higher ALR1 / ALR2 (rat) and 5-fold higher AKR1B10 / AKR1B1 (human) selectivity compare to **CMTI**. These results have been recently published.¹³¹

¹³¹ Hlavac, M.; Kovacikova, L.; Prnova, M.S.; Addova, G.; Majekova, M.; Hanquet, G.; Bohac, A.; Stefek, M. *J. Med. Chem.*, **2020**, *63*, 369 - 381.

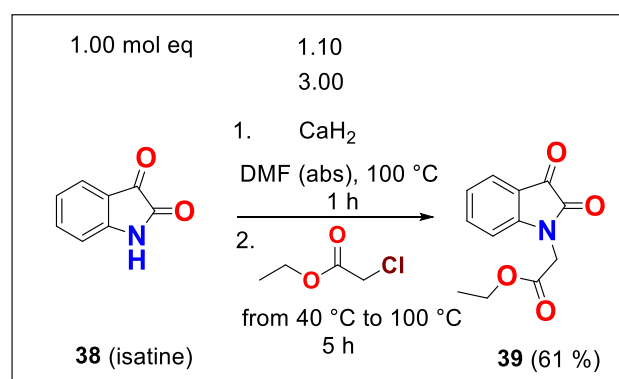
13.5. Experimental part

13.5.1. Synthesis of triazinoindol ALR2 inhibitor centirestat (CMTI)



Scheme 64. Synthesis of triazinoindol ALR2 inhibitor centirestat (CMTI).

Synthesis of ethyl 2-(2,3-dioxindolin-1-yl)acetate (39)

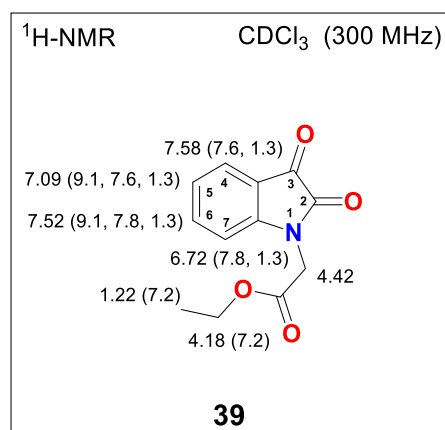


A mixture of 2.00 g (13.6 mmol, 1.00 mol eq) isatine (**38**) and 630 mg (15.0 mmol, 1.10 mol eq) of CaH_2 in 15 mL of DMF (abs) was stirred at $100\text{ }^\circ\text{C}$ for 1 h under Ar and then cooled to $40\text{ }^\circ\text{C}$. At this temperature 4.37 mL (40.8 mmol, 3.00 mol eq) of ethyl chloroacetate was added within 10 min into the reaction mixture. The resulting mixture was heated to $100\text{ }^\circ\text{C}$ for 5 h and then allowed to cool to rt. The reaction was poured into a vigorously stirred aqueous 0.5 M HCl solution (50 mL), which resulted in a red precipitate. The obtained solid material was filtered off and washed with H_2O . The crude product was further purified by trituration in a mixture of

hexane / ethyl acetate to afford 1.93 g (8.28 mmol, 61 %) of ethyl 2-(2,3-dioxindolin-1-yl)acetate (**39**) as a red solid material.

Novelty: The synthesis of compound **39** was previously described in the literature with quantitative yield and characterized by its M.P., ^1H -, ^{13}C -NMR, IR, MS and HRMS spectrum.¹³²

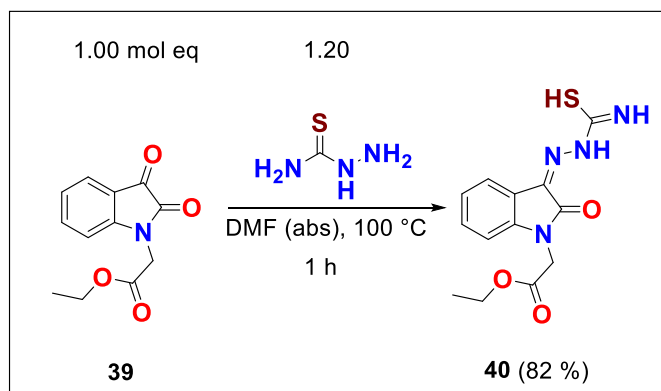
M.p.: 125.8 - 127.5 °C [DMF / H₂O] (lit. 132 - 133 °C).¹³²



^1H -NMR (300 MHz, CDCl_3): δ 7.58 (dd, 1H, $J(4,5) = 7.6$ Hz, $J(4,6) = 1.3$ Hz, H-C(4)), 7.52 (ddd, 1H, $J(5,6) = 9.1$ Hz, $J(6,7) = 7.8$ Hz, $J(4,6) = 1.3$ Hz, H-C(6)), 7.09 (ddd, 1H, $J(5,6) = 9.1$ Hz, $J(4,5) = 7.6$ Hz, $J(5,7) = 1.3$ Hz, H-C(5)), 6.72 (dd, 1H, $J(6,7) = 7.8$ Hz, $J(5,7) = 1.3$ Hz, H-C(7)), 4.42 (s, 2H, NCH_2COOEt), 4.18 (q, 2H, $J(\text{CH}_2, \text{CH}_3) = 7.2$ Hz, $-\text{OCH}_2\text{CH}_3$), 1.22 (t, 3H, $J(\text{CH}_2, \text{CH}_3) = 7.2$ Hz, $-\text{OCH}_2\text{CH}_3$).

¹³² Lötter, A.N.C.; Pathak, R.; Sello, T.S.; Fernandes, M.A.; Van Otterlo, W.A.L.; De Köning, Ch.B. *Tetrahedron*, **2007**, *63*, 2263 - 2274.

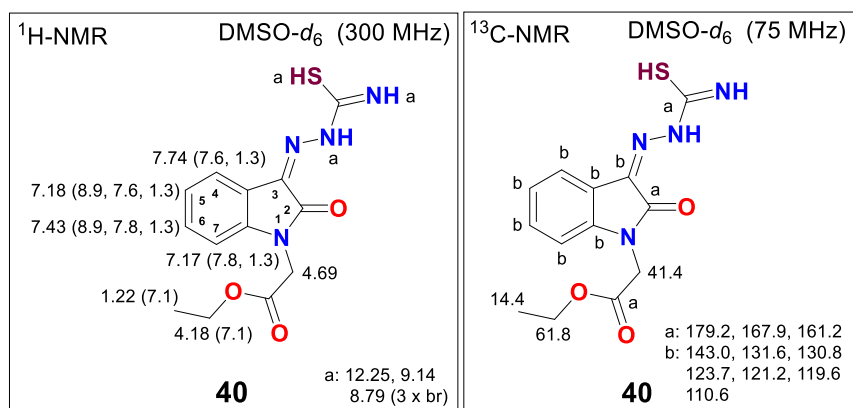
Synthesis of 2-(1-(2-ethoxy-2-oxoethyl)-2-oxoindolin-3-ylidene)hydrazinecarbimidothioic acid (**40**)



Ethyl 2-(2,3-dioxoindolin-1-yl)acetate (**39**) 500 mg (2.15 mmol, 1.00 mol eq) and 235 mg (2.58 mmol, 1.20 mol eq) of thiosemicarbazide were dissolved in 10 mL of DMF (abs) and stirred at 100 °C for 1 h. Then the reaction was cooled to rt and 20 mL of H₂O added. The obtained solution was extracted with EA (5 x 10 mL) and the combined organic layer washed with brine (3 x 10 mL), dried over Na₂SO₄, filtered and concentrated under reduced pressure. The crude product was purified by trituration in a mixture of hexole / ethyl acetate to yield 539 mg (1.76 mmol, 82 %) of 2-(1-(2-ethoxy-2-oxoethyl)-2-oxoindolin-3-ylidene)hydrazinecarbimidothioic acid (**40**) as a red - orange solid material.

Novelty: 2-(1-(2-ethoxy-2-oxoethyl)-2-oxoindolin-3-ylidene)hydrazinecarbimidothioic acid (**40**) is not described in the literature.

M.p.: 209.3 - 214.0 °C [EA].



$^1\text{H-NMR}$ (300 MHz, $\text{DMSO-}d_6$): δ 12.25, 9.14 and 8.79 (3 x br s, 3 x 1H, -NH-, =NH and -SH), 7.74 (dd, 1H, $J(4,5) = 7.6$ Hz, $J(4,6) = 1.3$ Hz, H-C(4)), 7.43 (ddd, 1H, $J(5,6) = 8.9$ Hz, $J(6,7) = 7.8$ Hz, $J(4,6) = 1.3$ Hz, H-C(6)), 7.18 (ddd, 1H, $J(5,6) = 8.9$ Hz, $J(4,5) = 7.6$ Hz, $J(5,7) = 1.3$ Hz, H-C(5)), 7.17 (dd, 1H, $J(6,7) = 7.8$ Hz, $J(5,7) = 1.3$ Hz, H-C(7)), 4.69 (s, 2H, NCH_2COOEt), 4.18 (q, 2H, $J(\text{CH}_2, \text{CH}_3) = 7.1$ Hz, $-\text{OCH}_2\text{CH}_3$), 1.22 (t, 3H, $J(\text{CH}_2, \text{CH}_3) = 7.1$ Hz, $-\text{OCH}_2\text{CH}_3$).

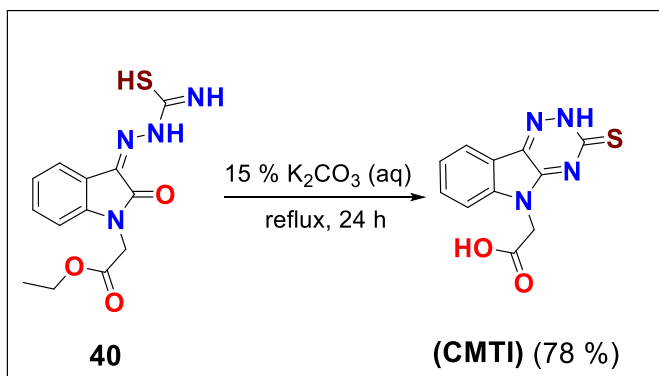
$^{13}\text{C-NMR}$ (75 MHz, $\text{DMSO-}d_6$): δ 179.2, 167.9, 161.2, 143.0, 131.6, 130.8, 123.7, 121.2, 119.6, 110.6, 61.8 ($-\text{OCH}_2\text{CH}_3$), 41.4 (NCH_2COOEt), 14.4 ($-\text{OCH}_2\text{CH}_3$).

FT-IR (solid, cm^{-1}): 3411 (m), 3240 (m), 3145 (m), 2985 (w), 2941 (w), 1736 (s), 1688 (s), 1612 (s), 1471 (s), 1452 (s), 1418 (m), 1375 (s), 1351 (s), 1295 (w), 1237 (s), 1154 (s), 1103 (s), 1062 (s), 1011 (s), 885 (m), 868 (m), 835 (m), 786 (m), 738 (m), 641 (m), 619 (m), 567 (w), 491 (s), 456 (s).

MS (ESI m/z): 307.0 $[\text{M}+\text{H}]^+$ (positive mode).

Anal. calcd for $\text{C}_{13}\text{H}_{14}\text{N}_4\text{O}_3\text{S}$ (306.34): C, 50.97; H, 4.61; N, 18.29 Found: C, 50.84; H, 4.49; N, 18.05.

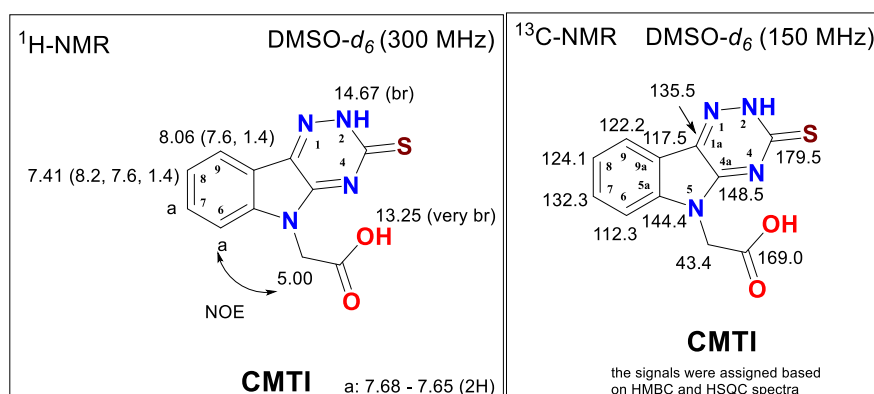
Synthesis of 2-(3-thioxo-2*H*-[1,2,4]triazino[5,6-*b*]indol-5(3*H*)-yl)acetic acid (CMTI)



Solution of hydrazinecarbimidothioic acid **40** 600 mg (1.96 mmol, 1.00 mol eq) was refluxed in 50 mL of 15 % aq solution of K_2CO_3 for 24 h. After cooling to rt the mixture was treated with HCl (1 M, aq) to pH = 2. Precipitated solid material was filtered off, washed with water and dried under reduced pressure to yield 398 mg (1.53 mmol, 78 %) of acid **CMTI** as an orange solid product.

Novelty: Synthesis and characterisation of 2-(3-thioxo-2*H*-[1,2,4]triazino[5,6-*b*]indol-5(3*H*)-yl)acetic acid (**CMTI**) is not described in the literature.

M.p.: 340 - 370 °C [H_2O] (dec).



¹H-NMR (300 MHz, DMSO-*d*₆): δ 14.67 (br s, 1H, -NH-), 13.25 (very br, 1H, -COOH) 8.06 (dd, 1H, *J*(8,9) = 7.6 Hz, *J*(7,9) = 1.4 Hz, H-C(9)), 7.68 - 7.65 (m, 2H, H-C(6 and 7)), 7.41 (ddd, 1H, *J*(7,8) = 8.2 Hz, *J*(8,9) = 7.6 Hz, *J*(6,8) = 1.4 Hz, H-C(8)), 5.00 (s, 2H, NCH₂COOH).

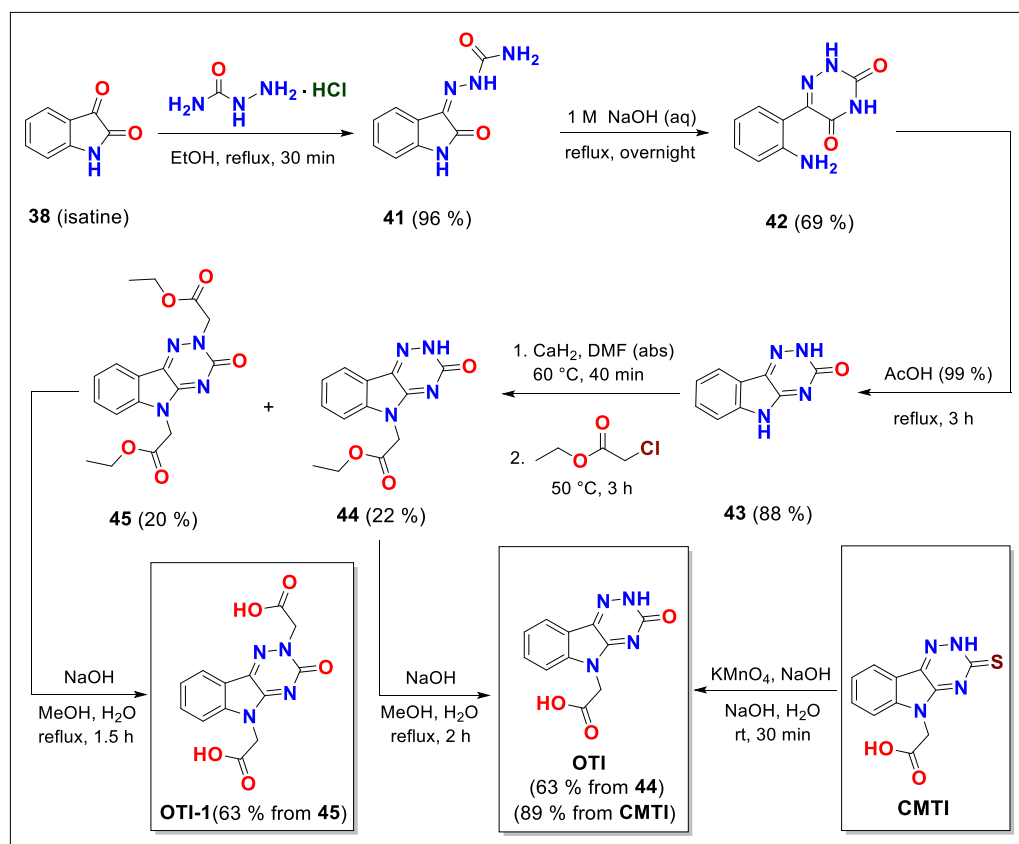
¹³C-NMR (150 MHz, DMSO-*d*₆): δ 179.5 (C=S), 169.0 (-COOH), 148.5 (C_{4a}), 144.4 (C_{5a}), 135.5 (C_{1a}), 132.3 (C₇), 124.1 (C₈), 122.2 (C₉), 117.5 (C_{9a}), 112.3 (C₆), 43.4 (NCH₂COOH).

FT-IR (solid, cm⁻¹): 3500 (w), 3099 (w), 3020 (w), 2978 (w), 2892 (w), 1736 (m), 1601 (m), 1575 (s), 1466 (m), 1438 (w), 1370 (m), 1258 (m), 1167 (s), 1147 (s), 1073 (w), 1018 (m), 945 (w), 811 (w), 784 (m), 754 (m), 639 (w), 526 (m).

MS (ESI *m/z*): 259.0 (10 %) [M-H]⁻, 214.9 (100 %) [M-CO₂-H]⁻ (negative mode).

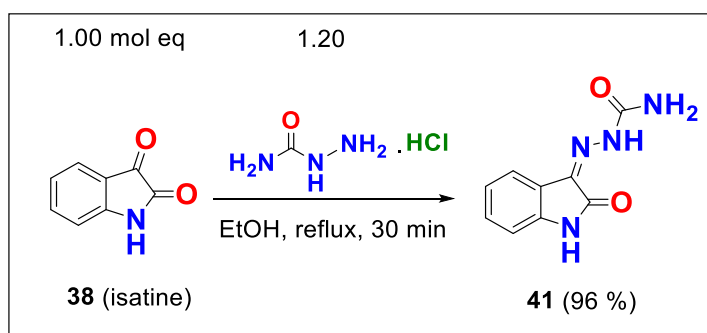
Anal. calcd for C₁₁H₈N₄O₂S (260.27): C, 50.76; H, 3.10; N, 21.53 Found: C, 50.92; H, 3.32 ; N, 21.84.

13.5.2. Synthesis of an oxo CMTI isostere (OTI) and its dicarboxylic derivative (OTI-1)



Scheme 65. Synthesis of an oxo CMTI isostere **OTI** and its dicarboxylic derivative **OTI-1**.

Synthesis of 2-(2-oxoindolin-3-ylidene)hydrazinecarboxamide (41)

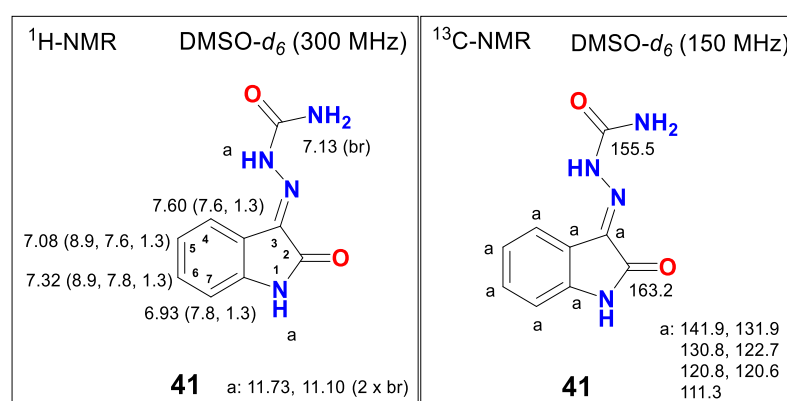


To a solution of 3.00 g (20.4 mmol, 1.00 mol eq) isatine **38** in 40 mL of EtOH, 2.73 g (24.5 mmol, 1.20 mol eq) of semicarbazide hydrochloride was added and the mixture refluxed for 30 min. Then, 40 mL of water was added to the reaction and the mixture cooled to rt and stirred

for another 30 min. The resulting yellow precipitate was filtered off, washed with water and dried under IR lamp and reduced pressure yielding 4.01 g (19.6 mmol, 96 %) of semicarbazone **41** as a yellow solid product.

Novelty: 2-(2-oxoindolin-3-ylidene)hydrazinecarboxamide (**41**) was described in the literature by its M.p., ¹H-NMR, bioactivity,¹³³ UV / VIS, IR¹³⁴ and HRMS spectral analyses.¹³⁵

M.p.: 248 - 270 °C (dec) [EtOH], (lit. 239 °C).¹³³



¹H-NMR (300 MHz, DMSO-*d*₆): δ 11.73 and 11.10 (2 x br s, 1H, -NH- and -NHCONH₂), 7.60 (dd, 1H, $J(4,5) = 7.6$ Hz, $J(4,6) = 1.3$ Hz, H-C(4)), 7.32 (ddd, 1H, $J(5,6) = 8.9$ Hz, $J(6,7) = 7.8$ Hz, $J(4,6) = 1.3$ Hz, H-C(6)), 7.13 (br s, 2H, -NH₂), 7.08 (ddd, 1H, $J(5,6) = 8.9$ Hz, $J(4,5) = 7.6$ Hz, $J(5,7) = 1.3$ Hz, H-C(5)), 6.93 (dd, 1H, $J(6,7) = 7.8$ Hz, $J(5,7) = 1.3$ Hz, H-C(7)).

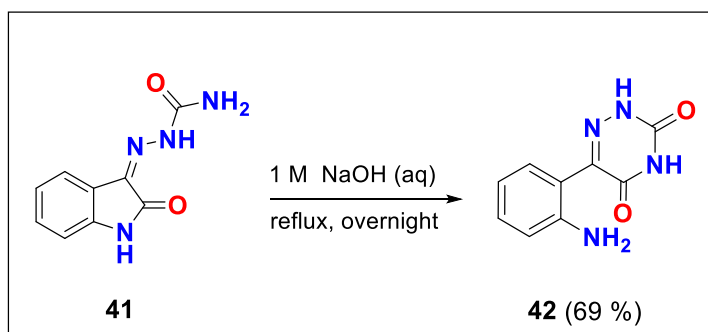
¹³C-NMR (150 MHz, DMSO-*d*₆): δ 163.2 (C₂), 155.5 (s, -NHCONH₂), 141.9, 131.9, 130.8, 122.7, 120.8, 120.6, 111.3.

¹³³ Seifi, M.; Sheibani, H. *Lett. Org. Chem*, **2013**, *10*, 478 - 481.

¹³⁴ Ilic, S.B.; Konstantinovic, S.S.; Savic, D.S.; Veljkovic, V.B.; Gojgic-Cvijovic, G. *Med. Chem. Res.*, **2010**, *19*, 690 - 697.

¹³⁵ Hall, M.D.; Salam, N.K.; Hellowell, J.L.; Fales, H.M.; Kensler, C.B.; Ludwig, J.A.; Szakacs, G.; Hibbs, D.E.; Gottesman, M.M. *J. Med. Chem.*, **2009**, *52*, 3191 - 3204.

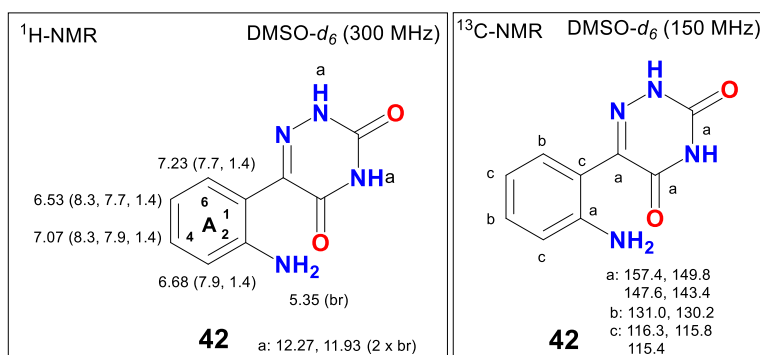
Synthesis of 6-(2-aminophenyl)-1,2,4-triazine-3,5(2H,4H)-dione (42)



A solution of 4.00 g (19.6 mmol, 1.00 mol eq) semicarbazone **41** was refluxed in 75 mL of 1 M aq solution of NaOH overnight. After cooling the reaction mixture was acidified with concentrated HOAc to pH = 5 and stirred 30 min. Resulting precipitate was filtered off, washed with water and dried under IR lamp and reduce pressure to yield 2.77 g (13.5 mmol, 69 %) of 6-(2-aminophenyl)-1,2,4-triazine-3,5(2H,4H)-dione (**42**) as a yellow solid product.

Novelty: 6-(2-aminophenyl)-1,2,4-triazine-3,5(2H,4H)-dione (**42**) was described in the literature with its M.p. and UV / VIS spectra.¹³⁶

M.p.: 270 - 320 °C (dec) [H₂O] (lit: 350 °C).¹³⁶



¹³⁶ Ioffe, I.S.; Tomchin, A.B.; Rusakov, E.A. *Zhurnal Obshchej Khimii*, **1969**, *39*, 2345 - 2351.

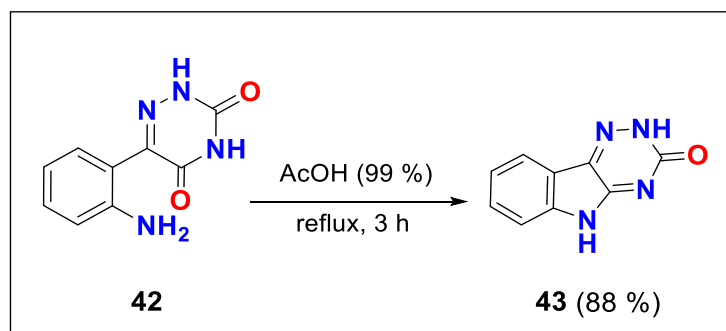
¹H-NMR (300 MHz, DMSO-*d*₆): δ 12.27 and 11.93 (2 x br s, 1H, -CONHCO- and =N-NHCO-), 7.23 (dd, 1H, *J*(A₅,A₆) = 7.7 Hz, *J*(A₄,A₆) = 1.4 Hz, H-C_A(6)), 7.07 (ddd, 1H, *J*(A₄,A₅) = 8.3 Hz, *J*(A₃,A₄) = 7.9 Hz, *J*(A₄,A₆) = 1.4 Hz, H-C_A(4)), 6.68 (dd, 1H, *J*(A₃,A₄) = 7.9 Hz, *J*(A₃,A₅) = 1.4 Hz, H-C_A(3)), 6.53 (ddd, 1H, *J*(A₄,A₅) = 8.3 Hz, *J*(A₅,A₆) = 7.7 Hz, *J*(A₃,A₅) = 1.4 Hz, H-C_A(5)), 5.35 (br s, 2H, -NH₂).

¹³C-NMR (150 MHz, DMSO-*d*₆): δ 157.4, 149.8, 147.6, 143.4; 131.0, 130.2; 116.3, 115.8, 115.4.

FT-IR (solid, cm⁻¹): 3491 (w), 3377 (w, NH), 3018 (m, NH₂), 1699 (s, C=O), 1609 (s, C=O), 1582 (m), 1542 (m), 1465 (m), 1311 (m), 1246 (m), 1154 (m), 1040 (w), 848 (m), 751 (s), 639 (m), 552 (m), 431 (s).

MS (ESI *m/z*): 202.9 (100 %) [M-H]⁻ (negative mode).

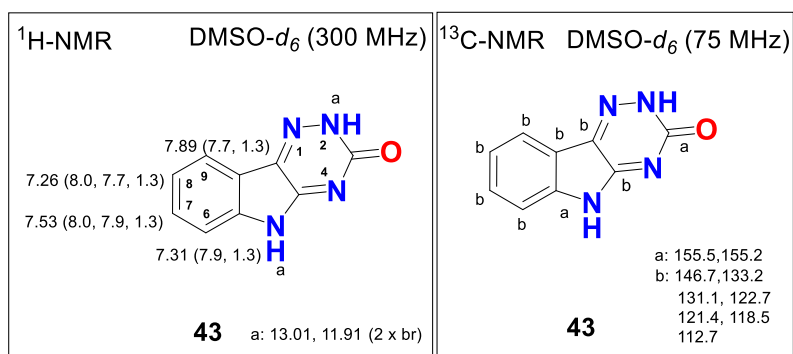
Synthesis of 2*H*-[1,2,4]triazino[5,6-*b*]indol-3(5*H*)-one (43)



A suspension of 2.77 g (13.5 mmol) **42** in 50 mL of conc. HOAc was refluxed for 3 h. After cooling to 0 °C 20 mL of water was added and resulting suspension stirred for another 30 min in an ice bath. An obtained solid material was filtered off, washed with water, dried under IR lamp and reduce pressure to yield 2.23 g (12.0 mmol, 88 %) of 2*H*-[1,2,4]triazino[5,6-*b*]indol-3(5*H*)-one (**43**) as a yellow solid product.

Novelty: 2H-[1,2,4]triazino[5,6-b]indol-3(5H)-one (**43**) is described in the literature with its M.p., ¹H-NMR, IR and MS spectrum.¹³⁷

M.p.: 320 - 360 °C (dec) [AcOH] (lit: 280 °C).¹³⁷



¹H-NMR (300 MHz, DMSO-*d*₆): δ 13.01 and 11.91 (2 x br s, 1H, -NHCO- and ArNH-), 7.89 (dd, 1H, $J(8,9) = 7.7$ Hz, $J(7,9) = 1.3$ Hz, H-C(9)), 7.53 (ddd, 1H, $J(7,8) = 8.0$ Hz, $J(6,7) = 7.9$ Hz, $J(7,9) = 1.3$ Hz, H-C(7)), 7.31 (dd, 1H, $J(6,7) = 7.9$ Hz, $J(6,8) = 1.3$ Hz, H-C(6)), 7.26 (ddd, 1H, $J(7,8) = 8.0$ Hz, $J(8,9) = 7.7$ Hz, $J(6,8) = 1.3$ Hz, H-C(8)).

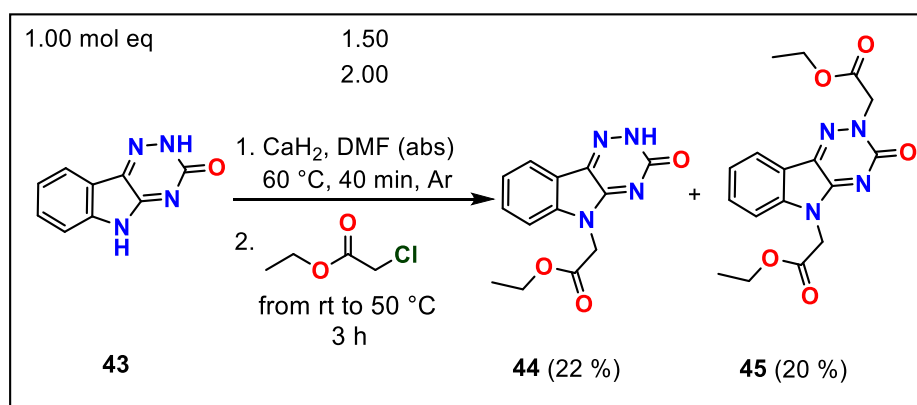
¹³C-NMR (75 MHz, DMSO-*d*₆): δ 155.5, 155.2; 146.7, 133.2; 131.1, 122.7; 121.4, 118.5, 112.7.

MS (ESI m/z): 184.9 (100 %) [M-H]⁻ (negative mode).

Anal. calcd for C₉H₆N₄O (186.17): C, 58.06; H, 3.25; N, 30.09; Found: C, 58.22; H, 3.43; N, 30.19.

¹³⁷ Abdel-Sayed, N.I. *Bulg. Chem. Commun.*, **2009**, 4, 362 - 367.

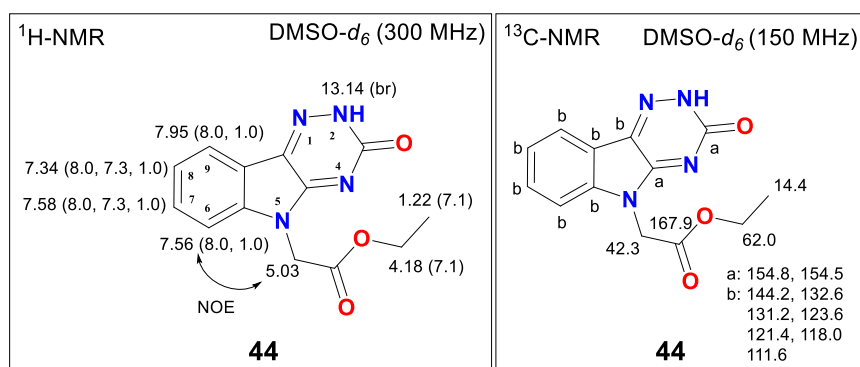
Synthesis of ethyl 2-(3-oxo-2H-[1,2,4]triazino[5,6-b]indol-5(3H)-yl)acetate (44) and diethyl 2,2'-(3-oxo-2H-[1,2,4]triazino[5,6-b]indole-2,5(3H)-diyl)diacetate (45)



A mixture of 1.40 g (7.52 mmol, 1.00 mol eq) **43** and 474 mg (11.30 mmol, 1.50 mol eq) of CaH₂ in 15 mL of DMF (abs) was stirred at 60 °C for 40 min under Ar and then cooled to rt. Then 1.61 mL (15.04 mmol, 2.00 mol eq) of ethyl chloroacetate was added dropwise to the reaction mixture within 10 min. Afterwards the mixture was heated to 50 °C for 3 h. After 3 h a TLC analysis confirmed formation of products **44**, **45** and the starting material **43** in a ratio: **44**/**45**/**43** = 2.0 / 2.5 / 1.0. The mixture was cooled to rt and poured into a stirred aqueous 0.5 M HCl solution (50 mL), which resulted in an orange precipitate. A solution obtained after filtration was extracted with EA (5 x 10 mL), washed with brine and water. A combined organic layer was dried over Na₂SO₄, filtered and concentrated under reduced pressure. A crude product was purified by FLC (SiO₂, DCM / MeOH = 14 / 1) to give 450 mg (1.65 mmol, 22 %) of monoester **44** as a white solid compound and 539 mg (1.51 mmol, 20 %) of diester **45** as an orange crystalline compound.

Novelty: ethyl 2-(3-oxo-2H-[1,2,4]triazino[5,6-b]indol-5(3H)-yl)acetate (**44**) is not described in the literature.

M.p.: 248.0 - 252.0 °C [MeOH / DCM].



¹H-NMR (300 MHz, DMSO-*d*₆): δ 13.14 (br s, 1H, -NH-), 7.95 (dd, 1H, $J(8,9) = 8.0$ Hz, $J(7,9) = 1.0$ Hz, H-C(9)), 7.58 (ddd, 1H, $J(6,7) = 8.0$ Hz, $J(7,8) = 7.3$ Hz, $J(7,9) = 1.0$ Hz, H-C(7)), 7.56 (dd, 1H, $J(6,7) = 8.0$ Hz, $J(6,8) = 1.0$ Hz, H-C(6)), 7.34 (ddd, 1H, $J(8,9) = 8.0$ Hz, $J(7,8) = 7.3$ Hz, $J(6,8) = 1.0$ Hz, H-C(8)), 5.03 (s, 2H, NCH₂COOEt), 4.18 (q, 2H, $J(\text{CH}_2, \text{CH}_3) = 7.1$ Hz, -OCH₂CH₃), 1.22 (t, 3H, $J(\text{CH}_2, \text{CH}_3) = 7.1$ Hz, -OCH₂CH₃).

¹³C-NMR (150 MHz, DMSO-*d*₆): δ 167.9 (-CH₂COO-); 154.8, 154.5, 144.2, 132.6; 131.2, 123.6, 121.4, 118.0, 111.6; 62.0 (-OCH₂CH₃), 42.3 (-CH₂COOEt), 14.4 (-OCH₂CH₃).

FT-IR (solid, cm⁻¹): 3151 (w), 3088 (w), 2980 (w), 2857 (m), 1733 (s), 1656 (s), 1595 (s), 1497 (s), 1408 (s), 1221 (s), 1171 (m), 1061 (m), 1012 (m), 965 (w), 919 (w), 788 (m), 746 (m), 659 (m), 604 (m), 575 (m), 486 (s).

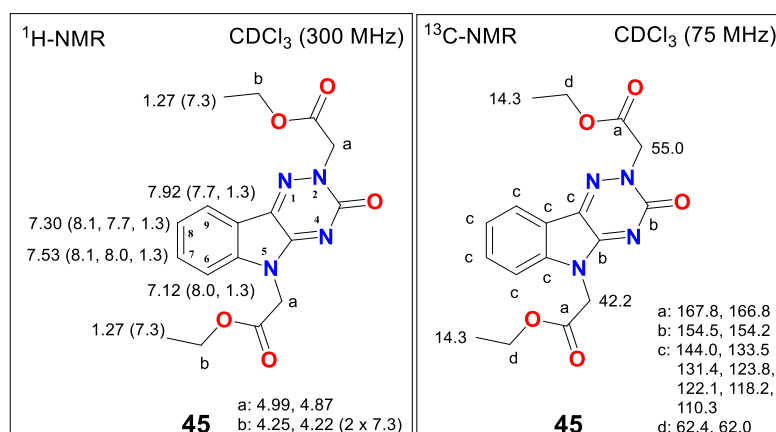
MS (ESI *m/z*): 271.0 [M-H]⁻ (negative mode).

Anal. calcd for C₁₃H₁₂N₄O₃ (272.26): C, 57.35; H, 4.44; N, 20.58; Found: C, 57.13; H, 4.16; N, 20.85.

Diethyl 2,2'-(3-oxo-2*H*-[1,2,4]triazino[5,6-*b*]indole-2,5(3*H*)-diyl)diacetate (45)

Novelty: diethyl 2,2'-(3-oxo-2*H*-[1,2,4]triazino[5,6-*b*]indole-2,5(3*H*)-diyl)diacetate (**45**) is not described in the literature.

M.p.: 182.0 - 184.1 °C [MeOH / DCM].



¹H-NMR (300 MHz, CDCl₃): δ 7.92 (dd, 1H, $J(8,9) = 7.7$ Hz, $J(7,9) = 1.3$ Hz, H-C(9)), 7.53 (ddd, 1H, $J(7,8) = 8.1$ Hz, $J(6,7) = 8.0$ Hz, $J(7,9) = 1.3$ Hz, H-C(7)), 7.30 (ddd, 1H, $J(7,8) = 8.1$ Hz, $J(8,9) = 7.7$ Hz, $J(6,8) = 1.3$ Hz, H-C(8)), 7.12 (dd, 1H, $J(6,7) = 8.0$ Hz, $J(6,8) = 1.3$ Hz, H-C(6)), 4.99 and 4.87 (2 x s, 2 x 2H, 2 x -CH₂COOEt), 4.25 and 4.22 (2 x q, 2 x 2H, $J(\text{CH}_2, \text{CH}_3) = 7.3$ Hz, 2 x -OCH₂CH₃), 1.27 (t, 2 x 3H, $J(\text{CH}_2, \text{CH}_3) = 7.3$ Hz, 2 x -OCH₂CH₃).

¹³C-NMR (75 MHz, CDCl₃): δ 167.8, 166.8, 154.5, 154.2, 144.0, 133.5, 131.4, 123.8, 122.1, 118.2, 110.3, 62.4 and 62.0 (2 x -OCH₂CH₃), 55.0 and 42.2 (2 x NCH₂COOEt), 2 x 14.3 (2 x -OCH₂CH₃).

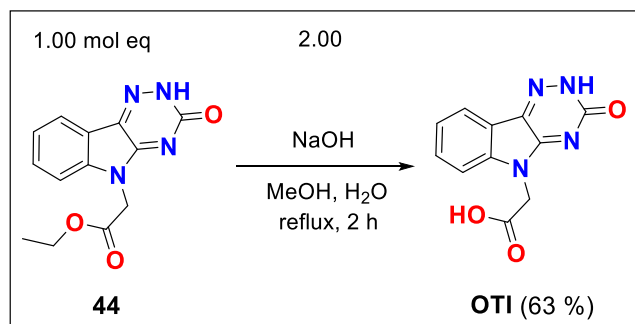
FT-IR (solid, cm⁻¹): 3020 (w), 2910 (w), 2083 (w), 1736 (s), 1683 (s), 1637 (s), 1604 (s), 1575 (m), 1498 (m), 1464 (m), 1421 (m), 1396 (s), 1374 (s), 1306 (m), 1275 (m), 1194 (s), 1138 (s), 1109 (s), 1058 (m), 1021 (m), 952 (m), 871 (w), 785 (m), 748 (s), 592 (m), 566 (m), 496 (w), 430 (s).

MS (ESI m/z): 359.1 (70 %) [M+H]⁺, 381.1 (100 %) [M+Na]⁺ (positive mode).

Anal. calcd for C₁₇H₁₈N₄O₅ (358.35): C, 56.98; H, 5.06; N, 15.63 Found: C, 57.05; H, 5.13; N, 15.74.

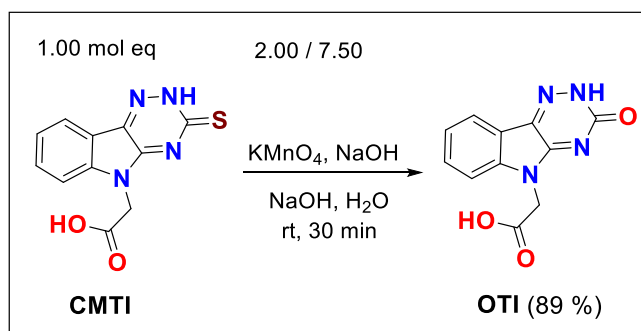
Synthesis of 2-(3-oxo-2H-[1,2,4]triazino[5,6-b]indol-5(3H)-yl)acetic acid (OTI)

Experiment 1



To a solution of 200 mg (0.74 mmol, 1.00 mol eq) ester **44** in 20 mL of MeOH, 59.0 mg (1.48 mmol, 2.00 mol eq) of NaOH in 5 mL of water was added and the resulted mixture refluxed for 2 h. After consumption of starting material **44** (confirmed by TLC analysis) the mixture was cooled down in an ice bath and acidified with 1 M aq HCl to adjust pH = 4. After 10 min of stirring formation of precipitate was observed. The mixture was stirred for another 20 min in an ice bath. Then the precipitate was filtered off and dried under reduced pressure to yield 113 mg (0.46 mmol, 63 %) of **OTI** as a pale orange solid product.

Experiment 2

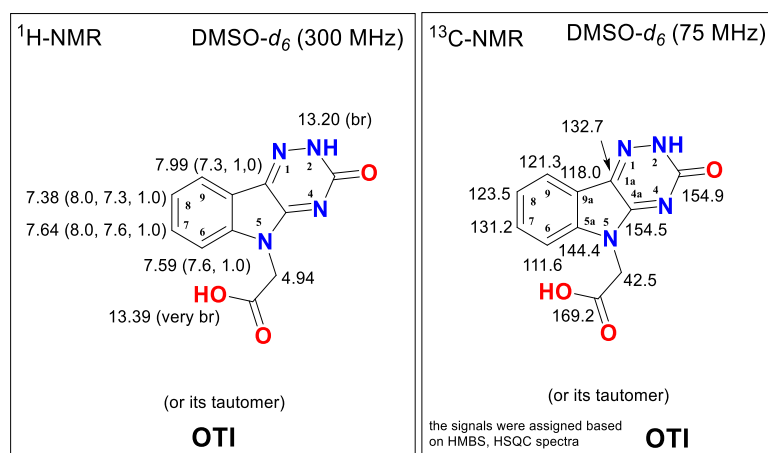


Compound **CMTI** 100 mg (0.38 mmol, 1.00 mol eq) was added to a solution of 30.0 mg (0.75 mmol, 2.00 mol eq) NaOH in 5 mL of water. An another solution consisting of 122 mg (0.77 mmol, 2.00 mol eq) KMnO₄ and 84.0 mg (2.10 mmol, 5.50 mol eq) of NaOH in 5 mL of water was added dropwise to the above mixture and a resulting suspension was stirred at rt for 30 min. Then, the solid material was filtered off, a filtrate acidified with 1 M aq HCl to pH = 1 and refluxed for 5 min to perform a clear solution, cooled down and concentrated to a half of its

volume by RVE. The additionally obtained **OTI** crude product was filtered off and washed with water. Collected product was purified by trituration in a mixture of hexole / ethyl acetate to afford 84.0 mg (0.34 mmol, 89 %) of **OTI** as a pale orange compound.

Novelty: 2-(3-oxo-2*H*-[1,2,4]triazino[5,6-*b*]indol-5(3*H*)-yl)acetic acid (**OTI**) is not described in the literature.

M.p.: 288.1 - 290.0 °C [H₂O / H⁺].



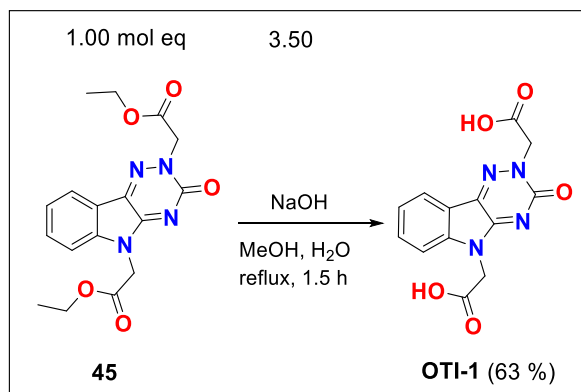
¹H-NMR (300 MHz, DMSO-*d*₆): δ 13.39 (very br s, 1H, -COOH), 13.20 (br s, 1H, H-N(2)), 7.99 (dd, 1H, $J(8,9) = 7.3$ Hz, $J(7,9) = 1.0$ Hz, H-C(9)), 7.64 (ddd, 1H, $J(7,8) = 8.0$ Hz, $J(6,7) = 7.6$ Hz, $J(7,9) = 1.0$ Hz, H-C(7)), 7.59 (dd, 1H, $J(6,7) = 7.6$ Hz, $J(6,8) = 1.0$ Hz, H-C(6)), 7.38 (ddd, 1H, $J(7,8) = 8.0$ Hz, $J(8,9) = 7.3$ Hz, $J(6,8) = 1.0$ Hz, H-C(8)), 4.94 (s, 2H, -CH₂COOH).

¹³C-NMR (75 MHz, DMSO-*d*₆): δ 169.2 (-COOH), 154.9 (-NHCO-), 154.5 (C_{4a}), 144.4 (C_{5a}), 132.7 (C_{1a}), 131.2 (C₇), 123.5 (C₈), 121.3 (C₉), 118.0 (C_{9a}), 111.6 (C₆), 42.5 (-CH₂-).

MS (ESI *m/z*): 242.9 (75 %) [M-H]⁻, 198.9 (100 %) [M-CO₂-H⁺]⁻ (negative mode).

Anal. calcd for C₁₁H₈N₄O₃ (244.21): C, 54.10; H, 3.30; N, 22.94; Found: C, 54.42; H, 3.61; N, 22.63.

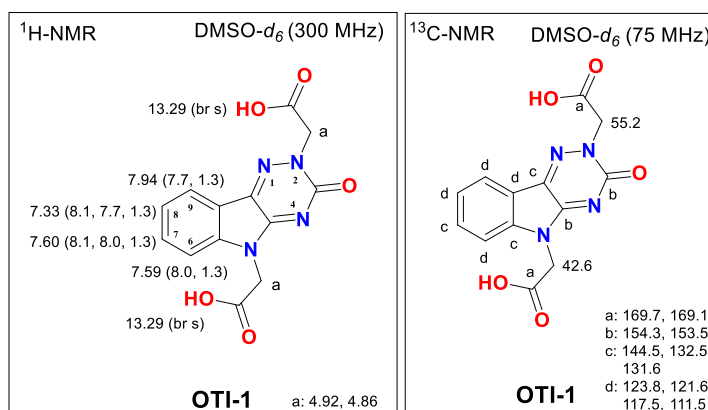
Synthesis of 2,2'-(3-oxo-2H-[1,2,4]triazino[5,6-b]indole-2,5(3H)-diyl)diacetic acid (OTI-1)



To a solution of 200 mg (0.56 mmol, 1.00 mol eq) diester **45** in 20 mL of MeOH, 78.0 mg (1.95 mmol, 3.50 mol eq) of NaOH in 5 mL water was added and the mixture refluxed for 1.5 h. After consumption of starting material **45** (confirmed by TLC analysis) the reaction was cooled down in an ice bath and acidified with 1 M aq HCl to pH = 4. After 10 min of stirring, formation of precipitate was observed and the mixture was stirred for another 20 min. Then the precipitate was filtered off and dried under reduce pressure to yield 106 mg (0.35 mmol, 63 %) of diacid **OTI-1** as a yellow solid product.

Novelty: 2,2'-(3-oxo-2H-[1,2,4]triazino[5,6-b]indole-2,5(3H)-diyl)diacetic acid (**OTI-1**) is not described in the literature.

M.p.: 296.0 - 299.0 °C [MeOH].



¹H-NMR (300 MHz, DMSO-*d*₆): δ 13.29 (2 x br s, 2 x 1H, 2x -COOH) 7.94 (dd, 1H, $J(8,9) = 7.7$ Hz, $J(7,9) = 1.3$ Hz, H-C(9)), 7.60 (ddd, 1H, $J(7,8) = 8.1$ Hz, $J(6,7) = 8.0$ Hz, $J(7,9) = 1.3$ Hz, H-C(7)), 7.33 (ddd, 1H, $J(7,8) = 8.1$ Hz, $J(8,9) = 7.7$ Hz, $J(6,8) = 1.3$ Hz, H-C(8)), 7.59 (dd, 1H, $J(6,7) = 8.0$ Hz, $J(6,8) = 1.3$ Hz, H-C(6)), 4.92 and 4.86 (2 x s, 2 x 2H, 2 x -CH₂COOH).

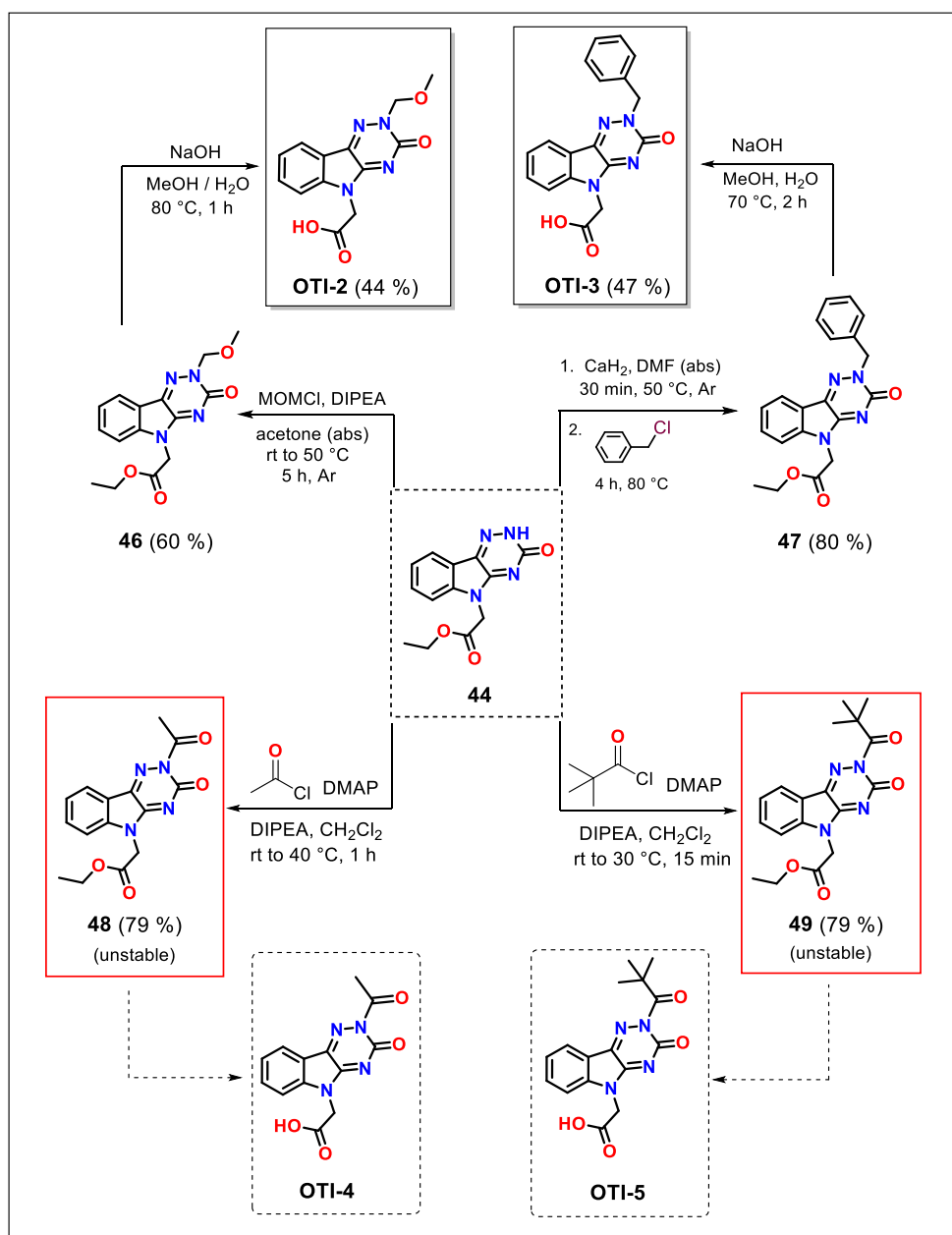
¹³C-NMR (75 MHz, DMSO-*d*₆): δ 169.7, 169.1, 154.3, 153.5, 144.5, 132.5, 131.6, 123.8, 121.6, 117.5, 111.5, 55.2 and 42.6 (2 x -CH₂COOH).

FT-IR (solid, cm⁻¹): 3010 (w), 2980 (w), 2606 (w), 2345 (w), 1733 (m), 1690 (m), 1602 (s), 1569 (s), 1503 (m), 1470 (m), 1400 (s), 1340 (m), 1275 (m), 1231 (s), 1142 (m), 1118 (m), 1069 (w), 1001 (m), 941 (m), 895 (m), 789 (m), 751 (s), 701 (m), 646 (m), 608 (m), 549 (m), 513 (m), 439 (s).

MS (ESI m/z): 323.0 (40 %) [M-2H+Na]⁻, 248.9 (100 %) [e.g. M-2CO₂+2H₂O+e]⁻ (negative mode).

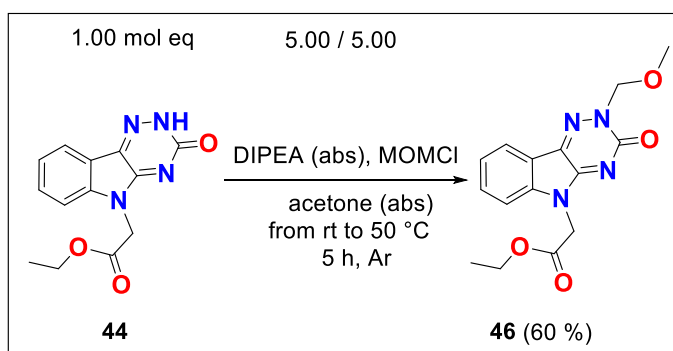
Anal. calcd for C₁₃H₁₀N₄O₅ (302.24): C, 51.66; H, 3.33; N, 18.54; Found: C, 51.85; H, 3.59; N, 18.90.

13.5.3. Synthesis of OTI derivatives OTI-(2-5)



Scheme 66. Synthesis of OTI derivatives OTI-(2-5).

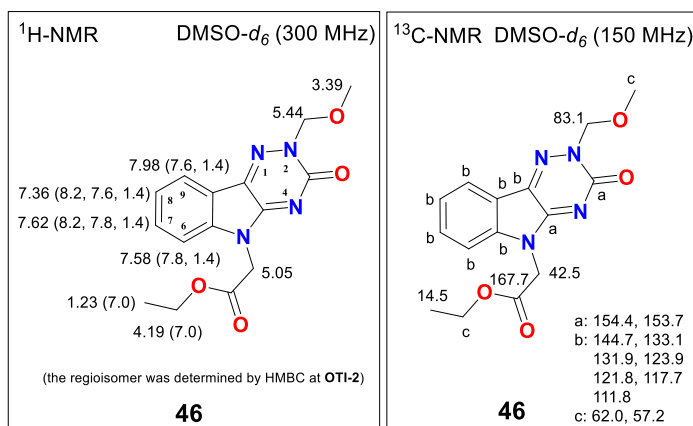
Synthesis of ethyl 2-(2-(methoxymethyl)-3-oxo-2H-[1,2,4]triazino[5,6-b]indol-5(3H)-yl)acetate (**46**)



To a solution of 100 mg (0.37 mmol, 1.00 mol eq) **44** in 20 mL of acetone (abs), 320 μ L (1.84 mmol, 5.00 mol eq) of DIPEA (abs) and 139 μ L (1.84 mmol, 5.00 mol eq) of MOMCl were added dropwise and while stirring at 50 °C under Ar. After 5 h TLC analysis confirmed presence of product **46**, traces of unknown side product and only small amount of starting material **44**. (after 16 h of heating almost no changes were seen by TLC analysis) Then, the reaction mixture was evaporated by RVE, dissolved in 20 mL of EA and extracted with water (3 x 15 mL). The isolated crude product was purified by crystallization in a mixture of hexane / ethyl acetate to afford 70.0 mg (0.22 mmol, 60 %) of ester **46** as a pale orange crystalline compound.

Novelty: ethyl 2-(2-(methoxymethyl)-3-oxo-2H-[1,2,4]triazino[5,6-b]indol-5(3H)-yl)acetate (**46**) is not described in the literature.

M.p.: 139.0 - 143.5 °C [EA].



¹H-NMR (300 MHz, DMSO-*d*₆): δ 7.98 (dd, 1H, $J(8,9) = 7.6$ Hz, $J(7,9) = 1.4$ Hz, H-C(9)), 7.62 (ddd, 1H, $J(7,8) = 8.2$ Hz, $J(6,7) = 7.8$ Hz, $J(7,9) = 1.4$ Hz, H-C(7)), 7.58 (dd, 1H, $J(6,7) = 7.8$ Hz, $J(6,8) = 1.4$ Hz, H-C(6)), 7.36 (ddd, 1H, $J(7,8) = 8.2$ Hz, $J(8,9) = 7.6$ Hz, $J(6,8) = 1.4$ Hz, H-C(8)), 5.44 (s, 2H, -CH₂OCH₃), 5.05 (s, 2H, -CH₂COOEt), 4.19 (q, 2H, $J(\text{CH}_2, \text{CH}_3) = 7.0$ Hz, -OCH₂CH₃), 3.39 (s, 3H, -CH₂OCH₃), 1.23 (t, 3H, $J(\text{CH}_2, \text{CH}_3) = 7.0$ Hz, -OCH₂CH₃).

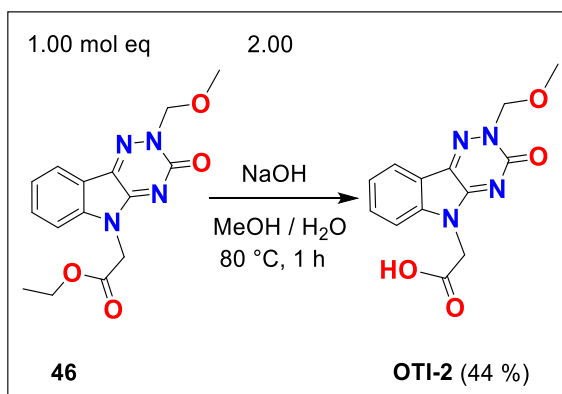
¹³C-NMR (150 MHz, DMSO-*d*₆): δ 167.7 (-C=O), 154.4, 153.7, 144.7, 133.1, 131.9, 123.9, 121.8, 117.7, 111.8, 83.1 (-CH₂OCH₃), 62.0, 57.2, 42.5 (-CH₂COOEt), 14.5 (-OCH₂CH₃).

FT-IR (solid, cm⁻¹): 3051 (w), 2987 (w), 2932 (w), 1750 (s), 1670 (s), 1631 (s), 1603 (s), 1570 (s), 1450 (m), 1456 (m), 1425 (m), 1406 (m), 1370 (m), 1329 (w), 1268 (w), 1215 (s), 1160 (s), 1092 (s), 1066 (s), 1003 (s), 975 (m), 915 (m), 909 (m), 788 (s), 607 (s).

MS (ESI *m/z*): 317.2 (75 %) [M+H]⁺, 339.2 (100 %) [M+Na]⁺ (positive mode).

Anal. calcd for C₁₅H₁₆N₄O₄ (316.32): C, 56.96; H, 5.10; N, 17.71; Found: C, 57.12; H, 5.22; N, 17.89.

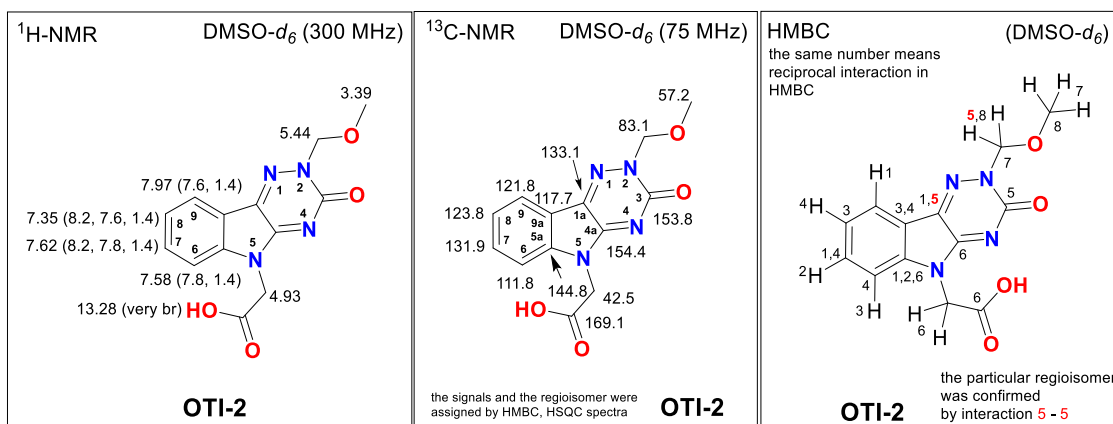
Synthesis of 2-(2-(methoxymethyl)-3-oxo-2*H*-[1,2,4]triazino[5,6-*b*]indol-5(3*H*)-yl)acetic acid (OTI-2)



To a solution of 70.0 mg (0.22 mmol, 1.00 mol eq) ester **46** in 15 mL of MeOH, 18.0 mg (0.45 mmol, 2.00 mol eq) of NaOH in 5 mL water was added and the mixture refluxed for 1 h. After consumption of starting material **46** (confirmed by TLC analysis) the reaction was cooled down in an ice bath and acidified with 1 M aq HCl to pH = 4. After 20 min of stirring, formation of precipitate was observed and the mixture was stirred for another 20 min. Then, the precipitate was filtered off, washed with ice water and dried under reduce pressure to yield 28.0 mg (0.10 mmol, 44 %) of **OTI-2** as a white solid product.

Novelty: 2-(2-(methoxymethyl)-3-oxo-2*H*-[1,2,4]triazino[5,6-*b*]indol-5(3*H*)-yl)acetic acid (**OTI-2**) was not yet described in the literature.

M.p.: 225 - 270 °C (dec) [MeOH].



¹H-NMR (300 MHz, DMSO-*d*₆): δ 13.28 (very br s, 1H, -COOH), 7.97 (dd, 1H, $J(8,9) = 7.6$ Hz, $J(7,9) = 1.4$ Hz, H-C(9)), 7.62 (ddd, 1H, $J(7,8) = 8.2$ Hz, $J(6,7) = 7.8$ Hz, $J(7,9) = 1.4$ Hz, H-C(7)), 7.35 (ddd, 1H, $J(7,8) = 8.2$ Hz, $J(8,9) = 7.6$ Hz, $J(6,8) = 1.4$ Hz, H-C(8)), 7.58 (dd, 1H, $J(6,7) = 7.8$ Hz, $J(6,8) = 1.4$ Hz, H-C(6)), 5.44 (s, 2H, -CH₂OCH₃), 4.93 (s, 2H, -CH₂COOEt), 3.39 (s, 3H, -CH₂OCH₃).

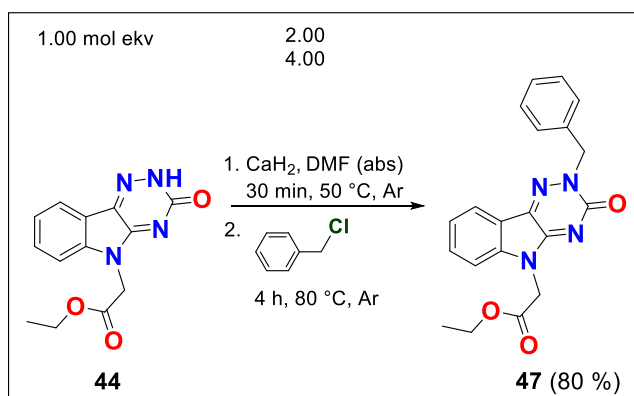
¹³C-NMR (75 MHz, DMSO-*d*₆): δ 169.1 (-COOH), 154.4 (C_{4a}), 153.8 (C₃), 144.8 (C_{5a}), 133.1 (C_{1a}), 131.9 (C₇), 123.8 (C₈), 121.8 (C₉), 117.7 (C_{9a}), 111.8 (C₆), 83.1 (-CH₂OCH₃), 57.2 (-CH₂OCH₃), 42.5 (-CH₂-).

FT-IR (solid, cm⁻¹): 3245 (m), 2919 (w), 2080 (w), 1741 (m), 1607 (s), 1576 (s), 1501 (m), 1465 (m), 1411 (m), 1369 (w), 1267 (w), 1217 (s), 1166 (s), 1088 (s), 1006 (m), 915 (m), 892 (w), 788 (m), 748 (s), 671 (m).

MS (ESI m/z): 287.2 (80 %) [M-H]⁻, 249.0 [e.g. M-CO₂-OMe+H₂O+e]⁻ (100 %), 243.1 (55 %) [e.g. M-(CH₂OCH₃)+e]⁻ (negative mode).

Anal. calcd for C₁₃H₁₂N₄O₄ (288.26): C, 54.17; H, 4.20; N, 19.44; Found: C, 54.35; H, 4.59; N, 19.84.

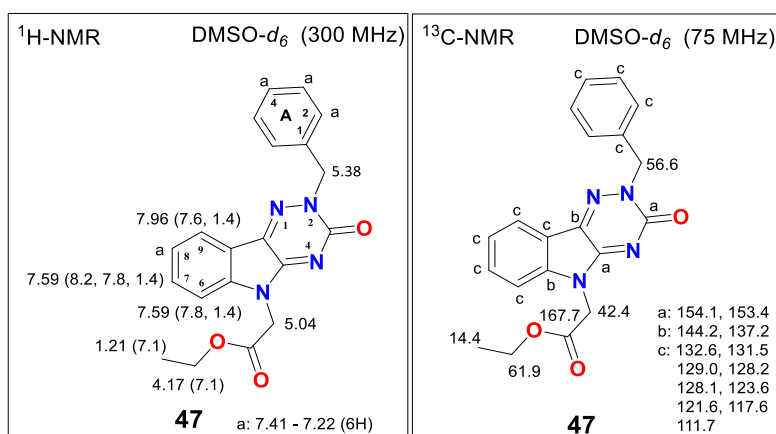
Synthesis of ethyl 2-(2-benzyl-3-oxo-2*H*-[1,2,4]triazino[5,6-*b*]indol-5(3*H*)-yl)acetate (47)



To a solution of 60.0 mg (0.22 mmol, 1.00 mol eq) ester **44** in 5 mL of DMF (abs), 19.0 mg (0.44 mmol, 2.00 mol eq) of CaH₂ was added and the reaction was stirred at 50 °C under Ar for 30 min. Then, the mixture was cooled to rt, 102 µl (0.88 mmol, 4.00 mol eq) of benzyl chloride was added dropwise. The resulted solution was stirred at 80 °C within 4 h under Ar. After consumption of ester **44** (confirmed by TLC analysis) the reaction was cooled down, 10 mL of water added and stirred for 20 min in an ice bath which led to formation of a precipitate. Obtained solid material was filtered off, washed with water and dried under reduced pressure to yield 20.0 mg (0.06 mmol) of product **47**. The filtrate was extracted with EA (3 x 10 mL). A combined organic layer was washed with brine and water, dried by Na₂SO₄, filtered off and concentrated under reduced pressure to yield another 44.0 mg (0.12 mmol) of product **47**. Overall yield of ester **47** was 64.0 mg, (0.18 mmol, 80 %).

Novelty: ethyl 2-(2-benzyl-3-oxo-2*H*-[1,2,4]triazino[5,6-*b*]indol-5(3*H*)-yl)acetate (**47**) is not described in the literature.

M.p.: 170.0 - 172.4 °C [DMF / H₂O].



¹H-NMR (300 MHz, DMSO-*d*₆): δ 7.96 (dd, 1H, *J*(8,9) = 7.6 Hz, *J*(7,9) = 1.4 Hz, H-C(9)), 7.59 (ddd, 1H, *J*(7,8) = 8.2 Hz, *J*(6,7) = 7.8 Hz, *J*(7,9) = 1.4 Hz, H-C(7)), 7.59 (dd, 1H, *J*(6,7) = 7.8 Hz, *J*(6,8) = 1.4 Hz, H-C(6)), 7.41 - 7.22 (m, 6H, H-C(8) and 5 x H_{Ar} from Bn), 5.38 (s, 2H, -CH₂Ph), 5.04 (s, 2H, -CH₂COOEt), 4.17 (q, 2H, *J*(CH₂,CH₃) = 7.1 Hz, -OCH₂CH₃), 1.21 (t, 3H, *J*(CH₂,CH₃) = 7.1 Hz, -OCH₂CH₃).

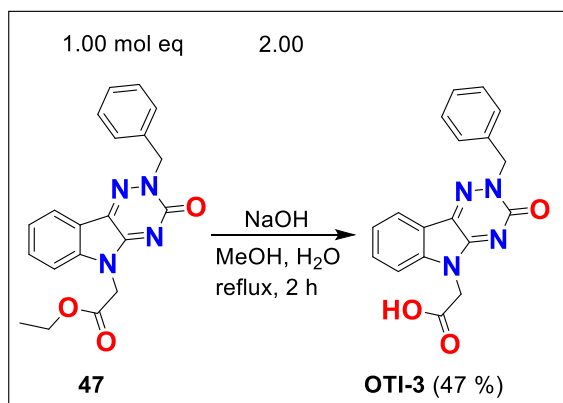
¹³C-NMR (75 MHz, DMSO-*d*₆): δ 167.7 (-COOEt), 154.1, 153.4, 144.2, 137.2, 132.6, 131.5, 129.0, 128.2, 128.1, 123.6, 121.6, 117.6, 111.7, 61.9 (-OCH₂CH₃), 56.6 (-CH₂Ph), 42.6 (NCH₂COOEt), 14.4 (-OCH₂CH₃).

FT-IR (solid, cm⁻¹): 3010 (w), 2337 (w), 2116 (w), 1735 (s), 1670 (s), 1635 (s), 1602 (s), 1570 (m), 1498 (m), 1466 (m), 1406 (m), 1373 (m), 1209 (s), 1094 (m), 1041 (m), 1016 (m), 785 (m), 748 (s), 705 (s), 493 (m).

MS (ESI *m/z*): 363.1 (100 %) [M+H]⁺, 385.1 (50 %) [M+Na]⁺ (positive mode).

Anal. calcd for C₂₀H₁₈N₄O₃ (362.38): C, 66.29; H, 5.01; N, 15.46; **Found:** C, 66.39; H, 5.10; N, 15.64.

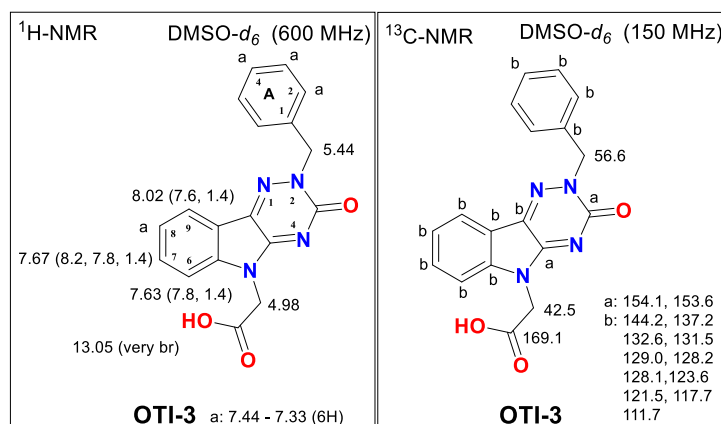
Synthesis of 2-(2-benzyl-3-oxo-2H-[1,2,4]triazino[5,6-b]indol-5(3H)-yl)acetic acid (OTI-3)



To a solution of 64.0 mg (0.18 mmol, 1.00 mol eq) **47** in 15 mL of MeOH, 14.0 mg (0.35 mmol, 2.00 mol eq) of NaOH in 5 mL of water was added and the mixture refluxed for 2 h. After consumption of **47** (confirmed by TLC analysis) the reaction mixture was cooled down in an ice bath and acidified with 1 M aq HCl to pH = 4. After 10 min formation of precipitate was observed and the mixture was stirred for 20 min. Then, the precipitate was filtered off, washed with ice water and dried under reduce pressure to yield 25.0 mg (82.8 μ mol, 47 %) of acid **OTI-3** as an orange solid product.

Novelty: 2-(2-benzyl-3-oxo-2H-[1,2,4]triazino[5,6-b]indol-5(3H)-yl)acetic acid (**OTI-3**) is described in the literature.

M.p.: 269.1 - 274.5 °C [MeOH].



¹H-NMR (600 MHz, DMSO-*d*₆): δ 13.05 (very br s, 1H, -COOH), 8.02 (dd, 1H, *J*(8,9) = 7.6 Hz, *J*(7,9) = 1.4 Hz, H-C(9)), 7.67 (ddd, 1H, *J*(7,8) = 8.2 Hz, *J*(6,7) = 7.8 Hz, *J*(7,9) = 1.4 Hz, H-C(7)), 7.63 (dd, 1H, *J*(6,7) = 7.8 Hz, *J*(6,8) = 1.4 Hz, H-C(6)), 7.44 - 7.33 (m, 6H, H-C(8) and 5 x H_{Ar} from Bn), 5.44 (s, 2H, -CH₂Ph), 4.98 (s, 2H, -CH₂COOH).

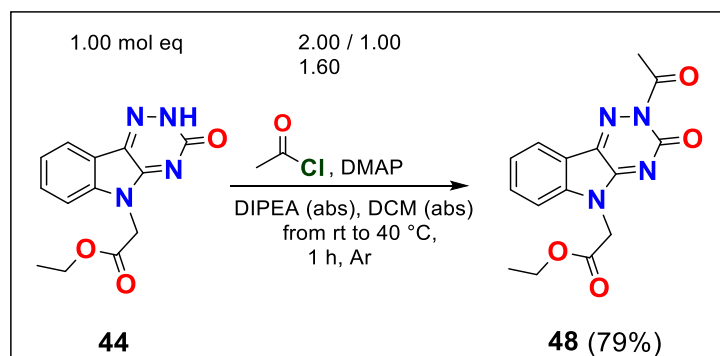
¹³C-NMR (150 MHz, DMSO-*d*₆): δ 169.1 (-COOH), 154.1, 153.6, 144.2, 137.2, 132.6, 131.5, 129.0, 128.2, 128.1, 123.6, 121.5, 117.7, 111.7, 56.6 (-CH₂Ph), 42.5 (NCH₂COOEt).

FT-IR (solid, cm⁻¹) 3651 (w), 2961 (w), 2100 (w), 1890 (w), 1726 (m), 1626 (m), 1601 (s), 1571 (s), 1500 (m), 1469 (m), 1408 (s), 1370 (m), 1245 (s), 1225 (s), 1097 (s), 1050 (s), 1014 (s), 926 (w), 796 (s), 749 (s), 696 (m), 665 (m), 609 (m).

MS (ESI *m/z*): 333.2 (40 %) [M-H]⁻, 289.1 (25 %) [M-CO₂-H]⁻, 249.1 (100 %) [e.g. M-Ph-CO₂+2H₂O+e]⁻ (negative mode).

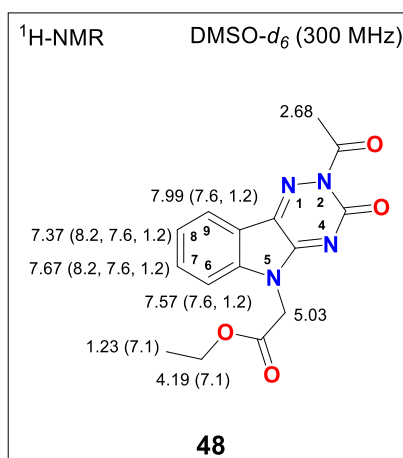
Anal. calcd for C₁₈H₁₄N₄O₃ (334.33): C, 64.66; H, 4.22; N, 16.76; Found: C, 64.50; H, 4.04; N, 16.54.

Synthesis of ethyl 2-(2-acetyl-3-oxo-2,3-dihydro-5H-[1,2,4]triazino[5,6-b]indol-5-yl)acetate (**48**)



To a suspension of 25.0 mg (0.90 mmol, 1.00 mol eq) ester **44** in 5 mL of DCM (abs), 24 μ l (0.14 mmol, 1.60 mol eq) of DIPEA (abs), 13 μ l (0.18 mmol, 2.00 mol eq) of acetyl chloride and 11.0 mg (0.09 mmol, 1.00 mol eq) of DMAP were added stepwise and resulting mixture stirred at 40 °C under Ar. After 1 h of stirring TLC analysis confirmed presence of product **48** without any side products. Then, the reaction mixture was extracted with water (3 x 10 mL), combined organic layer dried over Na₂SO₄, filtered and concentrated under reduced pressure to yield 26.0 mg (0.80 mmol, 79 %) of the crude product **48** as an orange solid compound.

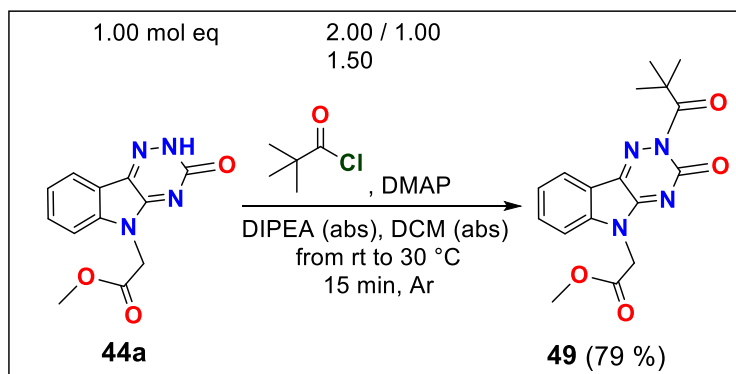
Novelty: ethyl 2-(2-acetyl-3-oxo-2,3-dihydro-5H-[1,2,4]triazino[5,6-b]indol-5-yl)acetate (**48**) is not described in the literature.



¹H-NMR (300 MHz, DMSO-*d*₆): δ 7.99 (dd, 1H, $J(8,9) = 7.6$ Hz, $J(7,9) = 1.2$ Hz, H-C(9)), 7.67 (ddd, 1H, $J(7,8) = 8.2$ Hz, $J(6,7) = 7.6$ Hz, $J(7,9) = 1.2$ Hz, H-C(7)), 7.57 (dd, 1H, $J(6,7) = 7.6$ Hz, $J(6,8) = 1.2$ Hz, H-C(6)), 7.37 (ddd, 1H, $J(7,8) = 8.2$ Hz, $J(8,9) = 7.6$ Hz, $J(6,8) = 1.2$ Hz, H-C(8)), 5.03 (s, 2H, -CH₂COOEt), 4.19 (q, 2H, $J(\text{CH}_2, \text{CH}_3) = 7.1$ Hz, -OCH₂CH₃), 2.68 (s, 3H, -COCH₃), 1.23 (t, 3H, $J(\text{CH}_2, \text{CH}_3) = 7.1$ Hz, -OCH₂CH₃).

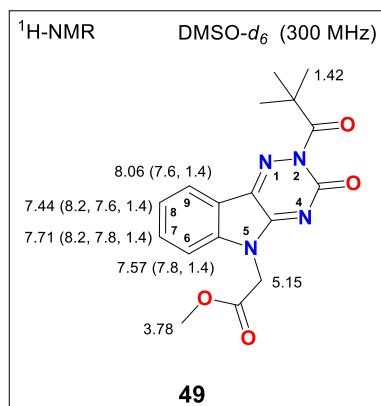
Due to instability of the compound **48** its M.p., ¹³C-NMR, IR, MS and el. anal. were not determined.

Synthesis of methyl 2-(3-oxo-2-pivaloyl-2,3-dihydro-5H-[1,2,4]triazino[5,6-*b*]indol-5-yl)acetate (**49**)



To a suspension of 25.0 mg (0.10 mmol, 1.00 mol eq) ester **44a** (prepared by reaction of **OTI** and CH₂N₂, not shown) in 5 mL of DCM (abs), 25 μ l (0.15 mmol, 1.50 mol eq) of DIPEA (abs), 24 μ l (0.20 mmol, 2.00 mol eq) of pivaloyl chloride and 12.0 mg (0.10 mmol, 1.00 mol eq) of DMAP were added stepwise and resulting mixture was stirred at 30 °C under Ar. After 15 min of stirring TLC analysis confirmed presence of product **49** without any side products. Then, the reaction mixture was extracted with water (3 x 10 mL), combined organic layer dried by Na₂SO₄, filtered and concentrated under reduced pressure to yield 26.0 mg (0.80 mmol, 79 %) of crude product **49** as an orange solid compound.

Novelty: methyl 2-(3-oxo-2-pivaloyl-2,3-dihydro-5H-[1,2,4]triazino[5,6-*b*]indol-5-yl)acetate (**49**) is not described in the literature.



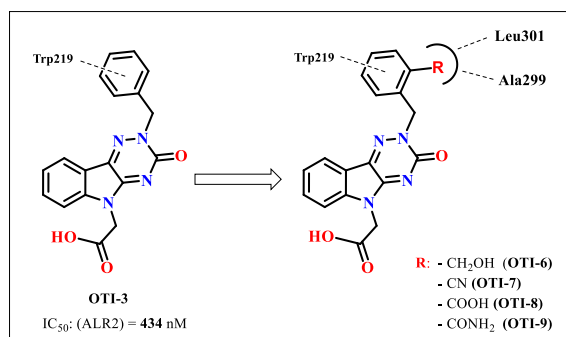
¹H-NMR (300 MHz, DMSO-*d*₆): δ 8.06 (dd, 1H, $J(8,9) = 7.6$ Hz, $J(7,9) = 1.4$ Hz, H-C(9)), 7.71 (ddd, 1H, $J(7,8) = 8.2$ Hz, $J(6,7) = 7.8$ Hz, $J(7,9) = 1.4$ Hz, H-C(7)), 7.57 (dd, 1H, $J(6,7) = 7.8$ Hz, $J(6,8) = 1.4$ Hz, H-C(6)), 7.44 (ddd, 1H, $J(7,8) = 8.2$ Hz, $J(8,9) = 7.6$ Hz, $J(6,8) = 1.4$ Hz, H-C(8)), 5.15 (s, 2H, -CH₂COOEt), 3.78 (s, 3H, -CH₂COOCH₃), 1.42 (s, 9H, -COC(CH₃)₃).

Due to a chemical instability of the compound **49** its M.p., IR and ¹³C-NMR were not determined.

Chapter 11. Project 4 - Synthesis and SAR study of novel OTI derivatives OTI-(6-9)

14. Project 4 - Synthesis and SAR study of novel OTI derivatives OTI-(6-9)

The last project was dedicated to a development of ALR2 inhibitors with inhibitory activity than leading inhibitor **OTI-3**, developed in the previous project.¹³¹ According to intermolecular interaction analysis we discovered an unoccupied pocket located in a close proximity to *N*(2) benzyl moiety of **OTI-3** consisting of Ala299, Leu301 and Trp219. In order to utilize these residues for additional interactions, we proposed novel *N*-benzyloxotriazinoindole derivatives **OTI-(6-9)**. (Scheme 67 and Figure 69)



Scheme 67. The structures of proposed *N*-benzyl(oxotriazinoindole) derivatives **OTI-(6-9)**.

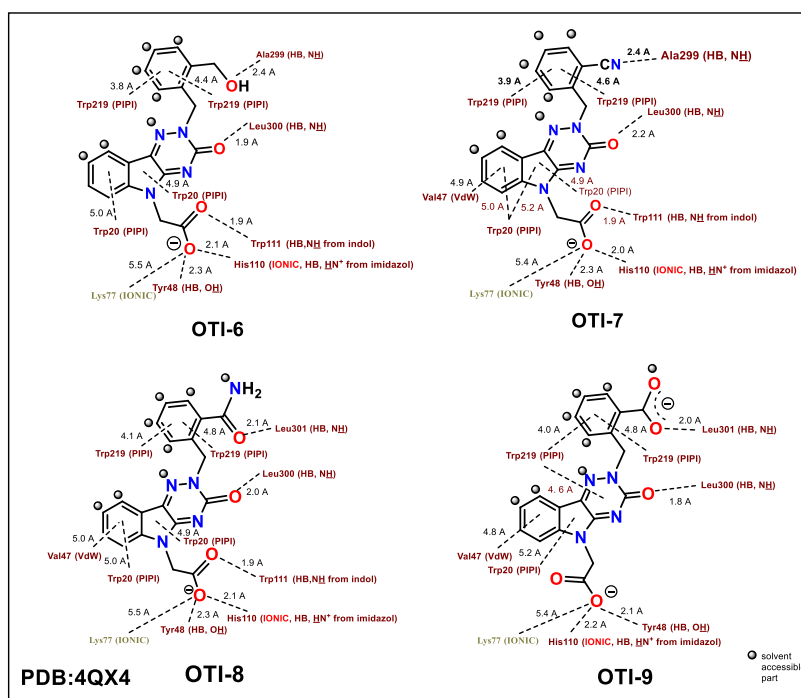
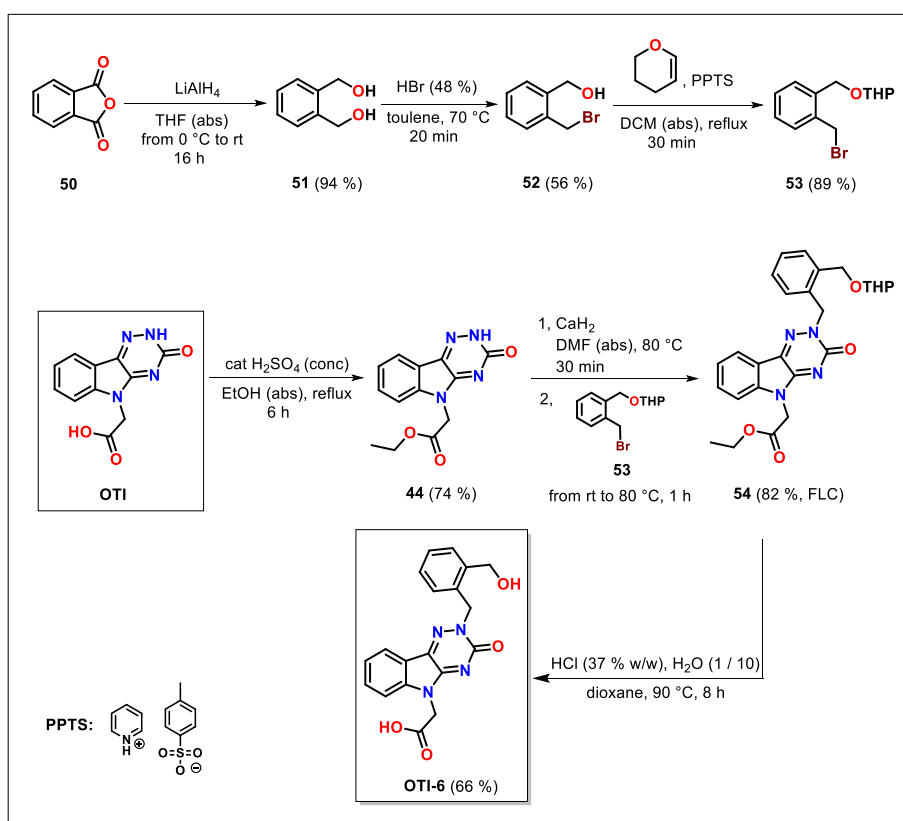


Figure 69. Interaction diagrams of proposed *N*-benzyl(oxotriazinoindole) derivatives **OTI-(6-9)**.

14.1. Synthesis of OTI-6

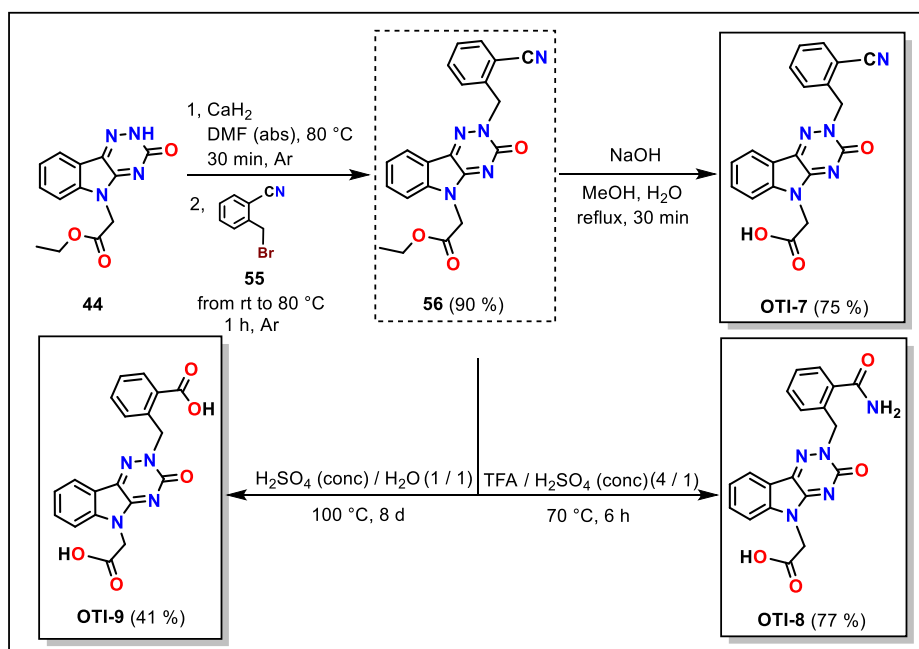
Synthesis of hydroxymethyl derivative **OTI-6** started from **OTI** and protected benzyl alcohol **53**, prepared in tree steps. (Scheme 68) Synthesis was initiated by reduction of phtalanhydride **50** with LiAlH_4 in THF (abs) at $0\text{ }^\circ\text{C}$ to give diol **51** in 94 % yield. Afterwards, a reaction of **51** with HBr (48 %) in toluene at $70\text{ }^\circ\text{C}$ provided required mono- **52** and small amount of bis brominated products. After FLC separation, desired intermediate **52** was obtained in 56 % yield. Finally, *O*-protected compound **53** was obtained by reaction of 3,4-dihydropyran (**DHP**) in a presence of cat amount of PPTS in refluxing DCM. Then, ester **44** was prepared in 74 % yield by acidic catalyzed esterification of **OTI** with EtOH (abs) Afterwards, alkylation of ester **44** with **53** by CaH_2 in DMF at $80\text{ }^\circ\text{C}$ performed an intermediate **54** in 82 % yield. Compound **54** was subsequently hydrolysed to required benzyl alcohol derivative **OTI-6** by aq HCl in dioxane at $90\text{ }^\circ\text{C}$ in 66 % yield. (Scheme 68)



Scheme 68. Synthesis of **OTI-6**.

14.2. Synthesis of OTI-(7-9)

Synthesis of proposed ALR2 inhibitors **OTI-(7-9)** was initiated by reaction of ester **44**, which was alkylated to **56** by 2-(bromomethyl)benzonitrile **55**. Obtained benzonitrile derivative **56** was used as a joint intermediate for a synthesis of the proposed compounds **OTI-(7-9)**. Hydrolysis of an ester group of **56** by aq solution of NaOH in MeOH / H₂O at reflux provided the benzonitrile compound **OTI-7**. Partial carbonitrile hydrolysis of **56** with TFA / H₂SO₄ (conc) (4 / 1) within 6 h provided benzamide derivative **OTI-8**. Benzoic acid derivative **OTI-9** was prepared by stronger hydrolysis of **56** with a mixture of H₂SO₄ (conc) / H₂O (1 / 1) at 100 °C within 8 days. (Scheme 69)

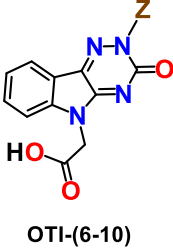
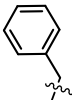
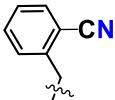
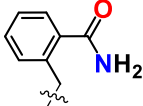
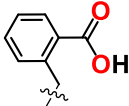
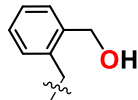


Scheme 69. Synthetic pathway to OTI-(7-9).

14.3. Evaluation of OTI-(6-9) ALR2 inhibitory activity

Inhibitors **OTI-(7-10)** were tested for their ability to inhibit the reduction of *D,L*-glyceraldehyde using ALR2 isolated from the rat eye lenses. Unsubstituted benzyl analogue **OTI-6** was used as a reference inhibitor. To assess selectivity we used a structurally related detoxification enzyme (an antitarget), aldehyde reductase (ALR1) isolated from the rat kidneys. (Table 1)

Table 1. Determined inhibitory activity and selectivity of substituted *N*-benzyl(oxotriazinoindole) inhibitors **OTI-(6-9)** in comparison to unsubstituted reference analogue **OTI-3**.

 OTI-(6-10)	Z:					
	compound	OTI-6	OTI-7 (5)	OTI-8 (6)	OTI-9 (7)	OTI-10 (13)
ALR2 IC ₅₀ [nM]		434 ± 14	76 ± 6	236 ± 5	139 ± 5	244 ± 3
ALR1 I (% , 100 μM)		38 ± 5	51 ± 1	50 ± 2	62 ± 1	33 ± 5
ALR1 IC ₅₀ [μM]		> 100	> 100	> 100	59 ± 6	> 100
S _F (selectivity factor)		> 230	> 1 333	> 424	424	> 410

Results are means ± SD from minimum of three independent repetitions. *I* is the % of enzyme inhibition observed at 100 μM inhibitor concentration. Selectivity factor: $S_F = IC_{50}(\text{ALR1}) / IC_{50}(\text{ALR2})$.

Obtained results confirmed proposed additional interactions of inhibitors **OTI-(6-9)** in the unoccupied interactive pocket of ALR2. The best ALR2 inhibition ($IC_{50} = 76$ nM) and selectivity relative to ALR1 ($SF > 1333$) was obtained for **OTI-7** derivative containing a *N*-(2-cyanobenzyl) group. (Table 1) According to predicted binding position of **OTI-7** in an active site of ALR2 (PDB: 4QX4) a present cyano group formed an additional H-bond with Ala299 (2.4 Å) and a benzyl moiety showed two good π - π stacking interactions with Trp219 (3.9 and 4.6 Å) from an investigated interactive pocket of ALR2. (Figure 70)

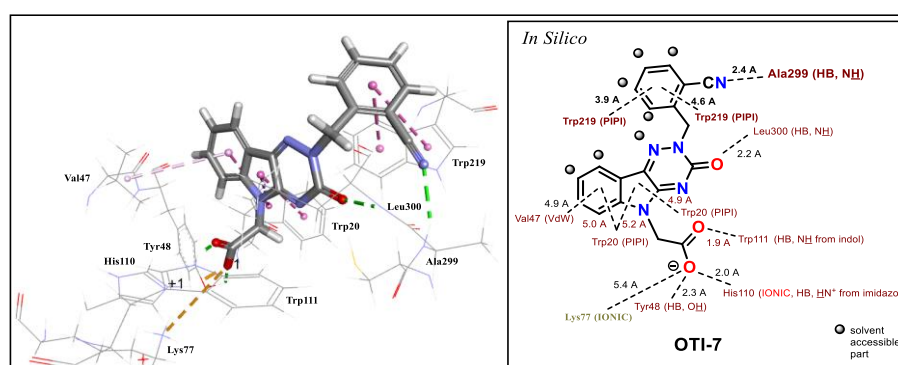


Figure 70. A predicted pose of the inhibitor **OTI-7** in the active site of ALR2 (PDB: 4QX4) and a diagram of its intermolecular interactions.

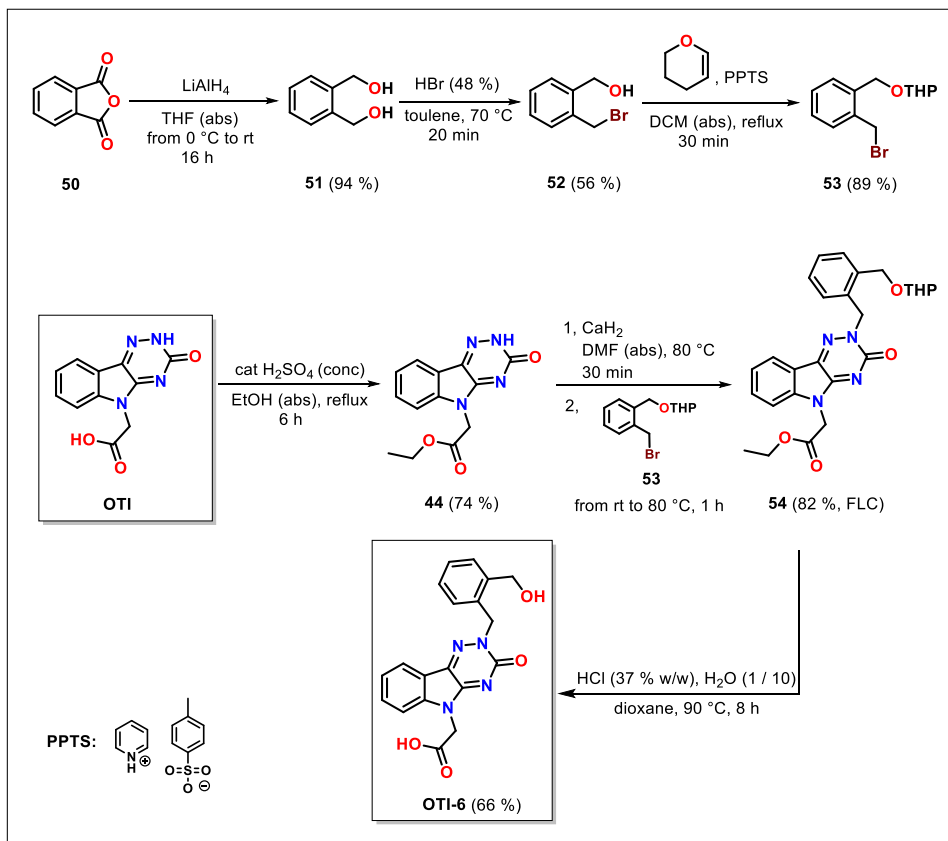
Hydroxymethyl derivative **OTI-6** exhibited the lowest inhibitory activity ($IC_{50} = 241$ nM, ALR2). Similar results were observed in the other derivatives **OTI-(8,9)** ($IC_{50} = 234$ and 139 nM, resp). (Table 1) The reason of lower activity of **OTI-(6,8,9)** could be assigned to a

desolvation and / or rotation penalty caused by a present polar functional group (-CH₂OH, -CONH₂ or -COOH) compare to a planar and less solvated carbonitrile moiety in **OTI-7**. Biscarboxylic acid **OTI-9** exhibits higher activity than hydroxymethyl and amide analogues **OTI-(6,8)**.

To sum up, we have developed four novel *N*-benzyl(oxotriazinoindole) inhibitors **OTI-(7-10)**, possessing polar functional groups (-CN, -CONH₂, -COOH, -CH₂OH, resp.) in *ortho* position on a benzyl group. They exhibited 2 to 6-fold better inhibitory activity than their *N*-(benzyl) lead compound **OTI-6**. Our findings confirmed expected additional interactions of novel **OTI** derivatives in a studied binding pocket of ALR2. Moreover, the novel derivatives also exhibited ALR1 inhibitory activity in high micromolar concentrations, which resulted in good to excellent ALR1 / ALR2 selectivity for developed compounds **OTI-(7-10)**. The most efficient ALR2 inhibitor **OTI-7** (IC₅₀ = 76 nM) contains a planar and less solvated -CN functional group on a benzyl ring. Other derivatives **OTI-(8-10)** (-CONH₂, -COOH and -CH₂OH, resp.) revealed 2 to 3-fold lower ALR2 inhibitory activity than **OTI-7**. The reason of lower activity of derivatives **OTI-(8-10)** was assigned to a desolvation and possibly also to a conformational penalty.

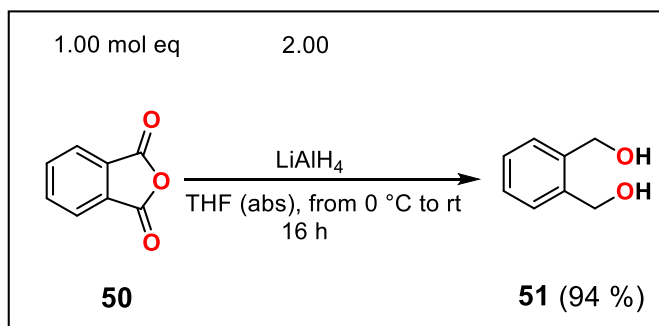
14.4. Experimental part

14.4.1. Synthesis of benzyl derivative (OTI-6)



Scheme 70. Synthesis of a benzyl analogue OTI-6.

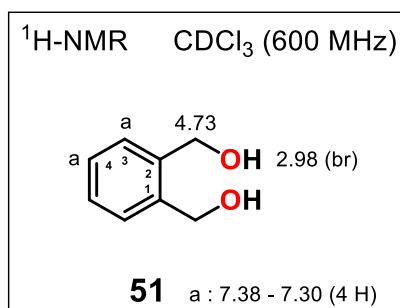
Synthesis of 1,2-phenylenedimethanol (51)



A solution of phthalic anhydride **50** (440 mg, 2.97 mmol, 1.00 mol eq) in 15 mL of THF (abs) was added dropwise at 0 °C to the stirred suspension of LiAlH₄ (226 mg, 5.96 mmol, 2.00 mol eq) in 20 mL of THF (abs) within 30 min. Then, the mixture was stirred overnight at room temperature. Afterwards, the reaction was cooled to 0 °C and 10 mL of isopropanol added slowly, followed by methanol (10 mL) and water (10 mL). Obtained wax-like precipitate was filtered through Celite and obtained filtrate washed with EA and DCM. Organic solution was evaporated and aqueous mixture extracted with EA (3x 20 mL) and DCM (3x 10 mL). Combined organic layer was dried over Na₂SO₄, filtered and concentrated over reduced pressure totally yielding 385 mg (2.79 mmol, 94 %) of diol **51** as a colourless oil, which solidified by storing in a refrigerator.

Novelty: 1,2-phenylenedimethanol (**51**) is described in the literature by its M.P., ¹H-NMR, ¹³C-NMR, IR and HRMS.¹³⁸

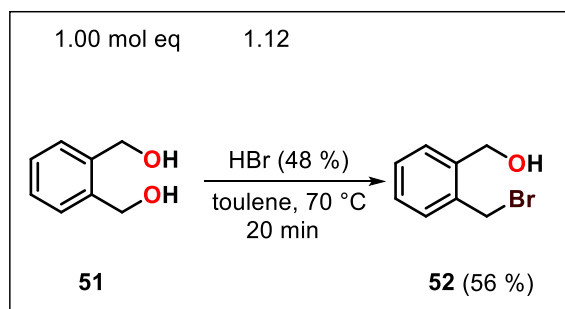
M.p.: 52.0 - 57.7 °C [EA / DCM], lit: 61 - 63 °C [EA].¹³⁸



¹H-NMR (600 MHz, CDCl₃): δ 7.38 - 7.30 (m, 4H, 2 x H-C(3 and 4)), 4.73 (s, 4H, 2 x -CH₂OH), 2.98 (br s, 2H, -CH₂OH).

¹³⁸ Dow, M.; Marchetti, F.; Abrahams, K.A.; Vaz, L.; Besra, G.S.; Warriner, S.; Nelson, A. *Chem.: Eur. J.*, **2017**, *23*, 7207 - 7211.

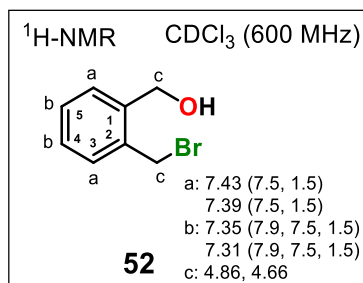
Synthesis of 2-(bromomethyl)phenyl]methanol (**52**)



A solution of 105 mg (0.76 mmol, 1.00 mol eq) 1,2-phenylenedimethanol (**51**) in 20 mL of toluene was heated to 70 °C. At this temperature, 80 μ L (0.85 mmol, 1.12 mol eq) of 48 % solution of HBr was added dropwise. After 20 min, TLC analysis confirmed a presence of product **52** and a small amount of probably bis brominated side product. Reaction mixture was cooled down, neutralized with saturated aq solution of Na₂CO₃ and extracted with diethyl ether (3 x 15 mL). Combined organic layer was evaporated and resulted mixture purified by FLC (Hex / EA = 5 / 1) to afford 80.0 mg (0.40 mmol, 56 %) of desired product **52** as a white solid compound.

Novelty: 2-(bromomethyl)phenyl]methanol (**52**) is described in the literature by its M.P., ¹H-NMR, IR¹³⁹ and MS spectra.¹⁴⁰

M.p.: 61.0 - 63.8 °C [Et₂O], lit: 55 °C [hexane].¹³⁹

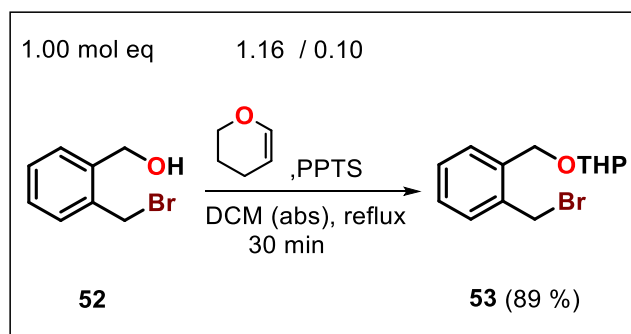


¹³⁹ Cowell, A.; Stille, J.K. *J. Am. Chem. Soc.*, **1980**, *102*, 4193 - 4198.

¹⁴⁰ Doyle, M.P.; Chapman, B.J.; Hu, W.; Peterson, C.S. *Org. Lett.*, **1999**, *1*, 1327 - 1329.

¹H-NMR (600 MHz, CDCl₃): δ 7.43 and 7.39 (2 x dd, 2 x 1H, $J(3,4$ or $5,6) = 7.5$ Hz, $J(3,5$ or $4,6) = 1.5$ Hz, H-C(3 and 6)), 7.35 and 7.31 (2 x ddd, 2 x 1H, $J(4,5) = 7.9$ Hz, $J(3,4$ or $5,6) = 7.5$ Hz, $J(3,5$ or $4,6) = 1.5$ Hz, H-C(4 and 5)), 4.86 and 4.66 (2 x s, 2 x 2H, -CH₂OH and CH₂Br).

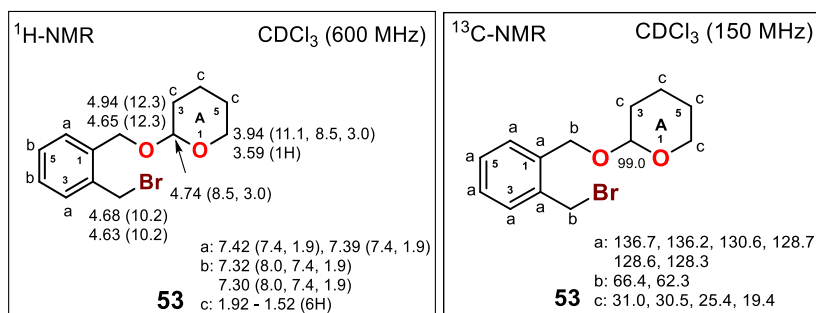
Synthesis of 2-([2-(bromomethyl)benzyl]oxy)tetrahydro-2H-pyran (**53**)



A solution of 245 mg (1.22 mmol, 1.00 mol eq) of arylmethanol **52** in 20 mL of DCM (abs), 130 μ L (1.42 mmol, 1.16 mol eq) of 3,4-dihydro-2H-pyran (DHP) and 30.6 mg (0.12 mmol, 0.10 mol eq) of PPTS (pyridinium *p*-toulenesulfonate), was stirred under Ar for 30 min at reflux. Subsequent TLC analysis confirmed presence of a new product and traces of two side products. Then, 20 mL of NaHCO₃ (sat aq sol.) was added and resulting mixture extracted with DCM (3 x 15 mL). Combined organic layer was dried over Na₂SO₄, filtered and concentrated under reduced pressure yielding 310 mg (1.09 mmol, 89 %) of tetrahydropyran **53** as a colourless oily product.

Novelty: 2-([2-(bromomethyl)benzyl]oxy)tetrahydro-2H-pyran (**53**) is described in the literature by its ¹H-NMR and crystal property description.¹⁴¹

¹⁴¹ Novartis AG; Novartis Pharma GMBH; Masuya, Keiichi - WO2006/74924, 2006, A1.



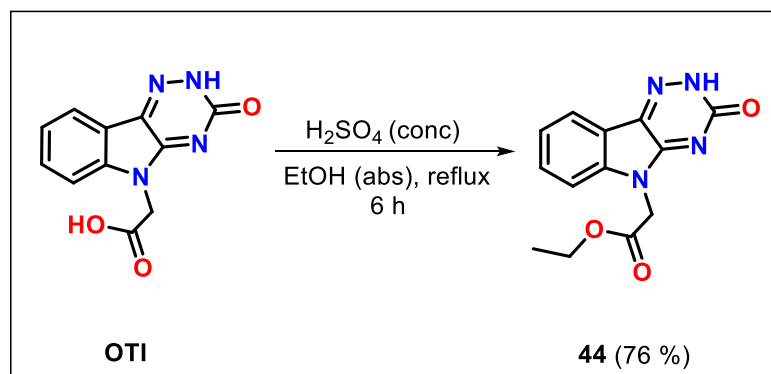
¹H-NMR (600 MHz, CDCl₃): δ 7.42 and 7.39 (2 x dd, 2 x 1H, $J(3,4$ or $5,6) = 7.4$ Hz, $J(3,5$ or $4,6) = 1.9$ Hz, H-C(3 and 6)), 7.32 and 7.30 (2 x ddd, 2 x 1H, $J(4,5) = 8.0$ Hz, $J(3,4$ or $5,6) = 7.4$ Hz, $J(3,5$ or $4,6) = 1.9$ Hz, H-C(4 and 5)), 4.94 (d, 1H, $J_{\text{gem}} = 12.3$ Hz, $-\text{CH}_2\text{OTHP}$), 4.74 (dd, 1H, $J(A_2, A_3) = 8.5$ Hz, $J(A_2, A_3) = 3.0$ Hz, H-C_A(2)), 4.68 (d, 1H, $J_{\text{gem}} = 10.2$ Hz, $-\text{CH}_2\text{Br}$), 4.65 (d, 1H, $J_{\text{gem}} = 12.3$ Hz, $-\text{CH}_2\text{OTHP}$), 4.63 (d, 1H, $J_{\text{gem}} = 10.2$ Hz, $-\text{CH}_2\text{Br}$), 3.94 (ddd, 1H, $J_{\text{gem}} = 11.1$ Hz, $J(A_5, A_6) = 8.5$ Hz, $J(A_5, A_6) = 3.0$ Hz, H-C_A(6)), 3.59 (m, 1H, H-C_A(6)), 1.92 - 1.52 (m, 6H, H-C_A(3-5)).

¹³C-NMR (150 MHz, CDCl₃): 136.7, 136.2, 130.6, 128.7, 128.6, 128.3, 99.0 (-OCHO-), 66.4, 62.3, 31.0, 30.5, 25.4, 19.4.

FT-IR (solid, cm⁻¹): 2939 (m), 2867 (w), 1723 (w), 1454 (m), 1385 (m), 1260 (w), 1200 (m), 1118 (s), 1076 (m), 1022 (s), 971 (m), 904 (m), 869 (m), 814 (w), 760 (m), 606 (m), 533 (w)

Due to moisture sensitivity of the product **53**, MS spectrum and elemental analysis were not measured.

Synthesis of ethyl 2-(3-oxo-2,3-dihydro-5H-[1,2,4]triazino[5,6-b]indol-5-yl)acetate (44)



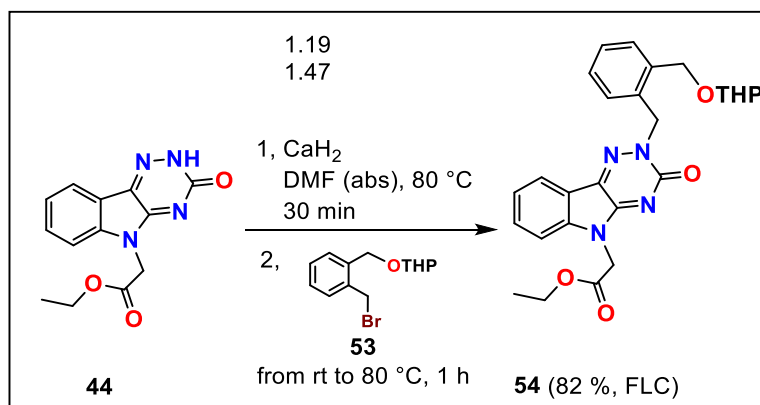
To a solution of 100 mg (0.41 mmol, 1.00 mol eq) of **OTI** dissolved in 30 mL of EtOH (abs), 1.00 mL of H₂SO₄ (conc) was added and the reaction mixture stirred at reflux under Ar. After 6 h TLC analysis confirmed a presence of a new product without starting compound. The mixture was cooled down and excess of EtOH was evaporated by RVE. Crude product was dissolved in 30 mL of DCM, washed with water (5 x 30 mL) and saturated aq solution of NaHCO₃ (3 x 30 mL). Separated organic layer was dried over Na₂SO₄, filtered and concentrated under reduced pressure yielding 85.0 mg (0.31 mmol, 76 %) of ester **44** as an orange solid product.

Novelty: ethyl 2-(3-oxo-2,3-dihydro-5H-[1,2,4]triazino[5,6-b]indol-5-yl)acetate (**44**) is described in the literature by its M.P., ¹H-NMR, ¹³C-NMR, IR, MS and elemental analysis.¹⁴²

M.p.: 247.0 - 253.0 °C [DCM], lit.: 248.0 - 252.0 °C [MeOH / DCM].¹⁴²

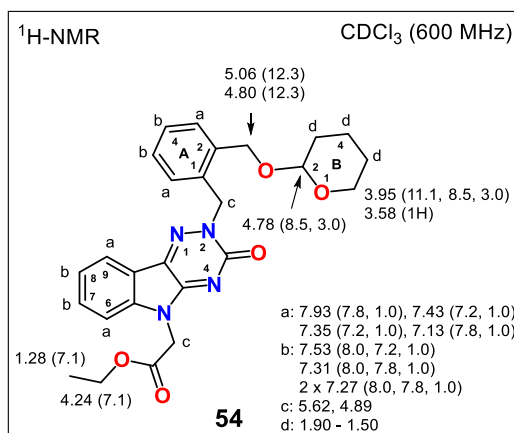
¹⁴² Hlavac, M.; Kovacikova, L.; Prnova, M.S.; Addova, G.; Majekova, M.; Hanquet, G.; Bohac, A.; Stefek, M. *J. Med. Chem.*, **2020**, *63*, 369 - 381.

Synthesis of ethyl 2-{3-oxo-2-{2-[[tetrahydro-2H-pyran-2-yl]oxy]methyl}benzyl}-2,3-dihydro-5H-[1,2,4]triazino[5,6-b]indol-5-yl}acetate (54**)**



To a solution of 200.0 mg (0.74 mmol, 1.00 mol eq) **44** in 5 mL DMF (abs), 37.0 mg (0.88 mmol, 1.19 mol eq) of CaH₂ was added and the mixture stirred at 80 °C under Ar within 30 min. Then, the reaction was cooled to rt and 310 mg (1.09 mmol, 1.47 mol eq) of tetrahydropyrane **53** was added dropwise and the solution was stirred at 80 °C within 1 h under Ar. After consumption of **44** (confirmed by TLC analysis) the reaction was cooled down, 10 mL of water added and then the mixture stirred for 10 min in an ice bath. Resulting mixture was extracted with DCM (3 x 15 mL), washed with brine (3 x 20 mL), dried over Na₂SO₄, filtered and concentrated under reduced pressure. A crude product was purified by FLC (SiO₂, Hex / EA = 1 / 5) to give 286 mg (0.60 mmol, 82 %) of **54** as red oil.

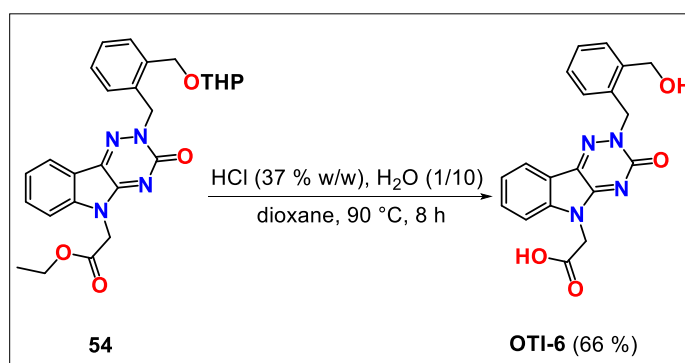
Novelty: ethyl 2-{3-oxo-2-{2-[[tetrahydro-2H-pyran-2-yl]oxy]methyl}benzyl}-2,3-dihydro-5H-[1,2,4]triazino[5,6-b]indol-5-yl}acetate (**54**) is not described in the literature.



¹H-NMR (600 MHz, CDCl₃): δ 7.93, 7.43, 7.35 and 7.13 (4 x dd, 4 x 1H, *J*(6,7 or 8,9 or A₃,A₄ or A₅,A₆) = 7.8 and 7.2 Hz, *J*(6,8 or 7,9 or A₃,A₅ or A₄,A₆) = 1.0 Hz, H-C(6, 9, A₃ and A₆)), 7.53, 7.31, 2 x 7.27 (4 x ddd, 4 x 1H, *J*(7,8 or A₄,A₅) = 8.0 Hz, *J*(6,7 or 8,9 or A₃,A₄ or A₅,A₆) = 7.8 and 7.2 Hz, *J*(6,8 or 7,9 or A₃,A₅ or A₄,A₆) = 1.0 Hz, H-C(7, 8, A₄ and A₅)), 5.06 (d, 1H, *J*_{gem} = 12.3 Hz, -OCH₂Ph), 5.62 and 4.89 (suprisingly 2 x s, 2 x 2H, -CH₂COOEt and -CH₂Ph), 4.80 (d, 1H, *J*_{gem} = 12.3 Hz, -OCH₂Ph), 4.78 (dd, 1H, *J*(B₂,B₃) = 8.5 Hz and *J*(B₂,B₃) = 3.0 Hz, H-C_B(2)), 4.24 (q, 2H, *J*(CH₂,CH₃) = 7.1 Hz, -OCH₂CH₃), 3.95 (ddd, 1H, *J*_{gem} = 11.1 Hz, *J*(B₅,B₆) = 8.5 Hz, *J*(B₅B₆) = 3.0 Hz, H-C_B(6)), 3.58 (m, 1H, H-C_B(6)), 1.90 - 1.50 (m, 6H, 3 x -CH₂- from C(B₃-B₅)), 1.28 (t, 3H, *J*(CH₂,CH₃) = 7.1 Hz, -OCH₂CH₃).

Due to moisture instability of the **54**, its other spectra and analysis were not recorded and compound **54** was used directly in the next step.

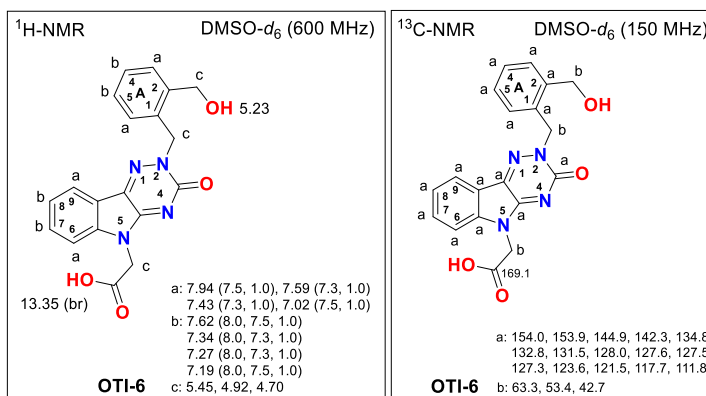
Synthesis of 2-{2-[2-(hydroxymethyl)benzyl]-3-oxo-2,3-dihydro-5H-[1,2,4]triazino[5,6-*b*]indol-5-yl}acetic acid (OTI-6)



To a solution of 50.0 mg (0.11 mmol, 1.00 mol eq) ester **54** in 10 mL of dioxane, 1 mL of H₂O and 0.1 mL of HCl (37 % w/w) were added and resulting solution stirred at 90 °C for 8 h. After that, TLC analysis confirmed presence of a one product without side products. Reaction mixture was cooled down, 30 mL of water added and extracted with DCM (3 x 15 mL). Combined organic layer was dried over Na₂SO₄, filtered and concentrated under reduce pressure yielding 25.0 mg (0.07 mmol, 66 %) of acid **OTI-6** as a yellow solid compound.

Novelty: 2-{2-[2-(hydroxymethyl)benzyl]-3-oxo-2,3-dihydro-5H-[1,2,4]triazino[5,6-b]indol-5-yl}acetic acid (**OTI-6**) is not described in the literature.

M.p.: 220.0 - 238.0 °C (dec) [DCM].



¹H-NMR (600 MHz, DMSO-*d*₆): δ 13.35 (br s, 1H, -COOH), 7.94, 7.59, 7.43 and 7.02 (4 x dd, 4 x 1H, $J(6,7$ or $8,9$ or A_3,A_4 or $A_5,A_6) = 7.5$ or 7.3 Hz, $J(6,8$ or $7,9$ or A_3,A_5 or $A_4,A_6) = 1.0$ Hz, H-C(6, 9, A_3 and A_6)), 7.62, 7.34, 7.27 and 7.19 (4 x ddd, 4 x 1H, $J(7,8$ or $A_4,A_5) = 8.0$ Hz, $J(6,7$ or $8,9$ or A_3,A_4 or $A_5,A_6) = 7.5$ or 7.3 Hz, $J(6,8$ or $7,9$ or A_3,A_5 or $A_4,A_6) = 1.0$ Hz, H-C(7, 8, A_4 and A_5)), 5.45, 4.92 and 4.70 (3 x s, 3 x 2H, -CH₂COOEt, -CH₂Ph and -CH₂OH), 5.23 (s, 1H, -OH).

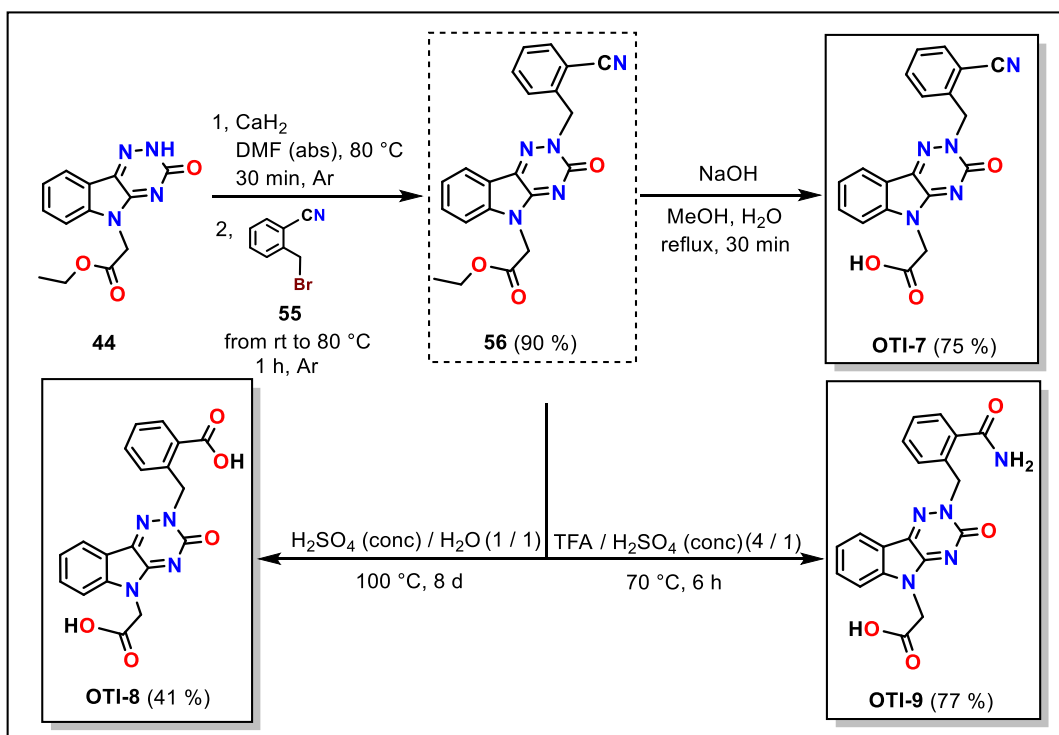
¹³C-NMR (150 MHz, DMSO-*d*₆): 169.1 (-COOH), 154.0, 153.9, 144.9, 142.3, 134.8, 132.8, 131.5, 128.0, 127.6, 127.5, 127.3, 123.6, 121.5, 117.7, 111.8, 63.3, 53.4, 42.7.

FT-IR (solid, cm⁻¹): 3207 (w), 2922 (w), 2712 (w), 2602 (w), 2522 (w), 2108 (w), 2087 (w), 1728 (s), 1606 (s), 1577 (s), 1502 (m), 1467 (m), 1414 (s), 1374 (m), 1228 (s), 1203 (s), 1116 (w), 1087 (w), 1045 (m), 997 (w), 954 (w), 937 (w), 893 (w), 786 (m), 751 (s), 670 (m), 610 (m), 585 (m), 478 (w), 434 (s).

MS (ESI m/z): 363.0 (95 %) [M-H]⁻, 319.1 (95 %) [M-CO₂-H]⁺ (negative mode).

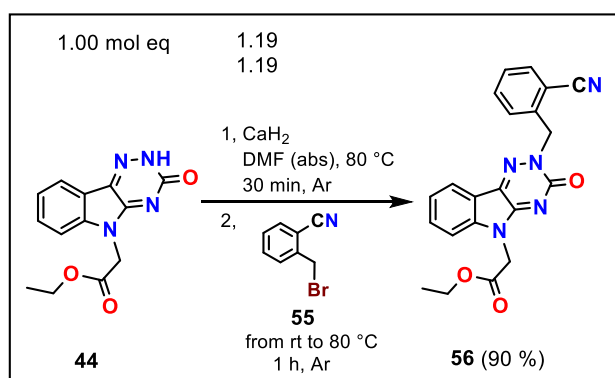
Anal. calcd for $C_{19}H_{16}N_4O_4$ (364.36): C, 62.63; H, 4.43; N, 15.38 Found: C, 62.75; H, 4.49; N, 15.55.

14.4.2. Synthesis of benzyl analogues OTI-(7-9)



Scheme 71. Synthesis of benzyl analogues OTI-(7-9).

Synthesis of ethyl 2-[2-(2-cyanobenzyl)-3-oxo-2,3-dihydro-5H-[1,2,4]triazino[5,6-b]indol-5-yl]acetate (56)



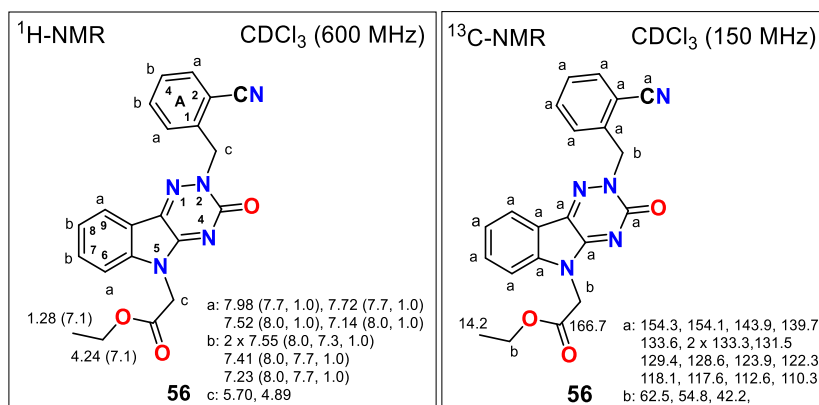
To a solution of 100.0 mg (0.37 mmol, 1.00 mol eq) **44** in 3 mL DMF (abs), 18.5 mg (0.44 mmol, 1.19 mol eq) of CaH_2 was added and the reaction stirred at 80 °C for 30 min. Then, the mixture was cooled to rt and 86.5 mg (0.44 mmol, 1.19 mol eq) of benzonitrile **55** was added

portionwise and the mixture stirred at 80 °C within 1 h. After consumption of **44** (confirmed by TLC analysis) the reaction was cooled down in an ice bath, 10 mL of water added and the reaction stirred for 10 min. Resulting mixture was extracted with DCM (3 x 15 mL), a combined organic phase washed with brine (3 x 20 mL), dried over Na₂SO₄, filtered and concentrated under reduced pressure. A crude product was purified by FLC (SiO₂, Hex / EA = 1 / 5) to give 128 mg (0.33 mmol, 90 %) of **56** as an orange solid material.

Novelty: ethyl 2-[2-(2-cyanobenzyl)-3-oxo-2,3-dihydro-5H-[1,2,4]triazino[5,6-*b*]indol-5-yl]acetate (**56**) is not described in the literature.

M.p.: 175.0 - 180.0 °C [Hex / EA].

NMR diagrams:



¹H-NMR (600 MHz, CDCl₃): δ 7.98, 7.72, 7.52 and 7.14 (4 x dd, 4 x 1H, *J*(6,7 or 8,9 or A₃,A₄ or A₅,A₆) = 7.7 or 8.0 Hz, *J*(6,8 or 7,9 or A₃,A₅ or A₄,A₆) = 1.0 Hz, H-C(6, 9, A₃ and A₆)), 2 x 7.55, 7.41 and 7.23 (4 x ddd, 4 x 1H, *J*(7,8 or A₄,A₅) = 8.0 Hz, *J*(6,7 or 8,9 or A₃,A₄ or A₅,A₆) = 7.7 or 7.3 Hz, *J*(6,8 or 7,9 or A₃,A₅ or A₄,A₆) = 1.0 Hz, H-C(7, 8, A₄ and A₅)), 5.70 and 4.89 (2 x s, 2H, -CH₂COOEt and -CH₂Ar), 4.24 (q, 2H, *J*(CH₂,CH₃) = 7.1 Hz, -OCH₂CH₃), 1.28 (t, 3H, *J*(CH₂,CH₃) = 7.1 Hz, -OCH₂CH₃).

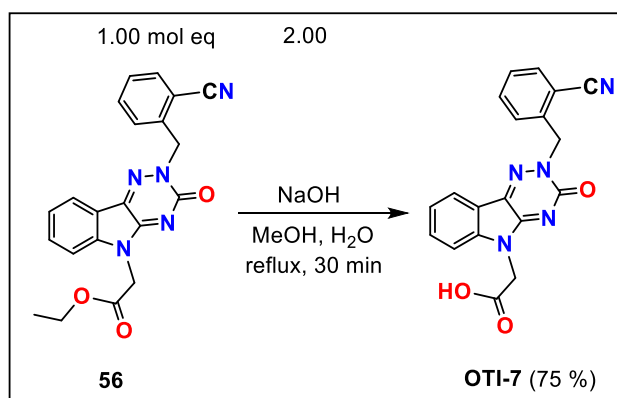
$^{13}\text{C-NMR}$ (150 MHz, CDCl_3): 166.7 ($-\text{COOEt}$), 154.3, 154.1, 143.9, 139.7, 133.6, 2 x 133.3, 131.5, 129.4, 128.6, 123.9, 122.3, 118.1, 117.6, 112.6, 110.3, 62.5, 54.8, 42.2, 14.2 ($-\text{OCH}_2\text{CH}_3$).

FT-IR (solid, cm^{-1}): 2983 (w), 2931 (w), 2228 (m, $-\text{CN}$), 1738 (s), 1662 (s), 1633 (s), 1600 (s), 1568 (s), 1498 (m), 1478 (s), 1408 (s), 1373 (m), 1314 (w), 1274 (m), 1200 (s), 1131 (w), 1104 (s), 1052 (s), 1015 (m), 955 (m), 936 (m), 874 (w), 786 (m), 755 (s), 730 (m), 697 (m), 670 (m), 557 (m), 486 (w), 465 (w), 430 (s).

MS (ESI m/z): 387.0 (95 %) [$\text{M}-\text{e}^-$] (negative mode).

Anal. calc. for $\text{C}_{21}\text{H}_{17}\text{N}_5\text{O}_3$ (387.39): C, 65.11; H, 4.42; N, 18.08; Found: C, 64.86; H, 4.49; N, 18.45.

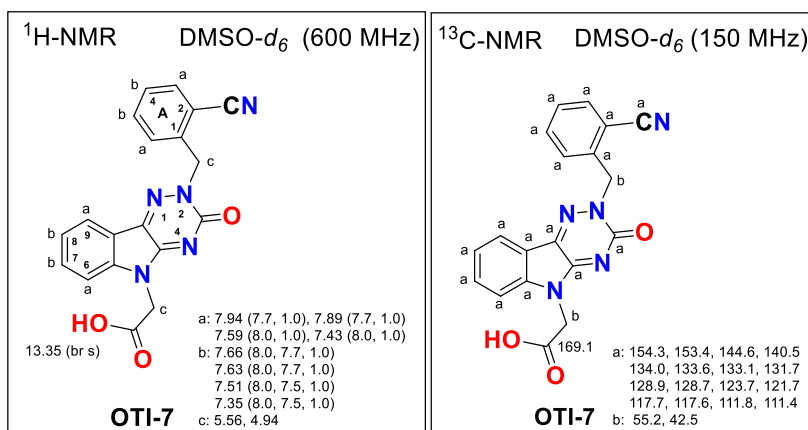
Synthesis of 2-[2-(2-cyanobenzyl)-3-oxo-2,3-dihydro-5H-[1,2,4]triazino[5,6-b]indol-5-yl]acetic acid (OTI-7)



To a solution of 100 mg (0.26 mmol, 1.00 mol eq) ester **56** in 20 mL of MeOH, 20.6 mg (0.52 mmol, 2.00 mol eq) of NaOH in 3 mL water was added and the mixture refluxed for 30 min. After consumption of starting material **56** (confirmed by TLC analysis) the reaction mixture was cooled down in an ice bath and acidified with 1 M HCl to pH = 3. After 10 min of stirring, formed precipitate was filtered off, washed with ice water and dried under reduce pressure to yield 70.0 mg (0.19 mmol, 75 %) of acid **OTI-7** as a brown solid product.

Novelty: 2-[2-(2-cyanobenzyl)-3-oxo-2,3-dihydro-5H-[1,2,4]triazino[5,6-b]indol-5-yl]acetic acid (**OTI-7**) is not described in the literature.

M.p.: 280.9 - 284.5 °C [MeOH / H₃O⁺].



¹H-NMR (600 MHz, DMSO-*d*₆): δ 13.35 (br s, 1H, -COOH), 7.94, 7.89, 7.59 and 7.43 (4 x dd, 4 x 1H, *J*(6,7 or 8,9 or A₃,A₄ or A₅,A₆) = 8.0 or 7.7 Hz, *J*(6,8 or 7,9 or A₃,A₅ or A₄,A₆) = 1.0 Hz, H-C(6, 9, A₃, A₆)), 7.66, 7.63, 7.51 and 7.35 (4 x ddd, 4 x 1H, *J*(7,8 or A₄,A₅) = 8.0 Hz, *J*(6,7 or 8,9 or A₃,A₄ or A₅,A₆) = 7.7 or 7.5 Hz, *J*(6,8 or 7,9 or A₃,A₅ or A₄,A₆) = 1.0 Hz, H-C(7, 8, A₄, A₅)), 5.56 and 4.94 (2 x s, 2 x 2H, -CH₂COOH and -CH₂Ar).

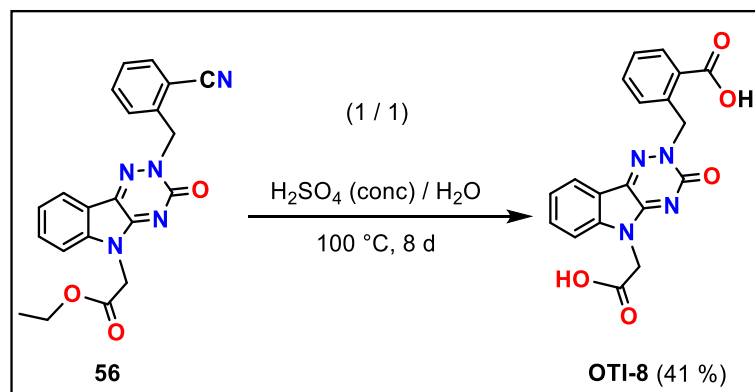
¹³C-NMR (150 MHz, DMSO-*d*₆): 169.1 (-COOH), 154.3, 153.4, 144.6, 140.5, 134.0, 133.6, 133.1, 131.7, 128.9, 128.7, 123.7, 121.7, 117.7, 117.6, 111.8, 111.4, 55.2, 42.5.

FT-IR (solid, cm⁻¹): 3300 - 2800 (br, COOH) 2226 (w), 1762 (m), 1626 (m), 1604 (s), 1572 (s), 1502 (m), 1468 (m), 1420 (m), 1381 (m), 1341 (m), 1316 (w), 1278 (m), 1229 (m), 1207 (m), 1162 (w), 1134 (w), 1115 (w), 1084 (w), 1058 (w), 1039 (w), 994 (w), 934 (w), 885 (w), 788 (s), 767 (s), 668 (m), 611 (m), 584 (m), 556 (m), 499 (w), 457 (w), 433 (s)

MS (ESI m/z): 358.1 (80 %) [M-H]⁻, 314.0 (100 %) [M-CO₂-H]⁻ (negative mode).

Anal. calcd for C₁₉H₁₃N₅O₃ (359.35): C, 63.51; H, 3.65; N, 19.49 Found: C, 63.30; H, 3.60; N, 19.50.

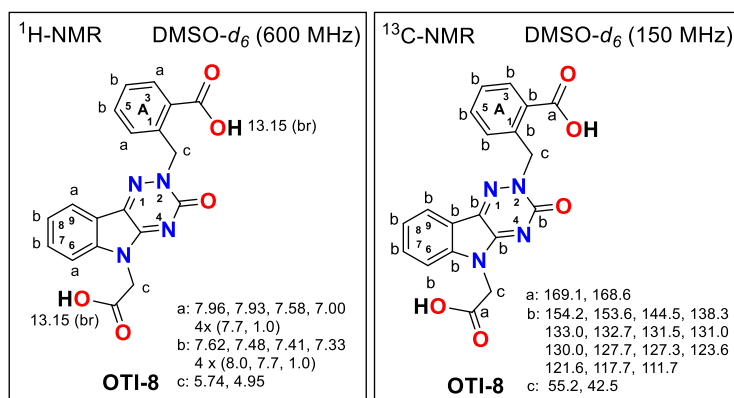
Synthesis of 2-[[5-(carboxymethyl)-3-oxo-3,5-dihydro-2H-[1,2,4]triazino[5,6-b]indol-2-yl]methyl]benzoic acid (OTI-8)



A solution of 30.0 mg (0.08 mmol, 1.00 mol eq) of ester **56** in 2 mL of H₂SO₄ (conc) and 2 mL of H₂O was stirred at 100 °C within 8 d. After complete consumption of starting compound **56** and its amidic intermediate (confirmed by TLC analysis), the reaction was cooled down, 20 mL of H₂O added and the resulting mixture extracted with EA (5 x 15 mL). Combined organic layer was dried over Na₂SO₄, filtered and concentrated to a half of its volume. After that, the solution was placed into a refrigerator, where the product **OTI-8** precipitated. After filtration, obtained precipitate was triturated with a mixture of Hex / EA to give 12.0 mg (0.03 mmol, 41 %) of bisacid **OTI-8** as a yellow solid compound.

Novelty: 2-[[5-(carboxymethyl)-3-oxo-3,5-dihydro-2H-[1,2,4]triazino[5,6-b]indol-2-yl]methyl]benzoic acid (**OTI-8**) is not described in the literature.

M.p.: 260 - 277 °C (dec) [EA].



¹H-NMR (600 MHz, DMSO-*d*₆): δ 13.15 (2 x br s, 2 x 1H, 2 x -COOH), 7.96, 7.93, 7.58 and 7.00 (4 x dd, 4 x 1H, $J(6,7$ or $8,9$ or A_3,A_4 or $A_5,A_6) = 7.7$ Hz, $J(6,8$ or $7,9$ or A_3,A_5 or $A_4,A_6) = 1.0$ Hz, H-C(6, 9, A₃ and A₆)), 7.62, 7.48, 7.41 and 7.33 (4 x ddd, 4 x 1H, $J(7,8$ or $A_4,A_5) = 8.0$ Hz, $J(6,7$ or $8,9$ or A_3,A_4 or $A_5,A_6) = 7.7$ Hz, $J(6,8$ or $7,9$ or A_3,A_5 or $A_4,A_6) = 1.0$ Hz, H-C(7, 8, A₄ and A₅)), 5.74 and 4.95 (2 x s, 2 x 2H, -CH₂COOH and -CH₂Ar).

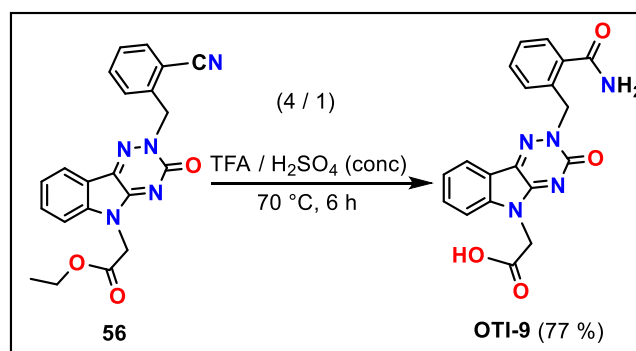
¹³C-NMR (150 MHz, DMSO-*d*₆): 169.1, 168.6, 154.2, 153.6, 144.5, 138.3, 133.0, 132.7, 131.5, 131.0, 130.0, 127.7, 127.3, 123.6, 121.6, 117.7, 111.7, 55.2, 42.5.

FT-IR (solid, cm⁻¹): 3000 - 2200 (br, -COOH) 2822 (m), 2606 (m), 2088 (w), 1725 (m), 1688 (m), 1635 (m), 1602 (s), 1569 (s), 1499 (m), 1467 (m), 1406 (m), 1313 (m), 1225 (s), 1203 (s), 1134 (w), 1107 (m), 1056 (w), 968 (m), 940 (s), 827 (w), 788 (s), 733 (s), 663 (s), 614 (w), 582 (w), 554 (w), 483 (w), 436 (s).

MS (ESI *m/z*): 377.0 (25 %) [M-H]⁻, 365.1 (100 %) [M-CO₂-H⁺+CH₃OH]⁻, 333.1 (100 %) [M-CO₂-H]⁻, 755 (30 %) [(2 x M)-H]⁻ (negative mode).

Anal. calcd for C₁₉H₁₄N₄O₅ (378.34): C, 60.32; H, 3.73; N, 14.81;; Found: C, 60.55; H, 4.05; N, 14.97.

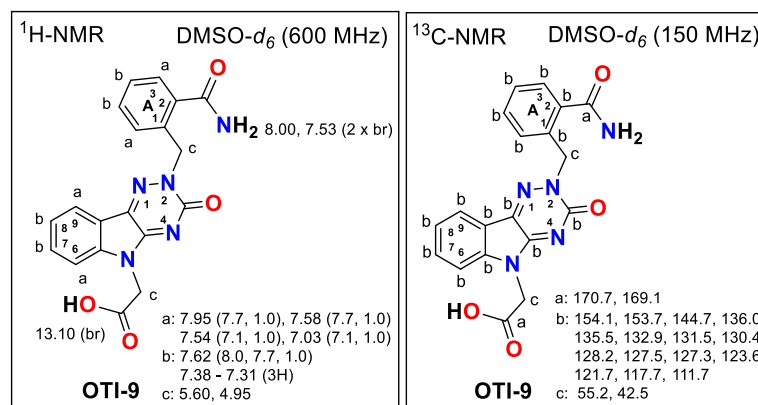
Synthesis of 2-[2-(2-carbamoylbenzyl)-3-oxo-2,3-dihydro-5H-[1,2,4]triazino[5,6-b]indol-5-yl]acetic acid (OTI-9)



A solution of 20.0 mg (0.05 mmol, 1.00 mol eq) ester **56** in 1 mL of CF₃COOH (TFA) and 0.25 mL of H₂SO₄ (conc) was stirred at 70 °C for 6 h. After complete consumption of starting compound **56** (confirmed by TLC analysis), the reaction was cooled down and 20 mL of H₂O and 20 mL of brine were added and the resulting mixture extracted with EA (5 x 15 mL). Combined organic layer was dried over Na₂SO₄, filtered and concentrated under reduced pressure. A crude product **OTI-9** was purified by trituration with a mixture of Hex / EA to give 15.0 mg (0.04 mmol, 77 %) of acid **OTI-9** as a solid compound.

Novelty: 2-[2-(2-carbamoylbenzyl)-3-oxo-2,3-dihydro-5H-[1,2,4]triazino[5,6-b]indol-5-yl]acetic acid (**OTI-9**) is not described in the literature.

M.p.: 221.3 - 225.1 °C [EA].



¹H-NMR (600 MHz, DMSO-*d*₆): δ 13.10 (br s, 1H, -COOH), 8.00 and 7.53 (2 x br s, 2 x 1H, -ArCONH₂), 7.95, 7.58, 7.54 and 7.03 (4 x dd, 4 x 1H, $J(6,7$ or $8,9$ and A_3,A_4 or $A_5,A_6) = 7.7$ or 7.1 Hz, $J(6,8$ or $7,9$ or A_3,A_5 or $A_4,A_6) = 1.0$ Hz, H-C(6, 9, A₃ and A₆)), 7.62 and 7.38 – 7.31 (1 x ddd and m, 1H and 3H, $J(7,8$ or $A_4,A_5) = 8.0$ Hz, $J(6,7$ or $8,9$ or A_3,A_4 or $A_5,A_6) = 7.7$ Hz, $J(6,8$ or $7,9$ or A_3,A_5 or $A_4,A_6) = 1.0$ Hz, H-C(7, 8, A₄ and A₅)), 5.60 and 4.95 (2 x s, 2 x 2H, -CH₂COOH and -CH₂Ar).

¹³C-NMR (150 MHz, DMSO-*d*₆): 170.7, 169.1, 154.1, 153.7, 144.7, 136.0, 135.5, 132.9, 131.5, 130.4, 128.2, 127.5, 127.3, 123.6, 121.7, 117.7, 111.7, 55.2, 42.5.

FT-IR (solid, cm⁻¹): 3357 (m), 3191 (m), 2959 (m), 2928 (m), 2858 (w), 2342 (w), 1736 (s), 1671 (s), 1606 (s), 1578 (s), 1498 (m), 1465 (m), 1413 (m), 1375 (w), 1282 (m), 1199 (s), 1122 (s), 941 (m), 748 (s), 678 (m), 631 (m), 504 (w), 438 (m).

MS (ESI *m/z*): 378.0 (100 %) [M+H⁺]⁺, 400.1 (20 %) [M+Na⁺]⁺, 777.2 (80 %) [(2 x M) + Na⁺]⁺ (positive mode).

Anal. calcd for C₁₉H₁₅N₅O₄ (377.36): C, 60.48; H, 4.01; N, 18.56; Found: C, 60.85; H, 4.39; N, 18.75.

Conclusion

15. Conclusion

Within the first project, we have successfully developed a synthesis of *N*,4-diaryloxazole-2-amine precursor **10**, which acts as a joint intermediate for preparation of all desired inhibitors **NBM(1-7)**. All proposed inhibitors **NBM(1-5,7)** were prepared by particular coupling reaction using either commercially available (**20-24**) or synthesized (**15** and **19**) coupling partners. Compound **NBM6** was synthesized previously in our group. Desired *N*-regioisomeric derivatives **NBM(1-7)** represent a new class of VEGFR2 TK inhibitors with expected similar binding position as their relative *O*-regioisomers **BM(1-7)**. Results from biological assays revealed lower VEGFR2 TK inhibitory activity for **NBM(1-6)** mostly in micromolar IC₅₀ range in comparison to **BM(1-6)** with nanomolar IC₅₀ activities. In spite of that, the obtained activities of **NBM(1-7)** confirmed an active and predicted binding conformation of regioisomeric inhibitors in the active site of VEGFR2 TK. In this case regioisomeric exchange of „N“ to „O“ in an oxazole ring in **NBM(1-6)** was presumably less preferred and causing their lower inhibitory activity compare to **BM(1-6)**. Determination of an inhibitory activity of **BM7** and **NBM7** is pending.

The second project was focused on the development of a second class of VEGFR2 TK inhibitors, possessing three key interactions in the SBCP pocket. Biomagi proposed nine *N*,5-diaryloxazole-2-amine inhibitors **BM(8-16)**, containing pyrrole-3-yl, pyrazole-3-yl and imidazole-4-yl substituents. As a first inhibitor we have successfully synthesized the pyrrole derivative **BM8**. Then, we explained the problems we faced during the synthesis of its analogues **BM(8-9)** in discussion. According to not favourable inhibitory activity of recently determined **NBM1**, synthesis of **BM8** analogues **BM(8-9)** was discontinued. Afterwards, we prepared three pyrazole derivatives **BM(11-13)** and two imidazole inhibitors **BM(14-15)**. Synthesis of imidazole **BM(16)** is pending. In addition, we have developed a preparation of tributylstannylimidazole **15** and pyrrole pinacol boronic ester **19** coupling reagents, that were used in the synthesis of proposed inhibitors **BM(7,8,14)** and *N*-regioisomers **NBM(1,7)**. Compound **BM(16)** should be also synthesized. Determination of an inhibitory activity of **BM(11-15)** is pending. Next part of this project was a synthesis of **NBM(8-14)**, containing *N*,4-diaryloxazole-2-amine scaffold. Unfortunately, we were not able to prepare *N*-regioisomeric intermediate **69** by reaction conditions developed previously for similar intermediate **10**. Reaction of benzonitrile **66** with Tf₂O provided a mixture of probably containing desired triflate **67** and the stable side product **68**, which structure has not been defined yet.

The third project was focused on a development of inhibitors of aldose reductase

Conclusion

(ALR2), implicated in various chronic diabetic complications. Herein, we developed a synthesis of very efficient ALR2 inhibitor cemtirestat (**CMTI**), which synthesis had not been described before. We also developed **CMTI** bioisosteric analogue **OTI**, containing an oxygen instead of a sulphur, and its derivatives **OTI-(1-3)**. Synthesis of the acyl and pivaloyl analogues **OTI-4** and **OTI-5** was not feasible due to their chemical instability. The most active inhibitor **OTI** exhibited 3-fold higher inhibitory activity than **CMTI** and remarkable 8-fold higher selectivity (SF > 2380, ALR2 & ALR1). Similar results we observed in assay on human enzymes with 1.5-fold higher activity of **OTI** and 5-fold higher selectivity (AKR1B1 & AKR1B10). On the other hand, antioxidant activity assay revealed lower activity for **OTI** in comparison to sulphur containing **CMTI**. Based on all these results, **OTI** inhibitor has become a promising lead compound suitable for further development towards inhibition of ALR2.

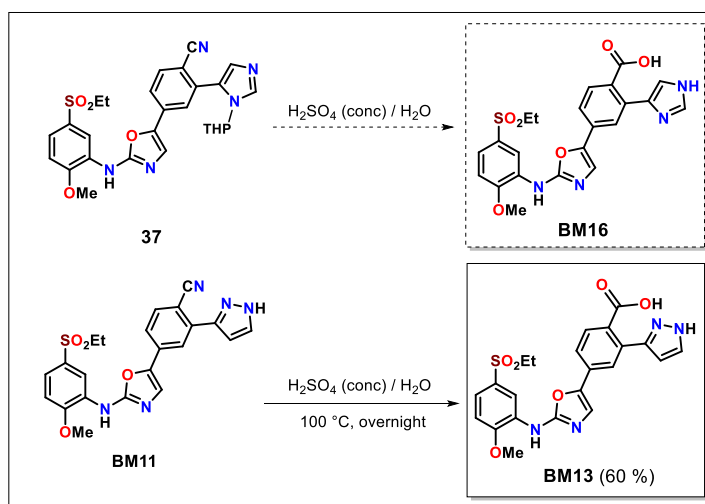
In the last project we performed a SAR study on the *N*-benzylated ALR2 inhibitor **OTI-3**, described in the previous project. According to molecular modeling we detected an unoccupied pocket in the active site of ALR2. Therefore four *N*-benzyl substituted derivatives **OTI-(6-9)** were proposed, possessing various functional groups attached on a benzyl moiety. After synthesis and screening we have seen that all predicted compounds **OTI-(6-9)** exhibited higher inhibitory activity than their unsubstituted analogue **OTI-3**, which proved the proposed additional interactions in the ALR2 binding pocket. We also proposed hypothesis of lower inhibitory activity of derivatives **OTI-(6,8,9)** compare to **OTI-7** and proposed further analogues **OTI-(10-17)** with expected better properties.

To sum up the dissertation thesis, we have prepared 78 compounds, from which 48 were new. From 30 predicted final compounds, we synthesized 22 while 16 of them were biologically evaluated (IC₅₀, VEGFR2 TK, ALR2 and ALR1).

Chapter 12. **Future perspective**

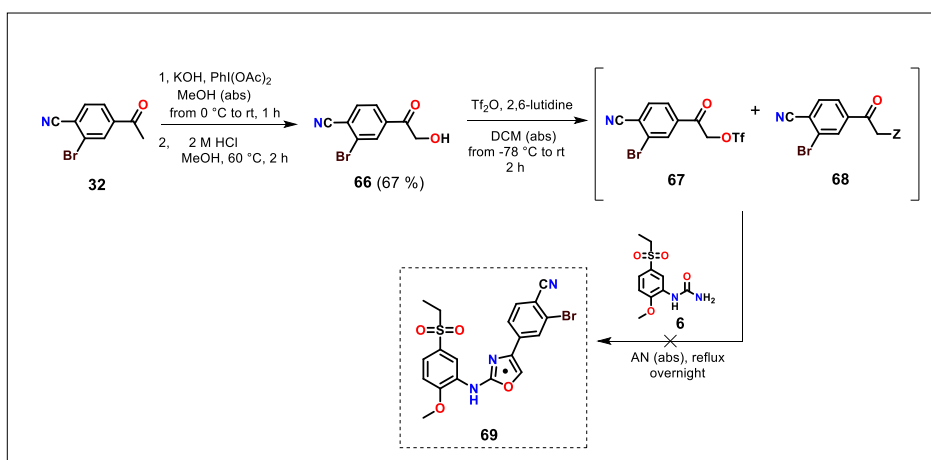
16. Future perspective

Considering the finalization of the first part of the dissertation thesis (**inhibition of VEGFR2 TK**), preparation of the imidazole inhibitor **BM16** is required. Proposed synthesis would start from the intermediate **37**, which would undergo acidic hydrolysis by using a mixture H_2SO_4 (conc) / H_2O , similar as it was applied in the pyrazole inhibitor **BM11**. (Scheme 72)



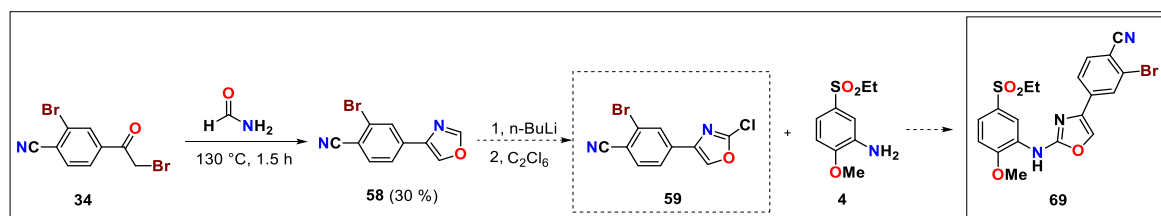
Scheme 72. Proposed synthesis of the inhibitor **BM16**.

Regarding the unsuccessful synthesis of the *N*-regioisomeric intermediate **69**, we would like to determine a structure of the unknown side product **68** by X-ray analysis. (Scheme 73) Since the synthesis of the intermediate **69** *via* triflate **67** was not successful, other synthetic pathway is required to apply.



Scheme 73. Unsuccessful synthesis of the intermediate **69** *via* triflate **67**.

Other synthesis of *N*,4-disubstituted aminooxazoles has been recently started in our research group. Synthesis was initiated from benzonitrile **34**, which was stirred in formamide at 130 °C to get an oxazole **58**. Next step would be a chlorination with *n*-BuLi / hexachloroethane and subsequent nucleophilic substitution with aniline **4** would afford aminooxazole **69**. (Scheme 74)



Scheme 74. New proposed synthesis of aminooxazole **69** by using formamide.

Within the second part of the thesis (**ALR2 inhibition**), we would like to proceed with optimization of OTI skeleton in order to improve pharmacokinetic properties (Project 4). Based on this assumption we have proposed some novel *N*-benzyl(oxotriazineindole) derivatives **OTI-(10-12)**, which may exhibit lower desolvation and conformational penalty with an aim to preserve important interactions in an unoccupied pocket. (Figure 71) Acetyl derivative **OTI-10** is a less polar (solvated) analogue to amide derivative **OTI-8** characterised by lower polarity and solvation. Methyl ester **OTI-11** is less polar analogue to carboxylic acid **OTI-9**. Besides of its lower solvation, it could also possess better penetration through the cell membrane in contrast to **OTI-9**. Other bioisostere of the carboxylic acid derivative **OTI-9** could be a nitro analogue **OTI-12** that could also exhibit lower desolvation and conformational penalty considering its mesomeric delocalization. Even though -NO₂ group is less favourable in drug like molecules.

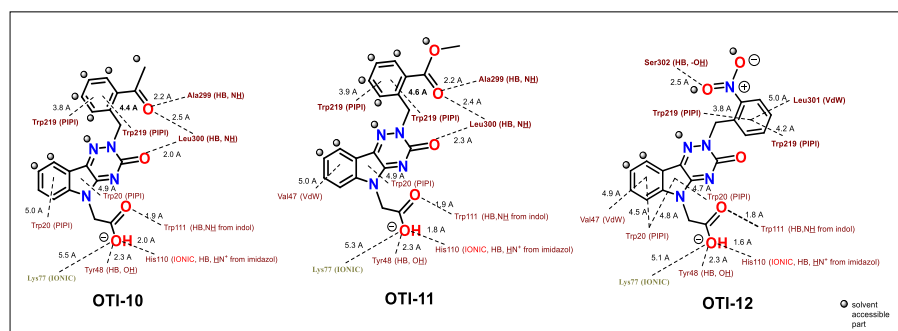


Figure 71. Structures of proposed analogues **OTI-(10-12)** with their interaction diagrams.

Apart from **OTI-(10-12)** analogues, we proceeded with a design of other *N*-substituted derivatives. We identified lipophilic naphthalene derivatives **OTI-(13-14)** with favourable docking predictions comprising four π - π interactions with Trp219 and Van der Waals interactions with Ala299 or Leu301. (Figure 72)

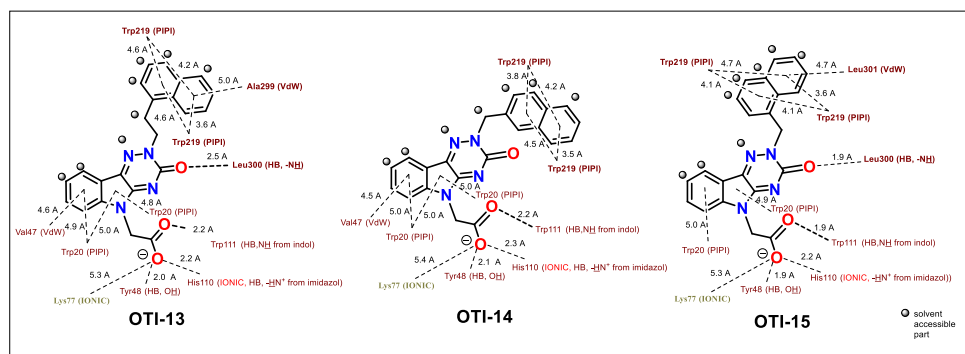


Figure 72. Structures and predicted poses of proposed naphthalene derivatives **OTI-(13-15)**.

Other polycyclic derivatives with convenient docking predictions and lower solvation includes **OTI-16** and **OTI-17** derivatives, containing 3,4-dihydronaphthalen-2(1*H*)-one and 2,3-dihydro-1*H*-inden-1-one moiety, resp. Besides of their π - π interactions with Trp219, they also revealed H-bond with Ala299 and **OTI-17** also with Leu300. (Figure 73)

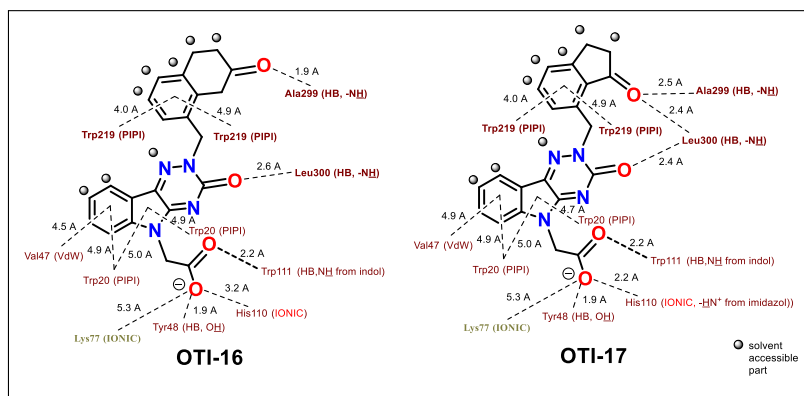


Figure 73. Structures and interaction diagrams of proposed polycyclic derivatives **OTI-16** and **OTI-17**.

Chapter 13. Characterization of the prepared compounds

17. Characterization of the prepared compounds

Compound			Identity												Purity					
Code	new	known	M.P.	¹ H NMR	¹³ C NMR	other NMR	IR	UV-VIS	Elemental analysis	HRMS	rtg analysis (ORTEP)	e.r./d.r.	chiropt. info. [α]/CD	ESI-MS	Fig. of ¹ H NMR spectr.	Fig. of ¹³ C NMR spectr.	Elemental analysis	Pict. of chromatogram	GC/HPLC	others
2	x		x	x	x		x		x					x	x	x	x			
3	x		x	x	x		x		x					x	x	x	x			
4		x	x	x											x					
5		x	x	x											x					
6		x	x	x											x					
8		x	x	x											x					
9 ^a	x			x																
10	x		x	x	x		x		x	x				x	x	x	x			
12		x		x											x					
14		x		x											x					
15	x			x	x		x								x	x				
17		x		x											x					
19		x	x	x											x					
NBM1	x		x	x	x		x		x					x	x	x	x			
NBM2	x		x	x	x		x		x					x	x	x	x			
NBM3	x		x	x	x		x		x					x	x	x	x			
NBM4	x		x	x	x		x		x					x	x	x	x			
NBM5	x		x	x	x		x		x					x	x	x	x			
25	x		x	x	x		x		x					x	x	x	x			
NBM7	x		x	x	x		x		x					x	x	x	x			
26 ^b		x		x																
27 ^b		x		x																
28 ^b		x		x																
29 ^b	x		x	x	x		x		x					x	x	x	x			
BM7	x		x	x	x		x		x					x	x	x	x			

Characterization of the prepared compounds

Code	new	known	M.P.	¹ H NMR	¹³ C NMR	other NMR	IR	UV-VIS	Elemental analysis	HRMS	rtg analysis (ORTEP)	e.r./d.r.	chiropt. info. [α]/CD	ESI-MS	Fig. of ¹ H NMR spectr.	Fig. of ¹³ C NMR spectr.	Elemental analysis	Pict. of chromatogram	GC/HPLC	others
31		x	x	x											x					
32		x	x	x	x										x	x				
34	x		x	x	x		x		x						x	x	x			
35	x		x	x	x		x		x					x	x	x	x			
36	x		x	x	x		x		x					x	x	x	x			
BM8	x		x	x	x		x		x					x	x	x	x			
BM11	x		x	x	x		x		x					x	x	x	x			
BM12	x		x	x	x		x		x					x	x	x	x			
BM13	x		x	x	x		x		x					x	x	x	x			
37	x		x	x	x		x		x					x	x	x	x			
BM14	x		x	x	x		x		x					x	x	x	x			
BM15	x		x	x	x		x		x					x	x	x	x			
32a-35c ^c	x			x	x															
36c ^d		x		x	x															
35b ^d	x			x	x															
36b ^d		x		x	x															
37c ^d	x			x	x															
36d ^d		x		x																
64	x			x																
66	x		x	x	x		x		x					x	x	x	x			
67	x			x ^e																
68	x		x	x	x	x ^f	x							x	x	x				
39		x	x	x											x					
40	x		x	x	x		x		x					x	x	x	x			
CMTI	x		x	x	x	x ^{ghi}	x		x					x	x	x	x			
41		x	x	x											x					
42		x	x	x	x		x							x	x	x	x			

Characterization of the prepared compounds

Code	new	known	M.P.	¹ H NMR	¹³ C NMR	other NMR	IR	UV-VIS	Elemental analysis	HRMS	rig analysis (ORTEP)	e.r./d.r.	chiropt. info. [α] _D /CD	ESI-MS	Fig. of ¹ H NMR spectr.	Fig. of ¹³ C NMR spectr.	Elemental analysis	Pict. of chromatogram	GC/HPLC	others
43		x	x	x	x				x					x	x	x	x			
44	x		x	x	x	x ^g	x		x					x	x	x	x			
45	x		x	x	x		x		x					x	x	x	x			
OTI	x		x	x	x	x ^{hi}	x		x					x	x	x	x			
OTI-1	x		x	x	x		x		x					x	x	x	x			
46	x		x	x	x		x		x					x	x	x	x			
OTI-2	x		x	x	x	x ^h	x		x					x	x	x	x			
47	x		x	x	x		x		x					x	x	x	x			
OTI-3	x		x	x	x		x		x					x	x	x	x			
48	x			x											x					
49	x			x											x					
51		x	x	x											x					
52		x	x	x											x					
53		x		x	x		x								x	x				
54	x			x											x					
OTI-6	x		x	x	x		x		x					x	x	x	x			
56	x		x	x	x		x		x					x	x	x	x			
OTI-7	x		x	x	x		x		x					x	x	x	x			
OTI-8	x		x	x	x		x		x					x	x	x	x			
OTI-9	x		x	x	x		x		x					x	x	x	x			

^a - Due to instability of product other analyses were not determined

^b - Synthesis and full experimental analysis is described by Peter Šramel in his dissertation thesis

^c - Synthesis of these four intermediate was not an aim of this thesis, therefore other experimental analyses and characterization were not determined and described in the experimental part of the thesis.

^d - Synthesis of this product was not an aim of this thesis, therefore other characterizations are not described in the experimental part of the thesis.

^e - Due to instability of the product, the structure is determined from a mixed spectrum with **68**

^f - ¹⁹F NMR

^g - NOE NMR

^h - HMBC NMR

ⁱ - HSQC NMR

Chapter 14. **Scientific contribution**

Scientific contribution

Some of the obtained results in this dissertation thesis were published in the following scientific papers and the last one has been recently submitted:

- 1, Hlaváč, M.; Kováčiková, L.; Šoltéssová Prnová, M.; Šramel, P.; Addová, G.; Májeková, M.; Hanquet, G.; Boháč, A.; Štefek, M. Development of Novel Oxotriazinoindole Inhibitors of Aldose Reductase: Isosteric Sulfur/Oxygen Replacement in the Thioxotriazinoindole Centirestat Markedly Improved Inhibition Selectivity *J. Med. Chem.*, **2020**, *63*, 369 - 381.
- 2, Dobiáš, J.; Ondruš, M.; Hlaváč, M.; Murár, M.; Kóňa, J.; Addová, G.; Boháč, A. Medicinal chemistry: an effect of a desolvation penalty of an amide group in the development of kinase inhibitors *Chem. Papers*, **2019**, *73*, 71 - 84.
- 3, Hlaváč, M.; Kováčiková, L.; Šoltéssová Prnová, M.; Addová, G.; Hanquet, G.; Štefek, M.; Boháč, A. Novel substituted *N*-benzyl(oxotriazinoindole) inhibitors of aldose reductase exploiting ALR2 unoccupied interactive pocket (recently submitted)

Also accomplished results were presented at following international conferences:

- 1, **26th Young Research Fellows Meeting in Paris, France (20.2. - 22.2.2019)**
- oral presentation
- 2, **8. Meeting of the Paul Ehrlich Euro-PhD Network in Porto, Portugal (12.7. - 14.7.2018)**
- poster presentation
- 3, **Journée des doctorants en chimie in Strasbourg, France (10.11.2017)**
- oral presentation

Développement rationnel d'inhibiteurs de kinases dédiés au traitement de maladies néoplasiques et des complications diabétiques

Résumé

Les récepteurs de la tyrosine kinase VEGFR2 sont des protéines transmembranaires cruciales pour la régénération tissulaire, la régulation des cycles cellulaires importants et la fonction des cellules endothéliales vasculaires. D'autre part, une activité accrue de VEGFR2 TK provoque une division incontrôlée des cellules cancéreuses et la formation de tumeur. En conséquence, le développement de petites molécules inhibitrices de la VEGFR2 TK est devenu un moyen prometteur et efficace pour le traitement du cancer. D'un autre côté une autre maladie tout aussi grave tel que le diabète, caractérisé par l'absence d'insuline ou sa résistance ou l'aldose réductase (ALR2) joue un rôle important dans la formation de diverses complications cardiaques et diabétiques est devenue une cible thérapeutique importante dans le traitement des maladies liées au diabète. Cette thèse a abouti à la découverte de 14 inhibiteurs de VEGFR2 TK et 9 inhibiteurs d'ALR2 tandis que 16 d'entre eux ont été évalués biologiquement (IC_{50} , VEGFR2 TK, ALR2 et ALR1).

Mot clés : inhibiteurs de tyrosine kinase, aldose réductase, VEGFR2 TK, ALR2, aminooxazoles, oxotriazinoindoles

Résumé en anglais

VEGFR2 tyrosine kinase receptors are transmembrane proteins that are crucial for tissue regeneration, regulation of important cell cycles and vascular endothelial cell function. On the other hand, enhanced activity of VEGFR2 TK causes uncontrolled division of cancer cells and formation of tumor. Accordingly, a development of small molecule VEGFR2 TK inhibitors has become a promising and effective way for cancer treatment. Another equally serious disease is diabetes mellitus, characterized by absence of insulin or its resistance. Aldose reductase (ALR2) plays an important role in a formation of various heart and diabetic complications and has become an important therapeutic target in treatment of illnesses related to diabetes mellitus. This dissertation thesis resulted in a discovery of 14 inhibitors of VEGFR2 TK and 9 inhibitors of ALR2 while 16 of them were biologically evaluated (IC_{50} , VEGFR2 TK, ALR2 and ALR1).

Key words: tyrosine kinase inhibitors, aldose reductase, VEGFR2 TK, ALR2, aminooxazoles, oxotriazinoindoles